DRVNA INDUSTRIJA

SCIENTIFIC JOURNAL
OF WOOD TECHNOLOGY

ZNANSTVENI ČASOPIS
IZ PODRUČJA DRVNE TEHNOLOGIJE

Fraxinus angustifolia Vahl.

UDK 674.031.677.7
ISO: Drv. Ind.
CODEN: DRINAT
JCR: DRVNA IND
ISSN 0012-6772

2/25
VOLUME 76

since 1913

UDK 630*8+674 Coden: Drinat ISSN 0012-6772

DRVNA INDUSTRIJA

SCIENTIFIC JOURNAL OF WOOD TECHNOLOGY

Znanstveni časopis iz područja drvne tehnologije

PUBLISHER AND EDITORIAL OFFICE
Izdavač i uredništvo
University of Zagreb
Faculty of Forestry and Wood Technology
Sveučilište u Zagrebu
Fakultet šumarstva i drvne tehnologije
www.sumfak.unizg.hr

CO-PUBLISHER / Suizdavač
Hrvatska komora inženjera šumarstva i drvne tehnologije

FOUNDER / Osnivač
Institut za drvnoindustrijska istraživanja, Zagreb

The journal Drvna industrija is an international open access peer-reviewed quarterly scientific journal for publishing research results on structure, properties and protection of wood and wood materials, application of wood and wood materials, mechanical woodworking, hydrothermal treatment and chemical processing of wood, all aspects of wood materials and wood products production and trade in wood and wood products.
The journal is published quarterly and financially supported by the Ministry of Science and Education of the Republic of Croatia.

Časopis Drvna industrija je međunarodni recenzirani tromjesečni znanstveni časopis otvorenog pristupa za objavu rezultata istraživanja građe, svojstava i zaštite drva i drvnih materijala, primjene drva i drvnih materijala, mehaničke i hidrotermičke obrade te kemijske prerade drva, svih aspekata proizvodnje drvnih materijala i proizvoda te trgovine drvom i drvnim proizvodima.
Časopis izlazi četiri puta u godini uz financijsku potporu Ministarstva znanosti i obrazovanja Republike Hrvatske.

Contents
Sadržaj

CIRCULATION: *400 pieces*

INDEXED IN: *Science Citation Index Expanded, Scopus, CAB Abstracts, Compendex, Environment Index, Veterinary Science Database, Geobase, DOAJ, Hrčak, Sherpa Romeo*

MANUSCRIPTS ARE TO BE SUBMITTED *by the link http://journal.sdewes.org/drvind*

CONTACT WITH THE EDITORIAL *e-mail: editordi@sumfak.hr*

SUBSCRIPTION: *Annual subscription is 55 EUR. For pupils, students and retired persons the subscription is 15 EUR. Subscription shall be paid to the IBAN HR0923600001101340148 with the indication "Drvna industrija".*

PRINTED BY: *DENONA d.o.o., Getaldićeva 1, Zagreb, www.denona.hr*

DESIGN: *Bernardić Studio*

THE JOURNAL IS AVAILABLE ONLINE: *https://drvnaindustrija.com*

COVER: *Radial-sectional view of Fraxinus angustifolia (Vahl), xylotheca of Institute for Wood Science, University of Zagreb Faculty of Forestry and Wood Technology*

DRVNA INDUSTRIJA · VOL. 76, 2 · P. 113-228 · SUMMER 2025. · ZAGREB EDITORIAL COMPLETED 1. 6. 2025.

NAKLADA: *400 komada*

ČASOPIS JE REFERIRAN U: *Science Citation Index Expanded, Scopus, CAB Abstracts, Compendex, Environment Index, Veterinary Science Database, Geobase, DOAJ, Hrčak, Sherpa Romeo*

ČLANKE TREBA SLATI *putem poveznice http://journal.sdewes.org/drvind*

KONTAKT S UREDNIŠTVOM: *e-mail: editordi@sumfak.hr*

PRETPLATA: *Godišnja pretplata za pretplatnike u Hrvatskoj i inozemstvu iznosi 55 EUR. Za đake, studente i umirovljenike 15 EUR. Pretplata se plaća na IBAN HR0923600001101340148 s naznakom "Drvna industrija".*

TISAK: *DENONA d.o.o., Getaldićeva 1, Zagreb, www.denona.hr*

DESIGN: *Bernardić Studio*

ČASOPIS JE DOSTUPAN NA INTERNETU: *https://drvnaindustrija.com*

NASLOVNICA: *Radijalni presjek drva poljskog jasena (Fraxinus angustifolia (Vahl)), ksiloteka Zavoda za znanost o drvu, Sveučilište u Zagrebu Fakultet šumarstva i drvne tehnologije*

DRVNA INDUSTRIJA · VOL. 76, 2 · STR. 113-228 · LJETO 2025. · ZAGREB REDAKCIJA DOVRŠENA 1. 6. 2025.

ORIGINAL SCIENTIFIC PAPERS
Izvorni znanstveni radovi 115-211

Influence of Focal Length Position of Focusing Lens on Plywood Discoloration Under Different Modes of CO_2 Laser Engraving
Utjecaj položaja žarišne duljine fokusne leće na promjenu boje furnirske ploče pri različitim parametrima graviranja CO_2 laserom
Zhivko Gochev, Pavlin Vichev 115

Testing of Bleaching Application on Kingwood (*Dalbergia cearensis* Ducke) Wood
Analiza primjene izbjeljivanja na drvu *kingwooda* (*Dalbergia cearensis* Ducke)
Hüseyin Peker, Ümit Ayata 125

Comparison of Various Feature Extractors and Classifiers in Wood Defect Detection
Usporedba različitih ekstraktora i klasifikatora svojstava u otkrivanju grešaka drva
Kenan Kılıç, Kazım Kılıç, İbrahim Alper Doğru, Uğur Özcan 133

Properties of Phenol-Formaldehyde Resin Modified with Kraft Lignin for Particleboard Production
Svojstva fenol-formaldehidne smole modificirane kraft ligninom za proizvodnju ploča iverica
Miroslav Němec, Luboš Prokůpek, Jaromír Hradecký, Vojtěch Obst, Tomáš Pipíška, Štěpán Hýsek 149

The Effect of Thermal Modification on Anatomical Properties of *Daniellia oliveri* (Rolfe) Hutch and Dalziel from Ghana
Utjecaj toplinske modifikacije na anatomska svojstva drva *Daniellia oliveri* (Rolfe) Hutch i Dalziel iz Gane
Issah Chakurah, Stephen Jobson Mitchual, Francis Kofi Bih, Kwaku Antwi, Enoch Gbapenuo Tampori 159

Forecasting and Comparison of Mechanical Properties of Wooden Structure Models
Predviđanje i usporedba mehaničkih svojstava modela drvnih konstrukcija
Darius Albrektas, Ernestas Ivanauskas, Ugnė Misiūnaitė 169

Constituent Elements, pH and Electrical Conductivity Values of Feedstock, Ash and Slow Pyrolysis Derived Biochar of Date Palm Wastes
Sastavni elementi, pH vrijednost i električna provodnost sirovine, pepela i biougljena dobivenoga sporom pirolizom od otpadaka palme datulje
Ghanbar Ebrahimi, Alireza Shakeri, Pyman Ahmadi, Mosayeb Dalvand, Masoud Shafee 177

Investigating Physical and Mechanical Properties of Mahogany Root Wood (*Khaya ivorensis*) for its Utilization
Istraživanje fizičkih i mehaničkih svojstava drva korijena afričkog mahagonija (*Khaya ivorensis*) radi njegove uporabe
Justine Wepia Apungu, Kwaku Antwi, Emmanuel Appiah-Kubi, Francis Kofi Bih, Joseph Zakaria 189

Potential Antioxidants in Bio-oil Obtained by Pyrolysis of Yew (*Taxus baccata* L.) Tree Bark
Potencijalni antioksidansi u bioulju dobivenom pirolizom kore drva tise (*Taxus baccata* L.)
Hadi Baseri, Seyyed Khalil HosseiniHashemi, Sayed Khosrow HossinAshrafi, Jakia Jerin Mehjabin 201

REVIEW PAPER
Pregledni rad 213-221

Thermal Pre-treatments of Woody Biomass: A High-Level Overview
Toplinski predtretmani drvne biomase: opći pregled
Marin Dujmović, Branimir Šafran, Matija Jug, Kristijan Radmanović 213

SPECIES ON THE COVER / Uz sliku s naslovnice 223-225

Zhivko Gochev*, Pavlin Vichev[1]

Influence of Focal Length Position of Focusing Lens on Plywood Discoloration Under Different Modes of CO_2 Laser Engraving

Utjecaj položaja žarišne duljine fokusne leće na promjenu boje furnirske ploče pri različitim parametrima graviranja CO_2 laserom

ORIGINAL SCIENTIFIC PAPER
Izvorni znanstveni rad
Received – prispjelo: 30. 11. 2023.
Accepted – prihvaćeno: 21. 1. 2025.
UDK: 674.07; 630*83
https://doi.org/10.5552/drvind.2025.0168

ABSTRACT • *This paper presents the results of a study of the laser engraving process on birch plywood samples. The influence of the focal distance of the focusing lens at different positions relative to the surface of the material on the discoloration of plywood samples, at different power and scanning speed of a CO_2 laser beam, was investigated. The change in the color shades of the plywood was studied with an LS173 calorimeter. For this research, the following parameters were used: ZnSe lens with focal length F = 50.8 mm; the position of the focal plane of the focusing lens relative to the surface of the material ΔF = 4, 6, and 8 mm; laser beam power P = 4.0; 5.6 and 7.2 W; feed rate of the laser beam V_f = 250; 260 and 270 mm/s. The color shade difference of the plywood samples was measured in the L*, a* and b* color space. The results allow to define modes for surface treatment with laser beam in the construction of complex graphic images on plywood products.*

KEYWORDS: *CO_2 laser beam; focal distance; calorimeter; discoloration; colour space; birch plywood; surface treatment*

SAŽETAK • *U ovom su radu predstavljeni rezultati istraživanja laserskog graviranja na uzorcima furnirske ploče od brezovine. Istražen je utjecaj položaja žarišne duljine fokusne leće u odnosu prema površini materijala na promjenu boje uzoraka furnirske ploče uz primjenu CO_2 laserske zrake različite snage i brzine. Promjene nijansi boje furnirske ploče proučavane su kolorimetrom LS173. U ovom je istraživanju primijenjena ZnSe leća žarišne duljine F = 50,8 mm; položaj žarišne ravnine fokusne leće s obzirom na površinu materijala bio je ΔF = 4; 6 i 8 mm; snaga laserske zrake P = 4,0; 5,6 i 7,2 W, a posmična brzina laserske zrake V_f = 250; 260 i 270 mm/s. Razlika u nijansama boje uzoraka furnirske ploče mjerena je u L*, a* i b* prostoru boja. Rezultati omogućuju pregled načina obrade površine laserskom zrakom pri izradi složenih grafičkih slika na proizvodima od furnirske ploče.*

KLJUČNE RIJEČI: *CO_2 laserska zraka; žarišna duljina; kolorimetar; promjena boje; prostor boja; furnirska ploča od brezovine; površinska obrada*

* Corresponding author
[1] Authors are researchers at University of Forestry Sofia, Faculty of Forest Industry, Sofia, Bulgaria. https://orcid.org/0000-0001-8689-695X, https://orcid.org/0000-0002-7193-6012

1 INTRODUCTION
1. UVOD

Laser engraving is one of the most up-to-date and effective methods for engraving wood and wood-based materials (WBM). Today, this technology can also be used at home thanks to the development of affordable and compact laser engravers. Different laser engravers are used for engraving wood and WBM based on diode lasers, CO_2 lasers and fiber lasers.

CO_2 lasers use a gas mixture to generate the laser beam; they are versatile, operate at higher speeds and power, and are widely used for cutting and engraving wood and WBM.

In laser engraving, the material is heated very strongly by the laser beam and the surface layer is vaporized or burned. The sharpness and the contrast of the engraving, as well as the resulting shade after the process is completed, depend on various factors, including adjustment of the focus distance, the power and speed of the laser beam, all depending on the type and thickness of the wood or WBM.

In a number of literature sources, the changes in the color of wood, as a result of the impact of CO_2 laser radiation, and the possibilities for engraving or decorating at different power and speeds of the laser beam, have been investigated (Pagano *et al.,* 2009; Leone *et al.,* 2009; Hernández-Castañeda *et al.,* 2011; Eltawahni *et al.,* 2013; Petutschnigg *et al.,* 2013; Kubovský and Kačík, 2013; Kubovský and Igaz, 2014; Kúdela *et al.,* 2018; Kubovský and Kačík, 2014; Yakimovich *et al.,* 2016; Gurau *et al.,* 2017; Martinez-Conde *et al.,* 2017; Vidholdová *et al.,* 2017; Sikora *et al.,* 2018; Jurek *et al.,* 2021; Kúdela *et al.,* 2022; Kúdela *et al.,* 2023; Chernykh *et al.,* 2024 and others). The influence of laser radiation with a CO_2 laser on the discoloration of different types of wood was analyzed: beech, oak, spruce, pine, birch, aspen, larch, lime, afromosia wood, beech veneer and others. The degree of discoloration of the wood surface depends on the amount and type of energy supplied and the absorption characteristics of the main wood components. The most frequently studied parameters were laser power, beam speed, laser beam emission mode (CW or pulse), and the number of laser scans. It was established through chemical analysis of the surface of spruce wood that discoloration is mainly due to heat-induced cleavage of C=O groups in the lignin and hemicellulose structures (Kúdela *et al.,* 2023).

Laser engraving of complex photographic images on the wood surface is a difficult task, and to optimize the result and quality of the output, it is necessary to control every aspect of the laser engraving process (Jurek *et al.,* 2021).

Most of the studies in the literature were conducted when the focus position of the laser beam focus point was located exactly on the surface of the engraving material (Figure 1A). In this case, the spot size of the focused laser beam is minimal, and the power density of the beam is maximal.

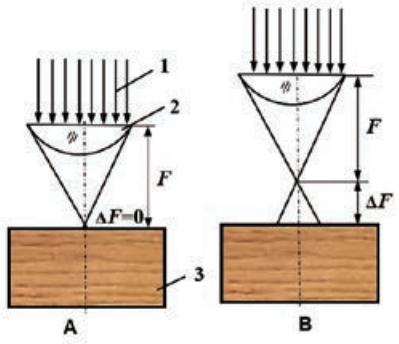

Figure 1 Position of focal plane of focusing lens on the surface (A) and above the surface (B) of the material: 1 – laser beam; 2 – focusing lens; 3 – processed material
Slika 1. Položaj žarišne ravnine fokusne leće na površini (A) i iznad površine (B) materijala: 1 – laserska zraka; 2 – fokusna leća; 3 – obrađivani materijal

The focus of the focusing lens and the position of the focal plane in relation to the workpiece surface are very important to the engraving process.

The focus position of the laser beam above the workpiece surface is considered negative ($-\Delta F$), on the surface zero ($\Delta F = 0$) and below the surface positive ($+\Delta F$).

The aim of the present work is to study the influence of CO_2 laser beam parameters, power and scanning speed at different focus positions above the surface of birch plywood samples and discoloration when engraving complex graphic images. The study is a continuation of the results obtained by the authors at the positions of the focus on the surface of the material with the same parameters of the laser beam (Gochev and Vichev, 2022; Gochev and Vichev, 2024).

2 MATERIALS AND METHODS
2. MATERIJALI I METODE

The experimental studies were carried out using a laser engraving and cutting machine of FormaTec, model K40 (China) with a power of 40 W (Figure 2).

Discoloration of the surface layer of the material was studied by varying the power of the laser beam (P, W) and scan speed (V_f, mm/s), wiht focal length of ZnSe lens, $F = 50.8$ mm. The focus position for each series of the matrix of the planned experiment was above the surface of the material: $\Delta F = -4$ mm; $\Delta F = -6$ mm and $\Delta F = -8$ mm.

Plywood samples – common birch (*Betula pendula* Roth.) with dimensions 200 mm × 200 mm × 3 mm, density $\rho = 400$ kg/m^3 and humidity $W = 6$ % were used as the research material.

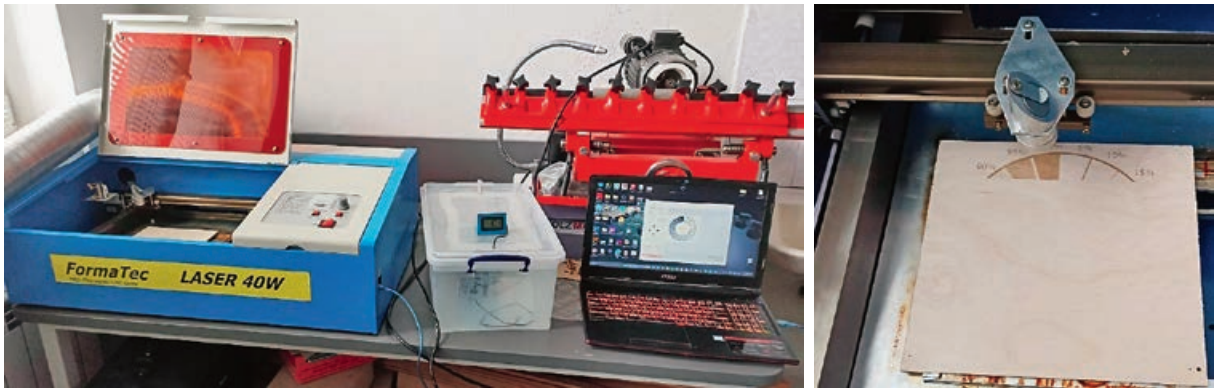

Figure 2 CO_2 laser machine for engraving and cutting
Slika 2. CO_2 laser za graviranje i rezanje

The dispersion analysis methodology was used to evaluate the results of the two-factor experiment (Vuchkov *et al.,* 1986). The regression equation for two variation factors is of the form

$$y_{pr.v.} = b_o + b_1 x_1 + b_2 x_2 + b_{11} x_1^2 + b_{22} x_2^2 + b_{12} x_1 x_2 \quad (1)$$

Where:
$y_{pr.v}$ – predicted value of output quantity,
b_o – coefficient before free member,
b_1 and b_2 – coefficients before linear member,
b_{11} and b_{22} – coefficients before non-linear equation members.

The values of the variable factors – power of the laser beam (P, W) and speed of scanning (feed rate) of the laser beam (V_f, mm/s) in explicit and coded form are given in Table 1. The matrix of the planned two-factor experiment is shown in Table 2.

To measure the difference in colors of a standard sample (without laser exposure) and on the examined sample (after exposure to a laser beam) a portable colorimeter for color difference, model LS173 (China), was used, as shown in Figure 3. The device allows measurements in two color spaces $L^*a^*b^*$ and $L^*c^*h^*$.

Table 1 Variable factor values
Tablica 1. Vrijednosti varijabilnih faktora

Variable factors *Varijabilni faktori*	**Minimum value** *Najmanja vrijednost*		**Average value** *Srednja vrijednost*		**Maximum value** *Najveća vrijednost*	
	Explicit value *Stvarna vrijednost*	Coded value *Kodirana vrijednost*	Explicit value *Stvarna vrijednost*	Coded value *Kodirana vrijednost*	Explicit value *Stvarna vrijednost*	Coded value *Kodirana vrijednost*
$X_1 = P$, W	4.0	-1	5.6	0	7.2	+1
$X_2 = V_f$, mm/s	250	-1	260	0	270	+1

Table 2 Matrix of planned two-factor experiment
Tablica 2. Matrica planiranoga dvofaktorskog eksperimenta

№ of experiment *Broj eksperimenta*	**Variable factors** / *Varijabilni faktori*			
	$X_1 = P$, W		**$X_2 = V_f$, mm/s**	
1	-1	4.0	-1	250
2	+1	7.2	-1	250
3	-1	4.0	+1	270
4	+1	7.2	+1	270
5	-1	4.0	0	260
6	+1	7.2	0	260
7	0	5.6	-1	250
8	0	5.6	+1	270
9	0	5.6	0	260
Experiments in the middle of the factor space *Eksperimenti u sredini faktorskog prostora*				
10	0	5.6	0	260
11	0	5.6	0	260
12	0	5.6	0	260

Figure 3 Colorimeter, model LS173
Slika 3. Kolorimetar, model LS173

3 RESULTS AND DISCUSSION
3. REZULTATI I RASPRAVA

The results of the studies on the changes in the discoloration of the plywood samples, according to the matrix of the planned two-factor experiment, are shown in Figures 4, 5 and 6 for different positions of the focus ΔF above the surface of the material. The arrangement of the samples was made vertically, in four rows, according to the experiment matrix of Table 2.

The difference in discoloration shades of the plywood samples is measured in a three-dimensional color model, with CIELAB (L^* a^* b^*) being used as a reference standard.

A system of isolated zones with different colors, from dark brown to light, approaching the natural color of birch plywood, was engraved on the surface of the samples. Specialized software *Inkscape* was used to conduct this research (https://wikibgbg.top/wiki/Inkscape; https://paradacreativa.es/bg/que-es-inkscape-y-como-funciona/). For each experiment from the planned matrix (Table 2), the power of the laser beam was changed from 100 % to 5 % in steps of 5 %.

To estimate the difference between two colors, the total color difference ΔE^* was used, estimated according to BDS EN ISO 11664-6:2016 and calculated by the formula

$$\Delta E^* = \sqrt{(\Delta L^*)^2 + (\Delta a^*)^2 + (\Delta b^*)^2} \qquad (2)$$

Figure 5 Results of an engraving test and changes in discoloration of birch plywood at ΔF = - 6 mm
Slika 5. Rezultati testa graviranja i promjene boje furnirske ploče od brezovine pri ΔF = - 6 mm

Figure 4 Results of an engraving test and changes in discoloration of birch plywood at ΔF = - 4 mm
Slika 4. Rezultati testa graviranja i promjene boje furnirske ploče od brezovine pri ΔF = - 4 mm

Figure 6 Results of an engraving test and changes in discoloration of birch plywood at ΔF = - 8 mm
Slika 6. Rezultati testa graviranja i promjene boje furnirske ploče od brezovine pri ΔF = - 8 mm

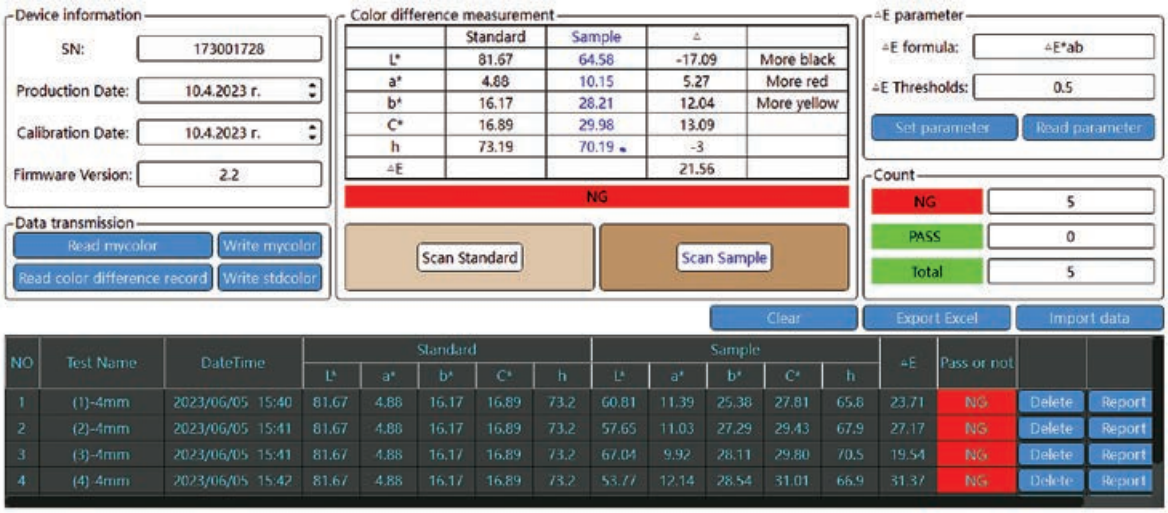

Figure 7 Results after measurement with colorimeter LS173 at ΔF = - 4 mm
Slika 7. Rezultati nakon mjerenja kolorimetrom LS173 pri ΔF = - 4 mm

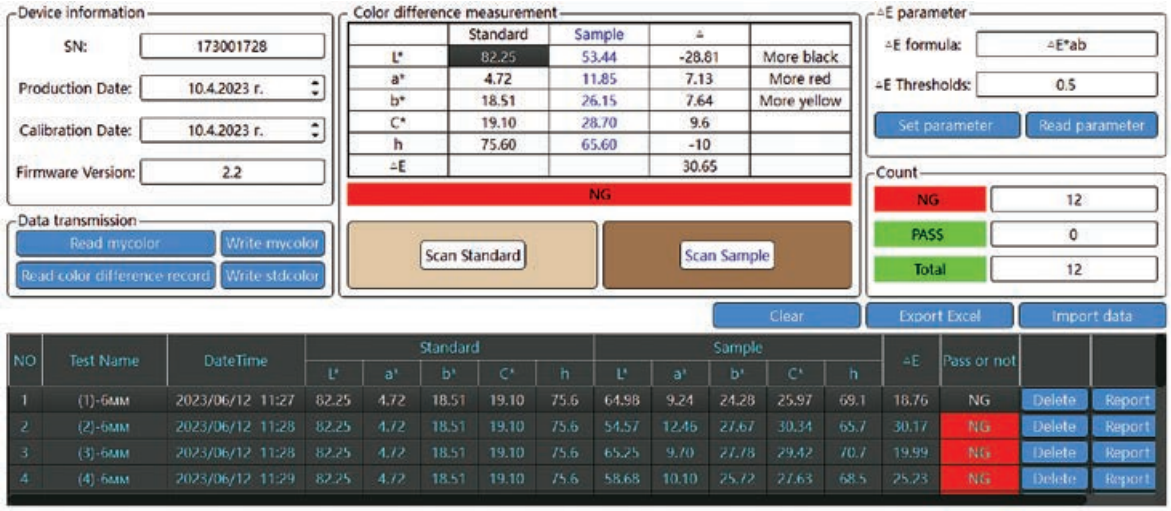

Figure 8 Results after measurement with colorimeter LS173 at ΔF = - 6 mm
Slika 8. Rezultati nakon mjerenja kolorimetrom LS173 pri ΔF = - 6 mm

Where ΔL^*, Δa^* and Δb^* are differences in individual axes (difference between values measured after laser exposure and reference sample).

The results of the measurements made using an LS173 colorimeter (Figure 3) of the changes in discoloration shades of the samples from Figures 4, 5 and 6 are represented in Figures 7, 8 and 9. Since the volume of measurements for each impact zone is very large, as seen in Figures 4, 5, and 6, only the results of the zones impacted with a 100 % power laser beam are presented here, according to the experiment matrix in Table 2.

Based on the experimental studies carried out and after mathematical processing of the data, regression equations (3); (4), and (5) were derived for ΔF = - 4 mm; ΔF = - 6 mm, and ΔF = - 8 mm using the specialized software Q-StatLab.

- Regression equation at ΔF = - 4 mm:
$$Y_1 = 23.829 + 3.683X_1 + 0.540X_2 + 2.179X_1^2 - 1.081X_2^2 + 2.092X_1X_2 \quad (3)$$
- Regression equation at ΔF = - 6 mm:
$$Y_1 = 29.772 + 4.420X_1 - 0.322X_2 + 0.829X_1^2 - 6.136X_2^2 - 1.542X_1X_2 \quad (4)$$
- Regression equation at ΔF = - 8 mm:
$$Y_1 = 35.067 + 8.343X_1 + 3.828X_2 - 1.630X_1X_1 - 3.085X_2X_2 - 4.692X_1X_2 \quad (5)$$

Where:

Y_1 – expected variation of ΔE^* indicator in coded form at corresponding focal length,

X_1 – laser beam power (P) in coded form,

X_2 – scan speed (V_f) in encoded form.

From the values of the regression coefficients of equations (3), (4) and (5), it is evident that, of the two factors investigated, the laser beam power (P) has a greater influence on the discoloration of the samples. Kubovský *et al.* (2014), Kubovský *et al.* (2021), Vidholdová *et al.* (2017) and others reached a similar conclusion for the irradiation dose (H, J/cm^2), but it depends proportionally on the laser beam power (P, W).

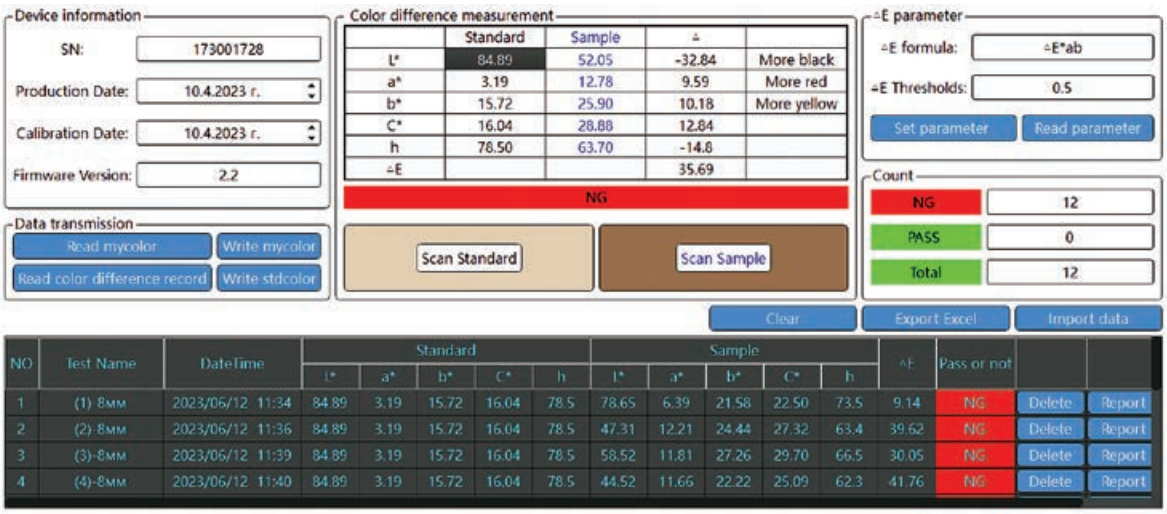

Figure 9 Results after measurement with colorimeter LS173 at ΔF = - 8 mm
Slika 9. Rezultati nakon mjerenja kolorimetrom LS173 pri ΔF = - 8 mm

Furthermore, the value of the regression coefficient b_1 increases with increasing position of the laser beam focus (ΔF) over the material being processed, indicating that the influence of the laser beam power on the variation of the total color difference ΔE^* also increases. Similar conclusions were reached by Gurau *et al.* (2017), who investigated color changes in beech wood under the interaction of a focused laser beam with a power of 5.2 W to 6.8 W.

Figures 10, 11 and 12 present graphically the variation of the total color difference ΔE^* as a function of the laser beam power (P) at different laser beam feed rates (V_f) for the three experimental focus positions above the material surface ΔF, respectively: Figure 1 – at ΔF = - 4 mm; Figure 2 – at ΔF = - 6 mm and Figure 3 – at ΔF = - 8 mm.

Through these graphs, comparisons of shades in the discoloration of plywood can be made, as the differences between them are specified with delta values.

The small value of ΔE^* means that the shades in the discoloration of the plywood are close to each other.

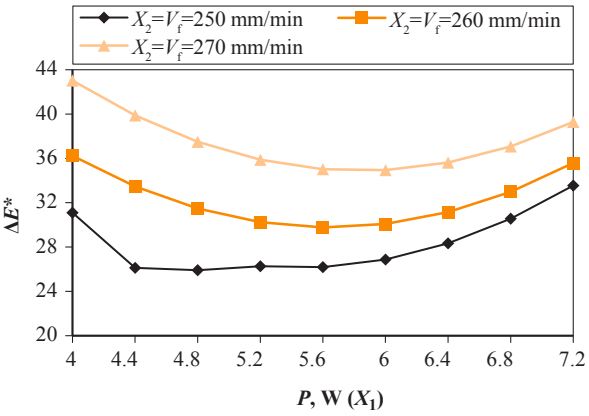

Figure 11 Variation of total color difference ΔE^* depending on laser beam power (P) at different feed rate of laser beam (V_f) and at focus position ΔF = - 6 mm
Slika 11. Varijacija ukupne razlike u boji ΔE^* ovisno o snazi laserske zrake (P) pri različitim brzinama pomicanja laserske zrake (V_f) i u položaju fokusa ΔF = - 6 mm

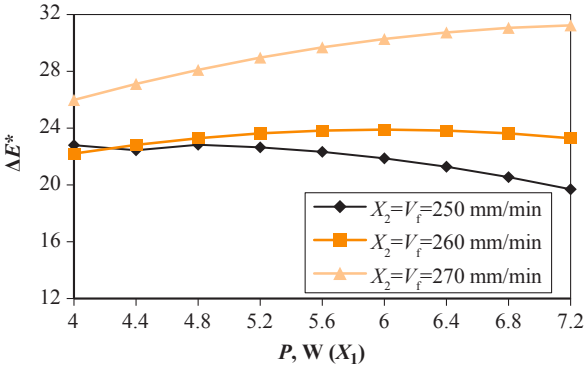

Figure 10 Variation of total color difference ΔE^* depending on laser beam power (P) at different feed rate of laser beam (V_f) and at focus position ΔF = - 4 mm
Slika 10. Varijacija ukupne razlike u boji ΔE^* ovisno o snazi laserske zrake (P) pri različitim brzinama pomicanja laserske zrake (V_f) i u položaju fokusa ΔF = - 4 mm

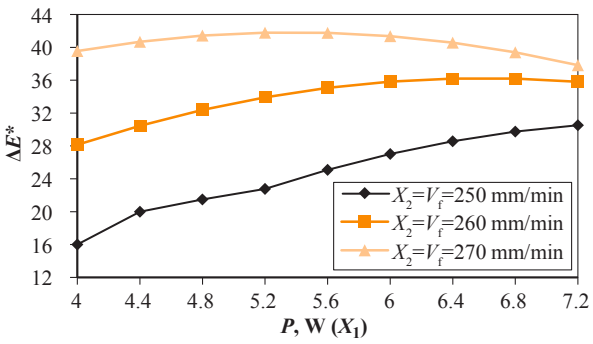

Figure 12 Variation of total color difference ΔE^* depending on laser beam power (P) at different feed rate of laser beam (V_f) and at focus position ΔF = - 8 mm
Slika 12. Varijacija ukupne razlike u boji ΔE^* ovisno o snazi laserske zrake (P) pri različitim brzinama pomicanja laserske zrake (V_f) i u položaju fokusa ΔF = - 8 mm

From the graphs in Figures 10-12, it can be clearly seen that the difference between the shades in total color difference ΔE^* in plywood discoloration is greatest at the highest feed rate of the laser beam (V_f = 270 mm/min).

At the focal position ΔF = - 4 mm, the value of the total color difference ΔE^* increased with increasing laser power (P) for the entire power interval studied at scanning speeds from 260 to 270 m/min, with a decreasing trend at 250 m/min (Figure 10).

As the position of the focus above the material surface (ΔF) increases from - 4 to - 6 mm, the value of the total color difference ΔE^* decreases with increasing laser beam power in the range from - 4 to - 6 W and starts to increase back with increasing power above 6 W (Figure 11). At the focal position ΔF = - 8 mm (Figure 12), a similar trend of the variation of the total color difference curves ΔE^* with that at ΔF = - 4 mm was observed.

Figures 13, 14 and 15 show graphically the variation of the total color difference ΔE^* depending on scanning speed (V_f) at different laser beam power (P) for the three selected focus positions ΔF: Figure 13 – at ΔF = - 4 mm; Figure 14 – at ΔF = - 6 mm; Figure 15 – at ΔF = - 8 mm.

As the scanning speed V_f increases, the total color difference ΔE^* also increases, and this is most pronounced at the focus position ΔF = - 8 mm above the material surface.

Figure 15 shows the variation of the lightness L^*, relative to the reference color (standard) depending on the position of the focus above the material surface (ΔF).

The measured L^* axis value (lightness) of the standard (reference) sample depending on the focal position ranged from 81.7 % to 84.9 % with the difference to absolute white (100 %) ranging from 18.3 % to 15.1 %. It can be seen from this figure that the resulting values for L^* of the treated samples for ΔF = - 4; - 6 and - 8 mm are close to those of the standard sample

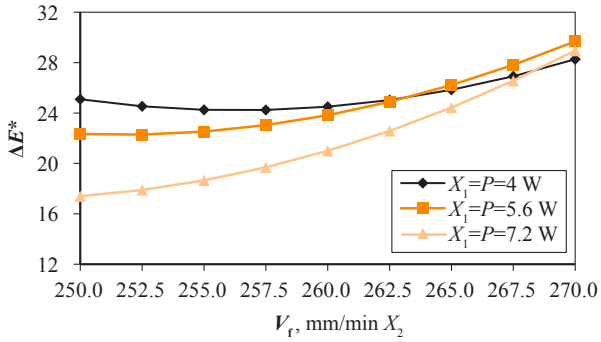

Figure 13 Variation of total color difference ΔE^* depending on laser beam feed rate (V_f) (P) and at focus position ΔF = - 4 mm

Slika 13. Varijacija ukupne razlike u boji ΔE^* ovisno o brzini pomicanja laserske zrake (V_f) pri različitim snagama laserske zrake (P) i u položaju fokusa ΔF = - 4 mm

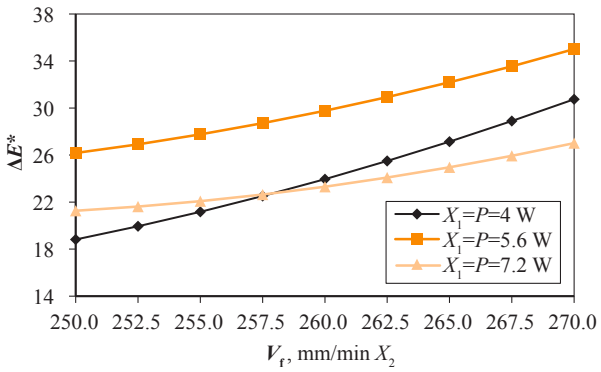

Figure 14 Variation of total color difference ΔE^* depending on laser beam feed rate (V_f) at different laser beam power (P) and at focus position ΔF = - 6 mm

Slika 14. Varijacija ukupne razlike u boji ΔE^* ovisno o brzini pomicanja laserske zrake (V_f) pri različitim snagama laserske zrake (P) i u položaju fokusa ΔF = - 6 mm

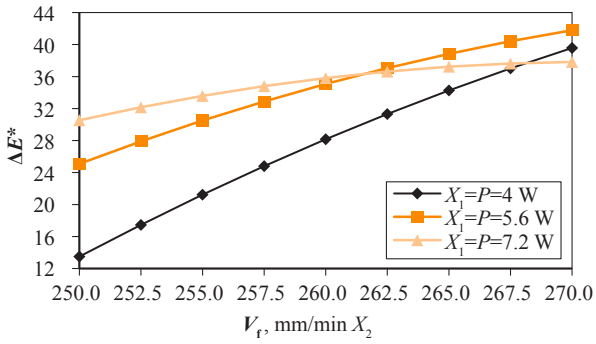

Figure 15 Variation of total color difference ΔE^* depending on laser beam feed rate (V_f) at different laser beam power (P) and at focus position ΔF = - 8 mm

Slika 15. Varijacija ukupne razlike u boji ΔE^* ovisno o brzini pomicanja laserske zrake (V_f) pri različitim snagama laserske zrake (P) i u položaju fokusa ΔF = - 8 mm

and less than 1.0, which is imperceptible to the human eye. Even if there are differences in hues based on numerical values, to the human eye they are one color and changes in hue contrast when building complex graphic images will be difficult to notice.

With increasing the laser beam power, the value of L^* decreases and the material surface becomes darker, which is consistent with Petutschnigg *et al.* (2021)

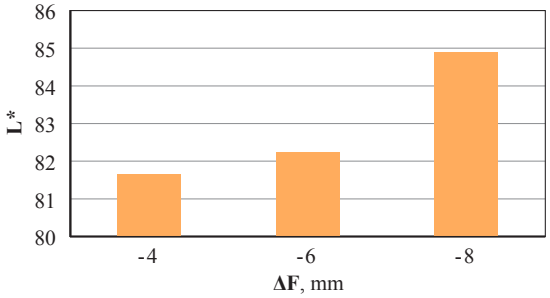

Figure 16 Variation of lightness L^* on workpiece surface depending on focus position above material surface (ΔF)

Slika 16. Varijacija svjetline L^* na površini obratka ovisno o položaju fokusa iznad površine materijala (ΔF)

and other authors. The laser beam focused on the surface of a material has a higher power density, which results in immediate sublimation and burning of the wood and its darkening to a dark brown color. The unfocused laser beam has a lower power density and acts on the material for a longer period of time, creating the conditions for the carbonization process to begin; black carbon is then formed on the surface of the wood and the shade changes to a deep black color (Jurek *et al.,* 2021). This is confirmed by the measurements made for the color change of the birch plywood surface in the L^* axis – lightness.

At ΔF = - 4 mm, ΔF = - 6 mm and ΔF = - 8 mm, the average results obtained were L^* = 64.6 (81.7 – reference sample value), L^* = 53.4 (82.2 – reference sample value) and L^* = 52.1 (84.9 – reference sample value), respectively (Figures 7, 8 and 9). As is known, L^* represents lightness from black to white on a scale of zero to 100. The average of the measured results that were obtained for L^* at the position of the beam focus on the surface for birch plywood samples (ΔF = 0 mm) were L^* = 72.18 (87.4 – reference sample value) (Gochev and Vichev, 2022).

4 CONCLUSIONS
4. ZAKLJUČAK

The study of the engraving process of wood and WBM, with a CO_2 laser beam, not only at the position of the focus on the surface of the material, but also at different positions above the surface of the engraved material, will allow to expand the diversity in the construction of complex graphic images - photography type, as well as to increase the effect in their perception by the human eye.

The presented results show the changes in discoloration of the plywood samples from the areas exposed to the laser beam at 100 % of the set power. As can be seen in Figures 4, 5 and 6, the variation in discoloration is extremely large when the laser beam power is changed from 100 % to 5 % in steps of 5 %.

This determines the necessity of in-depth research in this field in order to be able to propose the most rational regimes for engraving wood and WBM and achieve the maximum effect in the building of complex graphic images.

In order to control the engraving process when building complex graphic images, small differences or variations in the discoloration of the plywood samples must be able to be identified, i.e. it should be possible to choose the limit of acceptable difference between the color we want to achieve and its values in the actual laser engraving process.

In the future, research will be focused on changes in color shades for each impact zone in Figures 4, 5 and 6 with laser beam power other than 100 % and the development of focusing models for constructing complex photographic images.

Acknowledgements – Zahvala

We would like to thank the Research Sector of the University of Forestry, Sofia, Bulgaria, with whose support, through Contract No. NIS-B-1284/19.10.2023, this research was carried out.

5 REFERENCES
5. LITERATURA

1. Chernykh, M.; Korepanova, A.; Maksimova, E.; Sevryugin, V.; Gilfanov, M.; Stollmann, V., 2024: Selecting color of mosaic pattern elements for laser engraving on wood. Acta Facultatis Xylologiae Zvolen, 66 (2): 89-101. https://doi.org/10.17423/afx.2024.66.2.08
2. Eltawahni, H. A.; Rossini, N. S.; Dassisti, M.; Alrashed, K.; Aldaham, T. A.; Benyounis, K. Y.; Olabi, A. G., 2013: Evaluation and optimization of laser cutting parameters for plywood materials. Optics and Lasers in Engineering, 51 (9): 1029-1043. https://doi.org/10.1016/j.optlaseng.2013.02.019
3. Gochev, Z.; Vitchev, P.; Aziz, Y.; Stanev, T., 2022: Selection of modes for CO_2 laser heat treatment when engraving complex graphic images on plywood. In: Proceedings of 11th International Scientific Conference – Innovation in Woodworking industry and Engineering Design, Bulgaria, pp. 67-74.
4. Gochev, Z.; Vichev, P., 2022: Color modifications in plywood by different mode of CO_2 laser engraving. Acta Facultatis Xylologiae Zvolen, 64 (2): 77-86. https://doi.org/10.17423/afx.2022.64.2.08
5. Gochev, Z.; Vitchev, P., 2024: The effect of the focal length position of the focusing lens on the discoloration roughness of plywood under different CO_2 laser engraving modes. Acta Facultatis Xylologiae Zvolen, 66 (2): 75-87. https://doi.org/10.17423/afx.2024.66.2.06
6. Gurau, L.; Petru, A.; Varodi, A.; Timar, M., 2017: The influence of CO_2 laser beam power output and scanning speed on surface roughness and colour changes of beech (*Fagus sylvatica*). BioResources, 12 (4): 7395-7412. https://doi.org/10.15376/biores.12.4.7395-7412
7. Hernández-Castañeda, J. C.; Sezer, H. K.; Li, L., 2011: The effect of moisture content in fibre laser cutting of pine wood. Optics and Lasers in Engineering, 49 (9-10): 1139-1152. https://doi.org/10.1016/j.optlaseng.2011.05.008
8. Jurek, M.; Wagnerová, R., 2021: Laser beam calibration for wood surface colour treatment. European Journal of Wood and Wood Products, 79 (5): 1097-1107. https://doi.org/10.1007/s00107-021-01704-3
9. Kubovský, I.; Igaz, R., 2014: Utilization of CO_2 laser as an unconventional instrument to wood colour changes. Acta Facultatis Technicaes, XIX (1): 79-88.
10. Kubovský, I.; Kačík, F., 2013: Changes of the wood surface colour inducted by CO_2 laser and its durability after the xenon lamp exposure. Wood Research, 58 (4): 581-590.
11. Kubovský, I.; Kačík, F., 2014: Colour and chemical changes of the lime wood surface due to CO_2 laser thermal modification. Applied Surface Science, 321: 261-267. https://doi.org/10.1016/j.apsusc.2014.09.124
12. Kúdela, J.; Andrejko, M.; Kubovský, I., 2023: The effect of CO_2 laser engraving on the surface structure and prop-

erties of spruce wood. Coatings, 13 (12): 2006. https://doi.org/10.3390/coatings13122006
13. Kúdela, J.; Kubovský, I.; Andrejko, M., 2018: Impact of different radiation forms on beech wood discoloration. Wood Research, 63 (6): 924-934.
14. Kúdela, J.; Kubovský, I.; Andrejko, M., 2022: Influence of irradiation parameters on structure and properties of oak wood surface engraved with a CO_2 laser. Materials, 15 (23): 8384. https://doi.org/10.3390/ma15238384
15. Leone, C.; Lopresto, V.; Pagano, N.; Genna, S., 2009: Wood laser machining using CO_2 30W laser in CW and pulse regime. In: Innovative production machines and systems, p. 480.
16. Martinez-Conde, A.; Krenke, T.; Frybort, S.; Müller, U., 2017: Review: Comparative analysis of CO_2 laser and conventional sawing for cutting of lumber and wood-based materials. Wood Science and Technology, 51: 943-966. https://doi.org/10.1007/s00226-017-0914-9
17. Pagano, N.; Genna, S.; Leone, C.; Lopresto, V., 2009: Wood laser machining using CO_2 30 W laser in CW and pulse regime. In: Innovative production machines and systems, LAPT, Napoli, pp. 145-150.
18. Petutschnigg, A.; Stöckler, M.; Steinwendner, F.; Schnepps, J.; Gütler, H.; Blinzer, J.; Holzer, H.; T. Schnabel, 2013: Laser treatment of wood surfaces for ski cores: An experimental parameter study. Advances in Materials Science and Engineering, 2013: 123085. http://dx.doi.org/10.1155/2013/123085
19. Sikora, A.; Kačík, F.; Gaff, M.; Vondrová, V.; Bubeníková, T.; Kubovský, I., 2018: Impact of thermal modification on color and chemical changes of spruce and oak wood. Journal of Wood Science, 64: 406-416, https://doi.org/10.1007/s10086-018-1721-0
20. Vidholdová, Z.; Reinprecht, L.; Igaz, R., 2017: The impact of laser surface modification of beech wood on its color and occurrence of molds. BioResources, 12 (2): 4177-4186. https://doi.org/10.15376/biores.12.2.4177-4186
21. Vuchkov, I.; Stoyanov, S., 1986: Mathematical modeling and optimization of technological objects. SPH Tehnika, Sofia, p. 341 (in Bulgarian).
22. Yakimovich, B.; Chernykh, M.; Stepanova, A.; Siklienka, M., 2016: Influence of selected laser parameters on quality of images engraved on the wood. Acta Facultatis Xylologiae, 58 (2): 45-50. https://doi.org/10.17423/afx.2016.58.2.05
23. ***BDS EN ISO 11664-6, 2016: Colorimetry. Part 6: CIEDE2000 colour-difference formula (in Bulgarian).
24. ***https://wikibgbg.top/wiki/Inkscape (Accessed Nov. 30, 2023).
25. ***https://paradacreativa.es/bg/que-es-inkscape-y-como-funciona/ (Accessed Nov. 30, 2023).

Corresponding address:

ZHIVKO GOCHEV
University of Forestry, 10 Kliment Ohridski Blvd., 1797 Sofia, BULGARIA, e-mail: zhivkog@ltu.bg

Hüseyin Peker[1], Ümit Ayata*[2]

Testing of Bleaching Application on Kingwood (*Dalbergia cearensis* Ducke) Wood

Analiza primjene izbjeljivanja na drvu *kingwooda* (*Dalbergia cearensis* Ducke)

ORIGINAL SCIENTIFIC PAPER
Izvorni znanstveni rad
Received – prispjelo: 2. 3. 2024.
Accepted – prihvaćeno: 18. 11. 2024.
UDK: 630*83; 674.07
https://doi.org/10.5552/drvind.2025.0200

ABSTRACT • *In this study, surface changes (whiteness index: WI*, color parameters, and glossiness properties) occurring after bleaching with oxalic acid ($C_2H_2O_4$) and hydrogen peroxide (H_2O_2) + sodium hydroxide (NaOH) chemicals in kingwood (Dalbergia cearensis Ducke) wood, used for high-quality applications such as quality turning, marquetry, furniture, inlay work, musical instruments, and decorative items, were investigated. The ΔE* values were determined as 5.46 for the single component and 8.69 for the double component. Decreases in L* and h^o parameters were obtained by the action of the $C_2H_2O_4$ chemical, while increases were observed in the a*, C*, and b* parameters. Additionally, the use of H_2O_2 + NaOH chemicals in the bleaching process resulted in increases in L*, b*, C*, and h^o values, with a decrease noted in the a* parameter. Observations revealed reductions in glossiness values at 60 and 85 degrees when employing two distinct bleaching agents in both orientations. It can be said that the bleaching agents used in the study exert varying effects as modifiers on the surface of wooden materials.*

KEYWORDS: *kingwood; whiteness index; color; Dalbergia cearensis Ducke; bleaching; glossiness*

SAŽETAK • *U radu se istražuju površinske promjene (indeks bjeline WI*, parametri boje i sjaj) drva kingwooda (Dalbergia cearensis Ducke) nakon izbjeljivanja oksalnom kiselinom ($C_2H_2O_4$) i vodikovim peroksidom (H_2O_2) + natrijevim hidroksidom (NaOH). Drvo kingwooda upotrebljava se za izradu proizvoda visoke kvalitete kao što su tokareni elementi, intarzije, namještaj, glazbala i ukrasni predmeti. Nakon primjene jednokomponentnog sredstva za izbjeljivanje na površini drva dobivena je vrijednost ΔE* od 5,46, a nakon primjene dvokomponentnog sredstva vrijednost 8,69. Smanjenje parametara L* i h^o postignuto je djelovanjem kemikalije $C_2H_2O_4$, a istodobno je uočeno povećanje parametara a*, C* i b*. Nadalje, primjena kemikalija H_2O_2 + NaOH u procesu izbjeljivanja rezultirala je povećanjem parametara L*, b*, C* i h^o te smanjenjem parametra a*. Pri mjerenju paralelno i okomito na vlakanca drva nakon primjene obaju sredstava za izbjeljivanje rezultati su pokazali smanjenje vrijednosti sjaja pri kutu od 60 i 85°. Može se reći da sredstva za izbjeljivanje primijenjena u istraživanju imaju različite učinke kao sredstva za modifikaciju površine drva.*

KLJUČNE RIJEČI: *drvo kingwooda; indeks bjeline; boja; Dalbergia cearensis Ducke; izbjeljivanje; sjaj*

* Corresponding author
[1] Author is researcher at Artvin Çoruh University, Faculty of Forestry, Department of Forest Industrial Engineering, Artvin, Turkey. https://orcid.org/0000-0002-7771-6993
[2] Author is researcher at Bayburt University, Faculty of Arts and Design, Department of Interior Architecture and Environmental Design, Bayburt, Turkey. https://orcid.org/0000-0002-6787-7822.

1 INTRODUCTION
1. UVOD

Sodium hypochlorite bleach, often known by the brand name clorox, is widely available as a household bleach. It is considered a gentle bleaching agent and typically lightens the color of most woods by a few shades, though oak may experience a slight darkening. Nonetheless, it does not completely remove this coloration. When applied to colors stemming from water stains, sodium hypochlorite tends to be effective, yet it is less so on earthy tones and certain organic pigments (Zeilman, 1960).

Inadequate peroxide levels left in the bleaching process may cause a decrease in fiber brightness, while an excessive amount escalates the expenses associated with the bleaching agent, peroxide. Hence, closely monitoring the peroxide concentration is of utmost importance in wood fiber bleaching procedures (Chai *et al*., 2004).

In the literature, it is observed that bleaching applications are carried out on various tree species: bamboo (Nguyen *et al*., 2019), movingui (Peker *et al*., 2023b), lotofa (Peker, 2023b), canelo (Peker, 2023a), birch (Mononen *et al*., 2005), lime (Çamlıbel and Ayata, 2023a), maritime pine (Mehats *et al*., 2021), olon (Peker and Ayata, 2023), birch (Liu *et al*., 2015), bulletwood (Peker *et al*., 2023a), ayous, linden, poplar (Lu *et al*., 2023), izombé (Peker *et al*., 2023c), oak, birch, Norway maple, European larch (Möttönen *et al*., 2003), balau red (Shorea guiso) (Peker *et al*., 2024), satinwood ceylon (Ayata and Çamlıbel, 2023), ilomba (Ayata and Bal, 2023), black locust (Peker and Ulusoy, 2023), birch (Yamamoto *et al*., 2017), and ekop (Çamlıbel and Ayata, 2023b).

Information regarding color changes obtained using various bleaching chemicals has been provided in the above studies. While some surface changes resulting from bleaching applications have been identified, it has been noted that there are no records of bleaching applications being conducted on kingwood (*Dalbergia cearensis* Ducke) wood in the literature.

Here is further information about this tree species: kingwood (*Dalbergia cearensis* Ducke), also known as jacarandá-violet, miolo-de-negro, pau-violeta, or simply violet, is a distinctive species native to the caatinga region stretching from Ceará to the southern parts of Piauí and Bahia. It thrives in areas with dense tree cover, typically found in the foothills and hinterlands where deep soils and favorable microclimates support the growth of lush vegetation (Carvalho, 1997). Notably, kingwood is renowned for its epigeal germination of seeds, particularly in semi-arid regions where surface temperature fluctuations influence germination proximity to or on the soil surface (Gutierrez *et al*., 1988).

The distinctive samaras, characterized by flattened and undivided structures, disperse gradually throughout the year after detachment from compact axillary clusters. This distribution pattern is considered an evolutionary adaptation that reduces predation pressure, thereby enhancing the chances of successful germination and reproduction (Wheelwright, 1985).

As a deciduous species, kingwood can reach heights of 5-8 meters, featuring wood with a specific gravity of 1.01 g/cm^3. Lacking water storage structures in its trunk or roots, the tree sheds its leaves at the onset of the dry season. Leaves typically persist for four to six months, regenerating with new foliage and flowers at the onset of the rainy season, coinciding with fruit maturation (Lorenzi, 2009). With a high seed germination rate of 70 %, seeds of kingwood exhibit phanero-epigeal-storage germination, sprouting seedlings within three days after planting (Nogueira *et al*., 2010).

It dries quickly, and care must be taken to avoid excessive checking and splitting. The material is dried without deterioration (Lincoln, 1986). The wood has a slightly aromatic odor and, when fresh, has brown-light purple stripes at regular intervals (Didier, 1992). It works well with both hand and machine tools, with a moderate blunting effect on cutting edges. Maintaining sharp cutting edges can achieve a very smooth surface. Nails and screws hold well, and the wood can provide a thin, natural waxy surface. The timber is durable and highly resistant to protective treatments. Today, it is mainly used in veneer and marquetry as sliced veneer for plywood and in solid form for inlays, turning, and various decorative items (Lincoln, 1986).

Another source describes the wood as having "brown-purple and black or black-purple, alternating concentric layers. It is finely striped and has a pleasant smell. Fine-textured; irregular grain; heavy; hard; extremely durable; takes a high, waxy, natural polish. It is a highly valuable timber, available only in small sizes and used for high-quality applications such as fine furniture, marquetry, musical instruments, inlay work, turning, and fancy articles" (Uphof, 1959). The calorific value of kingwood wood is 4,327 kcal/kg, volatile matter is 87.86 %, ash is 0.26 %, and fixed carbon is 11.87 % (Oliveira *et al*., 2019).

This study investigates the surface changes occurring after bleaching applications on kingwood (*Dalbergia cearensis* Ducke) wood.

2 MATERIALS AND METHODS
2. MATERIJALI I METODE

2.1 Material
2.1. Materijal

2.1.1 Wood material
2.1.1. Drvni materijal

Climate conditioning was applied to test samples of kingwood (*Dalbergia cearensis* Ducke) with dimen-

sions of 100 mm × 100 mm × 18 mm at (20±2) °C and 65 % relative humidity (ISO 554, 1976).

2.1.2 Bleaching chemicals
2.1.2. Kemikalije za izbjeljivanje

Oxalic acid ($C_2H_2O_4$) and hydrogen peroxide (H_2O_2) + sodium hydroxide (NaOH) (in a ratio of 2:1) chemicals were used in the study.

2.2 Methods
2.2. Metode

2.2.1 Application of bleaching
2.2.1. Nanošenje sredstva za izbjeljivanje

The chemicals were applied to the wood material surfaces using the brushing technique.

2.2.2 Tests
2.2.2. Ispitivanja

The Shore D hardness value was determined according to ASTM D 2240, (2010) using a shore hardness testing device (Model Ld-J Loyka, Durometer: Shenzhen Yibai Network Technology Co., Ltd., China) with a 5 kg load applied. Ten measurements were taken. Glossiness tests were conducted at three different angles (20°, 60°, and 85°) perpendicular and parallel to the fibers (ISO 2813, 1994) using an ETB-0833 model gloss meter device, shore D hardness value was measured using a shore meter device (ASTM D 2240, 2010), whiteness index (*WI**) values were measured perpendicular and parallel to the fibers using a whiteness meter BDY-1 device (ASTM E313-15e1, 2015), and color properties were measured using a CS-10 device (ASTM D 2244-3, 2007).

In the literature, ΔC^* is defined as chroma difference or saturation difference and ΔH^* as hue difference or shade difference. Definitions for other parameters are provided in Table 1 (Lange, 1999), and comparison criteria for visual assessment of color difference (ΔE^*) are given in Table 2 (Barański *et al*., 2017).

Total color differences were determined using the following formulas:

$$\Delta a^* = [a^*_{\text{bleached}}] - [a^*_{\text{control}}] \quad (1)$$

$$\Delta C^* = [C^*_{\text{bleached}}] - [C^*_{\text{control}}] \quad (2)$$

$$\Delta L^* = [L^*_{\text{bleached}}] - [L^*_{\text{control}}] \quad (3)$$

$$\Delta b^* = [b^*_{\text{bleached}}] - [b^*_{\text{control}}] \quad (4)$$

$$\Delta H^* = [(\Delta E^*)^2 - (\Delta L^*)^2 - (\Delta C^*)^2]^{1/2} \quad (5)$$

$$\Delta E^* = [(\Delta L^*)^2 + (\Delta b^*)^2 + (\Delta a^*)^2]^{1/2} \quad (6)$$

$$C^* = [(a^*)^2 + (b^*)^2]^{1/2} \quad (7)$$

$$h^o = \arctan [b^*/a^*] \quad (8)$$

Δa^*: positive values of Δa^* indicate a shift towards a more pronounced red tone compared to the reference, while negative values suggest a shift towards a greener hue. ΔH^*: reflects changes in the hue angle or tint. ΔC^*: positive values of ΔC^* signify an increase in chroma or saturation, resulting in a more vibrant and luminous appearance compared to the reference. Conversely, negative values indicate a decrease in chroma or saturation, leading to a reduction in vibrancy and distinctiveness relative to the reference. ΔL^*: when ΔL^* values are positive, they indicate a shift towards a lighter color compared to the reference, while negative values suggest a shift towards a darker color. Δb^*: positive values of Δb^* indicate an increase in yellowness compared to the reference, while negative values suggest an increase in blueness (Lange, 1999).

2.3 Statistical analysis
2.3. Statistička analiza

Maximum and minimum values, standard deviations, homogeneity groups, means, variance analyses, and percentage (%) change rates were determined using a statistical program.

Table 1 Color change criteria by Barański *et al*. (2017)
Tablica 1. Kriteriji promjene boje prema Barański *et al*. (2017.)

Color change criteria / *Kriteriji promjene boje*	**ΔE^* value** *ΔE^* vrijednost*
Invisible color change / *promjena boje koja nije vidljiva*	$\Delta E^* < 0.2$
Slight change of color / *blaga promjena boje*	$2 > \Delta E^* > 0.2$
Color change visible in high filter / *promjena boje vidljiva uz kvalitetan filtar*	$3 > \Delta E^* > 2$
Color change visible with average quality of filter / *promjena boje vidljiva uz filtar prosječne kvalitete*	$6 > \Delta E^* > 3$
High color change / *izrazita promjena boje*	$12 > \Delta E^* > 6$
Different color / *različita boja*	$\Delta E^* > 12$

Table 2 Results of shore D hardness value determined in kingwood wood
Tablica 2. Rezultati Shore D tvrdoće drva *kingwood*

Number of measurements *Broj mjerenja*	**Mean (HD)** *Srednja vrijednost (HD)*	**Standard deviation** *Standardna devijacija*	**Minimum**	**Maximum**	**Coefficient of variation** *Koeficijent varijacije*
10	78.70	2.16	75.00	81.00	2.75

3 RESULTS AND DISCUSSION
3. REZULTATI I RASPRAVA

The result for the shore D hardness value determined on the kingwood specimen is given in Table 3. According to the determined result, the shore D hardness value for kingwood wood is 78.70 HD, ranging between 75.00 and 81.00 HD (Table 2).

The results for total color differences are shown in Table 3. The ΔE^* values were found to be 5.46 for the single component and 8.69 for the double component. The ΔL^* values were determined to be negative (darker than the reference) in the single component and positive (lighter than the reference) in the double component. Δa^* values were negative (greener than the reference) in the double component and positive (redder than the reference) in the single component (Table 3).

After the application of both bleaching chemicals, Δb^* (more yellow than the reference) and ΔC^* (clearer, brighter than the reference) values were obtained in the positive direction. Comparing the values obtained in this study with the color change criteria (Barański *et al.* 2017), it was determined that the single-component bleaching agent falls into the "color change visible with average quality of filter ($6>\Delta E^*>3$)" category, while the double-component chemical falls into the "high color change ($12>\Delta E^*> 6$)" category (Table 3).

The color differences (ΔE^*) for various wood species after being bleached using the Wood-Brite method with a 35 % hydrogen peroxide solution were as follows: teak (*Tectona grandis*) had a ΔE^* of 4.63, oak (*Quercus robur*) had a ΔE^* of 7.73, birch (*Betula pendula*) had a ΔE^* of 3.06, Norway maple (*Acer platanoides*) had a ΔE^* of 2.49, and European larch (*Picea abies*) had a ΔE^* of 1.03 (Möttönen *et al*., 2003).

All test results data are provided in Table 5. The double-component chemical yielded the highest L^* value (48.53), in contrast with the single-component chemical, which showed the lowest value (38.17). While the L^* parameter decreased by 10.31 % in the single-component chemical, it increased by 14.03 % in the double-component chemical (Table 5). In the literature, decreases with the application of $C_2H_2O_4$ and increases with H_2O_2 + NaOH were observed in Satinwood Ceylon (Ayata and Çamlıbel, 2023), balau red (Shorea guiso) (Peker *et al*., 2024), ekop (Çamlıbel and Ayata, 2023b), lime (Çamlıbel and Ayata, 2023a), and Izombé (Peker *et al*., 2023c) wood species.

The lowest a^* value (1.68) was recorded in the double-component chemical, whereas the highest value (8.39) was obtained in the single-component chemical. In the a^* test, there was a 28.68 % increase in the single-component chemical, whereas a notable decrease of 74.23 % was noted in the double-component chemical (Table 5). In the literature, increases in the a^* parameter due to $C_2H_2O_4$ application and decreases due to H_2O_2 + NaOH application have been reported in various wood types such as bulletwood (Peker *et al*., 2023a), movingui (Peker *et al*., 2023b), Satinwood ceylon (Ayata and Çamlıbel, 2023), ilomba (Ayata and Bal, 2023), olon (Peker and Ayata, 2023), canelo (Peker, 2023a), lotofa (Peker, 2023b), black locust (Peker and Ulusoy, 2023), lime (Çamlıbel and Ayata, 2023a), ekop (Çamlıbel and Ayata, 2023b), and izombé (Peker *et al*., 2023c).

The double-component chemical exhibited the highest b^* parameter value (14.59), whereas the lowest value was observed in the control experimental group samples (10.52). The b^* value increased by 25.29 % with the single-component chemical and by 38.69 % with the double-component chemical (Table 5). Increases in the b^* parameter have been identified with oxalic acid application and H_2O_2 + NaOH treatments in wood types such as ekop (Çamlıbel and Ayata, 2023b), izombé (Peker *et al*., 2023c), canelo (Peker, 2023a), bulletwood (Peker *et al*., 2023a), and movingui (Peker *et al*., 2023b).

In the C^* test, the single-component chemical yielded the highest result (15.3), while the control samples had the lowest (12.38). Both the single and double-component chemicals showed increases in the C^* value (26.25 % and 18.66 %, respectively), with an overall increase of 25.29 % (Table 6). Increases in the C^* parameter were observed with the application of $C_2H_2O_4$ and H_2O_2 + NaOH chemicals in wood types such as izombé (Peker *et al*., 2023c), ekop (Çamlıbel and Ayata, 2023b), bulletwood (Peker *et al*., 2023a), movingui (Peker *et al*., 2023b), and canelo (Peker, 2023a).

The highest h^o parameter value (83.42) was observed in the double-component chemical, whereas the lowest (57.48) was found in the single-component chemical. A decrease of 1.32 % was observed in the h^o

Table 3 Results of total color differences
Tablica 3. Rezultati ukupne promjene boje

Treatment / *Tretman*	ΔL^*	Δa^*	Δb^*	ΔC^*	ΔH^*	ΔE^*	**Color change criteria** / *Kriteriji promjene boje* (Barański *et al*., 2017)
Single-component chemical *jednokomponentna kemikalija*	-4.39	1.88	2.66	3.26	0.10	5.46	Color change visible with average quality of filter *promjena boje vidljiva uz filtar prosječne kvalitete* ($6 > \Delta E^* > 3$)
Double-component chemical *dvokomponentna kemikalija*	5.97	-4.84	4.07	2.31	5.88	8.69	High color change / *izrazita promjena boje* ($12 > \Delta E^* > 6$)

value with the single-component chemical, while the double-component chemical exhibited a significant increase of 43.21 % (Table 4). In the *h*° values, decreases with the use of oxalic acid for bleaching purposes and increases with the use of H_2O_2 + NaOH chemicals were achieved in wood types such as bulletwood (Peker *et al*., 2023a) and lime (Çamlıbel and Ayata, 2023a).

Decreases in the *WI** values measured in both directions were observed with the single component (⊥: 25.91 % and ||: 21.68 %) and increases were determined with the double component (⊥: 35.17 % and ||: 78.67 %). The highest results for *WI** values in both directions were found with the application of the double-component chemical (⊥: 12.26 and ||: 10.22), while the lowest results were obtained with the application of the single-component chemical to wooden surfaces (⊥: 6.72 and ||: 4.48) (Table 4).

It was observed that decreases in glossiness values were achieved at 60 and 85 degrees by using two different bleaching chemicals in both directions. When both chemicals were applied to wooden surfaces, no change in glossiness values perpendicular to the fibers was observed at 20 degrees. However, different outcomes were exhibited parallel to the fibers (an increase

Table 4 Measurement results for all tests
Tablica 4. Rezultati svih ispitivanja

Test	Treatment *Tretman*	*N*	Mean *Srednja vrijednost*	Change ratio, % *Stupanj promjene, %*	Homogeneity group *Homogenost grupe*	Standard Deviation *Standardna devijacija*	Min.	Max.	COV
*L**	Control	10	42.56	-	B	1.14	40.79	44.00	2.68
	Single Component	10	38.17	↓10.31	C**	1.12	35.74	39.31	2.95
	Double Component	10	48.53	↑14.03	A*	0.88	47.45	49.89	1.81
*a**	Control	10	6.52	-	B	0.49	5.72	7.07	7.48
	Single Component	10	8.39	↑28.68	A*	0.45	7.50	8.92	5.31
	Double Component	10	1.68	↓74.23	C**	0.37	1.15	2.28	21.78
*b**	Control	10	10.52	-	C**	0.50	9.58	11.15	4.75
	Single Component	10	13.18	↑25.29	B	0.90	11.18	14.02	6.84
	Double Component	10	14.59	↑38.69	A*	0.78	13.10	15.42	5.38
*C**	Control	10	12.38	-	C**	0.67	11.19	13.19	5.40
	Single Component	10	15.63	↑26.25	A*	0.99	13.47	16.46	6.34
	Double Component	10	14.69	↑18.66	B	0.80	13.15	15.56	5.46
h°	Control	10	58.25	-	B	0.92	56.83	59.50	1.58
	Single Component	10	57.48	↓1.32	B**	0.63	56.14	58.39	1.10
	Double Component	10	83.42	↑43.21	A*	1.28	81.30	85.15	1.53
⊥20°	Control	10	0.10	-	A	0.00	0.10	0.10	0.00
	Single Component	10	0.10	0.00	A	0.00	0.10	0.10	0.00
	Double Component	10	0.10	0.00	A	0.00	0.10	0.10	0.00
⊥60°	Control	10	0.76	-	A*	0.08	0.60	0.80	11.10
	Single-Component	10	0.25	↓67.11	C**	0.05	0.20	0.30	21.08
	Double Component	10	0.59	↓22.37	B	0.09	0.50	0.70	14.84
⊥85°	Control	10	0.20	-	A*	0.09	0.10	0.30	47.14
	Single Component	10	0.10	↓50.00	B**	0.00	0.10	0.10	0.00
	Double Component	10	0.10	↓50.00	B**	0.00	0.10	0.10	0.00
||20°	Control	10	0.12	-	A	0.04	0.10	0.20	35.14
	Single Component	10	0.13	↑8.33	A*	0.05	0.10	0.20	37.16
	Double Component	10	0.10	↓16.67	A**	0.00	0.10	0.10	0.00
||60°	Control	10	1.22	-	A*	0.08	1.10	1.30	6.47
	Single Component	10	0.97	↓20.49	B	0.32	0.60	1.40	32.62
	Double Component	10	0.83	↓31.97	B**	0.05	0.80	0.90	5.82
||85°	Control	10	1.16	-	A*	0.25	0.80	1.50	21.96
	Single Component	10	0.10	↓91.38	B**	0.00	0.10	0.10	0.00
	Double Component	10	0.10	↓91.38	B**	0.00	0.10	0.10	0.00
*WI** (⊥)	Control	10	9.07	-	B	0.05	9.00	9.10	0.53
	Single Component	10	6.72	↓25.91	C**	0.12	6.60	6.90	1.83
	Double Component	10	12.26	↑35.17	A*	0.36	11.90	12.80	2.91
*WI** (||)	Control	10	5.72	-	B	0.20	5.50	6.00	3.57
	Single Component	10	4.48	↓21.68	C**	0.18	4.20	4.70	4.05
	Double Component	10	10.22	↑78.67	A*	0.41	9.70	10.70	3.99

*Highest value, **Lowest value, *N* – Number of measurements, COV – Coefficient of variation / **najviša vrijednost, **najniža vrijednost, N – broj mjerenja, COV – koeficijent varijacije*

Table 5 Multivariate analysis of variance results
Tablica 5. Rezultati multivarijantne analize varijance

Test	**Sum of squares** *Zbroj kvadrata*	***df***	**Mean square** *Srednji kvadrat*	***F***	**Sig.**	$\alpha \leq 0.05$
Bleaching chemical type / *Vrsta sredstva za izbjeljivanje*	Lightness (L^*)	539.871	2	269.936	242.390	0.000*
	Red (a^*) color tone	239.780	2	119.890	630.287	0.000*
	Yellow (b^*) color tone	85.336	2	42.668	76.240	0.000*
	Chroma (C^*)	56.099	2	28.049	40.617	0.000*
	Hue (h^o) angle	4357.468	2	2178.734	2270.000	0.000*
	Glossiness at ⊥20°	0.000	2	0.000	.	.**
	Glossiness at ⊥60°	1.349	2	0.674	115.234	0.000*
	Glossiness at ⊥85°	0.067	2	0.033	11.250	0.000*
	Glossiness at ‖20°	0.005	2	0.002	1.703	0.201**
	Glossiness at ‖60°	0.781	2	0.390	10.776	0.000*
	Glossiness at ‖85°	7.491	2	3.745	173.158	0.000*
	*WI** perpendicular (⊥)	154.634	2	77.317	1604.580	0.000*
	*WI** parallel (‖)	182.451	2	91.225	1136.109	0.000*
Error / *Pogreška*	Lightness (L^*)	30.068	27	1.114		
	Red (a^*) color tone	5.136	27	0.190		
	Yellow (b^*) color tone	15.111	27	0.560		
	Chroma (C^*)	18.646	27	0.691		
	Hue (h^o) angle	25.914	27	0.960		
	Glossiness at ⊥20°	0.000	27	0.000		
	Glossiness at ⊥60°	0.158	27	0.006		
	Glossiness at ⊥85°	0.080	27	0.003		
	Glossiness at ‖20°	0.037	27	0.001		
	Glossiness at ‖60°	0.978	27	0.036		
	Glossiness at ‖85°	0.584	27	0.022		
	*WI** perpendicular (⊥)	1.301	27	0.048		
	*WI** parallel (‖)	2.168	27	0.080		
Total / *Ukupno*	Lightness (L^*)	56262.903	30			
	Red (a^*) color tone	1162.896	30			
	Yellow (b^*) color tone	4986.506	30			
	Chroma (C^*)	6150.955	30			
	Hue (h^o) angle	136587.118	30			
	Glossiness at ⊥20°	0.300	30			
	Glossiness at ⊥60°	10.040	30			
	Glossiness at ⊥85°	0.680	30			
	Glossiness at ‖20°	0.450	30			
	Glossiness at ‖60°	32.160	30			
	Glossiness at ‖85°	14.240	30			
	*WI** perpendicular (⊥)	2778.610	30			
	*WI** parallel (‖)	1574.540	30			
Corrected total / *Ukupno nakon ispravka*	Lightness (L^*)	569.940	29			
	Red (a^*) color tone	244.916	29			
	Yellow (b^*) color tone	100.446	29			
	Chroma (C^*)	74.744	29			
	Hue (h^o) angle	4383.382	29			
	Glossiness at ⊥20°	0.000	29			
	Glossiness at ⊥60°	1.507	29			
	Glossiness at ⊥85°	0.147	29			
	Glossiness at ‖20°	0.042	29			
	Glossiness at ‖60°	1.759	29			
	Glossiness at ‖85°	8.075	29			
	*WI** perpendicular (⊥)	155.935	29			
	*WI** parallel (‖)	184.619	29			

*Significant, **Insignificant / **značajno, **nije značajno*

of 8.33 % with the single component and a decrease of 16.67 % with the double component). At 60 and 85 degrees, the control experimental group samples exhibited the highest results in both directions (Table 4).

The results of the analysis of variance are presented in Table 5. When these results were examined, the type of bleaching chemical was found to be statistically significant across all tests (Table 5).

4 CONCLUSIONS
4. ZAKLJUČAK

A reduction in *WI** values was noted in both orientations with the single component, whereas an increase was observed with the double component. The application of the double-component chemical yielded the highest *WI** values in both orientations, while the lowest values were recorded when using the single-component chemical on wooden surfaces.

The ΔE^* values were calculated as 5.46 for the single component and 8.69 for the double component.

The $C_2H_2O_4$ chemical led to reductions in the L^* and h^o parameters, accompanied by increases in the a^*, C^*, and b^* parameters. Furthermore, the application of H_2O_2 + NaOH chemicals during bleaching resulted in increases in L^*, b^*, C^*, and h^o values, while a decrease was observed in the a^* parameter.

It was observed that employing two distinct bleaching agents in both orientations resulted in reductions in glossiness values at 60 and 85 degrees.

It is recommended to conduct experiments related to natural or artificial aging tests on the bleached materials obtained.

5 REFERENCES
5. LITERATURA

1. Ayata, Ü.; Bal, B. C., 2023: Effect of application of various bleaching chemicals on some surface properties of ilomba (*Pycnanthus angolensis* Exell) wood. In: Proceedings of 2nd International Conference on Health, Engineering and Applied Sciences, August 4-6, Belgrade, pp. 95-105.
2. Ayata, Ü.; Çamlıbel, Ç., 2023: A study on the application of bleaching treatment on Satinwood ceylon (*Chloroxylon swietenia* DC) wood used indoors and outdoors. The Journal of Graduate School of Natural and Applied Sciences of Mehmet Akif Ersoy University, 14 (2): 273-281. https://doi.org/10.29048/makufebed.1343434
3. Barański, J.; Klement, I.; Vilkovská, T.; Konopka, A., 2017: High temperature drying process of beech wood (*Fagus sylvatica* L.) with different zones of sapwood and red false heartwood. BioResources, 12 (1): 1861-1870. https://doi.org/10.15376/biores.12.1.1861-1870
4. Çamlıbel, O.; Ayata, Ü., 2023a: The bleaching application on linden wood (*Tilia tomentosa* - Moench.). In: Proceedings of 2nd International Conference on Applied Sciences, October 20-22, Manila, pp. 107-116.
5. Çamlıbel, O.; Ayata, Ü., 2023b: Application of wood bleaching chemicals on ekop wood (*Tetraberlinia bifoliolata* Haum.). In: Proceedings of International Conference on Applied Sciences, October 20-22, 2023, pp. 125-135.
6. Carvalho, A. M. A., 1997: Synopsis of the genus *Dalbergia* (Fabaceae, Dalbergieae) in Brazil. Brittonia, 49 (1): 87-109.
7. Chai, X. S.; Hou, Q. X.; Luo, Q.; Zhu, J. Y., 2004: Rapid determination of hydrogen peroxide in the wood pulp bleaching streams by a dual-wavelength spectroscopic method. Analytica Chimica Acta, 507 (2): 281-284. https://doi.org/10.1016/j.aca.2003.11.036
8. de With, G., 2018: Polymer Coatings: A Guide to Chemistry, Characterization, and Selected Spplication. Wiley-Vch.
9. Didier, N., 1992: Le commerce des bois d'Am´erique tropicale. In: Cahiers d'outre-mer, N◦179-180 – 45e ann´ee, Juillet/d´ecembre 1992. Les plantes am´ericaines` a la conqu^ete du monde, pp. 249-261. https://doi.org/10.3406/caoum.1992.3443
10. Gama, J. R. V.; Pinheiro, J. C., 2010: Inventário florestal para adequação ambiental da fazenda Santa Rita, município de Santarém. Estado do Pará. Floresta, 40 (3): 585-592. http://dx.doi.org/10.5380/rf.v40i3.18920
11. Gutierrez, J. R.; Aguilera, L. E.; Moreno, R. J., 1988: The effects of variable regimes of temperature and light on the germination of *Atriplex repanda* seeds in the semi-arid region of Chile. Revista Chilena de Historia Natural, 61: 61-65.
12. Huxley, A.; Griffiths, M., 1992: Dictionary of gardening (vol. 3). Macmillan Press.
13. Lange, D. R., 1999: Fundamentals of Colourimetry – Application Report No. 10e. DR Lange: New York, NY, USA.
14. Lincoln, W. A., 1986: World wood in colour. Stobart.
15. Liu, Y.; Guo, H.; Gao, J.; Zhang, F.; Shao, L.; Via, B. K., 2015: Effect of bleach pretreatment on surface discoloration of dyed wood veneer exposed to artificial light irradiation. BioResources, 10 (3): 5607-5619. https://doi.org/10.15376/biores.10.3.5607-5619
16. Liu, Y.; Guo, H.; Gao, J.; Zhang, F.; Shao, L.; Via, B. K., 2015: Effect of bleach pretreatment on surface discoloration of dyed wood veneer exposed to artificial light irradiation. BioResources, 10 (3): 5607-5619. https://doi.org/10.15376/biores.10.3.5607-5619
17. Lorenzi, H., 2009: Árvores brasileiras: manual de identificação e cultivo de plantas arbóreas nativas do Brasil, 1. ed. Nova Odessa: Instituto Plantarum, v. 3. (Nogueira; Medeiros Filho; Gallão, 2010).
18. Lu, D.; Xiong, X.; Lu, G.; Gui, C.; Pang, X., 2023: Effects of $NaOH/H_2O_2/Na_2SiO_3$ bleaching pretreatment method on wood dyeing properties. Coatings, 13 (2): 233. https://doi.org/10.3390/coatings13020233
19. Luo, M. R., 2016: Encyclopedia of color science and technology. Springer, New York.
20. Mehats, J.; Castets, L.; Grau, E.; Grelier, S., 2021: Homogenization of maritime pine wood color by alkaline hydrogen peroxide treatment. Coatings, 11 (7): 839. https://doi.org/10.3390/coatings11070839
21. Mononen, K.; Jääskeläinen, A. S.; Alvila, L.; Pakkanen, T. T.; Vuorinen, T., 2005: Chemical changes in silver birch (*Betula pendula* Roth) wood caused by hydrogen peroxide bleaching and monitored by color measurement (CIELab) and UV-Vis, FTIR and UVRR spectroscopy. Holzforschung, 59: 381-388. https://doi.org/10.1515/HF.2005.063

22. Möttönen, V.; Asikainen, A.; Malvaranta, P.; Öykkönen, M., 2003: Peroxide bleaching of parquet blocks and glue lams. Holzforschung, 57 (1): 75-80. https://doi.org/10.1515/HF.2003.012
23. Nguyen, Q. T.; Nguyen, T.; Nguyen, N. B., 2019: Effects of bleaching and heat treatments on *Indosasa angustata* bamboo in Vietnam. BioResources, 14 (3): 6608-6618. https://doi.org/10.15376/biores.14.3.6608-6618
24. Nogueira, F. C. B.; Medeiros Filho, S.; Gallão, M. I., 2010: Caracterização da germinação e morfologia de frutos, sementes e plântulas de *Dalbergia cearensis* Ducke (pau-violeta) – Fabaceae. Acta Botanica Brasilica, 24 (4): 978-985.
25. Oliveira, H. G. B.; Sousa, M. V. C.; Silva, L. S.; Ferraz Filho, A. C.; Ribeiro, A., 2019: Propriedades energéticas da madeira e casca de *Dalbergia cearensis* Ducke. Agropecuária Científica no Semiárido, 15: 232-237. https://doi.org/10.30969/acsa.v15i3.1188
26. Panigrahi, S.; Rout, S.; Sahoo, G.; Gupta, S.; Kumar, V. S., 2021: Finishing properties of poly urethane coating on bleached and ammonia fumigated mango wood surface. International Journal of Plant & Soil Science, 33 (16): 57-67. https://doi.org/10.9734/IJPSS/2021/v33i1630523
27. Park, K. C.; Kim, B.; Park, H.; Park, S. Y., 2022: Peracetic acid treatment as an effective method to protect wood discoloration by UV light. Journal of the Korean Wood Science and Technology, 50 (4): 283-298. https://doi.org/10.5658/WOOD.2022.50.4.283
28. Peker, H., 2023a: Canelo (*Drimys winteri* J. R. Forst. & G. Forst.) ahşabında ağartma uygulamaları, ICAFVP 3. Uluslararası Tarım, Gıda, Veteriner Ve Eczacılık Bilimleri Kongresi, 10-12 Kasım 2023, Beyrut, Lübnan, 165-174.
29. Peker, H., 2023b. Lotofa (*Sterculia rhinopetala*) odununda tek ve çift bileşenli ağartıcılarının uygulanması, ICAFVP 3. Uluslararası Tarım, Gıda, Veteriner Ve Eczacılık Bilimleri Kongresi, 10-12 Kasım 2023, Beyrut, Lübnan, 173-182.
30. Peker, H.; Ayata, Ü., 2023: Effects of bleaching chemicals on some surface characteristics of olon (*Zanthoxylum heitzii*) wood. Furniture and Wooden Material Research Journal, 6 (2): 210-218. https://doi.org/10.33725/mamad.1369843
31. Peker, H.; Bilginer, E. H.; Ayata, Ü.; Çamlıbel, O., 2023: A research on the application of single and double-component wood bleaching chemicals on movingui (*Distemonanthus benthamianus* Baillon) wood used in the furniture industry. Sivas Cumhuriyet University Journal of Science and Technology, 2 (2): 73-79.
32. Peker, H.; Bilginer, E. H.; Ayata, Ü.; Çamlıbel, O.; Gürleyen, L., 2023a: The application of bleaching chemicals (oxalic acid and hydrogen peroxide + sodium hydroxide) on bulletwood (*Manilkara bidentata* (A.DC.) A. Chev.) wood. Sivas Cumhuriyet University Journal of Engineering Faculty, 1 (2): 48-54.
33. Peker, H.; Bilginer, E. H.; Ayata, Ü.; Gürleyen, L.; Çamlıbel, O., 2023c: The application of different wood bleaching chemicals on izombé wood (*Testulea gabonensis* Pellegr.) used in indoor and outdoor designs. In: Proceedings of 2nd International Culture, Art and Communication Symposium, Bayburt, Turkey, December 15-17.
34. Peker, H.; Bilginer, E. H.; Ayata, Ü.; Çamlıbel, O.; Gürleyen, L., 2024: Identification of certain surface characteristics of balau red (*Shorea guiso*) wood treated with wood Bleaching chemicals followed by wax treatment. Turkish Journal of Science and Engineering (in press).
35. Peker, H.; Ulusoy, H., 2023: Ahşap ağartıcı kimyasalları uygulanmış yalancı akasya (*Robinia pseudoacacia* L.) odununda bazı yüzey özelliklerinin belirlenmesi, 8. Asya Pasifik Uluslararası Modern Bilimler Kongresi, 11-12 Eylül 2023, Delhi, India, 464-465.
36. Seidler, T. G.; Plotkin, J. B., 2006: Seed Dispersal and Spatial Pattern in Tropical Trees. PLOS Biology, 4 (11): 1877-1898. https://doi.org/10.1371/journal.pbio.0040344
37. Souza, L. A. G., 2020: Guia da biodiversidade de Fabaceae do Alto Rio Negro. 2012. p. 118.
38. Uphof, J. C. T., 1959: Dictionary of economic plants, Dictionary of economic plants.
39. Wheelwright, N. T., 1985: Competition for dispersers and the timing of flowering and fruting in a guild of tropical trees. Oikos, 44 (3): 465-477.
40. Yamamoto, A.; Rohumaa, A.; Hughes, M.; Vuorinen, T.; Rautkari, L., 2017: Surface modification of birch veneer by peroxide bleaching. Wood Science and Technology, 51: 85-95. https://doi.org/10.1007/s00226-016-0880-7
41. Yuan, B.; Ji, X.; Nguyen, T. T.; Huang, Z.; Guo, M., 2019: UV protection of wood surfaces by graphitic carbon nitride nanosheets. Applied Surface Science, 467-468: 1070-1075. https://doi.org/10.1016/j.apsusc.2018.10.251
42. Zeilman, J. M., 1960: Techniques and materials for finishing sculpture. PhD thesis, Bowling Green State University.
43. ***ASTM D 2240, 2010: Standard test method for rubber property-durometer hardness, American Society for Testing and Materials, West Conshohocken, Pennsylvania, United States.
44. ***ASTM D 2244-3, 2007: Standard practice for calculation or color tolerances and color, differences from instrumentally measured color coordinates, ASTM International, West Conshohocken, PA.
45. ***ASTM E313-15e1, 2015: Standard practice for calculating yellowness and whiteness indices from instrumentally measured color coordinates, ASTM International, West Conshohocken, PA.
46. ***ISO 2813, 1994: Paints and varnishes – determination of specular gloss of non-metallic paint films at 20 degrees, 60 degrees and 85 degrees, International Organization for Standardization, Geneva, Switzerland.
47. ***ISO 554, 1976: Standard atmospheres for conditioning and/or testing, International Standardization Organization, Geneva, Switzerland.

Corresponding address:

ÜMIT AYATA
Bayburt University, Faculty of Arts and Design, Department of Interior Architecture and Environmental Design, Bayburt, TURKEY, e-mail: umitayata@yandex.com

Kenan Kılıç*[1], Kazım Kılıç[2], İbrahim Alper Doğru[3], Uğur Özcan[4]

Comparison of Various Feature Extractors and Classifiers in Wood Defect Detection

Usporedba različitih ekstraktora i klasifikatora svojstava u otkrivanju grešaka drva

ORIGINAL SCIENTIFIC PAPER
Izvorni znanstveni rad
Received – prispjelo: 20. 5. 2024.
Accepted – prihvaćeno: 23. 12. 2024.
UDK: 630*85
https://doi.org/10.5552/drvind.2025.0217

ABSTRACT • *Detection of defects on wood during quality processes in the wood industry is extremely important both economically and in terms of production and use. In order to minimize the time and cost loss caused by products obtained with defective wood, manufacturers want to detect defects in wood early by applying quality control process. For this purpose, in this study, some experiments are carried out using texture analysis methods and machine learning classifiers to detect defective wood from wood images. The features of wood images in the dataset taken from literature are extracted separately with six texture feature extractors to detect defective wood. Features are classified using twelve different machine learning classifiers, primarily tree-based ensemble classifiers. Cross-validation is used in all experiments to reduce classifier bias. The results obtained are presented comparatively in terms of each feature and classifier. The findings show that the most effective features in detecting defective wood are extracted by the Local Binary Pattern (LBP) method and the most effective classifier is the Random Forest Algorithm. An accuracy rate of 96.75 % is achieved with the LBP-RandomForestClassifier and, classification performance is also presented for each algorithm by creating hybrid feature vectors.*

KEYWORDS: *wood defect detection; feature extraction; machine learning; wood products engineering; computer vision*

SAŽETAK • *Otkrivanje grešaka na drvu tijekom kontrole kvalitete u drvnoj industriji iznimno je važno kako u ekonomskom, tako i u proizvodnom smislu. Da bi se smanjili troškovi i gubitci vremena zbog drvnih proizvoda s greškama, cilj proizvođača je procesom kontrole kvalitete rano otkriti greške na drvu. Stoga je u ovoj studiji istražena mogućnost otkrivanja grešaka na drvu sa slika primjenom metoda analize teksture i klasifikatora strojnog učenja. Obilježja slika drva preuzetih iz literature izdvojena su uz pomoć šest ekstraktora teksture kako bi se otkrile greške na drvu, a zatim su klasificirane uz pomoć 12 različitih klasifikatora, ponajprije klasifikatora ansambla stabla odlučivanja dobivenih strojnim učenjem. U svim je eksperimentima primijenjena unakrsna provjera kako bi*

* Corresponding author
[1] Author is researcher at Gazi University, Graduate School of Natural and Applied Sciences, Department of Wood Products Industrial Engineering, Ankara, Turkey and at Yozgat Bozok University, Vocational School of Yozgat, Department of Design, Yozgat, Turkey.
[2] Author is researcher at Gazi University, Graduate School of Natural and Applied Sciences, Department of Computer Engineering, Ankara, Turkey and at Yozgat Bozok University, Vocational School of Yozgat, Department of Computer Programming, Yozgat, Turkey.
[3] Author is researcher at Gazi University, Faculty of Technology, Department of Computer Engineering, Ankara, Turkey.
[4] Author is researcher at Gazi University, Faculty of Technology, Department of Wood Products Industrial Engineering, Ankara, Turkey.

se smanjila eventualna pristranost klasifikatora. Dobiveni su rezultati prikazani komparativno, prema svojstvima i klasifikatorima. Rezultati pokazuju da su najučinkovitija svojstva za otkrivanje grešaka na drvu izdvojena metodom lokalnoga binarnog uzorka (LBP), a najučinkovitiji je klasifikator algoritam slučajnih šuma. Stopa točnosti od 96,75 % postiže se kombinacijom LBP metode i algoritma slučajnih šuma, a za svaki algoritam predstavljena je i izvedba klasifikacije stvaranjem hibridnih vektora svojstava.

KLJUČNE RIJEČI: *detekcija grešaka na drvu; ekstrakcija svojstava; strojno učenje; izrada proizvoda od drva; računalni vid*

1 INTRODUCTION
1. UVOD

Throughout history, wood has been used as a basic building material for many industries and continues to be used in a wide range of applications today. Wood is unique and its natural structure, aesthetic appeal, strength and environmentally friendly properties offer great value to a range of industries from construction to furniture manufacturing. However, the use of defective wood in the production process, and the defects that can occur as a result, can lead to serious economic losses as well as safety risks. Early detection and effective classification of such defects is therefore vital to the wood industry. In addition, the decline of wood resources has become an important focus for practitioners and researchers in recent years in order to use forest resources in a more sustainable manner. The rapid and effective detection of surface defects in wood can increase the utile efficiency of wood and reduce excessive wood consumption (Pölzleitner and Schwingshakl 1992; Schmoldt *et al*., 1997; Norlander *et al*., 2015).

Traditionally, wood grading has been done manually. Today, however, automatic grading machines are widely used to speed up the process. By using the same set of mechanical devices and changing the grading task, different sorting tasks can be easily performed. Among these tasks, classification is perhaps the most important (Hu *et al*., 2019). Unlike traditional methods that rely on visual inspection by operators, methods used to detect surface defects in wood involve computer analysis of images of the wood surface. A Charge-Coupled Device (CCD) camera is usually used for this process. The process of recognizing wood defects is based on the design of the image analysis algorithm, with frequent use of digital image processing (Xie, 2013). The classification process typically begins with image pre-processing, such as greyscale transformation, histogram equalization, spatial or frequency domain filtering. Next, the wood images are processed to extract defect features. Finally, a machine learning algorithm is used to classify the images (Chen *et al*., 2023a). Machine learning is a technology that can automatically generate predictions and decisions by learning from data. This technology makes it possible to develop solutions to complex problems with different algorithms used to obtain results. Each algorithm is designed to understand a specific data structure and make inferences, and is particularly effective with large data sets. These algorithms can be broadly categorized into three main types: unsupervized learning, supervized learning and reinforcement learning. The combination of digital image processing and machine learning algorithms is the preferred methodology for detecting and classifying wood knot defects (Qi *et al*., 2010; Mu and Qi, 2009). This methodology is not only used for wood defect detection but also for quality control in automated production lines in various sectors such as textiles fabrics, ceramic tiles and pharmaceuticals (Gao *et al*., 2021; Liu *et al*., 2021; Shahrabadi *et al*., 2022; Zhang *et al*., 2023).

The detection of defects on the surface of industrial products has become a very promising area of academic research. There are many studies in the literature dealing with fabric defect detection (Raheja *et al*., 2013; Liu and Zheng, 2020; Liu and Le, 2021), leather surface inspection (Hoang *et al*., 1997; Chen *et al*., 2024), detection of defect in pharma (Galata *et al*., 2021), defect detection in electronic surfaces (Tsai and Huang, 2019; Chen *et al*., 2023b), metallic surface defect detection (Tao *et al*., 2018), concrete crack detection (Lei *et al*., 2024) and defect detection of mobile phone surface (Jian *et al*., 2017). Studies specific to the wood industry are also available in the literature. Zhang *et al*. (2015) used principal component analysis (PCA) and compressed sensing to identify wood defects in wood plate images. YongHua and Jin-Cong (2015) focused on three common wood defects: dead knots, poles and living knots. In their study, they introduced a hybrid defect detection method based on wood surface texture features, which combines the advantages of Tamura texture and Grey-Level Co-occurrence Matrix (GLCM) methods. Li *et al*. (2017) presented a wood defect detection method leveraging linear discriminant analysis (LDA) and the utilization of compressed sensor images. Chang *et al*. (2018) applied convex optimization (CO) and the Otsu segmentation method to obtain a comprehensive image of wood surface defects. The results between the original image and the defect image are used to evaluate the segmentation performance. A classification and regression tree (CART) classifier is then constructed. Li *et al*. (2019)

proposed a classification algorithm for distinguishing between cracks and linear mineral lines on the surface of birch veneer. This algorithm relies on Local Binary Pattern and Local Binary Differential Excitation Pattern for effective classification. Urbonas *et al*. (2019) presented an automatic visual inspection system for locating and classifying defects on wood veneer surfaces using a faster Region-Based Convolutional Neural Network (faster R-CNN). Shi *et al*. (2020) introduced an efficient detection method with high accuracy and speed for online production. They developed an integrated model, the Glance Multi-Channel Mask Region Convolutional Neural Network (R-CNN), specifically designed for wood veneer defect detection. This model incorporates both a Glance network and a multi-channel mask R-CNN. Wu *et al*. (2022) developed a wood surface defect detection approach based on feature fusion. The Support Vector Machine (SVM) is used as the classifier for this approach. There is no previous literature on the classical machine learning approach in the form of binary classification regarding the dataset used in the study. Instead, a general literature summary is given in Table 1.

The proposed study aims to evaluate the effectiveness of different image processing methods and classification algorithms in detecting defects on wood surface. The primary objective is to improve the early detection of defects in wood and to evaluate the performance of different feature extraction methods and classification algorithms in achieving this objective. In addition, the study aims to contribute to the identification of potentially valuable techniques and algorithms for defect detection in both the production and utilization processes of wood. For this purpose, an extensive dataset of 20,276 images of both defective and undefect wood surfaces is used. Dataset balancing is a process to address sample count imbalances between classes. Usually, when there is a large difference between the classes, machine learning models may focus more on the majority class, making it difficult to correctly classify the minority class. For this reason, data set balancing was performed. Subsequently, different feature extraction methods were applied to obtain image features, followed by the implementation of classification processes using classifiers of different structures. In this study, binary classification for wood defect detection was performed using feature extraction and classical machine learning classifiers. The advantages of machine learning in the field of image processing are as follows: It has important features such as coping with complexity, feature extraction ability, flexibility, suitability for large data sets, transfer learning possibility, updatability, and complexity reduction. In this study, machine learning models were trained on a standard processor (CPU) instead of using a GPU. This choice aims to make computational resources more wide-

Table 1 Literature summary
Tablica 1. Sažetak literature

Reference *Navod iz literature*	**Methodology** *Metodologija*	**Techniques** *Tehnike*	**Application** *Primjena*	**Metrics** *Metrika*
Pölzleitner and Schwingshakl (1992)	Manual wood grading	Real Time / Feature vector	Spruce boards	95 % Accuracy
Zhang *et al*. (2015)	PCA and compressed sensing	Principal Component Analysis (PCA), Compressed Sensing	Wood plate defect identification	92 % Accuracy
YongHua and Jin-Cong (2015)	Hybrid method based on texture features	Tamura texture, Grey-Level Co-occurrence Matrix (GLCM)	Detection of dead knots, poles, and living knots	91.83 % Accuracy
Li *et al*. (2017)	LDA and compressed sensor images	Linear Discriminant Analysis (LDA), Compressed Sensor Images	Wood defect detection	94 % Accuracy
Chang *et al*. (2018)	Convex optimization and Otsu segmentation	Convex Optimization, Otsu Segmentation	Comprehensive wood surface defect image evaluation	94.1 % Accuracy
Li *et al*. (2019)	Local Binary Pattern and Local Binary Differential Excitation	Local Binary Pattern, Local Binary Differential Excitation	Classification of cracks and linear mineral lines on birch veneer surface	93 % Recall
Urbonas *et al*. (2019)	Faster R-CNN	Region-Based Convolutional Neural Network (faster R-CNN)	Automatic visual inspection of wood veneer surfaces	96.1 % Accuracy
Shi *et al*. (2020)	Glance Multi-Channel Mask R-CNN	Glance network, Multi-Channel Mask R-CNN	Efficient method for wood veneer defect detection	95.31 % Accuracy
Wu *et al*. (2022)	Feature fusion and Support Vector Machine	Support Vector Machine (SVM)	Wood surface defect detection based on feature fusion	91.26 % Accuracy

spread and accessible. Therefore, computers with high processing power were not required.

In this study, the existing dataset is analyzed and the wood images are classified into two categories: defective or undefect wood. Also, many methods are used in the feature extraction phase, and the performance of the feature extraction methods is presented comparatively. The extracted features are evaluated with different classifiers and a cross-validation technique is used to reduce classifier bias. All the different extracted features are combined and the classifier performances are measured when different features are combined.

The remaining sections of the paper are organized as follows: Section 2 presents the preprocessing steps, feature extraction methods, and classifiers used; Section 3 provides the experimental results and comparative analysis, while Section 4 presents the conclusions and future research directions.

2 MATERIALS AND METHODS
2. MATERIJALI I METODE

The following subsections provide details about the dataset and its features, pre-processing, feature extraction methods and classifiers used in the study.

2.1 Dataset
2.1. Skup podataka

The dataset is taken from Kodytek *et al*. (2021). There are 20,276 wood surface images in the dataset with ten common types of wood defects including various types of knots, cracks, blue stain, resin and heartwood. Figure 1 shows wood defects samples within the dataset.

While 1,992 of these images contain images of cut wood with no defects, 18,284 images contain images of wood with one or more surface defects. On average, each image contains 2.2 defects, with 6.7 % of the images having more than three defects, and with the maximum number of defects in a single image being 16.

The dataset initially had a serious imbalance between undefect and defect images. There were only 1,992 undefect images, while there were 18,284 defect images. In our opinion deep learning models tend to focus predominantly on the larger class in unbalanced data sets. Therefore, we balanced the dataset by increasing the defect class. The number of defect examples was increased to 18,284 with data augmentation techniques (rotation, shift, brightness variation, etc.) so as to become equal to the defect examples. This process is necessary to balance the learning across classes and improve model performance.

In addition, the original images have a high resolution of 2800×1024 pixels. However, training at this resolution increased the computational cost and made it difficult for the models to work efficiently. Therefore, the images were resized to 300×300 pixels. This resizing provided sufficient resolution to train the model faster while preserving the features of the defects in the image. The image resolution was reduced from 2800×1024 to 300×300 pixels in order to reduce the high computational cost and train the model more efficiently. In this process, the defect details were preserved by using bilinear interpolation. As a result, significant improvements were obtained in processing time and resource usage with an acceptable difference in accuracy. Bilinear interpolation is a mathematical method used to resize an image or estimate a set of data at a higher resolution. In this way, the resizing process was performed without any problems with the features in the existing images.

These methods were applied to both solve the imbalance problem and increase the accuracy and overall performance of the model.

In this study, various data augmentation techniques were applied to increase the generalization ability of the model. These augmentation techniques were performed using the Augmentor: An Image Augmentation Library for Machine Learning library developed by Bloice *et al*. (2017). The images were rotated to the right or left with a maximum of 25 degrees with a 70 % probability, thus providing variation at different angles and increasing the model robustness against transformations. In addition, the images were flipped horizontally with a 50 % probability, thus providing symmetrical features to the model and making the model more flexible. The contrast of the images was changed by a random factor between 0.5 and 1.5 with a 50 % probability, which aimed to allow the model to adapt to different lighting conditions. Similarly, the brightness levels were

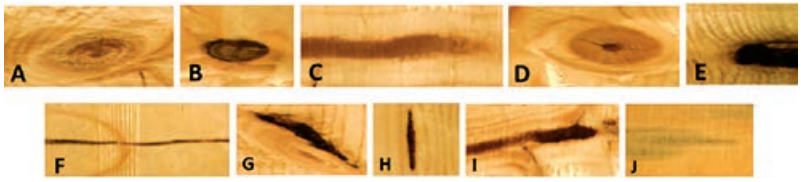

Figure 1 Wood defects within the dataset (A – live knot, B – dead knot, C – quartzity, D – knot with crack, E – knot missing, F – crack, G – overgrown, H – resin, I – marrow and J – blue stain)
Slika 1. Greške drva u skupu podataka (A – zdrava kvrga, B – nesrasla kvrga, C – inkrustacije minerala, D – ispucala kvrga, E – ispadajuća kvrga, F – pukotina, G – obrasla kvrga, H – smolenica, I – srčika, J – plavilo)

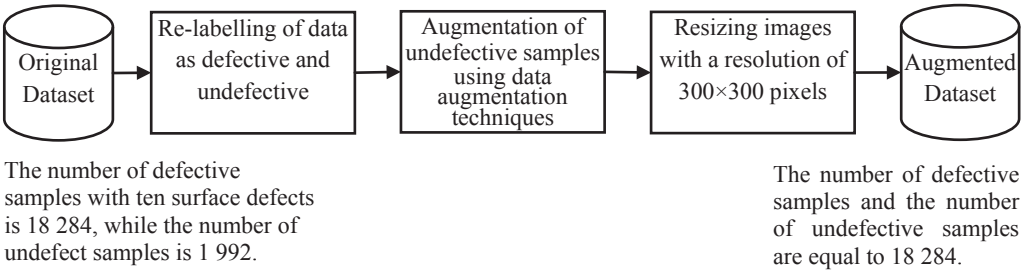

Figure 2 Data augmentation phase of data pre-processing
Slika 2. Faza porasta broja podataka u prethodnoj obradi podataka

randomly adjusted between 0.7 and 1.3 with a 50 % probability, thus increasing the sensitivity of the model to lighting changes in the images. These data augmentation processes allowed the model to be trained with a wider range of images, allowing it to generalize better under various conditions. The data augmentation phase of data pre-processing is shown in Figure 2.

2.2 Feature extraction
2.2. Izdvajanje svojstava

Feature extraction is the process of determining distinctive features from images. The purpose of this process is to represent the image with fewer values. In this way, decision making can be achieved with more meaningful and less dimensional values. Classification performances are directly dependent on good feature extraction. Well-extracted meaningful features increase classification performance. Many feature extraction methods have been proposed in the literature. In image analysis, especially in applications such as wood defect detection, the features used are generally grouped into four main groups: geometric features, statistical features, texture features, and color features (Mutlag *et al*., 2020). Another grouping made according to properties and models includes color based features, texture features, intensity features, human features, finger print features, conceptual features, and text features (Salau and Jain, 2009). In particular, a survey of texture feature extraction methods is also available in the literature (Humeau-Heurtier, 2019). Each has its pros and cons depending on the area in which they are used.

In this study, some well-known texture feature extraction methods are used to detect defective wood. These are Local Binary Pattern (LBP), Histogram of Oriented Gradients (HOG), Gray-Level Co-occurrence Matrix (GLCM), Sobel, Gabor and Multi Block LBP (MB-LBP). LBP (Local Binary Pattern) is a feature extraction method in which pixels are compared to their surrounding neighbouring pixels. Each pixel is compared with its neighbouring pixels to form a binary pattern. This pattern represents the texture and structure information in the image, so it is effective in recognizing small changes and patterns (Ojala *et al*., 2002). HOG is used for object recognition. It splits the image into small cells, calculates gradients in each cell, and then creates histograms of those gradients (Dalal and Triggs, 2005). GLCM captures the relationships between gray level pixels in an image (Haralick *et al*., 1973). Sobel is a filtering method used for edge detection. Sobel operators calculate the gradient of pixel intensity in the image (Duda and Hart, 1973). Gabor filters extract features from images using sinusoidal waves vibrating at different frequencies and in different directions (Daugman, 1985). MB-LBP is an expansion of the traditional LBP. MB-LBP divides an image into blocks of specific sizes. Within each block, pixels are compared with neighboring pixels around them using the LBP (Liu *et al*., 2019).

The selection of texture feature extraction methods to be used in the study is based on factors such as suitability to the problem addressed in this study, the class to which it belongs, computational cost and ease of implementation. LBP and its extension MB-LBP fall into the class of statistical approaches. They combine structural and statistical methods, resulting in improved performance for texture analysis. HOG is in human features group. GLCM is classified under the umbrella of statistical approaches. Sobel is a filtering method. Gabor is classified as transform-based approach. LBP focuses on local binary patterns, while MB-LBP extends this by using multi-bit representations for more detailed feature extraction. Sobel is an edge detection operator that focuses on gradient magnitudes in image processing. Gabor is a texture analysis filter that emphasises texture patterns at different scales and orientations. HOG emphasises the capture of shape and edge information through gradient orientations. GLCM uses information such as homogeneity, contrast, energy and correlation derived from pixel relationships.

In this study, different feature extraction techniques were applied using various image processing methods for wood defect detection. First, Local Binary Pattern (LBP) method was used. In this method, images

were converted to grayscale and LBP algorithm was applied. Radius=1 and n_points=8 were specified as parameters and 10 features were extracted for each image.

Another method, Histogram of Oriented Gradients (HOG), performs feature extraction by analyzing edges and orientations in images. For this method, pixels_per_cell=(16, 16) and cells_per_block=(2, 2) parameters are used. The HOG algorithm extracts 378 features from each image, providing a detailed representation of edges and orientations. The Gray Level Co-occurrence Matrix (GLCM) method extracts structural features such as contrast, similarity, homogeneity, energy and correlation in images. The parameters used here include distances=[5] and angles=[0], meaning that only horizontal neighborhood relationships are considered. With this method, 5 features are extracted from each image. Another important feature extraction method is Multiblock LBP (MB-LBP). By applying LBP in blocks, LBP histograms are extracted for each block. The parameters used are radius=2, n_points=4 and block_size=6 and 10 features are obtained for each block. As a result, 10 MB-LBP features are extracted from each image. The Gabor Filter method performs feature extraction by analyzing different frequencies and orientations in the images. With this method, Gabor kernels are created using sigma, theta, lambda and gamma parameters and applied to the image. The mean and standard deviation values are extracted for each Gabor filter, and approximately 36 features are obtained for each image in total. Finally, the Sobel Edge Detection method uses Sobel filters to detect edges in images. In this method, histograms of edge orientations are extracted and 9 features are obtained from each image. This is a feature known as the gradient orientation histogram and provides important information about the orientations of the edges. These methods create a rich feature set for wood defect detection and each of them increases the accuracy of the model by capturing different structural and textural information in the images.

Min-max scaling and standardization are two methods commonly used in data preprocessing. Min-max scaling transforms the values in the data set by compressing them into a certain range, usually between [0, 1]. This method is particularly preferred in distance-based algorithms. Standardization subtracts the data from the mean and divides it by the standard deviation, making the mean of the data 0 and the standard deviation 1. This method provides a more balanced modeling of data at different scales and is generally suitable for algorithms such as linear models and support vector machines. In order to improve the performance of the model used in the study, the data were processed by standardization method, because this method helps the model to obtain more accurate and reliable results.

2.3 Classification algorithms
2.3. Klasifikacijski algoritmi

Random Forest Classifier: Random Forest is an ensemble learning method that combines decision trees. Its advantages include that the model is resistant to overfitting, works well with missing data, and achieves high accuracy. It also has the ability to generalize on datasets with a large number of features. However, the interpretability of the model is difficult and the computational cost can increase on large datasets. In addition, memory and processing power requirements are high (Breiman, 2001).

K Neighbors Classifier: The K-nearest neighbor classifier is a simple and intuitive algorithm. Its advantages include the fast training phase and obtaining intuitive results by performing calculations on the test data. It gives good results especially on small data sets. However, calculations are slower on large data sets, and performance may decrease due to the "curse of dimensionality" effect on high-dimensional data (Cover and Hart, 1967).

Support Vector Machine (SVM): SVM is a powerful algorithm that can effectively classify high-dimensional datasets. Its advantages are its ability to perform nonlinear classification and its robustness against outliers. It also becomes very flexible with the right kernel functions. However, on large data sets the training time can be long and tuning the parameters is complex (Cortes and Vapnik, 1995).

Decision Tree Classifier: Decision trees create models that are understandable and visualizable. They can work with both numerical and categorical data. Their advantages include fast training time and simplicity of the model, while their disadvantages include their tendency to overfit and the large differences that small data changes can produce (Quinlan, 1986).

Naive Bayes: Naive Bayes is an algorithm based on Bayes theorem and provides high accuracy, especially in problems such as text classification. The training time is very fast and gives effective results on small data sets. However, the assumption that all features are independent of each other can affect accuracy, as it is generally not valid in real-world data sets (Lewis, 1998).

Logistic Regression: Logistic regression is a simple and fast algorithm used for binary classification. The outputs of the model are easily interpretable. However, its accuracy may be low in nonlinear relationships and complex data sets. Also, since it is based on linear features only, its ability to generalize is limited (Hosmer *et al.,* 2013).

GradientBoostingClassifier: Gradient Boosting combines weak learners to create a strong model. Its advantages include high accuracy and efficiency. This algorithm achieves effective results when hyperparameter settings are set correctly. Its disadvantages are that

the training time is long and the risk of overfitting is high (Friedman, 2001).

XGBClassifier: XGBClassifier is a fast and effective classifier developed by optimizing the Gradient Boosting algorithm. It offers high performance especially on large datasets and complex problems. Fast training time and low memory usage are its advantages. However, there is a risk of overfitting and complex parameter settings (Chen and Guestrin, 2016).

LightGBM: LightGBM is an algorithm with parallel processing capabilities that focuses on large datasets. It offers high efficiency and speed, and works very effectively on large datasets. However, its efficiency may be low on small datasets, and the complexity of the model can sometimes make tuning difficult (Ke *et al.,* 2017).

CatBoost: CatBoost is a gradient boosting library that can work effectively with categorical data. It stands out with its fast training time, low risk of overfitting, and strong performance. However, being a new method compared to other algorithms, it can sometimes lead to limited support and resources (Prokhorenkova, 2018).

AdaBoost: AdaBoost combines weak classifiers to create a strong model. Its advantages include high accuracy, low risk of overfitting, and flexibility. Its disadvantage is that the model may fail if the datasets contain noise and incorrect data (Freund and Schapire, 1997).

MLPClassifier: MLPClassifier is a powerful classifier that uses multilayer artificial neural networks. It works similarly to deep learning methods and can achieve high accuracy on very complex and large datasets. However, its training can take a long time and the model is difficult to interpret. It can also carry the risk of overfitting and its hyperparameter settings are complex (Haykin, 1999).

For the Random Forest model, a total of 500 decision trees were used with n_estimators=500, and the Gini coefficient and splitting criterion were determined by selecting criterion='gini'. The tree depth was not limited with max_depth=None, and the minimum sample numbers for splitting and leaf nodes were set with min_samples_split=2 and min_samples_leaf=1 parameters. max_features='sqrt' was used for feature selection and bootstrap sampling was enabled with bootstrap=True. In the KNN (K-Nearest Neighbors) classifier, a single neighbor was considered with n_neighbors=1, distance-based weighting was done by selecting weights='distance' and the KD tree algorithm was preferred by using algorithm='kd_tree'. In addition, the leaf size was determined as leaf_size=10 and the distance metric as metric='minkowski'.

SVM (Support Vector Machines) model was created with C=1.0 regularization parameter, linear kernel was selected as kernel='linear' and kernel degree was set as degree=4. Also, scaling of kernel function was provided with gamma='scale' parameter. In Decision Tree classifier, Gini coefficient was selected with criterion='gini', random splitting strategy was selected with splitter='random', depth was not limited with max_depth=None. Splitting and leaf node parameters were determined with min_samples_split=2 and min_samples_leaf=1 values; also, minimum decrease value was assigned for splitting with min_impurity_decrease=0.0.

For the Logistic Regression model, L2 regularization was applied with penalty='l2', optimization algorithm was determined as solver='liblinear', and maximum iteration number was determined as max_iter=100. GaussianNB(), which works with Gaussian distribution assumption, was used in Naive Bayes classifier. Gradient Boosting model was configured with parameters n_estimators=500, learning_rate=0.1 and max_depth=10, data subsampling rate was selected as subsample=1.0. XGBoost model was similarly configured with parameters n_estimators=500, learning_rate=0.1, max_depth=10, min_child_weight=1, subsample=1.0, colsample_bytree=1.0 and objective='binary:logistic'.

For LightGBM (LGBMClassifier), n_estimators=500, learning_rate=0.1, max_depth=10, min_child_weight=1, subsample=1.0, colsample_bytree=1.0 and objective='binary' were selected; while n_estimators=500 and learning_rate=0.1 were used in the AdaBoost model. For MLPClassifier (Multi-Layer Perceptron), the hidden layer structure was set as hidden_layer_sizes=(100, 50), the maximum iteration number was set as max_iter=500 and random_state=42 for randomness. All these hyperparameters were selected and optimized in accordance with the dataset used in the study and the nature of the problem.

2.4 Evaluation metrics
2.4. Evaluacijska mjerila

In this article, commonly used Accuracy, Precision, Recall, F1-Score and AUC score metrics are used to evaluate the performance of machine learning classification algorithms. The formulas for these metrics are given in Equations (1-4):

$$F1-Score=\frac{2\cdot Precision\cdot Recall}{Precision+Recall} \quad (1)$$

$$Accuracy=\frac{TP+TN}{TP+FN+FP+TN} \quad (2)$$

$$Precision=\frac{TP}{TP+FP} \quad (3)$$

$$Recall=\frac{TP}{TP+FN} \quad (4)$$

Where *TP*, *TN*, *FP* and *FN* are true positive, true negative, false positive and false negative, respectively.

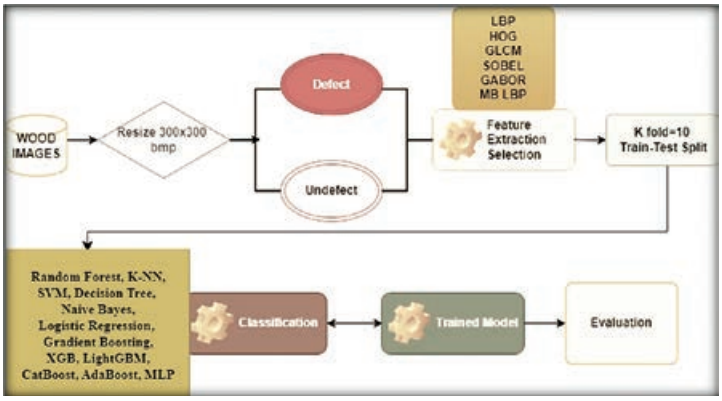

Figure 3 Schematic representation of methodology used in the study
Slika 3. Shematski prikaz metodologije primijenjene u istraživanju

Schematic representation of the methodology used in the study is shown in Figure 3.

3 RESULTS AND DISCUSSION
3. REZULTATI I RASPRAVA

In this section, the performances of the feature extraction and classification algorithms for defect detection are presented and interpreted. For the classification experiments, features are obtained with different feature extraction techniques (LBP, HOG, GLCM, SOBEL, GABOR, MB-LBP). Depending on these features, 12 different classifiers are used in the classification process and their performances are measured. Hyper-parameter settings are made for all classifiers. The same number of classifiers and the same hyper-parameters are used for all feature sets. Cross-validation technique is applied to increase the independence of the classification result and reduce its bias. For the cross-validation technique, the k value is determined as 10. 10-fold cross-validation divides the data set into 10 equal parts and uses each part of the model as a test set and the rest as a training set in turn. This process is repeated 10 times and the performance of the model is evaluated by averaging all results. This method provides more generalizable and reliable results. The results in Tables 2-8 are the average results obtaind after cross validation application. The performances of LBP and the classification algorithms in detecting defective wood are shown in Table 2.

According to this table, Random Forest Classifier is the algorithm that gives the best results in terms of performance metrics. This model has high values in all metrics, especially AUC, precision, sensitivity, F1-Score, and its accuracy values are quite high with 96.75 %. This shows that it can successfully classify data using LBP features. The algorithms with the second highest performance are Gradient Boosting Classifier and XGB-Classifier models. Among the classification algorithms on LBP features, LBP Random Forest Classifier has the highest accuracy rate of 96.75 % and this algorithm is highly effective in classifying data accurately. Other algorithms such as LBP Gradient Boosting Classifier 96.56 % and XGB Classifier 96.28 % also present high accuracy values, indicating that the data can be classified successfully. LBP CatBoost 95.39 % also has a very high accuracy rate, but is slightly lower than the others.

Random Forest Classifier has a high accuracy of 88.38 %. CatBoost comes right behind, achieving an accuracy of 86.25 %. Gradient Boosting Classifier,

Table 2 Performances of classification algorithms on LBP features
Tablica 2. Rezultati klasifikacijskih algoritama primijenjenih za LPB svojstva

Algorithms *Algoritmi*	**AUC**	**Precision** *Preciznost*	**Recall** *Opoziv*	**F1-Score** *F1-rezultat*	**Accuracy** *Točnost*
LBP RandomForestClassifier	0.9851	0.9680	0.9675	0.9675	0.9675
LBP KNeighborsClassifier	0.9198	0.9217	0.9199	0.9198	0.9199
LBP Support Vector Machine	0.8737	0.8701	0.8388	0.8353	0.8388
LBP DecisionTreeClassifier	0.9048	0.9081	0.9050	0.9047	0.9050
LBP Naive Bayes	0.8484	0.8319	0.8063	0.8025	0.8063
LBP LogisticRegression	0.8595	0.8504	0.8226	0.8190	0.8226
LBP GradientBoostingClassifier	0.9839	0.9661	0.9656	0.9656	0.9656
LBP XGBClassifier	0.9829	0.9631	0.9628	0.9628	0.9628
LBP LightGBM	0.9750	0.9289	0.9262	0.9261	0.9262
LBP CatBoost	0.9816	0.9546	0.9539	0.9539	0.9539
LBP AdaBoost	0.8966	0.8642	0.8398	0.8370	0.8398
LBP MLPClassifier	0.9048	0.8729	0.8458	0.8429	0.8458

Table 3 Performances of classification algorithms on HOG features
Tablica 3. Rezultati klasifikacijskih algoritama primijenjenih za HOG svojstva

Algorithms *Algoritmi*	**AUC**	**Precision** *Preciznost*	**Recall** *Opoziv*	**F1-Score** *F1-rezultat*	**Accuracy** *Točnost*
HOG RandomForestClassifier	0.9198	0.8903	0.8838	0.8834	0.8838
HOG KNeighborsClassifier	0.8232	0.8234	0.8232	0.8232	0.8232
HOG Support Vector Machine	0.8496	0.8451	0.8350	0.8338	0.8350
HOG DecisionTreeClassifier	0.8110	0.8118	0.8111	0.8110	0.8111
HOG Naive Bayes	0.8735	0.8433	0.8342	0.8331	0.8342
HOG LogisticRegression	0.8488	0.8432	0.8338	0.8326	0.8338
HOG GradientBoostingClassifier	0.9138	0.8839	0.8775	0.8770	0.8775
HOG XGBClassifier	0.9124	0.8760	0.8656	0.8646	0.8656
HOG LightGBM	0.9084	0.8726	0.8595	0.8582	0.8595
HOG CatBoost	0.9111	0.8750	0.8625	0.8614	0.8625
HOG AdaBoost	0.8918	0.8696	0.8517	0.8499	0.8517
HOG MLPClassifier	0.8940	0.8764	0.8552	0.8531	0.8552

XGBoost and MLP Classifier also have high accuracy scores. SVM and Naive Bayes achieve good accuracy if other performance metrics are put aside, but are slightly inferior to the best performers. K Neighbors Classifier, Decision Tree Classifier, and LightGBM achieve lower accuracy than other models.

In the experiments conducted on GLCM features, the Random Forest classifier gave the most successful results. The accuracy of Gradient Boosting and Random Forest classifiers is over 93 %. The XGB classifier achieved a value close to the most successful. Logistic Regression classifier showed the most unsuccessful result with an accuracy rate of 82.94 %.

Other algorithms also have high accuracy rates on SOBEL features such as Random Forest Classifier 88.44 %, Gradient Boosting Classifier 87.86 %, and XGB-

Table 4 Performances of classification algorithms on GLCM features
Tablica 4. Rezultati klasifikacijskih algoritama primijenjenih za GLCM svojstva

Algorithms *Algoritmi*	**AUC**	**Precision** *Preciznost*	**Recall** *Opoziv*	**F1-Score** *F1-rezultat*	**Accuracy** *Točnost*
GLCM RandomForestClassifier	0.9653	0.9415	0.9389	0.9388	0.9389
GLCM KNeighborsClassifier	0.8906	0.8918	0.8907	0.8906	0.8907
GLCM Support Vector Machine	0.8866	0.8762	0.8441	0.8407	0.8441
GLCM DecisionTreeClassifier	0.8735	0.8759	0.8736	0.8733	0.8736
GLCM Naive Bayes	0.8831	0.8557	0.8334	0.8362	0.8384
GLCM LogisticRegression	0.8729	0.8510	0.8294	0.8267	0.8294
GLCM GradientBoostingClassifier	0.9609	0.9352	0.9330	0.9330	0.9330
GLCM XGBClassifier	0.9592	0.9250	0.9217	0.9215	0.9217
GLCM LightGBM	0.9499	0.8993	0.8900	0.8894	0.8900
GLCM CatBoost	0.9546	0.9075	0.9006	0.9002	0.9006
GLCM AdaBoost	0.9034	0.8775	0.8523	0.8498	0.8523
GLCM MLPClassifier	0.9044	0.8808	0.8578	0.8557	0.8578

Table 5 Performances of classification algorithms on SOBEL features
Tablica 5. Rezultati klasifikacijskih algoritama primijenjenih za SOBEL svojstva

Algorithms *Algoritmi*	**AUC**	**Precision** *Preciznost*	**Recall** *Opoziv*	**F1-Score** *F1-rezultat*	**Accuracy** *Točnost*
SOBEL RandomForestClassifier	0.9326	0.8899	0.8844	0.8840	0.8844
SOBEL KNeighborsClassifier	0.8303	0.8304	0.8303	0.8303	0.8303
SOBEL Support Vector Machine	0.8209	0.8140	0.7834	0.7730	0.7834
SOBEL DecisionTreeClassifier	0.8078	0.8081	0.8078	0.8078	0.8078
SOBEL Naive Bayes	0.8424	0.8156	0.7776	0.7706	0.7776
SOBEL LogisticRegression	0.7248	0.7172	0.6935	0.6868	0.6935
SOBEL GradientBoostingClassifier	0.9256	0.8838	0.8786	0.8782	0.8786
SOBEL XGBClassifier	0.9264	0.8834	0.8777	0.8773	0.8777
SOBEL LightGBM	0.9226	0.8750	0.8671	0.8664	0.8671
SOBEL CatBoost	0.9271	0.8803	0.8732	0.8726	0.8732
SOBEL AdaBoost	0.8880	0.8502	0.8332	0.8311	0.8332
SOBEL MLPClassifier	0.9104	0.8754	0.8586	0.8571	0.8586

Table 6 Performances of classification algorithms on GABOR features
Tablica 6. Rezultati klasifikacijskih algoritama primijenjenih za GABOR svojstva

Algorithms *Algoritmi*	**AUC**	**Precision** *Preciznost*	**Recall** *Opoziv*	**F1-Score** *F1-rezultat*	**Accuracy** *Točnost*
GABOR RandomForestClassifier	0.9753	0.9521	0.9496	0.9495	0.9496
GABOR KNeighborsClassifier	0.9011	0.9022	0.9012	0.9011	0.9012
GABOR Support Vector Machine	0.9048	0.8861	0.8622	0.8600	0.8622
GABOR DecisionTreeClassifier	0.8866	0.8880	0.8866	0.8865	0.8866
GABOR Naive Bayes	0.8933	0.8766	0.8580	0.8562	0.8580
GABOR LogisticRegression	0.8918	0.8789	0.8586	0.8566	0.8586
GABOR GradientBoostingClassifier	0.9765	0.9543	0.9523	0.9522	0.9523
GABOR XGBClassifier	0.9756	0.9486	0.9460	0.9459	0.9460
GABOR LightGBM	0.9658	0.9216	0.9146	0.9142	0.9146
GABOR CatBoost	0.9704	0.9318	0.9265	0.9262	0.9265
GABOR AdaBoost	0.9157	0.8954	0.8770	0.8756	0.8770
GABOR MLPClassifier	0.9178	0.8989	0.8802	0.8788	0.8802

Classifier 87.77 %. Although Naive Bayes performs slightly lower than the others, with an accuracy rate of 77.76 %, it still has a very acceptable level of accuracy.

In the classification made on Gabor features, Gradient Boosting Classifier and XGBClassifier algorithms stand out by achieving a high accuracy rate of 95.23 % and 94.60 %. At the same time, Random Forest Classifier also shows a very successful result with 94.96 %. Other algorithms also have high accuracy rates, indicating that Gabor features allow effective classification.

In the classification processes performed on MB LBP features, Random Forest Classifier showed the highest performance with 89.58 % in terms of accuracy and also achieved successful results in other metrics. The Gradient Boosting Classifier ranked second with an accuracy of 88.86 %, while XGBClassifier and CatBoost performed well with an accuracy of 87.77 % and 86.03 %, respectively. LightGBM provided a satisfactory result with an accuracy of 84.07 %. In general, Random Forest provided the best results among these classification algorithms.

A "hybrid feature" is a feature or variable that is usually created by combining different types of features or information. This type of feature is usually created by combining information from two or more different sources. By combining all the features extracted in the study, hybrid features are created and their performance is examined.

The classification performances of the classifiers on the feature set obtained by combining all feature extraction methods are given in Table 8.

In the combined features, Gradient Boosting Classifier gives the highest accuracy with 95.16 % accuracy. XGB Classifier gives very successful results with 95.13 %. LightGBM and CatBoost had an accuracy of 94.70 % and 94.71 %, respectively. It has been observed that hybrid learning provides an increase in accuracy according to some feature extractions.

The accuracy values of all feature extraction and classification algorithms are given in Table 9.

A shematic view of Table 9 is also given in Figure 4. As it can be seen in Figure 4, classification algorithms RandomForestClassifier, GradientBoostingClassifier and XGBClassifier stand out in terms of total performance indicators.

The fact that certain methods perform better than others can be attributed to the characteristics of the fea-

Table 7 Performances of classification algorithms on MB-LBP features
Tablica 7. Rezultati klasifikacijskih algoritama primijenjenih za MB-LBP svojstva

Algorithms *Algoritmi*	**AUC**	**Precision** *Preciznost*	**Recall** *Opoziv*	**F1-Score** *F1-rezultat*	**Accuracy** *Točnost*
MB LBP RandomForestClassifier	0.9397	0.8984	0.8958	0.8956	0.8958
MB LBP KNeighborsClassifier	0.8307	0.8321	0.8308	0.8306	0.8308
MB LBP Support Vector Machine	0.7983	0.8025	0.7660	0.7586	0.7660
MB LBP DecisionTreeClassifier	0.8181	0.8201	0.8101	0.8178	0.8181
MB LBP Naive Bayes	0.7988	0.7961	0.7584	0.7504	0.7584
MB LBP LogisticRegression	0.7995	0.7742	0.7558	0.7516	0.7558
MB LBP GradientBoostingClassifier	0.9335	0.8907	0.8886	0.8844	0.8886
MB LBP XGBClassifier	0.9294	0.8802	0.8777	0.8775	0.8777
MB LBP LightGBM	0.9121	0.8486	0.8407	0.8398	0.8407
MB LBP CatBoost	0.9240	0.8638	0.8603	0.8600	0.8603
MB LBP AdaBoost	0.8365	0.7990	0.7673	0.7609	0.7673
MB LBP MLPClassifier	0.8575	0.8098	0.7893	0.7794	0.7839

Table 8 Performances of classification algorithms on hybrid features
Tablica 8. Rezultati klasifikacijskih algoritama primijenjenih na hibridna svojstva

Algorithms *Algoritmi*	**AUC**	**Precision** *Preciznost*	**Recall** *Opoziv*	**F1-Score** *F1-rezultat*	**Accuracy** *Točnost*
RandomForestClassifier	0.9778	0.9420	0.9364	0.9362	0.9364
KNeighborsClassifier	0.8985	0.8986	0.8986	0.8985	0.8986
Support Vector Machine	0.9262	0.9087	0.8896	0.8883	0.8896
DecisionTreeClassifier	0.8755	0.8762	0.8756	0.8755	0.8756
Naive Bayes	0.8822	0.8843	0.8645	0.8627	0.8645
LogisticRegression	0.9036	0.8886	0.8678	0.8660	0.8678
GradientBoostingClassifier	0.9820	0.9545	0.9516	0.9515	0.9516
XGBClassifier	0.9830	0.9538	0.9513	0.9513	0.9513
LightGBM	0.9811	0.9492	0.9470	0.9469	0.9470
CatBoost	0.9800	0.9504	0.9471	0.9470	0.9471
AdaBoost	0.9489	0.9058	0.8927	0.8918	0.8927
MLPClassifier	0.9581	0.9168	0.9072	0.9068	0.9072

Table 9 Accuracy values of all feature extraction and classification algorithms
Tablica 9. Točnost svih algoritama ekstrakcije i klasifikacije svojstava

Algorithms / Algoritmi	***LBP***	***HOG***	***GLCM***	***SOBEL***	***GABOR***	***MB-LBP***	***HYBRID***
RandomForestClassifier	0.9675	0.8838	0.9389	0.8844	0.9496	0.8958	0.9364
KNeighborsClassifier	0.9199	0.8232	0.8907	0.8303	0.9012	0.8308	0.8986
Support Vector Machine	0.8388	0.8350	0.8441	0.7834	0.8622	0.7660	0.8896
DecisionTreeClassifier	0.9050	0.8111	0.8736	0.8098	0.8866	0.8181	0.8756
Naive Bayes	0.8063	0.8342	0.8384	0.7776	0.8580	0.7584	0.8645
LogisticRegression	0.8226	0.8338	0.8294	0.6935	0.8586	0.7558	0.8678
GradientBoostingClassifier	0.9656	0.8775	0.9330	0.8786	0.9523	0.8886	0.9516
XGBClassifier	0.9628	0.8656	0.9217	0.8777	0.9460	0.8777	0.9513
LightGBM	0.9262	0.8595	0.8900	0.8671	0.9146	0.8407	0.9470
CatBoost	0.9539	0.8625	0.9006	0.8732	0.9265	0.8603	0.9471
AdaBoost	0.8398	0.8517	0.8523	0.8332	0.8770	0.7673	0.8927
LMLPClassifier	0.8458	0.8552	0.8578	0.8586	0.8802	0.7879	0.9072

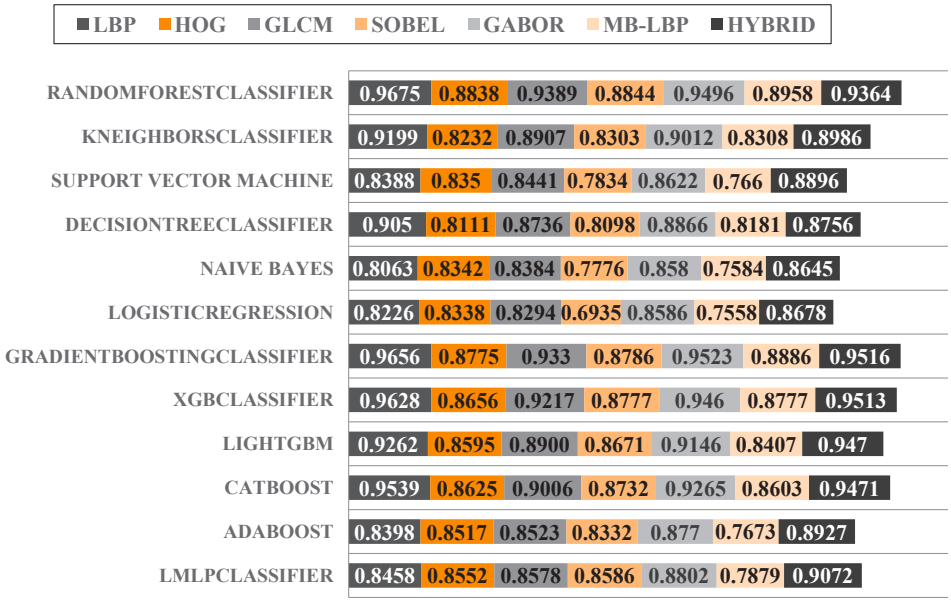

Figure 4 Accuracy values of classification algorithms
Slika 4. Točnost klasifikacijskih algoritama

ture extractors and classifiers used. LBP is very effective in capturing local patterns in the surface texture, which plays a critical role in detecting defects in texture-dense materials such as wood. This feature provides high performance, especially when combined with a powerful classifier such as RandomForestClassifier. On the other hand, HOG is successful in measuring edge density, but may be limited in recognizing

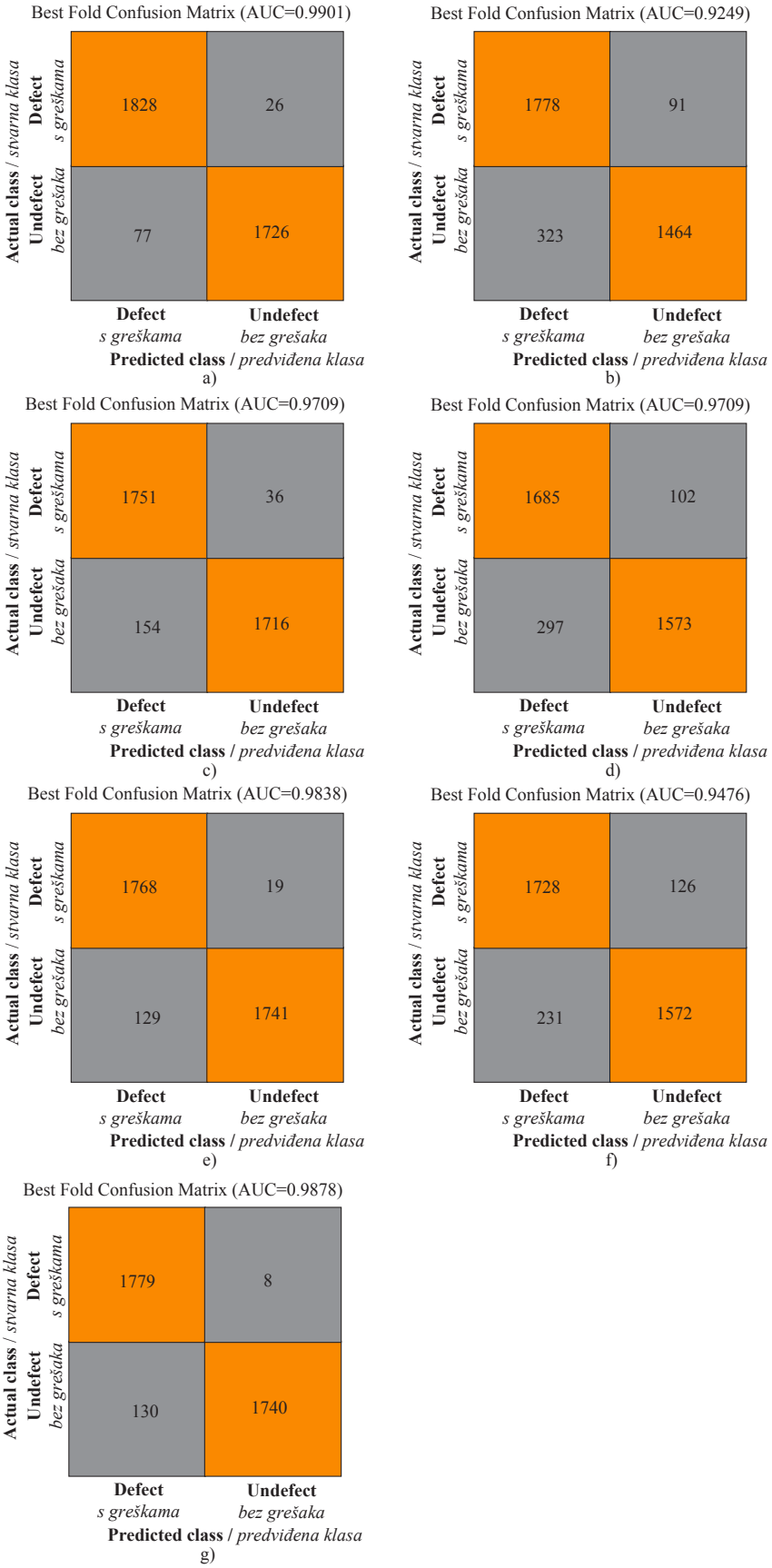

Figure 5 Complexity matrix of the most successful feature extraction and classification algorithms: a) LBP Random Forest Classifier, b) HOG Random Forest Classifier, c) GLCM Random Forest Classifier, d) SOBEL Random Forest Classifier, e) GABOR Gradient Boosting Classifier, f) MB LBP Random Forest Classifier, g) Hybrid Classifier

Slika 5. Matrica složenosti najuspješnijih algoritama ekstrakcije i klasifikacije svojstava: a) LBP Random Forest klasifikator, b) HOG Random Forest klasifikator, c) GLCM Random Forest klasifikator, d) SOBEL Random Forest klasifikator, e) GABOR Gradient Boosting klasifikator, f) MB LBP Random Forest klasifikator, g) hibridni klasifikator

finer defects on the wood surface. Similarly, GLCM is effective in describing texture patterns, but may be insufficient when more complex features are needed in high-dimensional datasets. While RandomForestClassifier stands out with its ability to handle high-dimensional data and reduce overfitting thanks to its ensemble of decision trees, other ensemble learning algorithms such as Gradient Boosting, XGBoost, and CatBoost also show high performance for similar reasons. Simpler modeling techniques such as Naive Bayes and Logistic Regression may show low accuracy in more complex datasets, and may be limited in understanding fine details such as wood surface defects. Although hybrid combinations aim to provide a wider information pool by combining multiple feature extractors, in this study, it was observed that hybrid features could not overcome the effect of individual features. This situation reveals that excessive complexity and redundancy of some features can limit performance. As a result, the obtained performance differences can be attributed to the internal properties of both feature extractors and classifiers and can be explained more clearly in this context.

The confusion matrices of the algorithms showing the most successful results for each feature extraction method on the test set are shown in Figure 5.

In this research, six different feature extraction methods are used and the performances of the same 12 different classifiers are analyzed in each feature extraction. In the experiments, it is observed that the LBP method made the most effective feature extraction. Over 90 % accuracy is achieved with tree-based algorithms on the features extracted with the LBP method. Additionally, the most successful performance of the study is achieved with the LBP-Random Forest combination. The worst performances are obtained for all classifiers in the features extracted with MB-LBP, SOBEL and HOG. Even tree-based ensemble classifiers could not reach 90 % accuracy. GABOR and GLCM extracted the most effective features after LBP.

In terms of classifier performance, tree-based classifiers such as Random Forest, Gradient Boosting and XgBoosting have achieved more successful results for all feature extraction methods in detecting defective wood.

The results obtained in this study show remarkable success compared to previous studies in the literature in wood defect detection. Pölzleitner and Schwingshakl (1992) achieved 95 % accuracy using manual wood classification and feature vectors, but manual methods are known to be less scalable compared to automated approaches. Zhang *et al*. (2015) achieved 92 % accuracy using PCA and compressed sensing methods, but the performance may be limited by the inability of PCA to provide sufficiently robust features in complex datasets. YongHua and Jin-Cong (2015) achieved 91.83 % accuracy with texture-based features such as GLCM and Tamura texture, but these methods do not capture as much detailed information as more modern feature extractors.

In a more advanced study, Li *et al*. (2017) achieved 94 % accuracy with LDA and compressed sensor images, while Li *et al*. (2019) achieved 93 % recall with LBP and local differential excitation methods. These methods, although focusing on texture analysis, were limited in distinguishing more complex surface defects. Urbonas *et al*. (2019) achieved 96.1 % accuracy using Faster R-CNN, and Shi *et al*. (2020) achieved 95.31 % accuracy with Multi-Channel Mask R-CNN. Although these deep learning-based methods provide high accuracy, their computational density and larger dataset requirements stand out as a disadvantage.

The combination of LBP and Random Forest used in this study has shown a competitive success with most of the methods in the literature and has reached an accuracy rate of 96.75 %. In particular, the success of LBP in capturing local texture patterns and the ability of the Random Forest algorithm to process high-dimensional data have made this result possible. In addition, the evaluation of hybrid feature combinations has provided an in-depth analysis, unlike other studies in the literature, but it has been observed that these combinations do not contribute to the performance increase. This situation reveals that excessive complexity may not be beneficial in certain cases. In general, the results of this study provide a strong alternative to the existing methods in the literature and provide both high accuracy and efficiency in the field of wood defect detection.

Since wood is a heterogeneous material, not every feature extraction method may give good results. The focus of this study is to find the most suitable feature extraction method to detect wood defects and to increase the binary classification performance with the obtained features. In this context, studies have been conducted to present the most suitable solution by considering the effects of different methods on the classification success.

LBP (Local Binary Pattern) has been used as a successful feature extraction method for wood defect detection. Wood contains textural differences and subtle defects due to its heterogeneous structure. LBP captures subtle textural changes by comparing each pixel with its surrounding neighboring pixels and thus detects subtle defects. The success of the method is due to the effective modeling of distinct texture structures on the wood surface and the ability to correctly identify small defects. The simple and efficient structure of LBP facilitates working with large data sets and increases the efficiency of the model.

4 CONCLUSIONS
4. ZAKLJUČAK

This study aimed to evaluate the performance of different feature extraction methods and classification algorithms for wood defect detection. Using different feature extraction methods (LBP, HOG, GLCM, SOBEL, GABOR and MB-LBP), with various classification algorithms (RandomForestClassifier, KNeighborsClassifier, Support Vector Machine, DecisionTreeClassifier, Naive Bayes, LogisticRegression, GradientBoostingClassifier, XGBClassifier, LightGBM, CatBoost, AdaBoost and MLPClassifier) has been tested for their defect detection capabilities. Based on the experiments carried out, the following conclusions can be drawn from this article: It has been observed that the LBP method extracts the most effective features in detecting defective wood. In addition, based on the classification results, GABOR and GLCM methods achieved very successful feature extraction. The most successful classification result is achieved by the Random Forest algorithm on LBP features. The performances of Gradient Boosting and Xgboosting classifiers have successful accuracy rates following the Random Forest classifier. In all feature sets, tree-based augmented ensemble methods are more successful than other classical machine learning algorithms. Although SOBEL, MB-LBP and HOG features are less effective than other methods, they provided successful results for detecting defective wood. Accuracy performance varies between 75 % and 97 % using all feature extraction methods and classifier combinations. In experiments performed by combining all features, the accuracy rate did not increase compared to the LBP-Random Forest combination result, but increased compared to other combinations. The most successful classification value obtained in the study is found to be 96.75 %.

In conclusion, this study evaluated how different feature extraction methods and classification algorithms perform in wood defect detection applications. These results provide valuable information that can be used in industrial defect detection and similar applications. According to the results obtained from the findings, the LBP-Random Forest model is expected to give successful results when used in industrial applications for the detection of defective woods.

Different feature extraction methods and different classification algorithms may be used in these fields of study in the future. Studies on wood defect detection can be carried out with deep learning methods. In addition, wood defect detection systems can be developed by extracting features with machine deep learning methods and making classifications with machine learning classification algorithms. Other feature extraction methods not used in this study are left to future studies. Studies on classifying wood defect types using this dataset is also left to future studies. In the future, it will be inevitable to ensure quality standards in production without using computer vision and artificial intelligence learning models in wood quality control processes.

There are several suggestions for future work in the field of deep learning. In particular, advanced architectures such as Vision Transformers (ViT) can improve model performance by performing robust feature extraction on large datasets. In addition, super-resolution methods can extract more details from low-resolution images, making it easier to detect small defects. Generative Adversarial Networks (GANs) can improve the learning capacity of the model by providing data augmentation in cases with few labeled data. Techniques such as attention mechanisms can also allow the model to focus on important areas in the image, allowing for more precise detection of small defects in particular.

Acknowledgements – Zahvala

This study represents a part of Kenan Kılıç's doctoral thesis titled "A Computer Vision-Based Machine Learning Approach for Wood Defect Detection" submitted to the Department of Wood Products Industrial Engineering, Institute of Science, Gazi University.

5 REFERENCES
5. LITERATURA

1. Bloice, M. D.; Stocker, C.; Holzinger, A., 2017: Augmentor: An ımage augmentation library for machine learning. Journal of Open Source Software, 2 (19): 432. https://doi.org/doi:10.21105/joss.00432
2. Breiman, L., 2001: Random forests. Machine learning, 45: 5-32. https://doi.org/10.1023/A:1010933404324
3. Chang, Z.; Cao, J.; Zhang, Y., 2018: A novel image segmentation approach for wood plate surface defect classification through convex optimization. Journal of Forestry Research, 29: 1789-1795. https://doi.org/10.1007/s11676-017-0572-7
4. Chen, K.; Cai, N.; Wu, Z.; Xia, H.; Zhou, S.; Wang, H., 2023b: Multi-scale GAN with transformer for surface defect inspection of IC metal packages. Expert Systems with Applications, 212: 118788. https://doi.org/10.1016/j.eswa.2022.118788
5. Chen, T.; Guestrin, C., 2016: Xgboost: A scalable tree boosting system. In Proceedings of the 22nd acm sigkdd international conference on knowledge discovery and data mining, pp. 785-794. https://doi.org/10.1145/2939672.2939785
6. Chen, Y.; Sun, C.; Ren, Z.; Na, B., 2023a: Review of the current state of application of wood defect recognition technology. BioResources, 18 (1): 2288-2302. https://doi.org/10.15376/biores.18.1.Chen
7. Chen, Z.; Xu, D.; Deng, J.; Chen, Y.; Li, C., 2024: Comparative study on deep-learning-based leather surface defect identification. Measurement Science and Technology, 35 (1): 015402. https://doi.org/10.1088/1361-6501/acfb9f

8. Cortes, C.; Vapnik, V., 1995: Support-vector networks. Machine Learning, 20: 273-297. https://doi.org/10.1007/BF00994018
9. Cover, T.; Hart, P., 1967: Nearest neighbor pattern classification. IEEE transactions on information theory, 13 (1): 21-27. https://doi.org/10.1109/TIT.1967.1053964
10. Dalal, N.; Triggs, B., 2005: Histograms of oriented gradients for human detection. IEEE Computer Society Conference on Computer Vision and Pattern Recognition (CVPR'05), San Diego, CA, USA, 1, 886-893. https://doi.org/10.1109/CVPR.2005.177
11. Daugman, J. G., 1985: Uncertainty relation for resolution in space, spatial frequency and orientation optimized by two-dimensional visual cortical filters. Journal of the Optical Society of America A, 2 (7): 1160-1169. https://doi.org/10.1364/JOSAA.2.001160
12. Duda, R. O.; Hart, P. E., 1973: Pattern classification and scene analysis. John Wiley & Sons, New York and London.
13. Freund, Y.; Schapire, R. E., 1997: A decision-theoretic generalization of on-line learning and an application to boosting. Journal of Computer and System Sciences, 55 (1): 119-139. https://doi.org/10.1006/jcss.1997.1504
14. Friedman, J. H., 2001: Greedy function approximation: a gradient boosting machine. Annals of Statistics, 29 (5): 1189-1232. http://www.jstor.org/stable/2699985 (Accessed Jan. 18, 2024).
15. Galata, D. L.; Mészáros, L. A.; Kállai-Szabó, N.; Szabó, E.; Pataki, H.; Marosi G.; Nagy, Z. K., 2021: Applications of machine vision in pharmaceutical technology: A review. European Journal of Pharmaceutical Sciences, 159: 105717. https://doi.org/10.1016/j.ejps.2021.105717
16. Gao, M.; Qi, D.; Mu, H.; Chen, J., 2021: A transfer residual neural network based on resnet-34 for detection of wood knot defects. Forests, 12 (2): 212. https://doi.org/10.3390/f12020212
17. Haralick, R. M.; Shanmugam, K.; Dinstein, I. H., 1973: Textural features for image classification. IEEE Transactions on Systems, Man and Cybernetics (SMC), 3 (6): 610-621. https://doi.org/10.1109/TSMC.1973.4309314
18. Hoang, K.; Wen, W.; Nachimuthu, A.; Jiang, X. L., 1997: Achieving automation in leather surface inspection. Computers in Industry, 34 (1): 43-54. https://doi.org/10.1016/S0166-3615(97)00019-5
19. Hosmer Jr, D. W.; Lemeshow, S.; Sturdivant, R. X., 2013: Applied logistic regression. John Wiley & Sons, Inc. https://doi.org/10.1002/9781118548387
20. Hu, J.; Song, W.; Zhang, W.; Zhao, Y.; Yilmaz, A., 2019: Deep learning for use in lumber classification tasks. Wood Science and Technology, 53: 505-517. https://doi.org/10.1007/s00226-019-01086-z
21. Humeau-Heurtier, A., 2019: Texture Feature Extraction Methods: A Survey. IEEE Access, 7: 8975-9000. https://doi.org/10.1109/ACCESS.2018.2890743
22. Jian, C.; Gao, J.; Ao, Y., 2017: Automatic surface defect detection for mobile phone screen glass based on machine vision. Applied Soft Computing, 52: 348-358. https://doi.org/10.1016/j.asoc.2016.10.030
23. Ke, G.; Meng, Q.; Finley, T.; Wang, T.; Chen, W.; Ma, W.; Ye, Q & Liu, T.Y., 2017: Lightgbm: A highly efficient gradient boosting decision tree. *Advances in neural information processing systems*, 30.
24. Kodytek, P.; Bodzas, A.; Bilik, P., 2021: A large-scale image dataset of wood surface defects for automated vision-based quality control processes. F1000Research, 10: 581. https://doi.org/10.12688/f1000research.52903.2
25. Lei, Q.; Zhong, J.; Wang, C.; Li, X., 2024: Integrating crack causal augmentation framework and dynamic binary threshold for imbalanced crack instance segmentation. Expert Systems with Applications, 240: 122552. https://doi.org/10.1016/j.eswa.2023.122552
26. Lewis, D. D., 1998: Naive (Bayes) at forty: The independence assumption in information retrieval. In: Machine Learning: ECML-98. ECML 1998. Lecture Notes in Computer Science, vol 1398. Springer, Berlin, Heidelberg. https://doi.org/10.1007/BFb0026666
27. Li, C.; Zhang, Y.; Tu, W.; Jun, C.; Liang, H.; Yu, H., 2017: Soft measurement of wood defects based on LDA feature fusion and compressed sensor images. Journal of Forestry Research, 28: 1285-1292. https://doi.org/10.1007/s11676-017-0395-6
28. Li, S.; Li, D.; Yuan, W., 2019: Wood defect classification based on two-dimensional histogram constituted by LBP and local binary differential excitation pattern. IEEE Access, 7: 145829-145842. https://doi.org/10.1109/ACCESS.2019.2945355
29. Liu, G.; Li, F., 2021: Fabric defect detection based on low-rank decomposition with structural constraints. Visual Computer, 38: 639-653. https://doi.org/10.1007/s00371-020-02040-y
30. Liu, G.; Zheng, X., 2020: Fabric defect detection based on information entropy and frequency domain saliency. Visual Computer, 37: 515-528. https://doi.org/10.1007/s00371-020-01820-w
31. Liu, X.; Song, L.; Liu, S.; Zhang, Y., 2021: A review of deep-learning-based medical image segmentation methods. Sustainability, 13: 1224. https://doi.org/10.3390/su13031224
32. Liu, Y.; Xu, K.; Xu, J., 2019: An improved MB-LBP defect recognition approach for the surface of steel plates. Applied Sciences, 9 (20): 4222. https://doi.org/10.3390/app9204222
33. Mu, H.; Qi, D., 2009: Pattern recognition of wood defects types based on Hu invariant moments. In: 2nd International Congress on Image and Signal Processing, Tianjin, China, pp. 1-5. https://doi.org/10.1109/CISP.2009.5303866
34. Mutlag, W. K.; Ali, S. K.; Aydam, Z. M.; Taher, B. H., 2020: Feature extraction methods: A review. Journal of Physics: Conference Series, 1591: 012028. https://doi.org/10.1088/1742-6596/1591/1/012028
35. Norlander, R.; Grahn, J.; Maki, A., 2015: Wooden knot detection using convNet transfer learning. In: Image Analysis, SCIA, Lecture Notes in Computer Science, 9127. Springer, Cham. https://doi.org/10.1007/978-3-319-19665-7_22
36. Ojala, T.; Pietikainen, M.; Maenpaa, T., 2002: Multiresolution gray-scale and rotation invariant texture classification with local binary patterns. IEEE Transactions on pattern analysis and machine intelligence, 24 (7): 971-987. https://doi.org/10.1109/TPAMI.2002.1017623
37. Pölzleitner, W.; Schwingshakl, G., 1992: Real-time surface grading of profiled wooden boards. Industrial Metrology, 2 (3-4): 283-298. https://doi.org/10.1016/0921-5956(92)80008-H
38. Prokhorenkova, L.; Gusev, G.; Vorobev, A.; Dorogush, A. V.; Gulin, A., 2018: CatBoost: unbiased boosting with categorical features. Advances in neural information processing systems, 31.
39. Qi, D.; Zhang, P.; Jin, X.; Zhang, X., 2010: Study on wood image edge detection based on Hopfield neural network. IEEE International Conference on Information and

Automation, ICIA 2010. https://doi.org/10.1109/ICINFA.2010.5512014
40. Quinlan, J. R., 1986: Induction of decision trees. Machine Learning, 1: 81-106. https://doi.org/10.1007/BF00116251
41. Raheja, J. L.; Kumar, S.; Chaudhary, A., 2013: Fabric defect detection based on GLCM and Gabor filter: A comparison. Optik, 124 (23): 6469-6474. https://doi.org/10.1016/j.ijleo.2013.05.004
42. Salau, A. O.; Jain, S., 2019: Feature extraction: a survey of the types, techniques, applications. In: International conference on signal processing and communication (ICSC), IEEE, pp. 158-164. https://doi.org/10.1109/ICSC45622.2019.8938371
43. Schmoldt, D. L.; Li, P.; Abbott, A. L., 1997: Machine vision using artificial neural networks with local 3D neighborhoods. Computers and Electronics in Agriculture, 16 (3): 255-271. https://doi.org/10.1016/S0168-1699(97)00002-1
44. Shahrabadi, S.; Castilla, Y.; Guevara, M.; Magalhães, L. G.; Gonzalez, D.; Adão, T., 2022: Defect detection in the textile industry using image-based machine learning methods: a brief review. Journal of Physics: Conference Series, 2224: 012010. https://doi.org/10.1088/1742-6596/2224/1/012010
45. Shi, J.; Li, Z.; Zhu, T.; Wang, D.; Ni, C., 2020: Defect detection of industry wood veneer based on NAS and multi-channel mask R-CNN. Sensors, 20 (16): 4398. https://doi.org/10.3390/s20164398
46. Tao, X.; Zhang, D.; Ma, W.; Liu, X.; Xu, D., 2018: Automatic metallic surface defect detection and recognition with convolutional neural networks. Applied Sciences, 8 (9): 1575. https://doi.org/10.3390/app8091575
47. Tsai, D. M.; Huang, C. K., 2019: Defect detection in electronic surfaces using template-based fourier image reconstruction. IEEE Transactions on Components. Packaging and Manufacturing Technology, 9 (1): 163-172. https://doi.org/10.1109/TCPMT.2018.2873744
48. Urbonas, A.; Raudonis, V.; Maskeliūnas, R.; Damaševičius, R., 2019: Automated identification of wood veneer surface defects using faster region-based convolutional neural network with data augmentation and transfer learning. Applied Sciences, 9 (22): 4898. https://doi.org/10.3390/app9224898
49. Wu, C.; Zou, X.; Yu, Z., 2022: A detection method for wood surface defect based on feature fusion. In: 4th International Conference on Frontiers Technology of Information and Computer (ICFTIC), Qingdao, China, pp. 876-880. https://doi.org/10.1109/ICFTIC57696.2022.10075158
50. Xie, D. Y., 2013: Analysis to situation and countermeasure of wood manufacture industry of our country. Forest Investigation Design, 3: 85-92. https://doi.org/10.3969/j.issn.1673-4505.2013.03.038
51. YongHua, X.; Jin-Cong, W., 2015: A study on the determination of wood surface defects based on texture features. Optics, 126 (19): 2231-2235. https://doi.org/10.1016/j.ijleo.2015.05.101
52. Zhang, T.; Wang, Z.; Li, F.; Zhong, H.; Hu, X.; Zhang, W.; Zhang, D.; Liu, X., 2023: Automatic detection of surface defects based on deep random chains. Expert Systems with Applications, Part A, 229: 120472. https://doi.org/10.1016/j.eswa.2023.120472
53. Zhang, Y.; Xu, C.; Li, C.; Yu, H.; Cao, J., 2015: Wood defect detection method with PCA feature fusion and compressed sensing. Journal of Forestry Research, 26 (3): 745-751. https://doi.org/10.1007/s11676-015-0066-4

Corresponding address:

KENAN KILIÇ
Gazi University, Graduate School of Natural and Applied Sciences, Department of Wood Products Industrial Engineering, Ankara, TURKEY, e-mail: kenan.kilic@bozok.edu.tr

Miroslav Němec[1], Luboš Prokůpek[2], Jaromír Hradecký[1], Vojtěch Obst[2], Tomáš Pipíška[3], Štěpán Hýsek*[4]

Properties of Phenol-Formaldehyde Resin Modified with Kraft Lignin for Particleboard Production

Svojstva fenol-formaldehidne smole modificirane kraft ligninom za proizvodnju ploča iverica

ORIGINAL SCIENTIFIC PAPER
Izvorni znanstveni rad
Received – prispjelo: 27. 9. 2024.
Accepted – prihvaćeno: 9. 1. 2025.
UDK: 630*86; 674.812
https://doi.org/10.5552/drvind.2025.0232

ABSTRACT • *Lignin is a natural polymer with a phenolic structure, which makes it suitable as a substitute in phenol-formaldehyde (PF) resins. In this study, unmodified kraft lignin was used as a substitute in a commercial phenol-formaldehyde resin, with the substitution rate being 10 %. This resin was further used to produce a single-layer particleboard using hot pressing in a laboratory press. Results of physical and mechanical tests showed that the addition of lignin to the PF resin negatively affected these properties, while particleboards bonded with lignin-modified PF resin met the requirements of the standard for lower-class particleboards. Scanning electron microscopy confirmed cohesive failures in ruptured particleboards bonded with both the reference resin and the lignin-modified PF resin. For the lignin-modified PF resin, particles of undissolved lignin were found in the resin. Further testing showed no difference in the emission of volatile organic compounds between the variants.*

KEYWORDS: *Wood-based composite; lignin; adhesive; mechanical properties; physical properties*

SAŽETAK • *Lignin je prirodni polimer fenolne strukture, što ga čini prikladnom zamjenom za fenol-formaldehidne (PF) smole. U ovom je istraživanju nemodificirani kraft lignin upotrijebljen kao zamjena za komercijalnu fenol-formaldehidnu smolu, a stopa supstitucije bila je 10 %. Takva je smola dalje rabljena za proizvodnju jednoslojne iverice vrućim prešanjem u laboratorijskoj preši. Rezultati ispitivanja fizičkih i mehaničkih svojstava tako proizvedenih ploča pokazali su da dodatak lignina PF smoli negativno utječe na svojstva ploča, ali ipak ploče iverice s PF smolom modificiranom ligninom udovoljavaju standardima za iverice niže klase. Pretražna elektronska mikroskopija potvrdila je kohezivne lomove u polomljenim ivericama s referentnom smolom i PF smolom modificiranom*

* Corresponding author
[1] Author is researcher at Czech University of Life Sciences Prague, Faculty of Forestry and Wood Sciences, Prague, Czech Republic. https://orcid.org/0009-0009-1712-1320
[2] Author is researcher at University of Pardubice, Faculty of Chemical Technology, Institute of Chemistry and Technology of Macromolecular Materials, Pardubice, Czech Republic. https://orcid.org/0000-0003-1621-2705
[3] Author is researcher at Mendel University in Brno, Faculty of Forestry and Wood Technology, Department of Wood Science and Technology, Brno, Czech Republic. https://orcid.org/0000-0001-8096-4376
[4] Author is researcher at University of Natural Resources and Life Sciences, Department of Material Sciences and Process Engineering, Institute of Wood Technology and Renewable Materials, Vienna, Austria. https://orcid.org/0000-0001-8642-0847

ligninom. U PF smoli modificiranoj ligninom pronađene su čestice neotopljenog lignina. Daljnjim ispitivanjima među istraživanim varijantama ploča iverica nije uočena razlika u emisiji hlapljivih organskih spojeva.

KLJUČNE RIJEČI: *kompozit na bazi drva; lignin; ljepilo; mehanička svojstva; fizička svojstva*

1 INTRODUCTION
1. UVOD

Particleboard (PB) is a composite material consisting of wood particles that are bonded together using synthetic adhesives, primarily urea-formaldehyde (UF), phenol-formaldehyde (PF), melamine-formaldehyde (MF), and isocyanate (Jiang *et al*., 2023). The European production of PB mainly used for furniture, interior elements and cladding was approximately 44 million m^3 in 2022 (42 % of global production) (Scharf *et al*., 2023). Wood particles of lower quality wood, wood residues (sawdust and shavings), recycled wood or non-wood alternative materials can be used for PB production (Auriga *et al*., 2024; Niemz and Sandberg, 2022). It is the use of recycled materials and the possibility to recycle the PB itself that is their essence in the circular economy (Petrova *et al*., 2023). The possibility of using lignin in binders for PB production would further enhance the environmental aspect of this product.

PF are synthetic resins produced by reacting phenol with formaldehyde (Kumar and Pizzi, 2019). The term synthetic resin means that the substances for their synthesis are products of the petrochemical industry (Zhao *et al*., 2011).

For wood and paper-based materials, PF resins are currently one of the most widely used resins for their production (Thébault *et al*., 2017). The reason for their considerable use is the relatively low cost associated with their resistance to moisture, weathering and high temperatures (Pizzi, 2014). Specifically, they are predominantly utilized in the production of wood-based composites that must be resistant to environmental factors (Pilato, 2010).

The use of formaldehyde-based resins results in the release of formaldehyde into the environment, which is a significant concern due to its carcinogenic effects (IARC, 2023). At the same time, phenol is also classified as a highly toxic substance and its exposure limits are carefully controlled (Gardziella *et al*., 2000).

Lignin is a complex polymeric substance located within the cell walls of vascular plants. It represents the second most abundant organic polymer in nature, following cellulose (Abhilash and Thomas, 2017; Nadányi *et al*., 2022). Its main function is to strengthen secondary cell walls and promote water transport in plants (Whetten and Sederoff, 1995). Its extraction is often linked to industrial processes such as pulp production in the paper industry. The by-product of this process, black liquor, is a source of lignin for further use (Bajpai, 2018).

In terms of utilization, lignin has traditionally been used for combustion in recovery boilers to provide additional energy (Dessbesell *et al*., 2020). However, modern technologies allow lignin to be used in various sectors. For example, it can be used in the production of polymers (resins or plastics), carbon fibers, as a binder in pelletizing, and it also finds applications in the pharmaceutical and cosmetic industries. Last but not least, other valuable chemical products can be obtained from lignin (Calvo-Flores *et al*., 2015).

The adhesive properties of lignin and its potential use in adhesives have been studied for over 100 years, but only a few industrial applications have been developed in that time. The appeal of lignin as a substitute in wood adhesives is attributed to its natural origin, phenolic characteristics, high availability, and low cost (Karthäuser *et al*., 2021; Saražin *et al*., 2022).

The biggest difficulty in the application of lignin in adhesive systems is its low reactivity. This leads to slow curing of adhesives, which is crucial in the production of composite materials. Untreated lignin is economically disadvantageous for applications that require fast curing. However, the reactivity of lignin can be enhanced through various modifications, such as phenolation, methylation, and demethylation, which improve its reactivity with formaldehyde (Hemmilä *et al*., 2013; Zhang *et al*., 2013).

It was the high phenolic content of lignin that led to the idea of the possibility of replacing phenolics with lignin in the production of PF resins (Solt *et al.*, 2019), where the resulting lignin-phenol-formaldehyde (LPF) resins were tested for use in the production of MDF, DTD or OSB to evaluate their potential applications (Jiang *et al*., 2021).

Based on many studies, it has been shown that the strength of the bonded joint inside wood-based composite materials decreases with increasing the content of unmodified lignin (Ghorbani *et al*., 2016; Moubarik *et al*., 2013; Pinheiro *et al*., 2017; Yang *et al*., 2015). This is the reason for the lower reactivity of lignin and, therefore, up to 30 – 50 % of phenol can be replaced by unmodified lignin in PF resins without significant changes in the resin properties (Xu and Ferdosian, 2017). The molecular weight of lignin, which affects the final viscosity of the synthesized resin, is an essential property for some applications *(Huang et al*., 2022).

The price of lignin depends on its quality and purity, with lower quality lignin priced at less than USD

300/t, while high quality lignin can exceed USD 750/t (Mason, 2021). Lignin modification increases the reactivity of lignin, but the feedstock and energy costs lead to an increase in the price of the modified lignin *(Liu et al., 2024; Nadányi et al., 2022; Paananen et al*., 2021) and these are challenging technological steps.

The primary objective of this study is to examine the effects of incorporating kraft lignin as an additive in phenol-formaldehyde (PF) resins on the properties of particleboards (PBs) produced using these modified resins. By applying the developed resins in PB manufacturing, the study aims to yield critical insights into the interactions between the resin and wood during the board formation process, as well as their influence on the mechanical and physical properties of the resulting particleboards. The results of the properties will then be compared with the requirements of ČSN EN 310 (1995) in order to compare the individual parameters with each other against this standard and subsequently classify them into a quality category.

The broader aim of this research is to develop a kraft lignin-modified PF resin with the potential for large-scale industrial production.

2 MATERIALS AND METHODS
2. MATERIJALI I METODE

2.1 Materials
2.1. Materijali

Softwood particles supplied by DDL Lukavec company (Dřevozpracující družstvo Lukavec, Czech Republic) were used to produce the middle layer of particleboards with a moisture content of 8 %. The phenol-formaldehyde resin Lignofen G/3/D (LERG SA, Poland) was used. This is a resol-type resin of dark red color that cures at a temperature of 130 °C, with a curing time of 80 to 120 seconds.

Kraft lignin used in the preparation of lignin-phenol-formaldehyde resin was obtained by precipitation from hardwood black liquor by Mondi company (Mondi SCP, a.s., Slovakia). Isolation was carried out by adding sulfuric acid to the black liquor until pH 2-3 was reached and lignin was precipitated. Subsequently, the lignin was filtered and washed three times with distilled water to achieve pH 5-6. After reaching the desired pH, the lignin was dried at 60 °C and then ground to the desired fraction using a knife mill IKA MF 10 basic (IKA, Germany).

2.2 Production of lignin-phenol-formaldehyde resins
2.2. Proizvodnja lignin-fenol-formaldehidnih smola

Phenol-formaldehyde resins with 0 % (reference) and 10 % lignin content (relative to the dry matter of the adhesive and lignin) were prepared. The desired amount of lignin was added to the phenol-formaldehyde resin. The lignin was first mixed using an anchor stirrer and then, for greater homogeneity of the adhesive mixture, a disperser Yellow line DI 25 basic (IKA, Germany) was used, and the mixture was stirred for 5 minutes.

2.3 Particleboard production
2.3. Proizvodnja iverice

For testing the properties of particleboards bonded with PF resin with 0 % and 10 % lignin content, single-layer PBs 12 mm thick with a target density of 650 kg/m^3 were manufactured. To maintain the correct resin-to-wood ratio, the moisture content of the particles was first measured using a moisture analyzer MB-23 (Ohaus, USA). Then, the desired amount of particles was weighed and placed into a rotary drum blender. The resin content in PB was chosen to be 10 % in dry matter of the resin. The adhesive mixture was heated to 60 °C to reduce viscosity and applied by spraying under pressure in the spreader to ensure even distribution onto the particles.

Subsequently, the adhesive-coated particles were layered into a mold, after which the particle mat was subjected to compression using a hydraulic press. The samples were pressed under a pressure of 3.5 MPa at a temperature of 140 °C for a duration of 4 minutes. Following the pressing process, the boards were removed and conditioned at 20 °C and 65 % relative humidity for a period of 96 hours.

2.4 Methodology of particleboards testing
2.4. Metodologija ispitivanja iverice

2.4.1 Vertical density profile
2.4.1. Gustoća iverica po debljini

Vertical density profile (VDP) analysis was performed employing a DPX300-LTE X-ray density analyzer (IMAL PAL GROUP, Italy). Four samples, each measuring 50 mm × 50 mm × 12 mm, were subjected to measurement for every variant. The VDP values were then averaged within each variant to construct density curves, enabling subsequent comparison among the individual variants VDP curves.

2.4.2 Moisture uptake and thickness swelling
2.4.2. Upijanje vode i debljinsko bubrenje

To evaluate moisture resistance, 20 samples with dimensions of 50 mm × 50 mm were prepared for each variant. The samples were first dried in an oven at 103 °C until a constant weight was achieved, ensuring a moisture content of 0 %. Initial thickness (t_0) and weight (m_0) measurements were recorded for the dried samples.

Following this, the samples were immersed in water at 20 °C for 24 hours. After immersion, the samples

were placed on a mat for 10 minutes to allow surface water to drain. Subsequently, measurements of thickness (t_w) and weight (m_w) were taken for each sample.

From these measurements, thickness swelling (TS) and moisture uptake (MU) were calculated as percentages using the following equations (ČSN EN 317, 1995):

$$TS\ (\%) = \frac{t_w - t_0}{t_0} \cdot 100 \quad (1)$$

Where t_w represents the board thickness after 24 hours of water immersion, and t_0 denotes the board thickness after drying to 0 % moisture content.

$$MU\ (\%) = \frac{m_w - m_0}{m_0} \cdot 100 \quad (2)$$

Where m_w represents the board weight after 24 hours of water immersion, and m_0 denotes the board weight after drying to 0 % moisture content.

2.4.3 Bending strength
2.4.3. Čvrstoća na savijanje

Bending strength (*MOR*) and modulus of elasticity in bending (*MOE*) were evaluated in accordance with the (ČSN EN 310, 1995) standard, utilizing the three-point bending test method on a TT 2850 universal testing machine (TIRA, Germany). For each variant, ten particleboard samples with dimensions of 290 mm × 50 mm × 12 mm were prepared. The support span (l) was set at 240 mm. *MOR* and *MOE* values were subsequently calculated using the standard equations prescribed in the testing protocol:

$$MOR\ (MPa) = \frac{3 \cdot F_{max} \cdot l}{2 \cdot b \cdot t^2} \quad (3)$$

Where F_{max} represents the maximum force applied to the sample, measured in newtons (N), l denotes the distance between supports (240 mm), b is the width, and t is the thickness of the sample, both measured in millimeters (mm).

$$MOE\ (MPa) = \frac{l^3 \cdot (F_2 - F_1)}{4 \cdot b \cdot t^3 \cdot (a_2 - a_1)} \quad (4)$$

Where l represents the support span of 240 mm, F_1 corresponds to 10 % and F_2 to 40 % of the maximum load (F_{max}) in newtons (N), and b and t represent the width and thickness of the sample, respectively, in millimeters (mm). Let a_1 and a_2 denote the deflection increments at the center of the test specimen, measured in millimeters (mm), corresponding to the load difference between F_1 and F_2.

2.4.4 Internal bonding
2.4.4. Čvrstoća na raslojavanje

The determination of internal bonding (*IB*) was conducted in accordance with the procedures specified in ČSN EN 319, 1994. For each variant, ten samples with dimensions of 50 mm × 50 mm × 12 mm were prepared. The exact surface dimensions of each sample were measured prior to testing. The samples were then bonded to beech wood boards using Bison Power adhesive, a two-component polyurethane glue, in preparation for *IB* testing.

After bonding, the samples were allowed to cure under constant pressure for 24 hours. The *IB* test was performed using a TT 2850 universal testing machine (TIRA, Germany). IB values were calculated using the specified equation:

$$IB\ (MPa) = \frac{F_{max}}{a \cdot b} \quad (5)$$

Where F_{max} denotes the maximum force applied to the sample, measured in newtons (N), while a represents the length and b signifies the width of the sample, both measured in millimeters (mm).

2.4.5 Microscopic analysis
2.4.5. Mikroskopska analiza

The PB samples were subjected to Scanning Electron Microscopy (SEM) analysis using a MIRA 3 electron microscope (Tescan Orsay Holding, Czech Republic) equipped with a secondary electron detector and operated at 15 kV acceleration voltage (Hýsek and Żółtowska, 2022). After the internal bonding test, breached samples were selected for SEM examination. Prior to microscopic sample preparation, the samples were coated with a thin layer of gold using a sputtering technique.

2.4.6 Volatiles emission analysis
2.4.6. Analiza emisije hlapljivih spojeva

Differences among the samples were investigated using solid-phase microextraction (SPME) coupled with two-dimensional comprehensive gas chromatography and time-of-flight mass spectrometry (GC×GC-TOF-MS).

The gas chromatograph used was an Agilent Technologies 7890B (USA), equipped with an HP-5MS UI capillary column (30 m, 0.25 mm inner diameter, 0.25 µm film thickness, Agilent USA). This was coupled via a consumable-free modulator to a second-dimensional column, VF-17 (1.5 m, 0.1 mm inner diameter, 0.1 µm film thickness, Agilent USA). Helium was employed as the carrier gas at a flow rate of 1 ml/min. A splitless injection was performed using a hot split/splitless injector set at 275 °C. After a 2-minute solvent delay, the oven temperature was raised from an initial 40 °C at a rate of 5 °C/min to 120 °C, followed by an increase of 20 °C/min to 300 °C. The second-dimensional GC oven and modulator adhered to this temperature program with offsets of 5 °C and 15 °C, respectively. The modulation period was set to 5 seconds, with a hold time of 2 minutes, resulting in a total GC run time of 29 minutes. The separated compounds were ionized in the ion source of the TOF mass spectrometer

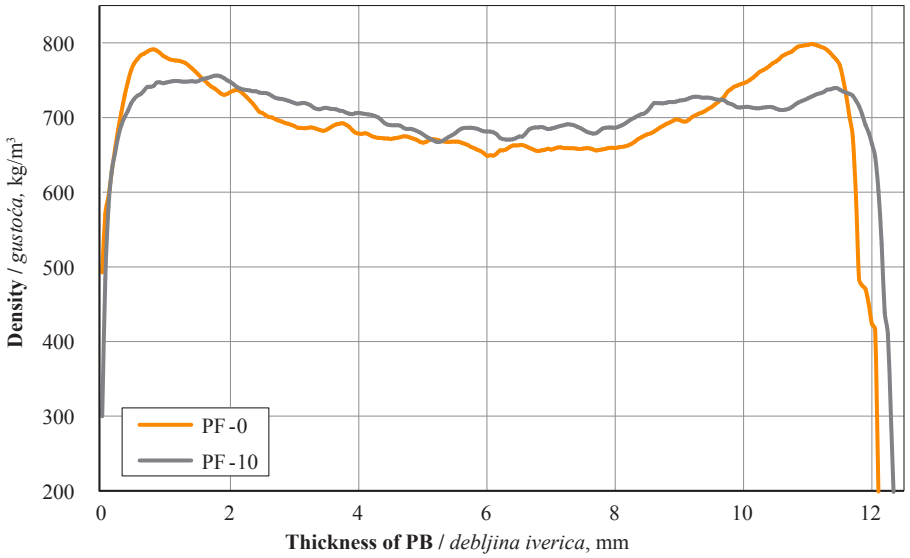

Figure 1 Vertical density profile of particleboards
Slika 1. Gustoća iverica po debljini

at 70 eV in electron impact mode, with full spectral information (35–500 Da) recorded at a rate of 100 times per second.

For tentative identification of the compounds, spectral similarity was assessed by comparing the measured and deconvoluted spectra with mass spectra in the National Institute of Standards and Technology mass spectral library (NIST, 2017).

3 RESULTS AND DISCUSSION
3. REZULTATI I RASPRAVA

3.1 Vertical density profile
3.1. Gustoća iverica po debljini

The vertical density profile (VDP) graph (Figure 1) illustrates that both variants exhibit highly comparable VDP curves, characterized by increased density at the surfaces and reduced density in the central region of the particleboard (PB). This phenomenon can be attributed to the compression of the PB. Notably, the PF-0 samples demonstrate higher density in the surface layers compared to the PF-10 samples, which exhibit a relatively flat VDP profile. The reason for the more flat VDP is probably due to the higher viscosity of the lignin-containing resin, which resulted in a less uniform distribution of the adhesive on the individual wood particles. However, the results indicate that the lignin content in the resin did not significantly influence the density distribution across the cross-section of the board.

3.2 Moisture uptake and thickness swelling
3.2. Upijanje vode i debljinsko bubrenje

The results of MU (Figure 2A) and TS (Figure 2B) show that the addition of lignin had a negative effect on the moisture interaction with the particleboards compared to the reference PF resin, which reaches the values required by (ČSN EN 302-1, 2013) for class P3. Although kraft lignin is inherently hydrophobic, it can be posited that the negative moisture interaction observed in PF bonded particleboards containing lignin is

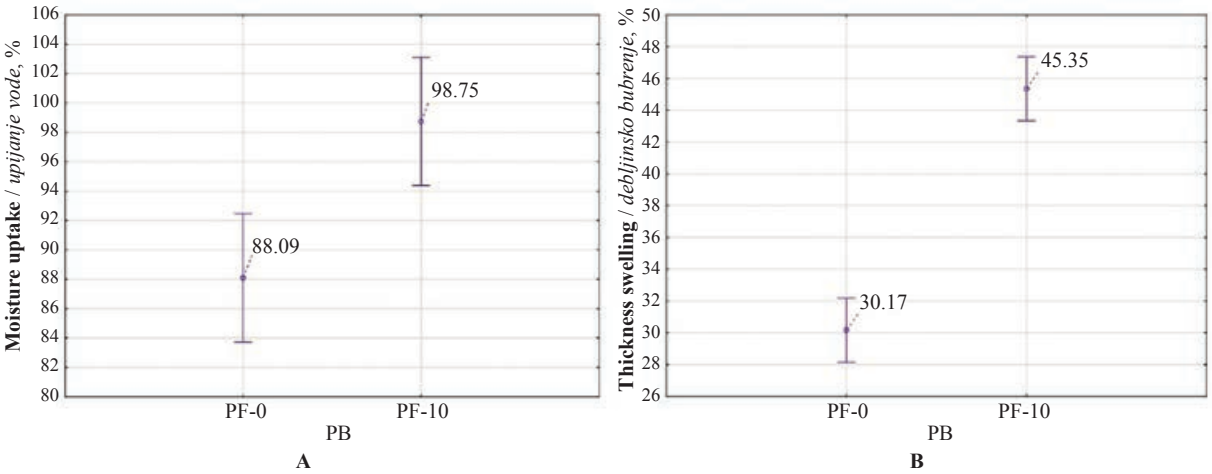

Figure 2 Moisture uptake (A) and thickness swelling (B) of particleboards
Slika 2. Upijanje vode (A) i debljinsko bubrenje (B) iverica

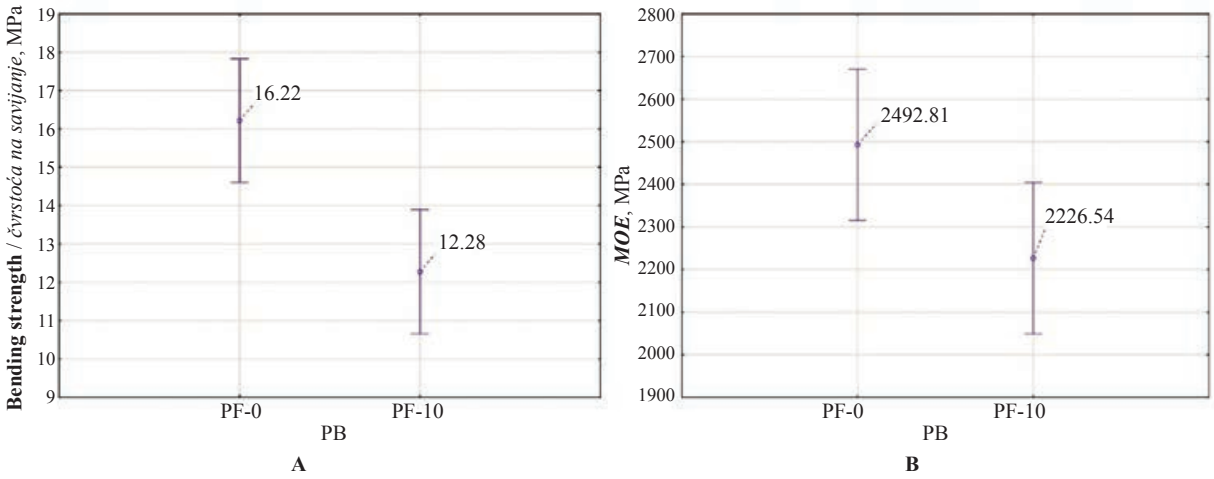

Figure 3 Bending strength (A) and modulus of elasticity (B) of particleboards
Slika 3. Čvrstoća na savijanje (A) i modul elastičnosti (B) iverica

attributable to the presence of lignin in the resin. This may lead to imperfect bonding sites between the wood particles and the resin, facilitating enhanced moisture penetration into the particleboard structure. Electron microscope images of the glued joint confirm our hypothesis (see chapter *3.5 Microscopic analysis*).

Similar results, where increasing substitution of unmodified lignin in PF resins leads to increased moisture uptake, were obtained in a study by (Younesi-Kordkheili, 2022). Here, the results are attributed to the degradation of free lignin particles by water absorption, since these particles, due to their nature, do not contribute to crosslinking with phenol and formaldehyde.

(Pizzi, 2014) further reports that, upon curing, PF resin forms methylene bridges, which are resistant to hydrolysis. In contrast, PF resins with added lignin form different bonds (e.g., C-O) that are more sensitive to moisture.

3.3 Bending properties
3.3. Svojstva savijanja

The incorporation of lignin also adversely affected the mechanical properties of the tested particleboards. With 10 % lignin replacement in PF resin, a significant decrease in PB properties can be seen compared to the use of commercial resin. The boards bonded with commercial resin reached the requirements for P4 class of PB according to (ČSN EN 302-1, 2013) (15 MPa and 2300 MPa) in *MOR* (Figure 3A) and *MOE* (Figure 3B) results (16.22 MPa and 2492.81 MPa). The boards bonded with PF-10 resin from the *MOR* and *MOE* point of view (12.28 MPa and 2226.54 MP) meet the requirements for PB category P2 for furniture purposes according to (ČSN EN 302-1, 2013) (11 MPa and 1800 MPa).

The findings of the study conducted by (Younesi-Kordkheili, 2022) indicate that the *MOR* and *MOE* of particleboard test samples decline as the proportion of kraft lignin in PF resins increases. This reduction is attributed to the lower reactivity of kraft lignin, resulting in a diminished formation of hydroxyl bonds. This reduces the crosslinking between lignin and resin components, causing a decrease in the cohesive strength of cured resin within PB.

The lower results of *MOR* and *MOE* of the PF-10 variant were expected due to the lower density in the surface layers of the PF-10 variant seen in the VDP results.

3.4 Internal bonding
3.4. Čvrstoća na raslojavanje

The *IB* results again show a decrease in mechanical properties for PB bonded with resin with the addition of lignin. However, despite the drop from 0.9 MPa for PF-0 samples to 0.57 MPa for PF-10 bonded boards, these boards met the requirements of (ČSN EN 302-1, 2013) for class P5 (0.45 MPa), and the results are only slightly below the 0.6 MPa required for class P6 boards.

In the tested samples, black colored areas could be observed inside the PB structure bonded with PF-10

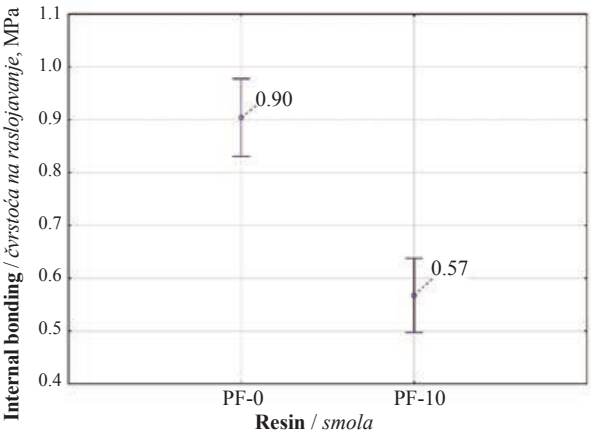

Figure 4 Internal bonding of particleboards
Slika 4. Čvrstoća iverica na raslojavanje

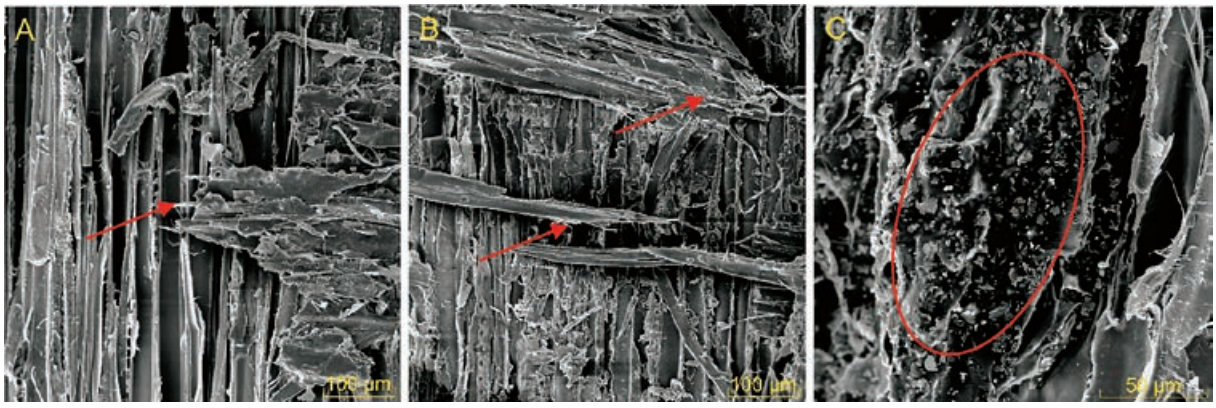

Figure 5 SEM images of ruptured samples of (A) PF-0 variant, (B) PF-10 variant showing cohesive failure of wood (red arrows) and (C) PF-10 variant showing lignin cumulation (red ellipse)
Slika 5. SEM slike polomljenih uzoraka: A varijanta PF-0, i B varijanta PF-10 pokazuju kohezijski lom po drvu (crvene strelice), a C varijanta PF-10 pokazuje nakupljanje lignina (crvena elipsa)

resin after the test. These spots identified clusters of lignin particles that were poorly mixed in the resin and could have caused poor bonding between the wood particles and the resin during manufacturing, which would have resulted in a deterioration of the mechanical properties of these PBs.

In their study, Donmez Cavdar *et al.* (2008) report that IB is very sensitive to the distribution of resin on the particles and to the VDP of individual panels. Here we assume that the decrease in IB for the PF-10 variant is partly due to the slightly lower density of the PB core layer.

Unmodified kraft lignin is less reactive and needs longer pressing time (Hu *et al*., 2011). In a previous study by (Němec *et al*., 2023), focusing on the production of lignin-PF resins for paper-based laminates, the effect of incomplete dissolution of lignin particles in the prepared resin was also observed, even with higher temperatures and longer pressing times. At the same time, extending the pressing time would significantly increase the economics of commercial scale PB production. This resulted in an increase in the molecular weight of the adhesive and therefore a deterioration in adhesion. Indeed, undissolved lignin molecules can behave as impurities forming a weak bond between the substrate, leading to a reduction in mechanical properties.

3.5 Microscopic analysis
3.5. Mikroskopska analiza

Figure 5a-b depicts the character of bond rupture in the ruptured boards. In both cases, cohesive failure of wood was observed, identifying the high performance of the adhesive variants used. In contrast to urea-formaldehyde resin modified with lignin, adhesive failures between wood and adhesive were not observed (Němec *et al*., 2024). However, thanks to the manual manufacturing of adhesive as well as the whole composite, insufficient dispersed lignin in the PF resin was found (Figure 5c). This failure of desperation could contribute to the lower mechanical properties of the composites in comparison with the reference.

3.6 Volatiles emission analysis
3.6. Analiza emisije hlapljivih spojeva

Typical compounds for wood-based materials e.g. terpenes, aldehydes and short chain fatty acids were detected in both board samples. Comparing the intensity of each selected compound in gas-chromatographic record of both samples, it was proved that both emitted the same profile of compounds. Within uncertainty of measurement, the intensity of responses, showing concentrations of compounds, was the same with exception of acetic acid. Modification of adhesive formula by addition of lignin leaded to significant (by 55 % lower) decrease in emission of this compound. While acetic acid is known to be evaporating from wood fibreboard containing phenolic glue (Roffael, 2017), it can be also used as a reactant in acetylation of kraft lignin (de Oliveira *et al*., 2020). In this reaction, the hydroxyl groups in lignin react with acetic acid, leading to the formation of acetylated lignin and water as a by-product. We assume that the emission decrease is due to the reaction of the present acetic acid with added lignin.

4 CONCLUSIONS
4. ZAKLJUČAK

Replacing part of the PF resin with lignin caused a decrease in moisture resistance and a decrease in mechanical properties. The results of *MOR* and *MOE* showed a decrease from 16.2 and 2492 MPa (PF-0) to 12.3 and 2227 MPa (PF-10), which still meets the requirements of the P2 board standard. For IB, there was a decrease in strength from 0.9 MPa (PF-0) to 0.57 MPa (PF-10), and this variant does not closely meet the requirements of the Type P6 standard (0.6 MPa). Scanning

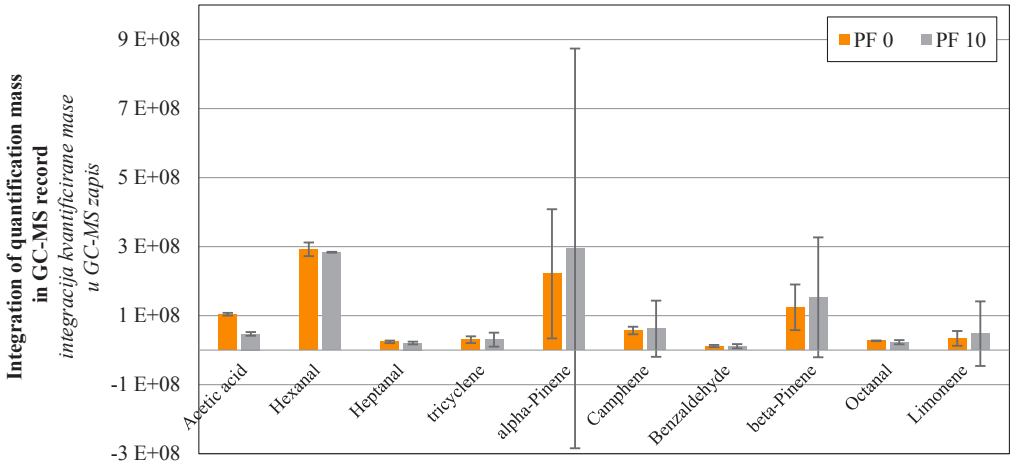

Figure 6 Comparison of selected volatile compounds mean emission in samples of board glued by standard phenolic (PF) and lignin modified glue (PF 10). Error bars represent expanded uncertainty of determination (U=2·SD) covering 95 % confidence interval.
Slika 6. Usporedba odabranih emisija hlapljivih spojeva u uzorcima ploča lijepljenih standardnim fenolnim ljepilom (PF) i ligninom modificiranim ljepilom (PF 10). Trake pogrešaka označavaju proširenu nesigurnost (U=2·SD) za interval pouzdanosti od 95 %.

electron microscopy showed cohesive failure in the wood for both tested variants. At the same time, the images showed the occurrence of small undissolved kraft lignin particles in the prepared resin. The tested modification of wood particleboard did not influence the emission of volatile organic compounds from material with exception of acetic acid, which decreased to one half of the original value. The presented method of PF resin modification is relatively simple and can be readily implemented in industry. By incorporating lignin content at 10 %, this method allows the production of particleboards that meet industry standards. Furthermore, it is believed that by selecting the appropriate technology, the standardized properties of these particleboards can be further enhanced. For future research, it is recommended to focus on solving the problem of increasing viscosity when lignin is added to the adhesive mixture, which negatively affects the subsequent uniform application of the resin to the wood particles during manufacturing. An interesting step would also be to test the behavior of a different type of lignin in the tested resin or, despite this being a technologically demanding and costly process, to test the effects of kraft lignin modification on the properties of particleboards compared to the variant tested in the present study.

Acknowledgements – Zahvala

This research was funded by the Faculty of Forestry and Wood Sciences at the Czech University of Life Sciences Prague (Internal Grant Agency, Project No. A_03_23). The authors wish to express their gratitude to Mondi AG for their support in supplying kraft lignin samples and to Dřevozpracující družstvo Lukavec (DDL) for providing wood particles for this project.

5 REFERENCES
5. LITERATURA

1. Abhilash, M.; Thomas, D., 2017: Biopolymers for biocomposites and chemical sensor applications. In: Biopolymer Composites in Electronics. Elsevier, pp. 405-435. https://doi.org/10.1016/B978-0-12-809261-3.00015-2
2. Auriga, R.; Borysiuk, P.; Jezierski, M., 2024: Drilling susceptibility of particleboard with *Cannabis sativa* L. Biuletyn Informacyjny Ośrodka Badawczo-Rozwojowego Przemysłu Płyt Drewnopochodnych w Czarnej Wodzie, pp. 121-126. https://doi.org/10.32086/biuletyn.2023.04
3. Bajpai, P., 2018: Brief description of the pulp and papermaking process. In: Biotechnology for Pulp and Paper Processing. Springer, Singapore, pp. 9-26. https://doi.org/10.1007/978-981-10-7853-8_2
4. Calvo-Flores, F. G.; Dobado, J. A.; Isac-García, J.; Martín-Martínez, F. J., 2015: Lignin and Lignans as Renewable Raw Materials: Chemistry, Technology and Applications. John Wiley & Sons.
5. de Oliveira, D. R.; Avelino, F.; Mazzetto, S. E.; Lomonaco, D., 2020: Microwave-assisted selective acetylation of Kraft lignin: Acetic acid as a sustainable reactant for lignin valorization. International Journal of Biological Macromolecules, 164: 1536-1544. https://doi.org/10.1016/j.ijbiomac.2020.07.216
6. Dessbesell, L.; Paleologou, M.; Leitch, M.; Pulkki, R.; Xu, C., 2020: Global lignin supply overview and kraft lignin potential as an alternative for petroleum-based polymers. Renewable and Sustainable Energy Reviews, 123: 109768. https://doi.org/10.1016/j.rser.2020.109768
7. Donmez Cavdar, A.; Kalaycioglu, H.; Hiziroglu, S., 2008: Some of the properties of oriented strandboard manufactured using kraft lignin phenolic resin. Journal of Materials Processing Technology, 202: 559-563. https://doi.org/10.1016/j.jmatprotec.2007.10.039
8. Gardziella, A.; Pilato, L.; Knop, A., 2000: Phenolic Resins. Springer-Verlag Berlin, Heidelberg, New York. https://doi.org/10.1007/978-3-662-04101-7

9. Ghorbani, M.; Liebner, F.; Van Herwijnen, H. W. G.; Pfungen, L.; Krahofer, M.; Budjav, E.; Konnerth, J., 2016: Lignin phenol formaldehyde resoles: the impact of lignin type on adhesive properties. BioResources, 11: 6727-6741. https://doi.org/10.15376/biores.11.3.6727-6741
10. Hemmilä, V.; Trischler, J.; Sandberg, D., 2013: Lignin: an adhesive raw material of the future or waste of research energy? Presented at the Meeting of the Northern European network for wood science and engineering : 11/09/2013 – 12/09/2013, pp. 98-103.
11. Hu, L.; Pan, H.; Zhou, Y.; Zhang, M., 2011: Methods to improve lignin's reactivity as a phenol substitute and as replacement for other phenolic compounds: A brief review. BioResources, 6 (3): 3515-3525.
12. Huang, C.; Peng, Z.; Li, J.; Li, X.; Jiang, X.; Dong, Y., 2022: Unlocking the role of lignin for preparing the lignin-based wood adhesive: A review. Industrial Crops and Products 187: 115388. https://doi.org/10.1016/j.indcrop.2022.115388
13. Hýsek, Š.; Żółtowska, S., 2022: Novel Lignin-Beeswax adhesive for production of composites from beech and spruce particles. Journal of Cleaner Production, 362: 132460. https://doi.org/10.1016/j.jclepro.2022.132460
14. Jiang, W.; Adamopoulos, S.; Hosseinpourpia, R.; Walther, T.; Medved, S., 2023: Properties and emissions of three-layer particleboards manufactured with mixtures of wood chips and partially liquefied bark. Materials, 16: 1855. https://doi.org/10.3390/ma16051855
15. Jiang, Z.; Duan, J.; Guo, X.; Ma, Y.; Wang, C.; Shi, B., 2021: Synthesis of Au/lignin-tannin particles and their anticancer application. Green Chemistry, 23: 6945-6952. https://doi.org/10.1039/D1GC01119G
16. Karthäuser, J.; Biziks, V.; Mai, C.; Militz, H., 2021: Lignin and lignin-derived compounds for wood applications – A review. Molecules, 26: 2533. https://doi.org/10.3390/molecules26092533
17. Kumar, R.; Pizzi, A. P., 2019: Adhesives for wood and lignocellulosic materials. John Wiley & Sons, Inc., Hoboken, New York, USA. https://doi.org/10.1002/9781119605584
18. Liu, L.-Y.; Chiang, W.-S.; Chang, H.; Yeh, T.-F., 2024: Phenolation to improve hardwood kraft lignin for wood adhesive application. Polymers, 16: 1923. https://doi.org/10.3390/polym16131923
19. Mason, S., 2021: Lignin valorisation opportunities from cellulosic sugar production – Prepared for the international council. NNFC Biocentre, New York, USA.
20. Moubarik, A.; Grimi, N.; Boussetta, N.; Pizzi, A., 2013: Isolation and characterization of lignin from Moroccan sugar cane bagasse: Production of lignin-phenol-formaldehyde wood adhesive. Industrial Crops and Products, 45: 296-302. https://doi.org/10.1016/j.indcrop.2012.12.040
21. Nadányi, R.; Ház, A.; Lisý, A.; Jablonský, M.; Šurina, I.; Majová, V.; Baco, A., 2022: Lignin modifications, applications and possible market prices. Energies, 15: 6520. https://doi.org/10.3390/en15186520
22. Němec, M.; Hájková, K.; Hýsek, Š., 2023: Paper-based laminates impregnated with a hybrid lignin-phenol-formaldehyde resin. Materials, 16: 2669. https://doi.org/10.3390/ma16072669
23. Němec, M.; Prokůpek, L.; Obst, V.; Pipíška, T.; Král, P.; Hýsek, Š., 2024: Novel kraft-lignin-based adhesives for the production of particleboards. Composite Structures, 344: 118344. https://doi.org/10.1016/j.compstruct.2024.118344
24. Niemz, P.; Sandberg, D., 2022: Critical wood-particle properties in the production of particleboard. Wood Material Science & Engineering, 17: 386-387. https://doi.org/10.1080/17480272.2022.2054726
25. Paananen, H.; Alvila, L.; Pakkanen, T. T., 2021: Hydroxymethylation of softwood kraft lignin and phenol with paraformaldehyde. Sustainable Chemistry and Pharmacy, 20: 100376. https://doi.org/10.1016/j.scp.2021.100376
26. Petrova, B.; Jivkov, V.; Yavorov, N., 2023: Possibilities for efficient furniture construction made of thin and ultra-thin materials by using mitre joints. Materials, 16: 6855. https://doi.org/10.3390/ma16216855
27. Pilato, L., 2010: Phenolic resins: a century of progress, phenolic resins: A century of progress. Springer-Verlag, Berlin, Heidelberg. https://doi.org/10.1007/978-3-642-04714-5
28. Pinheiro, F. G. C.; Soares, A. K. L.; Santaella, S. T.; Silva, L. M. A.; Canuto, K. M.; Cáceres, C. A.; Rosa, M. de F.; Feitosa, J. P. de A.; Leitão, R. C., 2017: Optimization of the acetosolv extraction of lignin from sugarcane bagasse for phenolic resin production. Industrial Crops and Products, 96: 80-90. https://doi.org/10.1016/j.indcrop.2016.11.029
29. Pizzi, A., 2014: Advanced Wood Adhesives Technology. CRC Press, Boca Raton. https://doi.org/10.1201/9781482293548
30. Roffael, E., 2017: Release of acetic acid and formaldehyde from particleboards bonded with phenolic resins. European Journal of Wood and Wood Products, 75: 1025-1026. https://doi.org/10.1007/s00107-017-1213-8
31. Saražin, J.; Poljanšek, I.; Pizzi, A.; Šernek, M., 2022: Curing kinetics of tannin and lignin biobased adhesives determined by DSC and ABES. Journal of Renewable Materials, 10: 2117-2131. https://doi.org/10.32604/jrm.2022.019602
32. Scharf, A.; Popescu, C.-M.; Dernegård, H.; Oja, J.; Ormondroyd, G.; Medved, S.; Sandberg, D.; Jones, D., 2023: Particleboards bonded by an imidazole-based adhesive system. Materials, 16: 7201. https://doi.org/10.3390/ma16227201
33. Solt, P.; Konnerth, J.; Gindl-Altmutter, W.; Kantner, W.; Moser, J.; Mitter, R.; van Herwijnen, H. W. G., 2019: Technological performance of formaldehyde-free adhesive alternatives for particleboard industry. International Journal of Adhesion and Adhesives, 94: 99-131. https://doi.org/10.1016/j.ijadhadh.2019.04.007
34. Thébault, M.; Müller, U.; Kandelbauer, A.; Zikulnig-Rusch, E.; Lammer, H., 2017: Review on impregnation issues in laminates manufacture: opportunities and risks of phenol substitution by lignins or other natural phenols in resins. European Journal of Wood and Wood Products, 75: 853-876. https://doi.org/10.1007/s00107-017-1206-7
35. Whetten, R.; Sederoff, R., 1995: Lignin Biosynthesis. The Plant Cell, 7: 1001-1013. https://doi.org/10.1105/tpc.7.7.1001
36. Xu, C.; Ferdosian, F., 2017: Conversion of lignin into bio-based chemicals and materials, green chemistry and sustainable technology. Springer-Verlag, Berlin, Heidelberg. https://doi.org/10.1007/978-3-662-54959-9
37. Yang, S.; Zhang, Y.; Yuan, T.-Q.; Sun, R.-C., 2015: Lignin-phenol-formaldehyde resin adhesives prepared with biorefinery technical lignins. Journal of Applied Polymer Science, 132. https://doi.org/10.1002/app.42493
38. Younesi-Kordkheili, H., 2022: Maleated lignin coreaction with phenol-formaldehyde resins for improved wood adhesives performance. International Journal of

Adhesion and Adhesives, 113: 103080. https://doi.org/10.1016/j.ijadhadh.2021.103080
39. Zhang, W.; Ma, Y.; Wang, C.; Li, S.; Zhang, M.; Chu, F., 2013: Preparation and properties of lignin-phenol-formaldehyde resins based on different biorefinery residues of agricultural biomass. Industrial Crops and Products, 43: 326-333. https://doi.org/10.1016/j.indcrop.2012.07.037
40. Zhao, L.; Liu, Y.; Xu, Z.; Zhang, Y.; Zhao, F.; Zhang, S., 2011: State of research and trends in development of wood adhesives. Forestry Studies in China, 13: 321-326. https://doi.org/10.1007/s11632-013-0401-9
41. ***ČSN EN 302-1, 2013: Adhesives for load-bearing timber structures – Test methods. Part 1: Determination of longitudinal tensile shear strength.
42. ***ČSN EN 310, 1995: Wood based panels. Determination of modulus of elasticity in bending and of bending strength.
43. ***ČSN EN 317, 1995: Particleboards and fibreboards. Determination of swelling in thickness after immersion in water.
44. ***ČSN EN 319, 1994: Particleboard and fibreboard. Determination of tensile strength perpendicular to the plane of the board.
45. ***List of Classifications – IARC: 2023: Monographs on the Identification of Carcinogenic Hazards to Humans. https://monographs.iarc.who.int/list-of-classifications (Accessed Nov. 12, 2023).

Corresponding address:

ŠTĚPÁN HÝSEK
University of Natural Resources and Life Sciences, Department of Material Sciences and Process Engineering, Institute of Wood Technology and Renewable Materials, Gregor-Mendel-Straße 33, 1180 Vienna, AUSTRIA,
e-mail: hyseks@fld.czu.cz

Issah Chakurah*[1], Stephen Jobson Mitchual[2], Francis Kofi Bih[3], Kwaku Antwi[3], Enoch Gbapenuo Tampori[4]

The Effect of Thermal Modification on Anatomical Properties of *Daniellia oliveri* (Rolfe) Hutch and Dalziel from Ghana

Utjecaj toplinske modifikacije na anatomska svojstva drva *Daniellia oliveri* (Rolfe) Hutch i Dalziel iz Gane

ORIGINAL SCIENTIFIC PAPER
Izvorni znanstveni rad
Received – prispjelo: 22. 5. 2024.
Accepted – prihvaćeno: 16. 12. 2024.
UDK: 630*81; 630*84; 674.038.17
https://doi.org/10.5552/drvind.2025.0218

ABSTRACT • *Understanding the biological changes from heat treatment is essential for effective wood application and quality control. Reliable evaluation ensures premium treated wood for the market. However, research on environmentally friendly thermal modification methods is limited. This gap must be addressed to evaluate the impact on lesser-known species like Daniellia oliveri. Five matured Daniellia oliveri trees were purposively selected and harvested from Du-West community and converted into standard sizes for the determination of the various properties. Fiber morphology, sectional characteristics as well as vessel measurements were evaluated in accordance with the International Association of Wood Anatomist (IAWA) Committee recommendations. The study revealed that, with the increase of the modification temperature, crystallization of wax occurred in the lumen of the modified specimens. The study further brought to light that with the increase in temperature fiber length decreased. Double fiber wall thickness and vessel diameter showed similar trends as their values decreased with the increase of the modification temperature. On the other hand, fiber lumen diameter and fiber diameter increased as temperature increased. This study highlights the significant impact of thermal modification on the anatomical properties of Daniellia oliveri wood. These insights underscore the importance of understanding the thermal modification response of wood species to enhance their application and ensure quality control.*

KEYWORDS: *thermal wood modification; anatomical wood properties; wood fiber morphology; Daniellia oliveri*

SAŽETAK • *Razumijevanje bioloških promjena drva zbog toplinske obrade ključno je za njegovu učinkovitu primjenu i kontrolu kvalitete. Pouzdana procjena utjecaja toplinske obrade osigurava vrhunsku kvalitetu modificiranog drva za tržište. Međutim, istraživanja ekološki prihvatljivih metoda toplinske modifikacije ograničena su.*

* Corresponding author
[1] Author is researcher at Mampong Technical College of Education, Department of Vocational and Technical Education, Mampong, Ghana. https://orcid.org/0000-0002-2055-0769
[2] Author is researcher at University of Education Winneba, Ghana. https://orcid.org/0000-0003-4267-804X
[3] Authors are researchers at Akenten Appiah-Menka University of Skills Training and Entrepreneurial Development, Department of Wood Science and Technology Education, Kumasi, Ghana. https://orcid.org/0000-0002-5197-5516, https://orcid.org/0000-0002-7715-3932
[4] Author is researcher at Tamale Technical University, Department of Wood Technology, Tamale, Ghana. https://orcid.org/0000-0002-0986-5129

Taj se nedostatak mora riješiti kako bi se procijenio utjecaj toplinske obrade na manje poznate vrste drva poput Daniellia oliveri. Za potrebe istraživanja odabrano je i posječeno pet zrelih stabala Daniellia oliveri iz područja Du-West te su pripremljene standardne veličine drva za određivanje različitih svojstava. Morfologija vlakana, obilježja presjeka, kao i promjeri traheja procijenjeni su u skladu s preporukama Međunarodnog udruženja anatoma drva (IAWA). Studija je otkrila da se s povećanjem temperature modifikacije vosak u lumenima uzoraka kristalizirao. Nadalje, ispitivanjem je uočeno da se s povećanjem temperature modifikacije duljina vlakana smanjuje. Također, s povećanjem temperature modifikacije smanjile su se i vrijednosti debljine dvostruke stijenke vlakana i promjera traheja. Nasuprot tome, s porastom temperature povećavali su se promjer lumena vlakana i promjer vlakana. Ova studija naglašava važnost utjecaja toplinske modifikacije na anatomska svojstva drva Daniellia oliveri. Rezultati upozoravaju na potrebu razumijevanja reakcije pojedinih vrsta drva na toplinsku modifikaciju kako bi se poboljšala njihova primjena i osigurala kontrola kvalitete.

KLJUČNE RIJEČI: *toplinska modifikacija drva; anatomska svojstva drva; morfologija drvnih vlakana; Daniellia oliveri*

1 INTRODUCTION
1. UVOD

There are over 800 different timber species found in the Ghanaian forests. However, only the commercially known species have been patronized by furniture and other timber users over the past decades (Appiah-Kubi *et al.*, 2019). A cursory look at the dwindling state of the traditionally known timber species in the furniture and construction industry in Ghana reveals a consistent decline in their volume. Therefore, mounting pressure on the few remaining commercial tree species such as Sapele, Mahogany, Odum, Ebony, Danta, Wawa amongst others that have been used for furniture and construction works since time immemorial (Asamoah *et al.*, 2023; Dumenu, 2019).

The imbalance between demand and supply of raw material for production purposes poses a bleak future for furniture and construction industries since there will be less supply of raw materials for continuous production (Antwi-Boasiako i Boadu, 2016). Despite difficulties with the availability of raw materials to the furniture and construction industries, a study conducted by Ofosu *et al.* (2019) asserted that the demand for wood-based products is still rising internationally. There are therefore significant ongoing efforts to expand the raw material base by finding alternative timber resources from tropical forests to compliment the endangered commercial timber species (Ofosu *et al.*, 2019).

Wood dimensional stability, appealing aesthetics as well as resistance to biodegradation when subjected to outdoor use are major wood qualities when purchasing and using wooden materials. However, not all timber species have these desired properties and to maximize and improve these properties, effective treatments such as wood preservation should be implemented. When these treatments are improperly done or managed, they turn to pose a concerning circumstance that will require immediate attention in seeking to achieve Sustainable Development Goals (SDGs) 14 and 15, i.e. "life below water and life on land", respectively.

The term wood modification refers to structural, mechanical, and chemical transformations occurring in the lignocellulosic material when gradually heated up to specific temperature ranges (Godinho *et al.*, 2021). It is still not quite apparent how the process will affect end-of-life circumstances, the environment, and product functionality in general despite the fact that many components of these treatments are well understood. The interactive evaluation of parameters used in the process, developed product attributes, and environmental implications must all be included. Much more data regarding all process-related environmental impacting aspects needs to be obtained to optimize modification processing with the aim of minimizing environmental impacts.

Heat treatment is a more environmentally friendly approach to changing wood properties than other methods such as chemical treatments (Elsheikh *et al.,* 2022; Garcia *et al.,* 2012; Kubovský *et al*., 2020; Lee *et al*., 2018; Teng *et al*., 2018). Although heat treatment generates major pleasant changes in the characteristics of wood, it also causes unwanted reductions in mechanical qualities such as the modulus of elasticity (*MOE*) and modulus of rupture (*MOR*) (Adebawo *et al.,* 2022; Kučerová *et al*., 2016; Rautkari *et al.,* 2014; Tang *et al.*, 2019). It is essential to identify the ideal heat treatment conditions (such as temperature levels, heating rate and time) In order to achieve that testing must be done to determine the value of the characteristics of heat-treated wood specimens at different temperatures.

By doing so, this research evaluated the anatomical changes and determined whether thermal modification can address the inherent limitations of *Daniellia oliveri* wood to enhance its performance, making it suitable for wider commercial and industrial applications.

According to Hutchison and Dalziel (1928), *Daniellia oliveri* is a member of the Fabaceae family and was named Paradaniellia oliveri Rolfe as the basionym. *Daniellia oliveri* (Rolfe) Hutch & Dalziel is a lesser-known timber species that, although not a significant species on the globally traded timber market, plays a crucial role in the lives of the individuals in its

surrounding zones (Schmelzer & Louppe, 2012). *Daniellia oliveri* (Rolfe) Hutch & Dalziel is called "Kanchil" by the Sissala tribe of Ghana where samples were collected. The wood is not long-lasting, and it is vulnerable to lumber-degrading micro-organisms such as fungi, pinhole borers, sea borers, and termites (Schmelzer & Louppe, 2012). As a result, a certain degree of efficient wood treatment is required to extend its useful lifespan. *Daniellia oliveri* (Rolfe) Hutch & Dalziel is a dominating species in humid savannah and abundant in deciduous woodland.

Although *Daniellia oliveri* (Rolfe) Hutch & Dalziel tends to be less durable, according to Schmelzer and Louppe (2012) its heartwood is commonly used for construction purposes such as roofing rafters, home furnishings, manufacturing packages and mortar (Achigan-Dako *et al.,* 2010). Because of the availability of *Daniellia oliveri* (Rolfe) Hutch & Dalziel in various geographical zones in Ghana, the wood is also used for charcoal and as fuel wood. *D. oliveri*, if treated effectively with strong preserving agents, can last longer in service, helping to prevent deforestation and its harm to commercial timber species.

According to Haeuser *et al.* (1970), *Daniellia oliveri* (Rolfe) Hutch & Dalziel is a big tropical plant that produces immense quantities of copal when its stem is injured. Since copal differs from other Amherstiae and solidifies when exposed to the atmosphere, they are widely used as varnishes. *Daniellia oliveri* (Rolfe) Hutch & Dalziel is also renowned for making copal resin. Copal has been used for ages in African traditional medicine, art, and faith-related rites as incense. It is obtained by creating slices in the bark of the tree and enabling the resin to flow out and solidify (Haeuser *et al.,* 1970). Copal has been marketed all over the world and is employed in a variety of cultural and religious traditions because of the brimming African population's reliance on medicinal plants. Various tribes have delved deeper into the plant for the cure of multiple conditions such as seizures and spasm pain, sexual dysfunction and to avoid premature births in pregnant women (Balogun *et al.,* 2023).

The aim of the present study therefore is to investigate the impact of thermal modification on the anatomical properties of *Daniellia oliveri* (Rolfe) Hutch & Dalziel wood from Ghana, with a focus on understanding how thermal modification influences its structural characteristics and potential applications.

2 MATERIALS AND METHODS
2. MATERIJALI I METODE

2.1 Research site
2.1. Lokalitet istraživanja

The Sissala West District is one of Ghana's 275 Metropolitan, Municipal, and District Assemblies (MMDAs), and is part of the Upper West Region consisting of 11 Municipalities and Districts. The Sissala West District is in Ghana's northern sector (Savannah ecological zone). It is located approximately at longitude 213w and 2:36w and latitude 10:00N 11:00N, with Gwollu serving as the administrative capital. Sissala West has a total land area of about 4, 11289 km^2, accounting for approximately 25 % of the total landmass of the Upper West Region. On the northern side of the Region, the district shares a border with Burkina Faso, which facilitates cross-border socioeconomic operations. The district shares boundaries with Sissala East Municipal in the east, Wa East District in the south, Jirapa Municipal and Lambussie Karni District in the west, and Daffiama Bussie Issa District in the southwest (GSS, 2010).

According to Fagariba *et al*. (2018), the annual rainfall in the Sissala West district ranges from 800 mm to 1,000 mm, which is lower than in the transition zone. This is due to the proximity of Guinea Savannah to the coast. This region encompasses the majority of Ghana and accounts for 63 % of the overall area of Ghana's major climate zone. This environment provides for a 180-200-day growing season. With barely a few rains from August through October, April and July are the wettest months of the year. The five Northern Regions of Ghana typically follow this pattern. The long dry season known as harmattan, which lasts from early November to March, is characterized by chilly and foggy weather and coincides with the rainy season. Relative humidity (RH) can drop to 20 % during the dry season, but it can reach 70 – 90 % during the rainy season. The mean yearly temperature of the Region is between 28 °C and 37 °C, although seasonal variations are occasionally brought about by variations in the local climate. The vegetation is made of perennial grasses interspersed with fire-resistant trees, including baobab (*Adansonia digitata*), *Daniellia oliveri* (Rolfe) Hutch & Dalziel, kapok (*Ceiba pentandra*), Shea trees (*Vitellaria paradoxa*), and others.

2.2 Sample collection and preparations
2.2. Prikupljanje i priprema uzoraka

Owing to their prominence and abundance in the area, in March 2024, five mature *Daniellia oliveri* (Rolfe) Hutch & Dalziel trees, ranging in age from 25 to 48 years, and with diameters between 60 – 80 cm, were harvested from the community's natural woodland in Duwest. The diameters of the five trees were purposefully chosen, and their straight trunks and defect-free state were noted before they were cut down. Following the felling of the chosen trees, a one-meter sectional length was removed from the base of each tree. Each tree was cut to the desired length, the trees had about 60 – 80 cm diameter clear boles that measured roughly 15 meters in

length. The billets were turned into boards using the quarter sawing technique, which minimizes warping boards and facilitates the easy separation of heartwood and sapwood for the determination of radial properties. At the wood workshop/lab of the AAMUSTED - Kumasi campus, the wood samples were produced to the required dimensions in conformity to IAWA committee recommendations. Defect-free specimens were carefully selected from the staked sawn wood together with the modified specimens and then conditioned for 6 days in a climate-controlled room with a temperature of (20 ± 2) °C and a relative humidity of (62 ± 2) % before being sawn into various sizes for further studies.

2.3 Thermal modification process
2.3. Proces toplinske modifikacije

Labline Technology Muffle furnace model MLF-1200/12 with a capacity of 12 liters and a maximum temperature of 1200 °C was used to modify 6 sets of heartwood and sapwood at 160 °C, 180 °C and 200 °C without oxygen, securely closed for 3 hours. Untreated set of 10 replicates of heartwood and sapwood served as the control. The oven was then adjusted to the temperatures at which the primary heat treatment was performed. The specimens were removed from Muffle furnace and allowed to cool in a desiccator filled with silica gel.

2.4 Determination of anatomical properties of control and modified specimens
2.4. Određivanje anatomskih svojstava kontrolnih i modificiranih uzoraka

The durability, physical, mechanical and chemical properties of fibrous lignocellulosic materials have been noted to be influenced by its anatomical structure. Using an optical microscope attached to a desk top computer and its peripherals, three sectionals (transverse, tangential and radial) slides were prepared from the study materials, which were used for the identification of cells of the materials that may contribute to the properties under study. Eight 20mm squared cubes samples were prepared from the control and modified specimens and from each of the five selected trees of *Daniellia oliveri* (Rolfe) Hutch & Dalziel wood for the anatomical test. Specimens were placed in a well labelled plastic vial containing water for about 21 days to ensure fibers are completely softened to enhance easy slicing with a microtome.

Thin sections of 25 µm thickness were cut from transverse, tangential and radial surfaces of the specimen using a sliding microtome. The sections were first washed in distilled water (Figure 1A) and then stained in 1 % safranin and in 50 % ethanol solution for about 10 – 15 min. Afterwards, the sections were rewashed in distilled water and dehydrated in increasing concentration of ethanol from 30 %, 50 %, 70 %, 95 %, and 100 % after keeping specimens in each concentration for 15 minutes to gradually remove the moisture from the thin sections and also to minimize crumbing during the test process. Specimens were then immersed in xylene for another 15 minutes to remove little traces of water. The sections were placed in a container and Canadian balsam was added. Thereafter, the specimens were placed on a slide with a cover slip carefully placed making sure there was no air bubbles trapped in the histological slides. The prepared slides were then oven-dried at 60 °C overnight (Figure 1B) before mounting them on the microscope for determining the various sectional measurements.

2.5 Maceration of specimens for fiber measurements
2.5. Maceracija uzoraka za mjerenje vlakanaca

In order to separate wood elements, the Franklin (1927) methods for wood maceration were used. Two matchstick-sized specimens were taken from each softened wood cube and placed in a labelled test tubes using cotton wool as cork. A mixture of 50mL of acetic acid and 50ml of hydrogen peroxide at a ratio of (1:1) was poured into the test tubes containing the specimens and left to soak for at least 7 days (Schweingruber, 2007). The specimens were boiled to facilitate the chemical re-

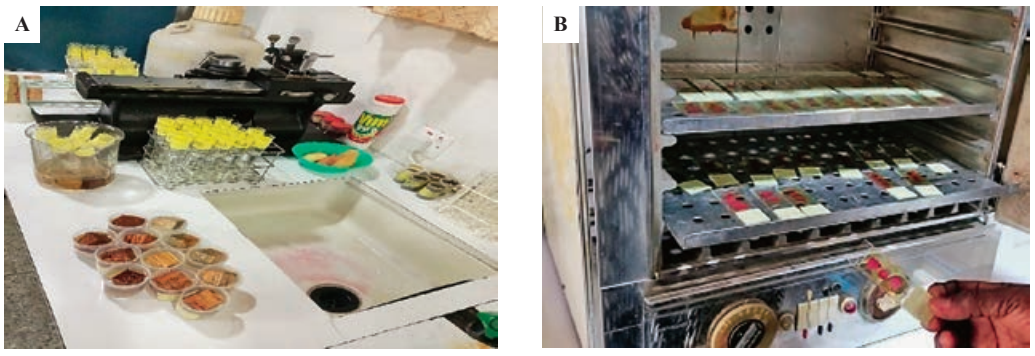

A) Specimens soaked in distill water
A) Uzorci potopljeni u destiliranu vodu

B) Slides kept in an oven to dry
B) Sušenje predmetnih stakalaca u sušioniku

Figure 1 Examining anatomical sections of control and thermally modified specimens for the study
Slika 1. Ispitivanje anatomskih presjeka kontrolnih i toplinski modificiranih uzoraka

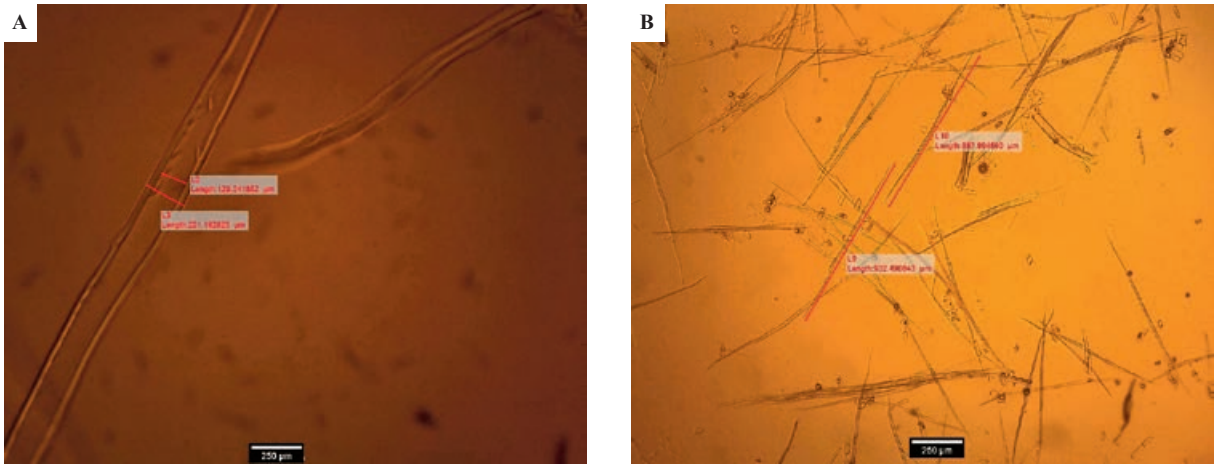

A) Measurement of fiber diameter and fiber lumen
A) Mjerenje promjena vlakana i lumena vlakana

B) Measurement of fiber length
B) Mjerenje duljine vlakana

Figure 2 Determination of fiber dimensions using an optical microscope attached to an HP desk top computer
Slika 2. Određivanje dimenzija vlakana uz pomoć optičkog mikroskopa spojenoga na HP stolno računalo

action on the wood; samples were checked every 24hr until wood was completely white (macerated); thereafter, specimens were washed to get rid of the chemicals. Distil water and alcohol were added to the macerate for preservation. A piece of the macerate was then taken into a petri dish and drops of glycerol were added. The specimen was then carefully teased out to separate individual wood components and poured into slides and properly covered with the slide cover. The slides were placed in an optical microscope where the fiber length, fiber diameter, vessel diameter, fiber lumen and cell wall thickness were measured (Figure 2A and 2B). Motic Image Plus (MIP) software and ImageJ software were used to do all anatomical measurements. Straight and unbroken pieces were measured for fiber length and vessel diameter.

2.6 Data analysis
2.6. Analiza podataka

All the trees in the study had their testing qualities determined. For every tree, experiments were carried out with different treatment temperatures and radial sections to examine variations in the quality of species tested. For the chosen parameters, the mean, standard deviation, and standard error of the mean were found. Two-way analysis of variance (ANOVA) was used to assess the significant difference between the two factors (temperature and wood section) and at an alpha value of $P<0.050$, differences were deemed significant.

3 RESULTS AND DISCUSSION
3. REZULTATI I RASPRAVA

The anatomical features of the modified and unmodified *Daniellia oliveri* (Rolfe) Hutch and Dalziel wood studied are presented in Figure 3 and 4, whereas Table 1 presents the results for the fiber morphology and vessel diameter. Generally, *Daniellia oliveri* (Rolfe) Hutch and Dalziel wood is a diffused-porous wood, as seen by the transverse section, and massive earlywood

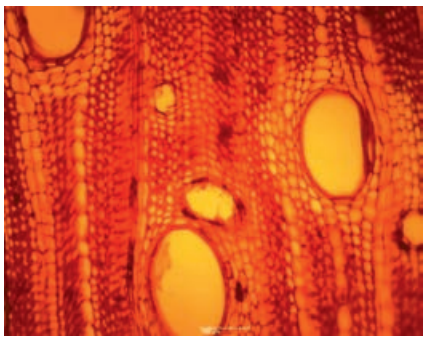

Transverse section of untreated *Daniellia oliveri* (Rolfe) Hutch and Dalziel specimen
Poprečni presjek nemodificiranog uzorka *Daniellia oliveri* (Rolfe) Hutch i Dalziel

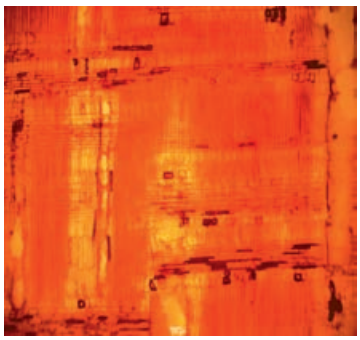

Radial section of untreated *Daniellia oliveri* (Rolfe) Hutch and Dalziel specimen
Radijalni presjek nemodificiranog uzorka *Daniellia oliveri* (Rolfe) Hutch i Dalziel

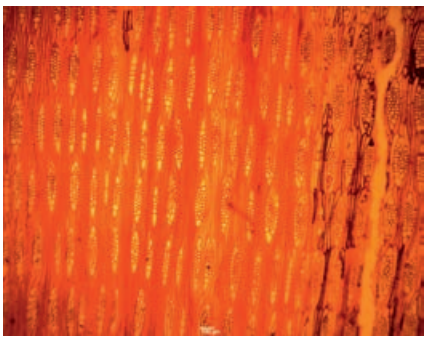

Tangential section of untreated *Daniellia oliveri* (Rolfe) Hutch and Dalziel specimen
Tangentni presjek nemodificiranog uzorka *Daniellia oliveri* (Rolfe) Hutch i Dalziel

Figure 3 Sectional images of untreated *D. oliveri* wood (magnification 100 µm)
Slika 3. Slike presjekâ nemodificiranog drva *D. oliveri* (povećanje 100 µm)

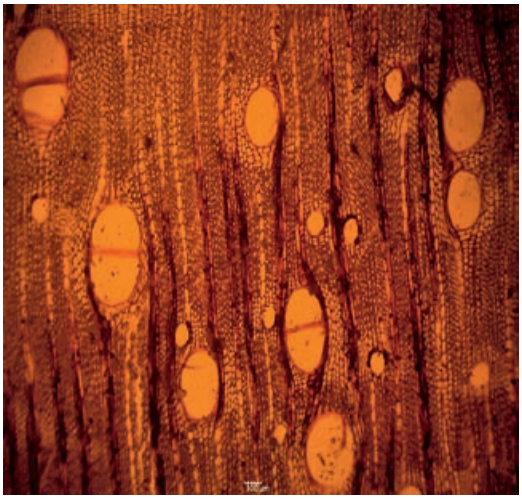

Transverse section of modified *Daniellia oliveri* (Rolfe) Hutch and Dalziel specimen
Poprečni presjek modificiranog uzorka *Daniellia oliveri* (Rolfe) Hutch i Dalziel

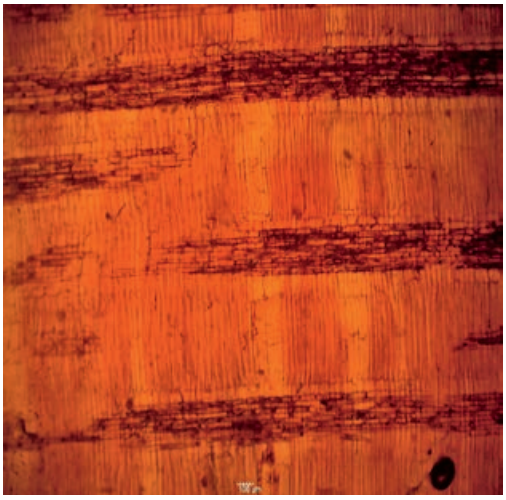

Radial section of modified *Daniellia oliveri* (Rolfe) Hutch and Dalziel specimen
Radijalni presjek modificiranog uzorka *Daniellia oliveri* (Rolfe) Hutch i Dalziel

Tangential section of modified *Daniellia oliveri* (Rolfe) Hutch and Dalziel specimen
Tangentni presjek modificiranog uzorka *Daniellia oliveri* (Rolfe) Hutch i Dalziel

Figure 4 Sectional images of modified *D. oliveri* wood (magnification 100 µm)
Slika 4. Slike presjekâ modificiranog drva *D. oliveri* (povećanje 100 µm)

vessels are lodged in parenchymatous tissues. Vessels are round to oval in shape, and primarily single with few multiples of two or three. Few vessels have been found to contain tyloses. The *Daniellia oliveri* (Rolfe) Hutch and Dalziel wood tangential section (Figure 3 and 4) reveals that the rays are primarily multi-seriate, with four to six cells per parenchyma strand.

Table 1 shows that there was a substantial variation in fiber morphology between the modification temperatures. The heat-treatment has brought about the formation of cross-fissures and crystallization of wax inside the pores as shown in Figure 4. The volatilization of extractives and rupture of polysaccharides also occurred to the heat-treated wood under study. Generally, it could be observed that there is great color change between the sections of the modified specimens and that of the unmodified specimens. The specimens became darker as the modification temperature rose to 200 °C, and it was also observed that the vessel diameter decreased as the modification temperature increased (Figure 5).

The result of the present study is in conformity with that of Johnson and Smith (2024), who demonstrated that heat treatment generally leads to a reduction in both vessel length and diameter. These changes in vessel dimensions were attributed to the thermal degradation of

Table 1 Measurement of selected anatomical properties of treated and untreated *Daniellia oliveri* (Rolfe) Hutch and Dalziel wood with standard deviation in parenthesis
Tablica 1. Rezultati mjerenja odabranih anatomskih svojstava modificiranoga i nemodificiranog drva *Daniellia oliveri* (Rolfe) Hutch i Dalziel sa standardnom devijacijom u zagradi

Properties, µm *Svojstva*, µm	**Tree section** *Dio stabla*	**Untreated (Control)** *Nemodificirani (kontrolni)*	**Modification at 160 °C** *Modificiran na 160* °C	**Modification at 180 °C** *Modificiran na 180* °C	**Modification at 200 °C** *Modificiran na 200* °C
Fiber length *duljina vlakana*	Heart / *srž*	1648.43 (172.41)	1632.37 (168.84)	1602.15 (166.74)	1561.29 (174.37)
	Sap / *bjeljika*	1616.55 (57.47)	1564.15 (91.51)	1535.76 (91.82)	1503.89 (99.72)
Fiber diameter *promjer vlakana*	Heart / *srž*	24.80 (3.34)	25.24 (3.31)	25.65 (3.35)	25.92 (3.30)
	Sap / *bjeljika*	26.35 (2.06)	26.83 (2.38)	27.26 (2.33)	27.56 (2.49)
Fiber lumen diameter *promjer lumena vlakana*	Heart / *srž*	16.28 (3.31)	16.72 (3.32)	17.21 (3.34)	17.44 (3.31)
	Sap / *bjeljika*	18.09 (2.09)	18.68 (2.04)	19.13 (2.02)	19.40 (1.97)
Double cell – wall thickness *debljina dvostruke stanične stijenke*	Heart / *srž*	8.46 (0.73)	8.46 (0.74)	8.40 (0.75)	8.42 (0.65)
	Sap / *bjeljika*	8.15 (0.71)	8.07 (0.62)	8.03 (0.58)	8.02 (0.64)

cell wall components, such as lignin and hemicellulose, which occur during the heat treatment process. The degradation of these components results in structural modifications within the vessels, leading to reductions in vessel size. Their study further noted that the magnitude of changes in vessel morphology varied depending on the specific heat treatment parameters used. According to Gupta *et al*. (2023) higher temperatures and prolonged treatment durations were associated with more pronounced alterations in vessel length and diameter, indicating the importance of treatment intensity in influencing vessel characteristics.

Moreover, Chen and Wang (2021) investigated the effects of different heat treatment conditions on vessel morphology and observed similar trends. They found that higher temperatures and longer treatment durations resulted in more pronounced reductions in vessel length and diameter. These changes are attributed to the increased degradation of cell wall components at higher temperatures and longer durations, leading to alterations in vessel structure and dimensions. Finally, in contrast to the result of the present study, Suri *et al*. (2021) observed in his study a similar trend, vessel lumen area and diameter of *Gmelina arborea* and *Melia azedarach* wood increased as temperature rose in both radial and tangential directions.

In terms of fiber morphology, this study shows that as the temperature increased, the fiber width and lumen diameter increased. However, the fiber wall thickness and fiber length decreased as the temperature

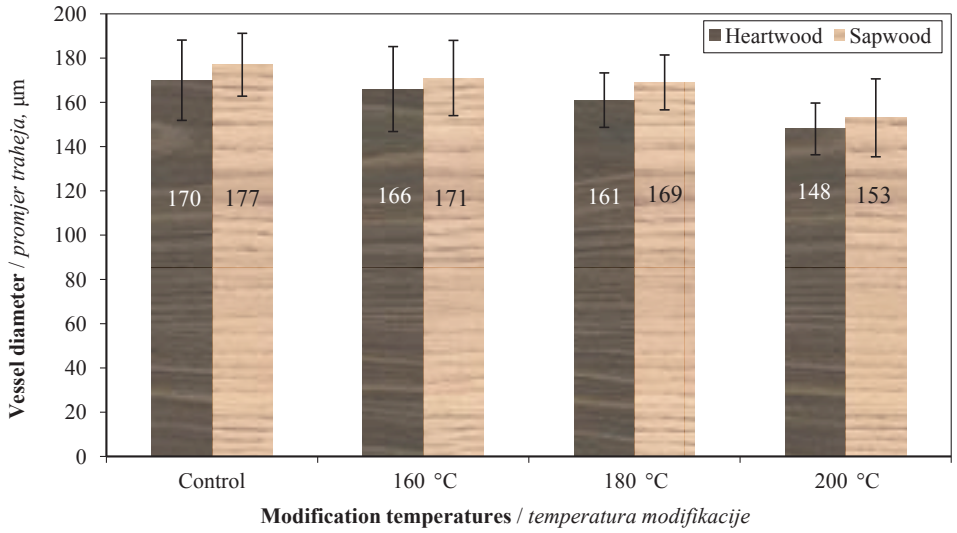

Figure 5 Measurement of Vessel diameter of thermally modified *Daniellia oliveri* (Rolfe) Hutch and Dalziel
Slika 5. Rezultati mjerenja promjera traheja toplinski modificiranog drva *Daniellia oliveri* (Rolfe) Hutch i Dalziel

increased as shown in Table 1. Similar results were obtained for vessel diameter, as temperature increased vessel diameter decreased (Figure 5). This result is in agreement with several other studies by scholars. Garcia and Lopez (2022) found that changes in fiber morphology induced by heat treatment can affect the mechanical performance of wood, including its tensile strength and modulus of elasticity. They observed that while heat treatment may lead to a decrease in fiber length and diameter, it can enhance the mechanical stability of wood fibers, thereby contributing to improved overall mechanical properties.

Furthermore, Chen and Wang (2021) explored the effects of heat treatment parameters on the fiber morphology of wood. They observed that higher temperatures and longer treatment durations resulted in more pronounced changes in fiber morphology, including greater reductions in fiber diameter. This observation suggests that the intensity and duration of heat treatment play crucial roles in influencing the extent of alterations in fiber morphology.

Moreover, Garcia and Lopez (2022) investigated the impact of heat treatment on fiber morphology across different wood species. Their research revealed that the response of fiber morphology to heat treatment varies among different species, with some species exhibiting more significant changes in fiber dimensions compared to others. This variation is attributed to differences in the composition and structure of wood fibers across species, which influence their susceptibility to heat-induced alterations.

Finally, Cabezas-Romero *et al*. (2021) conducted an investigation on the effects of the thermal modification process on the microstructure of *Pinus radiata* juvenile wood and revealed that the cell wall thickness decreased as treatment temperature increased, whereas the average lumen diameter increased slightly as temperature increased. This result is comparable to the present study.

4 CONCLUSIONS
4. ZAKLJUČAK

Wood preservation is a crucial component of effectively and efficiently prolonging the service life of wood when used in the furniture and construction industry. However, when preservatives are improperly handled, they turn out to be detrimental to both the users and the environment. In order to curb this menace associated with the use of these preservatives, alternatives and eco-friendly treatments are being sought. The present study therefore sets out to assess the anatomical properties of *Daniellia oliveri* (Rolfe) Hutch & Dalziel wood thermally modified at various temperatures for three hours. Thermal modification is a reliable and environmentally friendly method for improving the properties of wood. The reduction in vessel diameter, noticed in modified *Daniellia oliveri* (Rolfe) Hutch & Dalziel wood that has implications on its use, was found in modified specimens block lumens and prevents much intake of moisture when in service. Also, when thermally modified, reduction in vessel diameter could bring about reduction in moisture absorption improving dimensional stability of *Daniellia oliveri* (Rolfe) Hutch & Dalziel wood. Therefore, heat treatment may be recommended to improve the utilization of lesser-known timber species such as *Daniellia oliveri* (Rolfe) Hutch & Dalziel. In conclusion, the results of this study highlight the need for a deeper anatomical understanding of thermal modification processes, particularly for *Daniellia oliveri* wood as a lesser-known species, to optimize their utilization and maintain quality standards. The study further bridges a critical gap, contributing to the development of environmentally friendly and effective thermal modification methods for sustainable wood applications. Future research should prioritize exploring effective techniques for assessing crack development and investigating alternative methods for analyzing cellular structures, such as gray-scale image analysis or pixel-based measurements.

Acknowledgements – Zahvala

The authors are thankful to Akenten Appiah-Menka University of Skills Training and Entrepreneurial Development (AAMUSTED) and CSIR-Forestry Research Institute of Ghana for providing human resources, materials, and infrastructure for the study.

5 REFERENCES
5. LITERATURA

1. Achigan-Dako, E. G.; Pasquini, M. W.; Assogba Komlan, F.; N'Danikou, S.; Dansi, A.; Ambrose-Oji, B., 2010: Traditional vegetables in Benin. Institut National des Recherches Agricoles du Bénin. Imprimeries du CENAP, Cotonou, pp. 278.
2. Adebawo, F. G.; Adegoke, O. A.; Adelusi, E. A.; Adekunle, E. A.; Odeyale, O. C., 2022: Effect of thermal treatment on chemical, biological and mechanical properties of African whitewood (*Triplochiton scleroxylon* K. Schum). *Jou*rnal of Applied Sciences and Environmental Management, 26 (7): 1219-1224. https://doi.org/10.4314/jasem.v26i7.5
3. Antwi-Boasiako, C.; Boadu, K. B., 2016: The level of utilization of secondary timber species among furniture producers. 7 (1): 39-47. https://doi.org/10.15177/seefor.16-08
4. Appiah-Kubi, E.; Kankam, C. K.; Ansa-Asare, K., 2019: Mechanical properties of four lesser – Known Ghanaian timber species. International Journal of Trend in Research and Development, Conference proceeding IPMESS-19: 29-35.
5. Asamoah, O.; Danquah, J. A.; Bamwesigye, D.; Verter, N.; Acheampong, E.; Macgregor, C. J.; Boateng, C. M.; Kuittinen, S.; Appiah, M.; Pappinen, A., 2023: The perception of the locals on the impact of climate variability on non-

timber forest products in Ghana. Ecological Frontiers, 44: 489-499. https://doi.org/10.1016/j.chnaes.2023.07.004
6. Balogun, F. O.; Ajao, A. A.; Sabiu, S., 2023: A review of indigenous knowledge and ethnopharmacological significance of African Copaiba Balsam Tree, *Daniellia oliveri* (Fabaceae). Heliyon, 9 (9): e20228. https://doi.org/10.1016/j.heliyon.2023.e20228
7. Cabezas-Romero, J. L.; Salvo-Sepúlveda, L.; Contreras-Moraga, H.; Pérez-Peña, N.; Sepúlveda-Villarroel, V.; Wentzel, M.; Ananías, R. A., 2021: Microstructure of thermally modified Radiata Pine wood. BioResources, 16 (1): 1523-1533. https://doi.org/10.15376/biores.16.1.1523-1533
8. Chen, X.; Wang, L., 2021: Effects of heat treatment on vessel morphology in wood. Journal of Wood Science, 68 (4): 210-218.
9. Dumenu, W. K., 2019: Assessing the impact of felling/export ban and CITES designation on exploitation of African rosewood (*Pterocarpus erinaceus*). Biological Conservation, 236: 124-133. https://doi.org/10.1016/j.biocon.2019.05.044
10. Elsheikh, A. H.; Panchal, H.; Shanmugan, S.; Muthuramalingam, T.; El-Kassas, A. M.; Ramesh, B., 2022: Recent progresses in wood-plastic composites: Pre-processing treatments, manufacturing techniques, recyclability and eco-friendly assessment. Cleaner Engineering and Technology, 8: 100450. https://doi.org/10.1016/j.clet.2022.100450
11. Fagariba, C. J.; Song, S.; Soule, S. K. G., 2018: Factors influencing farmers' climate change adaptation in Northern Ghana: Evidence from subsistence farmers in sissala west, Ghana. Journal of Environmental Science and Management, 21 (1): 61-73.
12. Garcia, M.; Lopez, R.; 2022: Influence of heat treatment on mechanical properties of wood vessels. Wood Research, 75 (2): 89-97.
13. Garcia, R. A.; De Carvalho, A. M.; De Figueiredo Latorraca, J. V.; De Matos, J. L. M.; Santos, W. A.; De Medeiros Silva, R. F., 2012: Nondestructive evaluation of heat-treated Eucalyptus grandis Hill ex Maiden wood using stress wave method. Wood Science and Technology, 46 (1-3): 41-52. https://doi.org/10.1007/s00226-010-0387-6
14. Godinho, D.; Araújo, S. de O.; Quilhó, T.; Diamantino, T.; Gominho, J., 2021: Thermally modified wood exposed to different weathering conditions: A review. Forests, 12 (10): 1400. https://doi.org/10.3390/f12101400
15. Gupta, A.; Jain, L.; Dutt, B.; Kumar, R.; Sharma, S., 2023: Behavioral change in physical, anatomical and mechanical characteristics of thermally treated Pinus roxburghii wood. BioResources 18 (4): 7769-7795. https://doi.org/10.15376/biores.18.4.7769-7795
16. Haeuser, J.; Hall, S. F.; Oehlschlager, A. C.; Ourisson, G., 1970: The structure and stereochemistry of oliveric acid. Tetrahedron, 26 (14): 3461-3465. https://doi.org/10.1016/S0040-4020(01)92925-4
17. Hutchison, J.; Dalziel, J. M., 1928: Flora of west tropical Africa. The Crown Agents for the Colonies, London.
18. Johnson, R.; Smith, T., 2024: Variability in the Impact of Heat Treatment on Water Absorption Across Different Wood Species. Journal of Forestry, 57 (2): 112-120.
19. Kubovský, I.; Kačíková, D.; Kačík, F., 2020: Structural changes of oak wood main components caused by thermal modification. Polymers, 12 (2): 485. https://doi.org/10.3390/polym12020485
20. Kučerová, V.; Lagaňa, R.; Výbohová, E.; Hýrošová, T., 2016: The effect of chemical changes during heat treatment on the color and mechanical properties of fir wood. BioResources, 11 (4): 9079-9094. https://doi.org/10.15376/BIORES.11.4.9079-9094
21. Lee, S. H.; Ashaari, Z.; Lum, W. C.; Abdul Halip, J.; Ang, A. F.; Tan, L. P.; Chin, K. L.; Md Tahir, P., 2018: Thermal treatment of wood using vegetable oils: A review. Construction and Building Materials, 181: 408-419. https://doi.org/10.1016/j.conbuildmat.2018.06.058
22. Ofosu, S.; Boadu, K. B.; Afrifah, K. A., 2019: Suitability of *Chrysophyllum albidum* from moist semi-deciduous forest in Ghana as a raw material for manufacturing paper-based products. Journal of Sustainable Forestry, 39 (2): 153-166. https://doi.org/10.1080/10549811.2019.1623052
23. Rautkari, L.; Honkanen, J.; Hill, C. A. S.; Ridley-Ellis, D.; Hughes, M., 2014: Mechanical and physical properties of thermally modified Scots pine wood in high pressure reactor under saturated steam at 120, 150 and 180 °C. European Journal of Wood and Wood Products, 72 (1): 33-41. https://doi.org/10.1007/s00107-013-0749-5
24. Schmelzer, G. H.; Louppe, D., 2012: *Daniella oliveri* (Rolfe) Hutch and Dalziel. In: Plant resources of tropical Africa. Prota 7(2): timber 2. Lemmens RHMJ, Louppe Dominique, Oteng-Amoako AA. PROTA. Wageningen: PROTA, pp. 307-312.
25. Schweingruber, F. H., 2007: Wood Structure and environment, vol 1. Springer, Berlin.
26. Suri, I. F.; Purusatama, B. D.; Lee, S. H.; Kim, N. H.; Hidayat, W.; Ma'ruf, S. D.; Febrianto, F., 2021: Characteristic features of the oil-heat treated woods from tropical fast growing wood species. Wood Research, 66 (3): 365-378. https://doi.org/10.37763/wr.1336-4561/66.3.365378
27. Tang, T.; Chen, X.; Zhang, B.; Liu, X.; Fei, B., 2019: Research on the physico-mechanical properties of moso bamboo with thermal treatment in tung oil and its influencing factors. Materials, 12 (4): 599. https://doi.org/10.3390/ma12040599
28. Teng, T. J.; Arip, M. N. M.; Sudesh, K.; Nemoikina, A.; Jalaludin, Z.; Ng, E. P.; Lee, H. L., 2018: Conventional technology and nanotechnology in wood preservation: A review. BioResources, 13 (4): 9220-9252. https://doi.org/10.15376/biores.13.4.Teng
29. ***Ghana Statistical Service, 2010: Population and housing census. District analytical report, Sissala west district.

Corresponding address:

ISSAH CHAKURAH
Mampong Technical College of Education, Department of Vocational and Technical Education, Mampong, GHANA, e-mail: academiachakurah@gmail.com

LIN

Laboratorij za namještaj
Laboratory for Furniture

accredited testing laboratory for furniture according to HRN EN ISO/IEC 17025

more than 40 methods in the scope of the testing of furniture

outside the scope of accreditation:
coatings and parts for furniture
children's playgrounds and playground equipment
research of constructions and ergonomics of furniture
testing of finishing materials and proceses
testing of flammability and ecology of upholstered furniture
furniture expertise

Laboratory is a member of the Laboratoria Croatica CROLAB – an association whose goal is the development of Croatian laboratories as an infrastructure for the development of production and the economy within a demanding open market, using common potentials and synergy effects of the association, while the

Faculty of Forestry and Wood technology is a full member of the INNOVAWOOD – association whose aim it to contribute to business successes in forestry, wood industry and furniture industry, stressing the increase of competitiveness of the European industry.

Research of beds and sleeping, research of children's beds, optimal design of tables, chairs and corpus furniture, healthy and comfort sitting at school, office and in home are some of numerous researches performed by the *Institute for furniture and wood in construction*, which enriched the treasury of knowledge on furniture quality.

17025 HAA 1838 TEST

Good cooperation with furniture manufacturers, importers and distributors makes us recognizable

Knowledge is our capital

CROLAB

INNOVAWOOD

University of Zagreb • Faculty of forestry and wood technology
Testing laboratory for furniture and playground equipment
Institute for furniture and wood in construction
Svetošimunska cesta 23
HR-10000 Zagreb, Croatia

Darius Albrektas*[1], Ernestas Ivanauskas[2], Ugnė Misiūnaitė[2]

Forecasting and Comparison of Mechanical Properties of Wooden Structure Models

Predviđanje i usporedba mehaničkih svojstava modela drvnih konstrukcija

ORIGINAL SCIENTIFIC PAPER
Izvorni znanstveni rad
Received – prispjelo: 12. 8. 2024.
Accepted – prihvaćeno: 23. 12. 2024.
UDK: 630*83; 674.038.5
https://doi.org/10.5552/drvind.2025.0227

ABSTRACT • *In this study, different methods were used to compare the mechanical properties of spruce wood. The aim was to evaluate the potential of predicting the properties and behavior of wooden structural elements containing holes and voids. The modulus of elasticity (MOE) was determined using three methods: the static 4-point bending method according to the standard EN 408:2010+A1:2012, the original dynamic transverse resonance vibration method, and the ANSYS design program. The research was carried out in two phases. In the first phase, the dynamic modulus of elasticity (MOEd) of the samples was determined without causing them any damage. In the second phase, the bending resistance and static modulus of elasticity (MOE) of the same samples were determined. Using the ANSYS program and considering the dynamic modulus of elasticity, density, and other parameters, the bending resistance and static modulus of elasticity (MOEa) were predicted. During the first stage of the study, the modulus of elasticity (MOE) was measured for different groups of samples using different methods. The results showed that the average values of MOE differed by up to 4.6 % between the different groups. In the second stage, additional samples were divided into 5 groups, and holes or voids were formed in them according to 5 different schemes. The MOE, bending resistance, MOEa, and bending resistance were determined for each group, and it was found that the average MOE values differed by up to 17 % between the different groups. The presence of holes and voids in the wood increased the anisotropy of the material, which had the most significant impact on the results. Regardless of the number of holes and voids, the damping factor increased by up to 2.1 times.*

KEYWORDS: *modulus of elasticity; coefficient of damping; predicting of mechanical properties; hole; void*

SAŽETAK • *U ovom su istraživanju primijenjene različite metode za usporedbu mehaničkih svojstava smrekovine. Cilj je bio procijeniti mogućnost predviđanja svojstava i ponašanja drvenih konstrukcijskih elemenata koji imaju rupe i šupljine. Modul elastičnosti (MOE) određen je trima metodama: statičkom metodom savijanja u četiri točke prema normi EN 408:2010+A1:2012, metodom izvorne dinamičke transverzalne rezonantne vibracije te programom za projektiranje ANSYS. Istraživanje je provedeno u dvije faze. U prvoj je fazi određen dinamički modul elastičnosti (MOEd) uzoraka bez nanošenja ikakvih oštećenja. U drugoj je fazi određen otpor na savijanje i statički modul elastičnosti (MOE) istih uzoraka. Otpor na savijanje i statički modul elastičnosti (MOEa) predviđen je uz pomoć programa ANSYS, pri čemu su uzeti u obzir dinamički modul elastičnosti, gustoća drva i drugi parametri. Tijekom prve faze istraživanja izmjeren je modul elastičnosti (MOE) za različite skupine uzoraka različitim metodama. Rezultati su pokazali da su se prosječne vrijednosti modula elastičnosti različitih skupina*

* Corresponding author
[1] Author is researcher at Kauno kolegija Higher Education Institution, Kaunas, Lithuania. https://orcid.org/0009-0000-0641-347X
[2] Authors are researchers at Kaunas University of Technology, Kaunas, Lithuania. https://orcid.org/0000-0002-2014-8390, https://orcid.org/0009-0001-9699-4366

uzoraka međusobno razlikovale do 4,6 %. U drugoj fazi dodatni su uzorci podijeljeni u pet skupina, na kojima su napravljene rupe ili šupljine prema pet različitih shema. Za svaku skupinu određeni su MOE, MOEa i otpornost na savijanje, a utvrđeno je da se prosječne vrijednosti modula elastičnosti među različitim skupinama razlikuju do 17 %. Postojanje rupa i šupljina u drvu povećalo je anizotropiju materijala, što je najviše utjecalo na rezultate istraživanja. Bez obzira na broj rupa i šupljina, faktor prigušenja povećao se do 2,1 put.

KLJUČNE RIJEČI: *modul elastičnosti; koeficijent prigušenja; predviđanje mehaničkih svojstava; rupa; šupljina*

1 INTRODUCTION
1. UVOD

Wood has been widely used as a building material since ancient times. In addition to natural wood, other wood materials are also extensively used in construction. By gluing wood (Abed *et al*., 2022; Hildebrandt *et al.,* 2017; Ramage *et al.,* 2017; Risse *et al.*, 2019; Sanscartier Pilon *et al.,* 2019), it is possible to manufacture elements of various dimensions and alter some of their properties. This includes reducing the variability of mechanical properties, minimizing the environmental impact on dimensional and shape stability, eliminating defects or anatomical elements negatively affecting mechanical properties, and expanding the range of applications.

In the near future, wood will play an even more significant role in construction. This is due to the European Climate Law signed on June 24, 2021, obliging participants in the construction market to reduce greenhouse gas (GHG) emissions by at least 55 % by 2030 and achieve climate neutrality by 2050. The European Commission introduced the Green Deal to transform the EU into a modern, resource-efficient, and competitive economy, aiming for the EU to become the world's first climate-neutral continent by 2050, with no emissions of greenhouse gases and economic growth decoupled from resource use (The European Green Deal).

To predict the behavior of an element in a construction, precise knowledge of its mechanical properties is essential. Wood exhibits a wide range of properties, including mechanical variability. For example, the modulus of elasticity along the grain of elements cut from the same wood species can vary up to 2 times (Wood Handbook, 2010; Wagenführ, 2000). The properties of elements cut from the same tree trunk can also differ (Vobolis and Albrektas, 2007). Various defects, sometimes invisible to the naked eye (e. g. internal cracks, splits, resin cavities, fiber wrap, biological damage), and anatomical elements, which are often unavoidable, further influence mechanical properties. Thus, the mechanical properties of individual specimens, even those from the same sample, can vary by 30 % or more. The dispersion of values can be further increased by defects (Albrektas and Styraite, 2022).

It is advised to employ non-destructive methods for determining mechanical properties. By doing so, the test object remains unscathed and can be utilized subsequently. As a result, when constructing crucial structures, all the elements used can be examined, rather than just a small subset.

It is a well-established fact that values obtained for a particular property of a sample may differ based on the method employed to determine it. For instance, the dynamic modulus of elasticity, ascertained by non-destructive methods, can be higher than the static modulus of elasticity of the same element (Shan-qing and Feng, 2007; Divos and Tanaka, 2005; Nzokou *et al.,* 2006). This difference must be considered while designing structures or predicting the behavior of individual elements within them.

Holes or voids are often needed for various communication purposes in static structures. By cutting or drilling voids, there is a potential crack formation and propagation risk. The spread of these cracks changes the way structures collapse, and fractures may occur even under significantly lower loads (Ardalany *et al.,* 2013). Various methods are applied to prevent the formation and spread of such cracks, including the use of screws, steel plates, plywood, fiber-reinforced polymers (FRP), etc. An effective means of reinforcing elements made from fine wood panels is through reinforcement (Yerlikaya and Karaman, 2020). Karaman (2021) determined that the effects of joints reinforced BFRP and GFRP.

Depending on the size and location of voids, they can affect the elements strength, elasticity, and plasticity in various ways (Ardalany *et al.,* 2013; Zhang *et al.,* 2018; Gauronskaitė *et al.,* 2022). It is important to understand the impact of voids and holes on the behavior of structural elements. Static destructive methods are not suitable for evaluating the individual mechanical properties of each element, as the tested object will not be suitable for use after the study. Dynamic non-destructive methods, while not damaging the test object, often indicate average material properties. A typical example is measuring the dynamic modulus of elasticity by evaluating the sound propagation speed (Baltrušaitis and Mišeikytė, 2011). In this case, the average density of the sample, the average sound propagation speed, and the average dynamic modulus of elasticity are determined without isolating the "weakest" point (which could be a hole, in the case of a wooden element, a large branch, etc.). Yet, this "weak-

est" point can significantly influence the behavior of the element in a structure or the behavior of the entire structure.

Computer-aided design programs can be used in scenarios where it is imperative to assess the conduct of a structure or an element following the creation of a cavity or void. By acquiring knowledge of the pertinent physical and mechanical properties of an element, it is possible to model the alterations that may occur based on the location, size, and quantity of voids.

Objective of the study: To evaluate the possibility of predicting the behavior and properties of an element using computer-aided design software.

2 MATERIALS AND METHODS
2. MATERIJALI I METODE

The research employed spruce wood specimens that were free from visible defects, large branches, or other anatomical features that could have influenced the mechanical properties of the wood. The wood was purchased from a company selling wood products in Lithuania. Before testing, the cut samples were kept for two weeks in laboratory conditions with the temperature of 20-22 °C and the relative humidity of 55 – 60 %. A total of 70 specimens were examined, with dimensions measuring approximately 600 mm × 40 mm × 30 mm, and a moisture content ranging between 10.4 % and 11.6 %. The density of the specimens ranged from 403 to 451 kg/m^3. The length of the specimens was measured with a ruler with a precision of 1 mm, while the width and thickness were measured with a caliper having a precision of 0.05 mm. The mass of the specimens was measured with scales having a precision of 0.01 g, and the moisture content was measured using an electronic moisture meter in line with standard EN 13183-2:2003, EN 13183-2:2003/AC:2004, with a precision of 0.1 %.

The dynamic modulus of elasticity (*MOEd*) and coefficient of damping of the specimens were determined using an original methodology based on the transverse resonance vibration method (Vobolis and Albrektas, 2007; Gauronskaitė *et al.,* 2022). The bending resistance and static modulus of elasticity of the specimens were also determined using the methodology of standard LST EN 408:2010+A1:2012. Additionally, the behavior of the specimens was simulated using the ANSYS design program.

The four-point bending scheme and the specimen in the testing machine are presented in Figure 1.

ANSYS is one of the most popular engineering analysis programs due to its versatility, used for modeling, analysis and optimization in various engineering fields. This program allows you to perform element analysis (mechanical load, deformations, stresses). It is used in the development, optimization of product design, analysis of structural strength, stability, etc.

The study was conducted in two stages. In the first stage, 20 specimens were randomly selected, and their dynamic modulus of elasticity and coefficient of damping were determined. Subsequently, bending resistance and static modulus of elasticity were measured. The ANSYS design program used the available data (specimen density, dynamic modulus of elasticity) to determine the bending resistance and static modulus of elasticity. Finally, all the obtained values were statistically analyzed, and the results are presented in Table 1.

In the second stage, the remaining specimens were randomly divided into 5 groups of 10 specimens each (Groups II-VI), and holes and voids were drilled in accordance with the provided diagrams (see Figure 2).

The holes and voids are shaped in such a way as to have the greatest influence on the mechanical properties of the specimens during bending according to a scheme developed by the authors of this work. Subsequently, the dynamic modulus of elasticity and coefficient of damping of these specimens were determined. Bending resistance and static modulus of elasticity were also measured using the "four-point" bending method. Using the available data (specimen density, dynamic modulus of elasticity), the ANSYS design program determined the bending resistance and static modulus of elasticity. All values obtained were statistically processed (standard deviation (SD) was calculated).

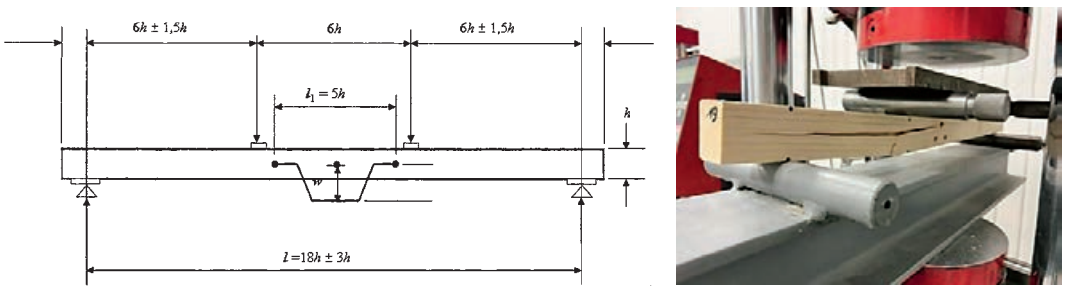

Figure 1 Four-point bending scheme (a) and specimen in testing machine (b); here *h* – specimen thickness; *l* – distance between supports

Slika 1. Shema savijanja u četiri točke (a) i uzorak u ispitnom uređaju (b); *h* – debljina uzorka, *l* – udaljenost između nosača

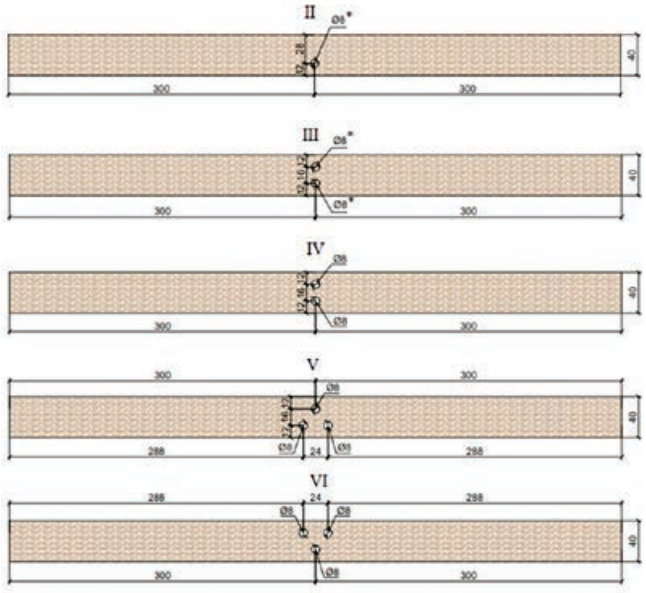

Figure 2 Schematics of drilling holes and voids in specimens: here II–VI are numbers of groups; * denotes a non-through hole in specimen, and holes have a depth of 15 mm (we called it „the void“)
Slika 2. Sheme bušenja rupa i šupljina u uzorcima: II. – VI. su brojevi skupina; * označava neprolaznu rupu na uzorku, a rupe su dubine 15 mm (nazvali smo ih *šupljinama*)

3 RESULTS AND DISCUSSION
3. REZULTATI I RASPRAVA

In the first stage of the study, the average values and standard deviations of the mechanical properties were determined for the tested specimens within each group, as presented in Table 1.

As expected, it was discovered that the (*MOEd*) is higher than the (*MOE*). The difference between the two is around 360 MPa, which is equivalent to 4.6 %. Other studies conducted by different researchers also showed similar differences between the static and dynamic modulus of elasticity (Divos and Tanaka, 2005; Nzokou *et al.,* 2006; Shan-qing and Feng, 2007). The ANSYS design program yielded an average static modulus of elasticity of 285 MPa, which is 3.7 % higher than the actual bending case. The differences are most likely due to the fact that the design program does not consider material heterogeneity. Additionally, fractures tend to occur at the weakest point of the specimen, which could be a result of a minor crack, a defect in the fiber structure, or other factors. The design program may not take into account these “weakest points,” which could also explain the lower average bending resistance obtained in real-life situations compared to the design program. The standard deviation could also be related to these differences. Typical examples of specimen failure are presented in Figure 3, illustrating the behavior of wood during bending.

It was noticed that the failure of one specimen (Figure 3a) happened at the location where it was under load, whereas another specimen (Figure 3b) did not fail in the location where the highest stresses were expected, but rather in its close vicinity. The location of the sample breakdown can be determined by any internal structural feature, including the aforementioned invisible one. The reasons for this variation in failure locations were the structural characteristics of each specimen. The compared design program ANSYS does not “see” these material structure features. For this reason, there may be a discrepancy between the mechanical properties determined in the laboratory and those

Table 1 Average mechanical properties values of specimen groups without voids and holes
Tablica 1. Srednje vrijednosti mehaničkih svojstava skupina uzoraka bez *šupljina* i rupa

Group *Skupina*	***MOEd***		**tgδ**		σ_w		***MOE***		σ_{wa}		MOE_a	
	Average value, MPa	*SD*, MPa	Average value, r. u.	*SD*, r. u.	Average value, MPa	*SD*, MPa	Average value, MPa	*SD*, MPa	Average value, MPa	*SD*, MPa	Average value, MPa	*SD*, MPa
I	7859	544	0.029	0.0023	62.2	4.7	7499	464	71.4	2.9	7784	360

Note: here *MOEd* – dynamic modulus of elasticity, *tgδ* – coefficient of damping, σ_w – bending resistance; *MOE* – static modulus of elasticity, σ_{wa} – bending resistance, calculated with ANSYS; MOE_a – modulus of elasticity, calculated with ANSYS
Napomena: MOEd – dinamički modul elastičnosti, tgδ – koeficijent prigušenja, σ_w – otpor na savijanje; MOE – statički modul elastičnosti, σ_{wa} – otpor na savijanje izračunan uz pomoć programa ANSYS; MOE_a – modul elastičnosti izračunan primjenom programa ANSYS

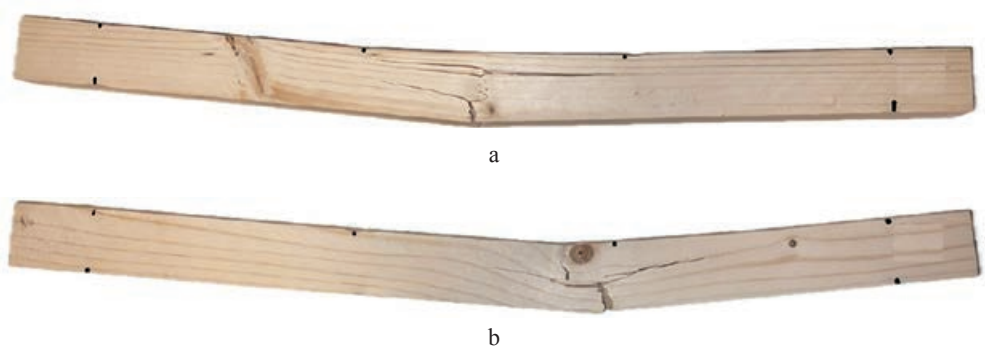

a

b

Figure 3 Typical examples of samples fracture
Slika 3. Tipični primjeri loma uzoraka

Table 2 The average mechanical property values and their standard deviations for specimen groups with voids and holes
Tablica 2. Srednje vrijednosti mehaničkih svojstava i njihove standardne devijacije za skupine uzoraka sa *šupljinama* i rupama

Group *Skupina*	***MOEd***		**tgδ**		σ_w		***MOE***		σ_{wa}		***MOEa***	
	Average value, MPa	*SD*, MPa	Average value, r. u.	*SD*, r.u.	Average value, MPa	*SD*, MPa	Average value, MPa	*SD*, MPa	Average value, MPa	*SD*, MPa	Average value, MPa	*SD*, MPa
II	6655	631	0.047	0.0058	46.5	4.4	5462	719	61.1	5.2	7132	664
III	6943	574	0.044	0.0030	52.6	3.9	5803	421	63.7	5.0	7355	436
IV	6215	208	0.049	0.0040	41.5	2.0	5144	380	56.6	2.1	6619	75
V	7085	650	0.046	0.0040	43.9	3.0	6195	553	64.1	6.2	7171	702
VI	7218	55	0.043	0.0050	44.3	3.8	5295	492	65.4	0.5	7626	22

Note: here *MOEd* – dynamic modulus of elasticity, *tgδ* – coefficient of damping, σ_w – bending resistance; *MOE* – static modulus of elasticity, σ_{wa} – bending resistance, calculated with ANSYS; MOE_a – modulus of elasticity, calculated with ANSYS
Napomena: MOEd – dinamički modul elastičnosti, tgδ – koeficijent prigušenja, σ_w – otpor na savijanje; MOE – statički modul elastičnosti, σ_{wa} – otpor na savijanje izračunan uz pomoć programa ANSYS; MOE_a – modul elastičnosti, izračunan primjenom programa ANSYS

calculated. The obtained coefficient of damping corresponds to the values of wood coefficient of damping obtained in previous studies (Vobolis and Albrektas, 2007; Gauronskaitė *et al.,* 2022; Albrektas and Styraite, 2022). The average mechanical property values and their standard deviations for specimen groups with voids and holes formed according to the discussed schemes are presented in Table 2.

Apparently, the average modulus of elasticity for specimens with voids or holes is lower than for those without them. It can be concluded that both specimens with voids and those with holes have statically obtained modulus of elasticity values close in magnitude (around 1000 MPa) or about 13-17 % lower than the dynamic modulus. This difference is significantly greater than when evaluating specimens without voids. The reason for this is that, during assessment of dynamic modulus of elasticity, voids only facilitate the bending of the specimen, whereas during static bending, they significantly weaken the bending zone, leading to specimen failure. Figure 4 presents several typical specimen fracture cases.

It has been observed that specimens typically fail where the highest load is applied and where voids or holes are formed. Group VI stands out from all other groups as in this case, the difference between static and dynamic modulus of elasticity is approximately 1900 MPa or about 27 %. Upon analyzing the results and failure zones of specimens, it has been concluded that the fiber in the failure zone of several specimens in this group was weaker and further weakened by the presence of voids. After excluding these specimens, the difference is significantly smaller. Figure 4 presents variant "e" as an example of such a specimen.

The ANSYS design program determined a modulus of elasticity that was slightly higher than the *MOEd* (about 400 MPa or about 6-7 %). This can be explained by the fact that the dynamic modulus of elasticity determines the frequency of vibrations when the specimen deflects in one mode (Vobolis and Albrektas, 2007; Gauronskaitė *et al.,* 2022). Voids are where the specimen bends and they "facilitate" the bending. The design program also evaluates voids in the bending zone. However, the real result is worse than the theoretical one, likely due to the anisotropy in materials and uneven distribution of properties. This is also true for average bending resistance, which is practically 17 – 31 % lower than that determined by the design program. Figure 5 shows examples of specimen failure and stress distribution simulated by the design program.

It has been observed that the highest stresses that should make the specimens fail, are supposed to form

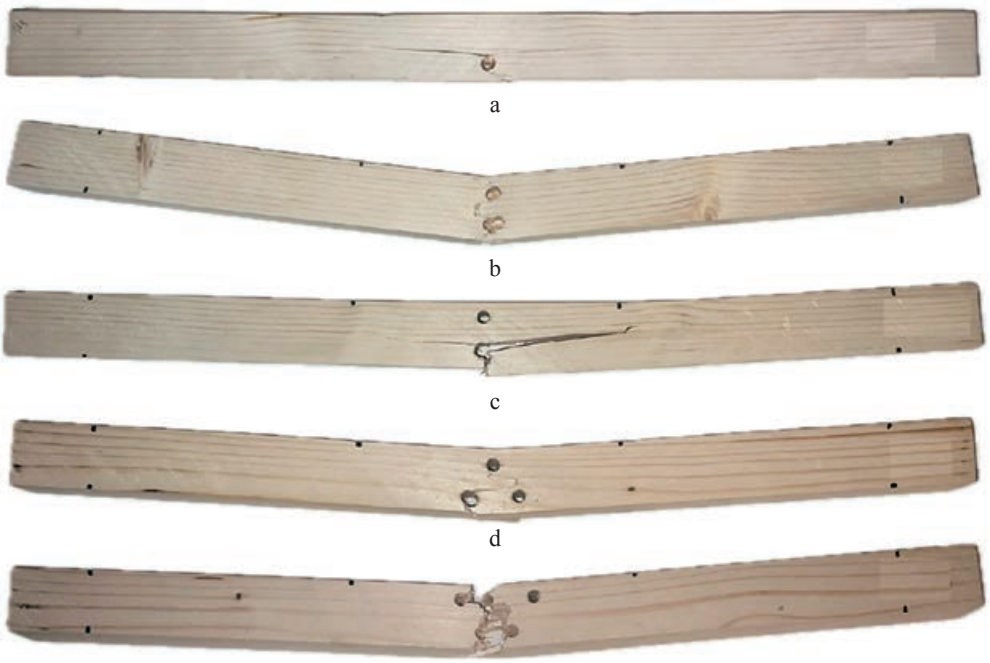

a

b

c

d

e

Figure 4 Typical specimen fracture cases
Slika 4. Tipični primjeri loma uzoraka

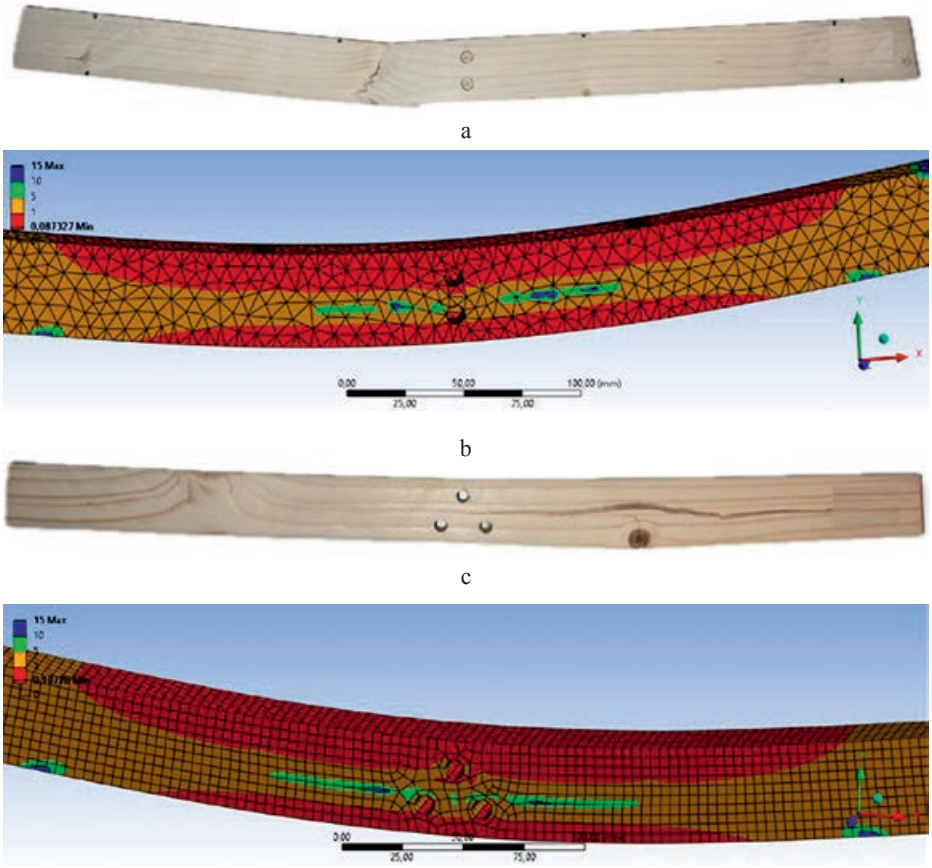

a

b

c

d

Figure 5 Examples of stress distribution simulated by design program for specimen failure (a, b – one from group III, c, d – one from group V)
Slika 5. Primjeri raspodjele naprezanja simuliranog programom za proračun loma uzorka (a, b – jedan uzorak iz skupine III., c, d – jedan uzorak iz skupine V.)

symmetrically around the voids that are created. However, in practice, due to the unique nature of wood structure, the specimens fail asymmetrically under load, most likely at the weakest points.

The coefficient of damping increased up to two times regardless of the formation of a void or a hole. Such defects compromise specimen integrity, and results are consistent with similar studies (Gauronskaitė *et al.,* 2022; Albrektas and Styraitė, 2022). These studies also evaluated the influence of element integrity on the coefficient of damping. In the first case, holes required for fittings to secure furniture parts were modeled, and in the second, wood drying defects (cracks formed during improper drying) were modeled.

4 CONCLUSIONS
4. ZAKLJUČAK

The values of mechanical properties for wood specimens were determined through various methods and simulated using a design program. The correlation between the different methods and the program simulation showed a relatively small margin of error. However, the modulus of elasticity for the same specimen varied up to 7.1 % when determined by different methods, with an average group difference of up to 4.6 %.

When a significant defect (especially in the bending area) is present in a specimen, its resistance to static bending or static modulus of elasticity decreases more than when evaluated by dynamic transverse resonance vibration method or simulated by the design program. This is because the dynamic method only partially eliminates the anisotropy of wood. The design program "assumes" that wood is an isotropic and homogeneous material and evaluates only the defects that are specified by the designer. As a result, the modulus of elasticity determined by different methods for the same specimen can differ by up to 24 %, with the average group difference being up to 17 %.

The standard deviation of the modulus of elasticity values in all specimen groups has been calculated to be large, up to 13 % from the average value. This suggests that there is a significant variation in the mechanical properties of the material, regardless of the nature or quantity of voids formed in the specimen.

The study found that the place of presence of voids and holes did not impact the coefficient of damping. However, when voids or holes were present in individual specimens, the coefficient of damping increased by a factor of 1.5 to 2.1.

In order to improve the precision of computer-aided design programs in predicting the characteristics and behavior of an element, extensive testing is required. This testing should involve altering the location, quantity, and size of voids, as well as analyzing different wood properties and design programs. The research conducted in this study has shown that this method is feasible and can be partially relied upon to obtain results. Although the results obtained by different methods are quite different, the general trends remain. Also, a large dispersion of results has been obtained, which is typical for most research results due to the peculiarities of wood structures.

5 REFERENCES
5. LITERATURA

1. Abed, J.; Rayburg, S.; Rodwell, J.; Neave, M, 2022: A Review of the performance and benefits of mass timber as an alternative to concrete and steel for improving the sustainability of structures. Sustainability, 14 (9): 5570. https://doi.org/10.3390/su14095570
2. Albrektas, D.; Styraite, A., 2022: Modelling and investigating real-world drying defects in wood. Drvna industrija, 73 (2): 115-123. https://doi.org/10.5552/drvind.2022.2040
3. Ardalany, M.; Fragiacomo, M.; Carradine, D.; Moss, P., 2013: Experimental behavior of Laminated Veneer Lumber (LVL) joists with holes and different methods of reinforcement. Engineering Structures, 56: 2154-2164. https://doi.org/10.1016/j.engstruct.2013.08.034
4. Baltrušaitis, A.; Mišeikytė, S., 2011: Strength and stiffness properties of the Lithuanian grown scotis pine (*Pinus sylvestris*): non destructive testing methods vs static bending. Wood Research, 56 (2): 157-168.
5. Divos, F.; Tanaka, T., 2005: Relation between static and dynamic modulus of elasticity of wood. Acta Silvatica & Lignaria Hungarica, 1: 105-110.
6. Gauronskaitė, S.; Dobilaitė, V.; Jucienė, M.; Albrektas, D., 2022: Effect of open-holes on mechanical properties of wood composite materials. Wood Research, 67 (1): 41-50. https://doi.org/10.37763/wr.1336-4561/67.1.4150
7. Hildebrandt, J.; Hagemann, N.; Thrän, D., 2017: The contribution of wood-based construction materials for leveraging a low carbon building sector in Europe. Sustainable Cities and Society, 34: 405-418. https://doi.org/10.1016/j.scs.2017.06.01
8. Karaman, A., 2021: Bending moment resistance of t-type joints reinforced with basalt and glass woven fabric materials. Maderas. Ciencia y Tecnología, 23: 1-12. https://doi.org/10.4067/s0718-221x2021000100444
9. Karaman, A.; Yildirim, M. N.; Tor, O., 2021: Bending characteristics of laminated wood composites constructed with black pine wood and aramıd fiber reinforced fabric. Wood Research, 66 (2): 309-320. https://doi.org/10.37763/wr.1336-4561/66.2.309320
10. Karaman, A.; Yildirim, M. N., 2021: Effects of wood species of the dowels and fiber woven fabric types on bending moment resistance of l-shaped joints. Wood Industry and Engineering, 3 (2): 12-22.
11. Nzokou, P.; Freed, J.; Kamden, D. P., 2006: Relationship between non destructive and static modulus of elasticity of commercial wood plastic composites. Holz als Roh und Werkstoff, 64: 90-93. https://doi.org/10.1007/s00107-005-0080-x
12. Ramage, M. H.; Burridge, H.; Busse-Wicher, M.; Fereday, G.; Reinolds, T.; Shah, D. U.; Wu, G.; Yu, L.; Fleming, P.; Densley-Tingley, D.; Allwood, J.; Dupree, P.; Linden, P. F.; Scherman, O., 2017: The wood from the trees: The use

of timber in construction. Energy Reviews, 68 (1): 333-359. https://doi.org/10.1016/j.rser.2016.09.107
13. Risse, M.; Weber-Blaschke, G.; Richter, K., 2019: Eco-effi ciency analysis of recycling recovered solid wood from construction into laminated timber products. Science of The Total Environment, 661: 107-119. https://doi.org/10.1016/j.scitotenv.2019.01.117
14. Sanscartier Pilon, D.; Palermo, A.; Sarti, F.; Salenikovich, A., 2019: Benefits of multiple rocking segments for CLT and LVL Pres-Lam wall systems. Soil Dynamics and Earthquake Engineering, 117: 234-244. https://doi.org/10.1016/j.soildyn.2018.11.026
15. Shan-qing, L.; Feng, F., 2007: Comparative study on three dynamic modulus of elasticity and static modulus of elasticity for Lodgepole pine lumber. Journal of Forestry Research, 18 (4): 309-312. https://doi.org/10.1007/s11676-007-0062-4
16. Vobolis, J.; Albrektas, D., 2007: Comparison of viscous elastic properties in wood of leaf and coniferous tree. Materials Science, 13 (2): 147-151.
17. Wagenführ, R., 2000: Holzatlas: mit zahlreichen Abbildungen München: Fachbuchverlag Leipzig im Carl Hanser Verlag, Leipzig (in German).
18. Yerlikaya, N. C.; Karaman, A., 2020: Effect of the fabric reinforcement of structural holes in wood based panels. Wood Research, 65 (3): 485-496. https://doi.org/10.37763/wr.1336-4561/65.3.485496
19. Yildrim, M. N.; Karaman, A.; Zor, M., 2021: Bending characteristics of laminated wood composites made of poplar wood and GFRP. Drvna industrija, 72 (1): 3-11. https://doi.org/10.5552/drvind.2021.1913
20. Zhang, X.; Que, Y.; Wang, X.; Li, Z.; Zhang, L.; Han, C.; Que, Z.; Komatsu, K., 2018: Experimental behavior of laminated veneer lumber with round holes, with and without reinforcement. BioResources, 13 (4): 8899-8910. https://doi.org/10.15376/biores.13.4.8899-8910
21. *** EN 408, 2010+A1:2012: Timber structures – Structural timber and glued laminated timber – Determination of some physical and mechanical properties European Committee for Standardization, Brussels.
22. ***The European Green Deal. Striving to be the first climate-neutral continent. An official website of the European Union. https://ec.europa.eu/newsroom/know-4pol/items/664852
(Accessed Jan. 15, 2024).
23. ***Wood Handbook, 2010: Wood as an Engineering Material. Centennial Edition. Forest Products Laboratory. Wood handbook – Wood as an engineering material. General Technical Report FPL-GTR-190. WI: U.S. Department of Agriculture, Forest Service, Forest Products Laboratory, Madison.

Corresponding address:

DARIUS ALBREKTAS
Kauno Kolegija Higher Education Institution, Pramones st. 20, LT-50468 Kaunas, LITHUANIA,
e-mail: darius.albrektas@ktu.lt

Ghanbar Ebrahimi*[1], Alireza Shakeri[2], Pyman Ahmadi[1], Mosayeb Dalvand[1], Masoud Shafee[1]

Constituent Elements, pH and Electrical Conductivity Values of Feedstock, Ash and Slow Pyrolysis Derived Biochar of Date Palm Wastes

Sastavni elementi, pH vrijednost i električna provodnost sirovine, pepela i biougljena dobivenoga sporom pirolizom od otpadaka palme datulje

ORIGINAL SCIENTIFIC PAPER
Izvorni znanstveni rad
Received – prispjelo: 22. 6. 2024.
Accepted – prihvaćeno: 12. 1. 2025.
UDK: 631.831
https://doi.org/10.5552/drvind.2025.0223

ABSTRACT • *Date palm wastes (rachis and dried stems) are feasible biomass to be treated and used for soil improvement and restoration purposes. Identified properties of processed forms of such biomass are required for their deliberated applications in compensating for any types of soil deficiencies. For this task constituent elements, pH and electrical conductivity (EC) values of fiber bundles, ash and slow pyrolysis derived biochar of these wastes were determined. Test materials were from two palm groves, differentiated by governing ecological conditions, named tropical and dry zones, to study climate impacts on the same palm species. Experimental data have shown that discrepancies in the percentages of C, H, N and S in three types of waste from the humid zone are not drastic. Their ashes are alkaline, but feedstock and biochar are acidic. EC values are high in ashes, but low in feedstock and biochar. C/N ratios do not change considerably. The same results were also observed for dry zone wastes, except their C/N ratio which is drastically higher. Percentages of measured properties of wastes from sampled groves were also compared for climate impacts. In terms of properties, differences between three forms of waste from two groves require to be considered when used for soil improvement purposes.*

KEYWORDS: *palm waste; constituent element; biochar; ash; fiber bundles; pyrolysis*

SAŽETAK • *Otpatke od palme datulje (lisne osi i osušene stabljike) moguće je iskoristiti za biomasu koja se može obrađivati i dalje upotrebljavati za poboljšanje i obnovu tla. Za promišljenu primjenu u nadoknadi bilo kakvog nedostatka tla potrebno je poznavati svojstva prerađenih oblika te biomase. Stoga su u ovom istraživanju određeni sastavni elementi, pH vrijednost i električna provodnost (EC) snopova vlakana, pepela i biougljena dobivenoga*

* Corresponding author
[1] Authors are researchers at Department of Wood and Paper Sciences, Faculty of Natural Resources, University of Tehran, Karaj, Iran
[2] Author is researcher at Faculty of Chemistry, University of Tehran, Tehran, Iran

sporom pirolizom otpadaka palme datulje. Kako bi se proučili klimatski utjecaji na tu vrstu palme, odabrani su uzorci iz dvaju nasada palmi koje su rasle u različitim ekološkim uvjetima nazvanima vlažna i suha zona. Eksperimentalni podatci pokazali su da odstupanja u postotcima elemenata C, H, N i S u sirovim vlaknima, pepelu i biougljenu palminih otpadaka iz vlažne zone nisu značajna. Pepeo je alkalan, ali su sirova vlakna i biougljen kiseli. EC vrijednosti su u pepelu visoke, ali su u sirovim vlaknima i biougljenu niske. C/N omjeri značajno se ne razlikuju. Jednaki rezultati dobiveni su i za otpadak od palmi iz suhe zone, osim što su C/N omjeri znatno viši. Izmjerena svojstva palminih otpadaka uspoređena su i s obzirom na klimatske utjecaje na nasad palmi, odnosno uspoređeni su uzorci iz vlažne i suhe zone. Pri uporabi palmine biomase za poboljšanje tla moraju se uzeti u obzir razlike između svojstava sirovih vlakana, pepela i biougljena iz dvaju nasada palmi.

KLJUČNE RIJEČI: *otpadci od palmi; sastavni element; biougljen; pepeo; snopovi vlakana; piroliza*

1 INTRODUCTION
1. UVOD

Date palm *(Phoenix dactilyfera)* wastes include rachis and dried stems. Rachis is more abundant since date farmers prune about 15 dried rachises from each fruit producing palm tree every year. Weight of trimmed rachis (fronds) comprises million metric tons annually. Dried stems are also rather plentiful wastes in date palm groves (palm trees stands). There are no official referable records of palm wastes (from both fruit bearing and nonfruit bearing palm stands), except a local date (Ahmadi *et al*., 2015). Proper utilization of these biomass has no history so far, although they contain valuable chemical substances (Ebrahimi *et al*., 2021; Ebrahimi *et al*., 2022). Some basic compositions of these wastes were studied in laboratory scale (see Tables 3, 4, 13 in Jonoobi *et al*., 2019). Some unpublished results of case studies on date palm wastes were reviewed as well.

Their use as raw material in producing fiber-based products was proposed, since these wastes are fibrous materials (Prasad and Power, 1991). Such concept of utilizing these residuals requires continuous removal of these wastes from palm groves as they would damage the groves environmentally, because end products are unreturnable to palm groves as fertilizer or any kind of soil amendment agent. Therefore, in the long run, the soil of groves would not be nutritious for the trees.

The right procedure for managing these residuals (Brewer *et al*., 2011) is to convert them into useful additives for soil amendment and restoration. This concept is compatible with environmental issues as well (Kamperidou *et al.,* 2021).

During recent decade, the concept of conversion of crop biomass through thermochemical process (pyrolysis) into solid (biochar) and liquid (vinegar) substances as returnable additives to soils under cultivations has been developed (Kloss *et al*., 2012).

Application of this kind of treatment on biomass residual has been extended to date palm wastes conversion as well. However, quite a few instructive research reports dealing with properties of biochar (Ronsse *et al*., 2013; Jouiad *et al*., 2015; Bensidhom *et al*., 2018; Usman *et al*., 2015), its uses as green sorbents of organic and inorganic pollutants (Usman *et al*., 2016; Al-Wabel *et al*., 2019), improving soil fertility, upgrading and remediation degraded soils (Al-Wabel *et al*., 2019; Beesley *et al*., 2011) and climate change mitigation (Hussain *et al*., 2014) have been published.

The above studies have clearly shown the positive functions of pyrolysis derived biochars. As mentioned earlier, the pyrolysis process is not harmful to the environment and pyroligneous gases from biomass pyrolysis can mostly be condensed by a properly designed system.

Another known pyrolytic product is bio-oil or vinegar, also called bio-fuel (Woolf *et al*., 2010), which results from condensing volatiles emitted from pyrolysis reactors with chemical content depending on temperature used in pyrolysis processes.

The objectives of this investigation were to characterize feedstock, ash and biochar samples from date palm wastes for their constituent elements, pH and EC (Index of soluble salt in soil solution) values, comparing rachis (fronds) and stem from each sampled grove and from groves in tropical and dry zones for finding ecological impact on the above variables. These objectives were designed to evaluate the potentiality of three forms of palm wastes mainly for their farming purposes. Results of this work will be useful for making proper use of such plentiful biomass (Prasad and Power, 1991; Power and Prasad, 1997).

2 MATERIALS AND METHODS
2. MATERIJALI I METODE

For this study, date palm wastes (dry rachis and stems) samples were collected from palm groves in Lamerd (southern territory of Fars province, in hot and humid climate zone) and Kerman (southeast province of Iran, a hot and dry climate zone). The purpose of collecting test materials from date palm groves in two different climate zones was to find discrepancies in wastes elemental contents due to ecological impacts, if any; however, the palm species was the same.

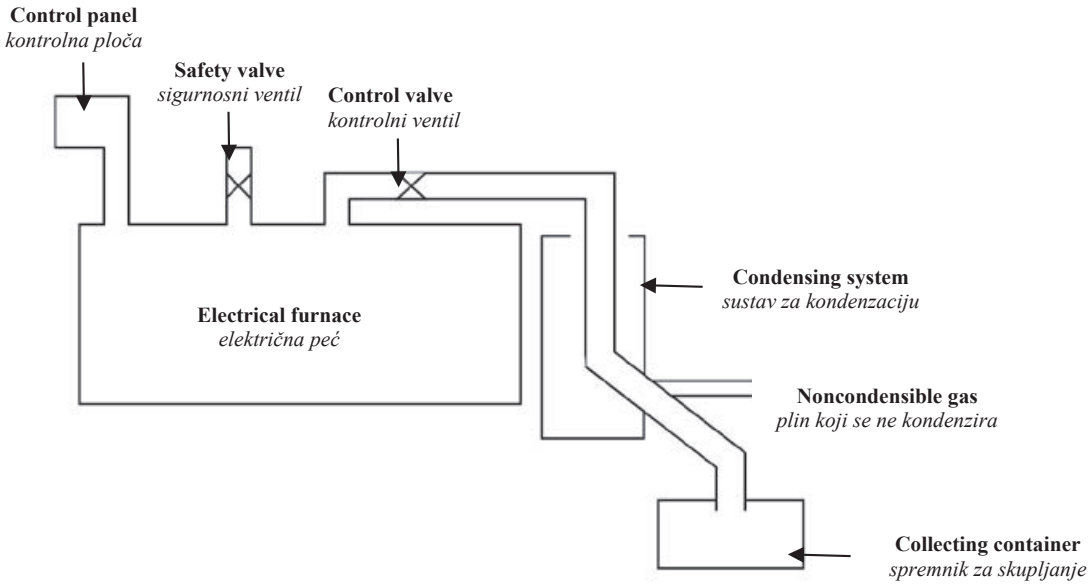

Figure 1 Pyrolysis apparatus
Slika 1. Oprema za pirolizu

Test materials were air dried to about 12, 7.5, 5 % moisture content, then chipped into particles, measuring 10-15 mm in length, less than several millimeters in thickness. Samples of rachis and stem (types of waste) were separately divided into three randomized sets. A set of each type of waste was mechanically defibrated for receiving fiber bundles (feedstock specimens). A slow pyrolysis process was conducted on one set in a laboratory scale electrical furnace (designed and shop fabricated, Figure 1). The third set of samples of each type of waste was burnt down to ash in an open fire. From each set of samples after the application of designated treatment, random specimens were drawn for C, H, N, S analysis.

2.1 C, H, N, S analysis
2.1. Analiza elemenata C, H, N i S

As mentioned above, randomly chosen specimens of feedstock (fiber bundles), ash and biochar (out of rachis & stem wastes of date palm) were analyzed (by Flash EA 1112 Series, Thermos Finnegan, Mass. USA) for their constituent elements, namely C, H, N and S. Table 1 presents accumulated data (mean and coefficient of variation) on percentages of elemental

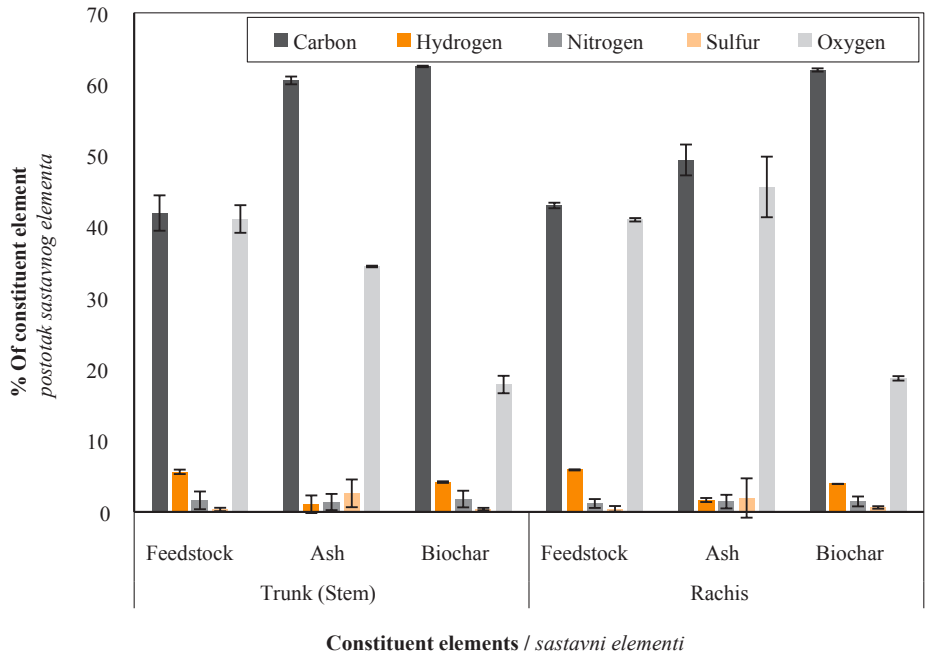

Figure 2 Mean percentages and corresponding error bars of C, H, N, S and O in feedstock, ash and biochar of date palm wastes from groves in humid climate zone (Lamerd)
Slika 2. Srednja vrijednost postotaka i odgovarajući stupci pogrešaka za elemente C, H, N, S i O u sirovim vlaknima, pepelu i biougljenu od otpadaka palme datulje iz nasada u zoni vlažne klime (Lamerd)

Table 1 Average and coefficient of variation of percentages of constituent elements, pH, EC and calculated molar ratios of feedstock, ash and biochar from date palm wastes (stem and rachis) from grove in humid climate zone (Lamerd)
Tablica 1. Srednja vrijednost i koeficijent varijacije postotaka sastavnih elemenata, pH, EC i izračunanih molarnih omjera sirovih vlakana, pepela i biougljena od otpadaka palme datulje (stabljike i lisne osi) iz nasada u zoni vlažne klime (Lamerd)

Variables *Varijable*	**Trunk (Stem)** / *Deblo*						**Rachis (Fronds)** / *Lisne osi (lišće)*					
	Feedstock* *Sirovina**		**Ash** *Pepeo*		**Biochar** *Biougljen*		**Feedstock** *Sirovina*		**Ash** *Pepeo*		**Biochar** *Biougljen*	
	Ave.	CV%**	Ave.	CV%	Ave.	CV%	Ave.	CV%	Ave.	CV%	Ave.	CV%
MC, % *sadržaj vode, %*	12.60	8.45					11.65	14.05				
Biochar, % *biougljen, %*	49.72						51.61					
Bio-oil, % *bioulje, %*	31.61						29.64					
Volatiles, *hlapljivi spojevi,* %	18.67						18.75					
Ash content, % *sadržaj pepela, %*	8.55				13.27		8.55				13.27	
Content of element, % *Sadržaj elemenata, %*												
C	41.91	5.92	60.51	0.89	62.47	0.19	42.90	0.91	49.36	4.37	61.98	0.36
H	5.62	5.53	1.07	115	4.18	0.11	5.89	1.35	1.70	16.8	3.93	0.56
N	1.62	76.82	1.38	82.31	1.80	64.60	1.18	52.50	1.45	65.50	1.47	47
S	0.34	70.59	2.61	74.33	0.40	42.5	0.43	91.85	1.95	141.40	0.63	34.92
O	41.10	4.71	34.42	0.33	17.86	6.85	40.97	0.59	45.57	9.32	18.73	1.70
pH***	4.10		10.30		6.30		4.23		11.23		6.11	
EC***	4.23 ds/m		15.42 ds/m		3.51 ds/m		4.20 ds/m		15 ds/m		3.50 ds/m	
Molar ratio												
O/C	0.98		0.56		0.28		0.95		0.92		0.30	
H/C	0.13		0.02		0.07		0.14		0.03		0.06	
(O+N/C)	1.02		0.56		0.31		0.98		0.95		0.32	
O+N+S/C)	1.03		0.63		0.32		1		1		0.33	
C/N	35.88	72.57	66.25	82.72	43.78	54.50	42.40	53.62	44.33	69.45	47.48	47.46

Due to seasonal dependency of *MC*, feedstock density is variable as well. / *Zbog sezonske ovisnosti sadržaja vode gustoća sirovine također je promjenjiva.*
**CV was adopted rather than standard deviation. / ***CV je odabran umjesto standardne devijacije.*
***In the extract for measuring pH and EC values, ratio of solid substance to water was maintained 1:2.5. / ****U ekstraktu za mjerenje pH i EC omjer suhe tvari i vode bio je 1:2,5.*

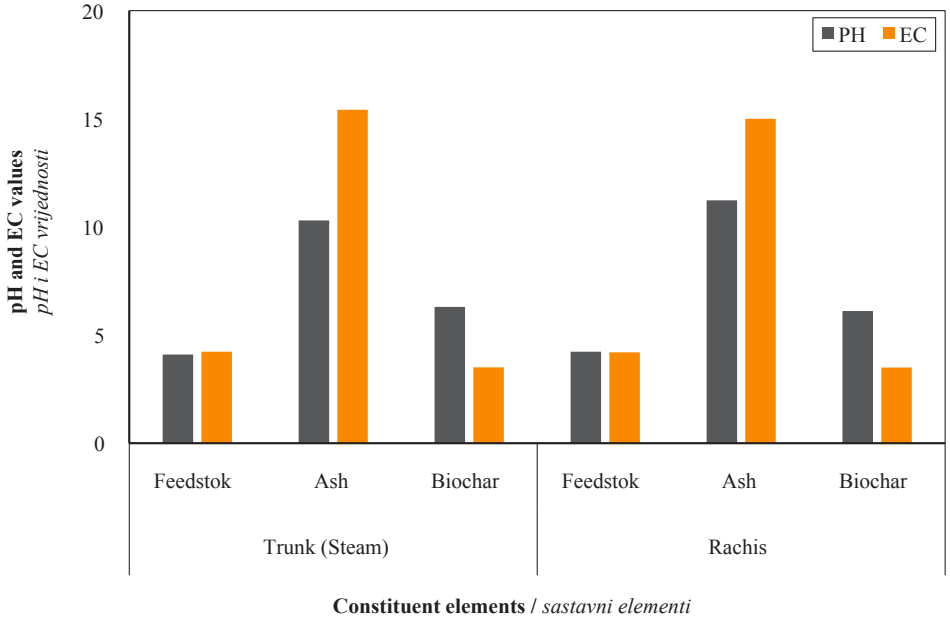

Figure 3 pH and EC values of feedstock, ash and biochar of date palm wastes from groves in humid zone (Lamerd)
Slika 3. pH i EC vrijednosti sirovih vlakana, pepela i biougljena od otpadaka palme datulje iz nasada u zoni vlažne klime (Lamerd)

Table 2 Average and coefficient of variation of percentages of constituent elements of feedstock, ash and biochar from date palm wastes (stem and rachis) from groves in dry climate zone (Kerman)
Tablica 2. Srednja vrijednost i koeficijent varijacije postotaka sastavnih elemenata, pH, EC i izračunanih molarnih omjera sirovih vlakana, pepela i biougljena od otpadaka palme datulje (stabljike i lisne osi) iz nasada u zoni suhe klime (Kerman)

Variables *Varijable*	**Trunk (Stem)** / *Deblo*						**Rachis (Fronds)** / *Lisne osi (lišće)*					
	Feedstock *Sirovina*		**Ash** *Pepeo*		**Biochar** *Biougljen*		**Feedstock** *Sirovina*		**Ash** *Pepeo*		**Biochar** *Biougljen*	
	Ave.	CV%	Ave.	CV%	Ave.	CV%	Ave.	CV%	Ave.	CV%	Ave.	CV%
MC, % *sadržaj vode, %*	7.50	8.21					4.89	6.34				
Biochar, % *biougljen, %*	57.15						51.70					
Bio-oil, % *bioulje, %*	32.21						34.90					
Volatiles, % *hlapljivi spojevi, %*	10.63						13.40					
Ash content, % *sadržaj pepela, %*	8.50				12.5		8.50				13.30	
Content of element, % *Sadržaj elemenata, %*												
C	40.78	6.30	15.53	105	58.60	5.37	40.78	4.60	32.89	31.53	59	9.34
H	5.45	15	1.13	0.66	2.25	102	4.52	2.45	1.46	5.82	4	0.25
N	0.27	50	0.45	142	0.63	117	0.55	114	0.40	52.50	1	3.60
S	0.47	59.60	2.76	64	2.29	77	0.51	16.70	1.35	78.50	0.61	4.64
O	44.53	9.10	80.59	19.7	23.74	18.65	44.12	2.32	63.40	14.53	22	25.20
pH	4.20		10.25		6.30		4.60		11.20		6.11	
EC	4.91 ds/m		4.20 ds/m		10.50 ds/m		15.35 ds/m		10 ds/m		11.70 ds/m	
Molar ratio												
O/C	1.09		5.18		0.41		1.08		1.92		0.37	
H/C	0.13		0.07		0.04		0.11		0.18		0.68	
(O+N/C)	1.10		5.22		0.42		1.10		1.94		0.39	
O+N+S/C)	1.11		5.40		0.45		1.11		1.98		0.40	
C/N	39.45	141	15	142	308	117	211	115	103.70	77.80	61.2	0.16

contents in feedstock, ash and biochar of stem and rachis from humid climate zone (Lamerd) date palm grove. In Table 1 molar rations were calculated through determination of the percentages of oxygen by Eq. 1 (Al-Wabel *et al.,* 2019):

$$Percentage\ of\ oxygen = 100 - (C + H + N + S + ash\%) \quad (1)$$

Figure 2 graphically shows the mean percentages, coefficient of variation and corresponding error bar of each constituent element of feedstock, ash and biochar out of sampled stem and rachis from groves in humid zone (Lamerd).

The pH and EC values of feedstock, ash and biochar of palm residuals from humid climate zone were measured as well.

Table 1 also contains data of these variables. Figure 3 presents these data graphically.

The same procedure was used for presenting data of sampled stem and rachis of date palm wastes from palm groves in Kerman territory, the dry climate zone. Table 2 presents relevant experimental data of these groves. Figure 4 is the graphical presentation of data in Table 2. pH and electrical EC values of related samples are shown graphically in Figure 5.

Volatiles in each Table (1, 2) are the remainder of feedstock weight minus sum of the produced bio-oil and biochar weights. Determination of volatiles by adopting either ASTM4 D1762-8 specification or applying A proposed modified method for analysis of biochar biochar (Skjemstad *et al.,* 2002) was not possible, due to the lack of the proper equipment.

3 RESULTS AND DISCUSSION
3. REZULTATI I RASPRAVA

As mentioned in the introduction, plentiful date palm residual is not utilized nor used in a beneficial manner. Mostly these wastes are scattered left in dry slashes form over palm groves floor. They are partially burnt, risking the expansion of flames and producing smoke that pollutes the environment. The ashes resulting from the waste burning process are not distributed evenly across the groves. Surface run-offs coming from precipitation and irrigation may contribute to the distribution of these ashes to some extent. Dealing with these valuable wastes in such a primitive manner is not productive. These wastes deserve to be utilized methodically based on scientific and technological achievements in order to develop products with higher added value.

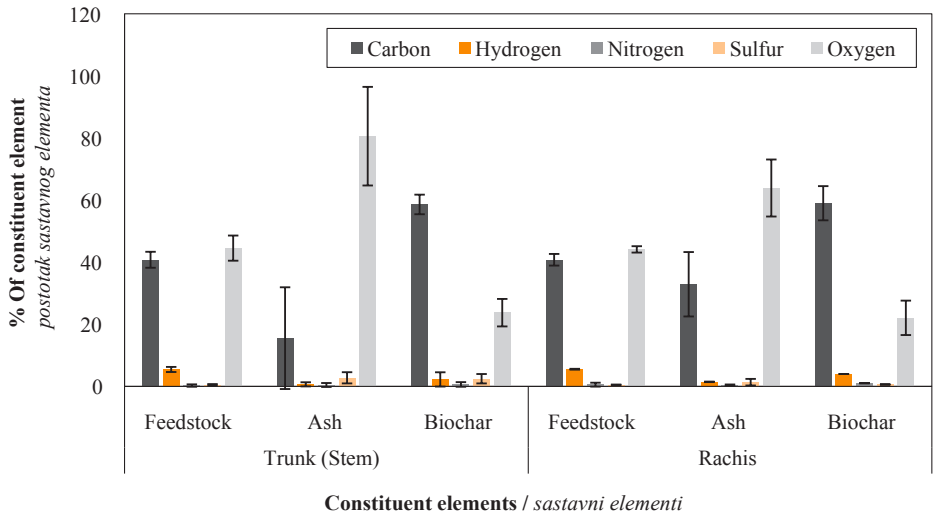

Figure 4 Mean percentages and corresponding error bars of C, H, N, S and O in feedstock, ash and biochar of date palm wastes from groves in dry climate zone (Kerman)
Slika 4. Srednja vrijednost postotaka i odgovarajući stupci pogrešaka za elemente C, H, N, S i O u sirovim vlaknima, pepelu i biougljenu od otpadaka palme datulje iz nasada u zoni suhe klime (Kerman)

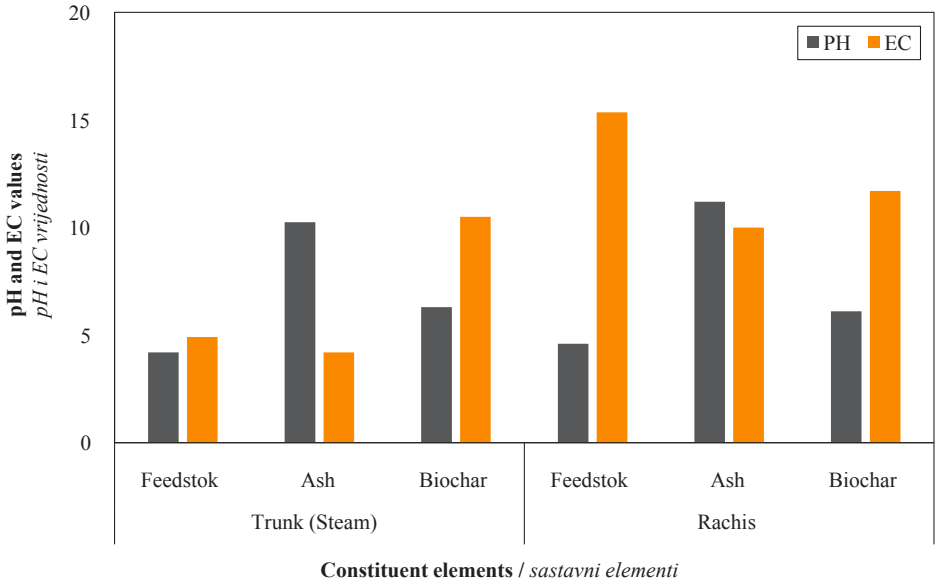

Figure 5 pH and EC values of feedstock, ash and biochar of date palm wastes from groves in dry zone (Kerman)
Slika 5. pH i EC vrijednosti sirovih vlakana, pepela i biougljena od otpadaka palme datulje iz nasada u zoni suhe klime (Kerman)

3.1 Applicable forms of date palm wastes for soil amendment
3.1. Primjenjivi oblici otpadaka palme datulje za poboljšanje tla

3.1.1 Fiber bundles (feedstock)
3.1.1. Snopovi vlakana (sirovina)

The most abundant date palm waste comes from rachis (fronds), since twice a year rachis trimming takes place. Palm trees last a long time, mostly more than a century, however their dried slashes are found rather frequently throughout the old palm groves. Palm tree stem (trunk) is mostly the remainder of pruned rachis in its circumference and therefore it should contain elements that are present in rachis. Thus, this type of waste should not be ignored.

The addition of feedstock fiber bundles to soil either from stem or rachis is not recommended because it takes a longer time to decay and decompose completely and it has been also recognized that organic soil improvement with organic decomposable substrates can contribute to global warming and greenhouse gases (Al-Wabel *et al.,* 2019). However, the basic elements (C, H, N, S, O) as well as C/N ratio, pH and EC values in fiber bundles (feedstock) are comparable to those in ash and biochar. Therefore, it may function better in some areas of farming activities, like in fish and shrimp farming ponds.

Preparing ash from date palm waste seems the simplest way of converting these residuals into soil additive, and soil exports generally agree with such additive as a soil amendment agent, but it cannot be as good as biochar.

3.1.2 Biochar
3.1.2. Biougljen

Biochar is the preferred type of converted biomass through thermo-chemical process, due to its desired properties when compared with any other soil additives. Biochar was evaluated as green sorbent (Al-Wabel *et al.,* 2019) for removing organic and inorganic pollutants in aqueous solutions. All three kinds of date palm wastes are functional additives to the soil.

3.2 Comparisons of three types of date palm wastes from stem and rachis in each sampled grove
3.2. Usporedbe triju vrsta otpadaka palme datulje sa stabljike i lisnih osi u svakoj uzorkovanoj brazdi

3.2.1 Wastes from palm grove in humid climate zone
3.2.1. Otpadci iz palmine brazde u zoni vlažne klime

Fiber bundles, ash and biochar of stem and rachis were compared for their elemental contents in Table 3. This Table shows as follows:

In feedstock:

Carbon - carbon in stem feedstock is less than that of rachis by 2.52 %.

Hydrogen - rachis has more hydrogen (4.80 %) than stem.

Nitrogen - nitrogen is more pronounced in stem feedstock than in rachis by 27 %, a noticeable difference.

Sulfur - stem fiber bundles contain more sulfur than fiber bundles of rachis by 26 %, a rather significant difference.

Oxygen - the amount of oxygen is 10.87 % higher in rachis than in stem.

C/N ratio - this ratio in fiber bundles of rachis is greater than that of stem by 18 %, a slight discrepancy.

pH values of the feedstock of both stem and rachis are acidic, fiber bundles of rachis are less acidic by 3.17 %, which is a little discrepancy.

EC values - fiber bundles (feedstock) of stem and rachis have the same EC values.

In ash:

Carbon - the percentage of carbon in stem ash is 41 % greater than that of rachis.

Hydrogen - hydrogen content in stem ash is 58 % higher than in rachis ash.

Nitrogen - the percentage of nitrogen in stem ash is only 5.80 % higher than in rachis ash.

Sulfur - this element is higher by 34 % in stem ash than in rachis ash.

Oxygen - rachis ash is richer in oxygen than stem ash by 32 %.

pH values - ashes of both segments (stem and rachis) are alkaline. Alkalinity of ash made from rachis is slightly higher, by 9 %.

EC values - this variable has almost the same value in ashes from stem and rachis.

C/N ratio - this ratio in stem ash is 49% greater than that of rachis.

In biochar:

Carbon - the percentages of carbon in biochar of stem and rachis is almost the same, an ignorable discrepancy of 0.8 % is calculated.

Hydrogen - biochar of stem contains 6.36 % more hydrogen than rachis biochar.

Nitrogen - this element in stem biochar is 22 % greater than in rachis biochar, this being considered a moderate difference.

Sulfur - rachis biochar is more sulfur-rich, by 57 %, comparing with that of stem, a noticeable difference.

Oxygen - calculated amount of oxygen in rachis biochar is 4.87 % greater than in stem biochar.

pH values, biochar of both segments stem and rachis of palm waste are acidic, almost equally, with only a 3 % difference.

EC values - this variable has equal values in biochar of both segments of palm wastes.

C/N ratio - in this ratio, rachis biochar is 8.57 % richer than stem biochar.

3.2.2 Wastes from palm grove in dry climate zone
3.2.2. Otpadci od palmi iz nasada u zoni suhe klime

Fiber bundles, ash and biochar of stem and rachis are compared in terms of percentages of constituent elements in Table 4. This table shows as follows:

In feedstock:

Carbon - rachis feedstock has equal amount of carbon with that in stem.

Hydrogen - in stem feedstock, hydrogen is 21 % higher compared to that of rachis.

Nitrogen - in rachis feedstock, nitrogen is 2 times richer than in stem feedstock.

Sulfur - in rachis feedstock, the percentage of sulfur is 8.5 % higher.

Oxygen - calculated value of oxygen is equal to that in stem and rachis feedstock.

pH values - rachis feedstock is 9.5 % less acidic than that of stem.

EC values - this parameter is 3 times higher in rachis feedstock than in stem.

C/N ratio - this ratio in rachis feedstock is 5.35 times greater than in stem feedstock.

In ash:

Carbon - rachis ash is 2.11 times richer in carbon with respect to stem ash.

Hydrogen - this parameter in rachis ash is 29 % higher than that of ash generated from stem.

Nitrogen - the amount of this element in stem ash is greater than in rachis ash by 12.5 %.

Table 3 Comparison of percentage of constituent elements (C, H, N, S, O), pH, EC and C/N ratio in types of waste (stem and rachis) – Lamerd date palm grove (humid climate zone)
Tablica 3. Usporedba postotaka sastavnih elemenata (C, H, N, S, O), pH, EC i C/N omjera u vrstama otpadaka (deblo i lisne osi) – nasad datulje Lamerd (zona vlažne klime)

Segment sampled *Uzorkovani segment*		**C, %**		**H, %**		**N, %**		**S, %**		**O, %**		**pH**		**EC, ds/m**		**C/N**	
		Value *Vrijednost*	% diff. or ratio*	Value *Vrijednost*	% diff. or ratio	Value *Vrijednost*	% diff. or ratio	Value *Vrijednost*	% diff. or ratio	Value *Vrijednost*	% diff. or ratio	Value *Vrijednost*	% diff. or ratio	Value *Vrijednost*	% diff. or ratio	Value *Vrijednost*	% diff. or ratio
Feedstock *Sirovina*	Stem / *deblo*	41.10	2.52	5.62	4.80	1.62	1.37	2.34	1.26	41.10	0.32	4.10	3.17	4.23	0.71	35.88	1.18
	Rachis / *lisne osi*	42.97		5.89		1.18		0.43		40.97		4.23		4.20		42.40	
Ash *Pepeo*	Stem / *deblo*	60.51	1.41	1.07	1.58	1.38	5.80	2.61	1.34	34.42	1.32	10.30	9	15.42	2.80	66.25	1.49
	Rachis / *lisne osi*	42.97		1.70		1.46		1.95		45.57		11.23		15		44.33	
Biochar *Biougljen*	Stem / *deblo*	62.47	0.80	4.18	6.36	1.80	1.22	0.40	1.57	17.86	4.87	6.30	3	3.51	0.28	43.73	8.57
	Rachis / *lisne osi*	61.98		2.93		1.47		0.63		18.73		6.11		3.50		47.48	

*% diff. were calculated with respect to lower values, and ratios were determined by higher values to lower ones
**Postotne su razlike izračunane s obzirom na niže vrijednosti, a omjeri su određeni odnosom viših vrijednosti prema nižima.*

Table 4 Comparison of percentage of constituent elements (C, H, N, S, O), pH, EC values and C/N ratio in types of waste (stem & rachis) – Kerman date palm grove (dry climate zone)
Tablica 4. Usporedba postotaka sastavnih elemenata (C, H, N, S, O), pH, EC i C/N omjera u vrstama otpadaka (deblo i lisne osi) – nasad palme datulje Kerman (zona suhe klime)

Segment sampled *Uzorkovani segment*		**C, %**		**H, %**		**N, %**		**S, %**		**O, %**		**pH**		**EC, ds/m**		**C/N**	
		Value *Vrijednost*	% diff. or ratio*	Value *Vrijednost*	% diff. or ratio	Value *Vrijednost*	% diff. or ratio	Value *Vrijednost*	% diff. or ratio	Value *Vrijednost*	% diff. or ratio	Value *Vrijednost*	% diff. or ratio	Value *Vrijednost*	% diff. or ratio	Value *Vrijednost*	% diff. or ratio
Feedstock *Sirovina*	Stem / *deblo*	40.78	1	5.45	1.21	0.27	2	0.47	8.50	44.53	0.92	4.20	9.50	4.91	3	39.45	5.35
	Rachis / *lisne osi*	40.78		4.52		0.55	times	0.51		44.12		4.60		15.35	times	211	
Ash *Pepeo*	Stem / *deblo*	15.53	2.11	1.13	1.29	0.45	12.5	2.76	2.04	80.59	27	10.25	9.26	4.20	2.40	15	6.91
	Rachis / *lisne osi*	32.89		1.46		0.40		1.25		63.40		11.20		10	Times	103.70	
Biochar *Biougljen*	Stem / *deblo*	58.60	0.70	2.25	1.78	0.63	1.58	2.29	3.75	23.74	7.90	6.30	1.47	10.50	1.11	308	5
	Rachis / *lisne osi*	59		4	times	1		0.61	times	22		6.11		11.7		61.2	times

*% diff. were calculated with respect to lower values, and ratios were determined by higher values to lower ones
**Postotne su razlike izračunane s obzirom na niže vrijednosti, a omjeri su određeni odnosom viših vrijednosti prema nižima.*

Table 5 Comparison of date palm wastes from groves in humid and dry climate zones, in terms of constituent elements (C, H, N, S, O), pH, EC values, and C/N ratios
Tablica 5. Usporedba otpadaka palme datulje iz nasada u vlažnoj i suhoj klimatskoj zoni s obzirom na sastavne elemente (C, H, N, S, O), pH, EC vrijednosti i omjer C/N

Segment sampled *Uzorkovani segment* Humid zone *Vlažna zona*		**C, %**			**H, %**			**N, %**			**S, %**						**pH**			**EC, ms**			**C/N**	
		Dry zone *Suha zona*	% diff. or ratio* *Postotna razlika*	Humid zone	Dry zone	% diff. or ratio*	Humid zone	Dry zone	% diff. or ratio*	Humid zone	Dry zone	% diff. or ratio*	Humid zone	Dry zone	% diff. or ratio*	Humid zone	Dry zone	% diff. or ratio*	Humid zone	Dry zone	% diff. or ratio*	Humid zone	Dry zone	% diff. or ratio*
Feedstock / *Sirovina* Ash / *Pepeo*	Stem *deblo* Rachis *lisne osi*	41.91	40.78	2.80	5.62	5.45	3.11	1.62	0.27	6.00 times	0.34	0.27	25.90	41.10	44.53 8.34		4.10	4.20 2.43		4.23	4.91 16		35.88	39.45 10
	Stem *deblo* Rachis *lisne osi*	-42.91	40.78	5.20	5.89	2.45	2.40 times	1.18	0.40	2.95 times	0.43	0.45	4.65	40.97	44.12 7.68		4.23	4.60 8.74		4.20	15.36 3.70 times		42.40	211 5 times
Biochar / *Biougljen* Feedstock / *Sirovina*	Stem *deblo*	60.51	15.53	3.90 times	1.07	1.13	5.60	1.38	0.45	3.10 times	2.61	2.76	5.75	34.42	80.59 2.34 times		1030	10.25 0.48		15.42	4.20 3.67 times		66.25	15 4.42 times
	Stem *deblo* Rachis *lisne osi*	49.36	32.89	1.50 times	1.35	1.45	7.40	1.45	0.55	2.63 times	1.96	1.35	44	45.57	63.40 39		11.23	11.20 0.27		15	10 1.50 times		44.33	163.70 2.34 times
Ash / *Pepeo*	Stem *deblo* Rachis *lisne osi*	62.47	58.60	6.60	4.12	2.25	1.83	1.80	0.63	2.85 times	0.40	2.29	5.72 times	17.86	23.74 32.93		6.30	6.30 1		3.51	10.50 3 times		43.73	308 7 times
	Stem *deblo*	61.98	59	5.10	3.93	4	1.78	1.47	1	47	0.63	0.61	3.27	18.73	22 17.45		6.11	6.11 1		3.50	11.7 3.34 times		47.48	61.2 28.90

% diff. were calculated with respect to lower values, and ratios were determined by higher values to lower ones / *Postotne su razlike izračunane s obzirom na niže vrijednosti, a omjeri su određeni odnosom viših vrijednosti prema nižima.*

Sulfur - stem ash is twice as rich in sulfur as rachis ash.

Oxygen - calculated amount of oxygen in stem ash is 27 % higher.

pH values - rachis ash is more alkaline by 9.26 % than stem ash.

EC values - this parameter in rachis ash is 2.4 times greater than in stem ash.

C/N ratio - this ratio in rachis ash is 6.91 times higher than that of stem.

In biochar:

Carbon - the percentage of carbon in rachis biochar is 0.70 % higher than that of stem biochar.

Hydrogen - rachis biochar is 78 % richer than biochar from stem.

Nitrogen - the percentage of nitrogen in rachis biochar is 58 % higher than that in stem biochar.

Sulfur - this element in stem biochar is 3.75 times greater than in rachis biochar.

Oxygen - calculated amount of oxygen in stem biochar is 7.90 % higher.

pH values - the difference between biochar of stem and rachis in pH is small, 1.47 %.

C/N ratio - this ratio in stem biochar is 5 times higher than that of rachis biochar.

3.2.3 Comparisons of climatological impacts on date palm wastes through characterized parameters

3.2.3. Usporedbe klimatoloških utjecaja na otpatke od palme datulje uz pomoć karakterističnih parametara

Samples of date palm wastes were collected from two different palm groves in terms of governing climatical conditions (Lamerd, hot and humid zone, Kerman, hot and dry zone), to evaluate discrepancies collected from three types of waste (feedstock, ash and biochar) are compared in Table 5.

Feedstock:

Carbon - stem feedstock from the humid zone contains more carbon, by 2.80 %. Carbon content of rachis feedstock from the same zone is slightly higher, by 5.20 %. Therefore, in terms of carbon content, no drastic differences have been observed in stem and rachis feedstock from either zone.

Hydrogen - hydrogen percentage in stem feedstock from the humid zone differs by 3.11 % from that of the dry zone. In rachis feedstock from the humid zone, the percentage of hydrogen is 2.40 times greater than that of the dry zone. It can be concluded that percentages of hydrogen in stem and rachis feedstock from either zone differ by 3.11 % to 2.40 times, respectively, which may not be considered negligible.

Nitrogen - nitrogen percentage is 6 times greater in stem feedstock in the humid zone. Therefore, the stem feedstock from the humid zone might be considered rather nitrogen-rich. In the rachis feedstock from the humid zone, the percentage of nitrogen is 2.95 times higher than that of the dry zone.

Sulfur - in the stem feedstock from the humid zone, the percentage of sulfur is 25.90 % greater than that of the dry zone. In rachis feedstock from the dry zone, sulfur content is 4.65 % higher than that of the humid zone.

Oxygen - the percentage of oxygen in feedstock from the dry zone is 8.34 % higher than that of the humid zone. Rachis feedstock from the dry zone contains more oxygen by 7.68 %.

pH value - stem feedstock from both zones has close acidic pH values (4.10, 4.20) and that of rachis has slightly less acidic pH, with an insignificant difference (4.23, 4.60).

EC values - in the stem feedstock from both sampled zones, EC values are close (4.23 ms and 4.91 ms) with a negligible difference. EC value in the rachis feedstock from the dry zone is 3.7 times greater than that of the humid zone. This might be important to consider when selecting feedstock (fiber bundles) of rachis from the dry zone as a soil additive.

C/N ratio - in stem feedstock from the dry zone, C/N ratio is 10 % richer than that of stem feedstock from the humid zone. The C/N ratio in rachis feedstock from the dry zone is 5 times greater than that of rachis feedstock from the humid zone.

Ash:

Carbon - Carbon content in the stem ash from the humid zone is 3.90 times higher than that of the dry zone. This difference is considerable.

In rachis ash from the humid zone carbon content is higher by 50 % (1.50 times). This is a relatively significant difference, and might be important, depending on cases of applications.

Hydrogen - the ash of the stem from the humid zone contains less hydrogen than corresponding ash from the dry zone by 5.60 %. The difference in hydrogen contents might be of interest in conjunction with areas of application.

The discrepancy in hydrogen content of rachis ash from the dry zone is 7.40 % higher compared with that of the humid zone.

Nitrogen - stem ash from the humid zone is 3.10 times higher than in stem ash from the dry zone. In rachis ash from the humid zone, nitrogen content is 2.63 times greater than nitrogen content in rachis ash from the dry zone.

Sulfur - the percentage of sulfur in the stem ash from the dry zone is 5.75 % higher than that in stem ash from the humid zone, but it is greater by 44 % in the rachis ash from the humid zone.

Oxygen - the amount of oxygen calculated in stem ash from the dry zone is 2.34 times higher than in stem ash from the humid zone. In rachis ash from the dry zone, oxygen is calculated to be 39 % higher than in rachis ash from the humid zone.

pH values - the stem ash from both zones had close pH values, 10.3 and 10.26, practically the same.

pH values in the rachis ash from both zones were close also, 11.23 and 11.20.

EC values - this parameter in stem ash from the humid zone is 3.67 times greater compared with that of ash from the dry zone. This drastic difference would be important considering cases of applications.

EC in rachis ash from the humid zone is greater in comparison with that of rachis ash from the dry zone by 50 %. This difference is noticeable as well.

C/N ratio - this ratio had a value of 66.25 % in the stem ash from the humid zone and 15 % in stem ash from the dry zone, the latter being 4.42 times smaller.

C/N ratio in the rachis ash from the dry zone is 2.34 times higher compared with its value in rachis ash from the humid zone.

Biochar:

Carbon - the percentage of carbon in stem biochar from the humid zone is 6.60 % higher than its percentage in stem biochar from the dry zone.

In rachis biochar from the humid zone, the percentage of carbon is 5.10 % greater if compared with that of the dry zone. This difference in carbon contents in rachis biochar can be considered modest.

Hydrogen - the percentage of hydrogen in stem biochar from the humid zone differs from that of the dry zone by 83 %, which is a great difference.

In the rachis biochar from the dry zone, the percentage of hydrogen is higher by 1.78 %, which is not significant.

Nitrogen - the percentage of nitrogen in stem biochar from the humid zone is 2.85 times higher compared with that of the stem biochar from the dry zone. This difference is high enough to be considered, depending on cases of applications.

Nitrogen content in rachis biochar from the humid zone is 47 % greater than that in rachis biochar from the dry zone, which is a relatively drastic difference and deserves to be considered with respect to areas of use.

Sulfur - in the stem biochar from the dry zone, the percentage of sulfur is 5.72 times larger, but in the rachis biochar from the humid zone, the percentage of sulfur is 3.27 % higher, a negligible difference.

Oxygen - calculated percentages of oxygen in stem biochar from the dry zone is 32.92 % greater, while in rachis biochar from the same zone, the percentage of oxygen is higher by 17.45 %.

pH values - the stem and rachis biochar from both climate zones are considered acidic. Rachis biochar is slightly less acidic.

EC values - the value of this parameter in stem biochar from the dry zone is 3 times larger than its value in stem biochar from the humid zone.

In rachis biochar from the dry zone, EC is 3.34 times higher than EC value in the rachis biochar from the humid zone.

C/N ratio - this ratio in the stem biochar from the dry zone is 7 times larger than its amount in the stem biochar from the humid zone, the difference being meaningful.

In the rachis biochar from the dry zone, C/N ratio is 28.90 % higher. Such difference in C/N ratio might be of importance considering areas of uses.

4 CONCLUSIONS
4. ZAKLJUČAK

Valuable Wastes

Based on the collected experimental data, wastes of rachis (fronds) and stems in date palm groves, especially rachis which are plentiful compared to stem slashes (trunk of palm tree), contain considerable amounts of constituent elements (C, H, N, S, O), carbon in particular. Among the necessary elements in the soil for the growth of agricultural crops, carbon (absorbable), hydrogen, nitrogen and sulfur are ranked 1st, 2nd, 4th and 9th, respectively (Aller *et al.,* 2017).

Returning crops residuals to the soil, improves its physical properties (Brewer *et al.,* 2011). This concept can be generalized for date palm wastes, since they contain useful organic substances that can restore degraded soils in palm groves.

Producing fiber bundles by mechanically defibrating date palm wastes might be considered a low-cost organic soil amendment agent. However, fiber decomposition process can be a source of gaseous emission from the soil, which will contribute to increasing greenhouse gases (Al-Wabel *et al.* 2019). Ash carbon is less desirable when compared with absorbable biochar. Biochar is a biologically more stable soil additive that changes the soil microbial community composition and enzyme activities (Prasad and Power, 1991).

C/N Ratio

In all three forms of date palm waste (fiber bundles, ash and biochar), C/N ratio has a rather high value. Therefore, any of these forms of waste (biochar is preferred) can be used for maintaining this ratio within its desired range in the soil and in fish and shrimp farming ponds, depending on the expertise of an experienced field specialist.

The percentages of constituent elements in the biochar of date palm waste in its commercial production, which is the right option in making use of this biomass, can be mentioned on their packaging for warning and to avoid any misuse.

Green Sorbent

It has been substantiated that biochar is a functional green sorbent (Lehmann *et al.,* 2011). Great amounts of biochar can be produced by applying py-

rolysis process on date palm wastes to meet demands for recycling polluted waters, which is currently a major environmental concern.

Experimental data obtained through this investigation reveal that data palm wastes are valuable biomass, and their derived biochar is effective in soil improvement (fertilizing and restoring) and recycling polluted water. Proper utilization of these wastes can help reduce greenhouse gases emitted from their natural decomposition.

Further investigations are recommended on developing the uses of biochar and on refining pyrolysis derived vinegar out of palm waste for their applications in producing liquid fertilizer or drug items.

5 REFERENCES
5. LITERATURA

1. Ahmadi, K., 2015: Iran statistical yearbook of agriculture horticulture prodcuts. Ministry of agriculture. Tehran I. R. Iran, Vol. 3.
2. Aller, D.; Bakshi, S.; Laird, D. A., 2017: Modified method for proximate analysis of biochars. Journal of Analytical and Applied Pyrolysis, 124: 335-342. https://doi.org/10.1016/j.jaap.2017.01.012
3. Al-Wabel, M. I.; Usman, A. R. A.; Al-Farraj, A. S.; Ok, Y. S.; Abduljabbar, A.; Al-Faraj, A. I.; Sallam, A. S., 2019: Date palm waste biochars alter a soil respiration, microbial biomass carbon and heavy metal mobility in contaminated mined soil. Environ. Geochem. Health, 41 (4): 1705-1722. https://doi.org/10.1007/s10653-017-9955-0
4. Beesley, L.; Moreno-Jiménez, E.; Gomez-Eyles, J. L.; Harris, E.; Robinson, B.; Sizmur, T., 2011: A review of biochars' potential role in the remediation, revegetation and restoration of contaminated soils. Environmental Pollution, 159 (12): 3269-3282. https://doi.org/10.1016/j.envpol.2011.07.023
5. Bensidhom, G.; Hassen-Trabelsi, A. B.; Alper, K.; Sghairoun, M.; Zaafouri, K.; Trabelsi, I., 2018: Pyrolysis of Date palm waste in a fixed-bed reactor: Characterization of pyrolytic products. Bioresource Technology, 247: 363-369. https://doi.org/10.1016/j.biortech.2017.09.066
6. Brewer, C. E.; Unger, R.; Schmidt-Rohr, K.; Brown, R. C., 2011: Criteria to select biochars for field studies based on biochar chemical properties. BioEnergy Research, 4 (4): 312-323. https://doi.org/10.1007/s12155-011-9133-7
7. Ebrahimi, G.; Ahmadi, P.; Efhamisisi D.; Shakeri, A., 2021: Application of pyrolysis acid from date palm waste as wood preservative. BioResources. 16 (3): 5000-5010. https://doi.org/10.15376/biores.16.3.5000-5010
8. Ebrahimi, G.; Shakeri, A.; Ahmadi, P.; Dalvand, M.; Shafie, M.; Hosseinabadi, H. Z., 2022: Chemical constituents of palm wastes slow pyrolysis derived vinegar. Maderas. Ciencia y Tecnología, 47: 1-8. http://dx.doi.org/10.4067/s0718-221x2022000100447
9. Hussain, A.; Farooq, A.; Bassyouni, M. I.; Sait, H. H.; El-Wafa, M. A.; Hasan, S. W.; Ani, F. N., 2014: Pyrolysis of Saudi Arabian date palm waste: A viable option for converting waste into wealth. Life Science Journal, 11 (12): 667-671. https://doi.org/10.7537/marslsj111214.126
10. Jonoobi, M.; Shafie, M.; Shirmohammadli, Y.; Ashori, A.; Hosseinabadi, H. Z.; Mekonnen, T., 2019: A review on date palm tree: properties, characterization and its potential applications. Journal of Renewable Materials, 7 (11): 1055-1075. https://doi.org/10.32604/jrm.2019.08188
11. Jouiad, M.; Al-Nofeli, N.; Khalifa, N.; Benyettou, F.; Yousef, L. F., 2015: Characteristics of slow pyrolysis biochars produced from rhodes grass and fronds of edible date palm. Journal of Analytical and Applied Pyrolysis, 111: 183-190. https://doi.org/10.1016/j.jaap.2014.10.024
12. Kamperidou, V.; Terzopoulou, P.; Barboutis, I., 2021: Marginal lands providing tree-crop biomass as feedstock for solid biofuels. Biofuels, Bioproducts and Biorefining, 15 (5): 1395-1405. https://doi.org/10.1002/bbb.2235
13. Kloss, S.; Zehetner, F.; Dellantonio, A.; Hamid, R.; Ottner, F.; Liedtke, V.; Schwanninger, M.; Gerzabek, M. H.; Soja, G., 2012: Characterization of slow pyrolysis biochars: effects of feedstocks and pyrolysis temperature on biochar properties. Journal of Environmental Quality, 41 (4): 990-1000. https://doi.org/10.2134/jeq2011.0070
14. Lehmann, J.; Rillig, M. C.; Thies, J.; Masiello, C. A.; Hockaday, W. C.; Crowley, D., 2011: Biochar effects on soil biota – A review. Soil Biology and Biochemistry, 43 (9): 1812-1836. https://doi.org/10.1016/j.soilbio.2011.04.022
15. Power, J. F.; Prasad, R., 1997: Soil fertility management for sustainable agriculture. CRC press.
16. Prasad, R.; Power, J. F., 1991: Crop residue management. In: Advances in soil science. Springer, New York, NY, pp. 205-251. https://doi.org/10.1007/978-1-4612-3030-4_5
17. Ronsse, F.; Van Hecke, S.; Dickinson, D.; Prins, W., 2013: Production and characterization of slow pyrolysis biochar: influence of feedstock type and pyrolysis conditions. GCB Bioenergy: Bioproducts for a Sustainable Bioeconomy, 5 (2): 104-115. https://doi.org/10.1111/gcbb.12018
18. Skjemstad, J. O.; Reicosky, D. C.; Wilts, A. R.; McGowan, J. A., 2002: Charcoal carbon in US agricultural soils. Soil Science Society of America Journal, 66 (4): 1249-1255. http://dx.doi.org/10.2136/sssaj2002.1249
19. Usman, A.; Sallam, A.; Zhang, M.; Vithanage, M.; Ahmad, M.; Al-Farraj, A.; Ok, Y. S.; Abduljabbar, A.; Al-Wabel, M., 2016: Sorption process of date palm biochar for aqueous Cd (II) removal: Efficiency and mechanisms. Water, Air & Soil Pollution, 227 (12): 1-16. https://doi.org/10.1007/s11270-016-3161-z
20. Usman, A. R.; Abduljabbar, A.; Vithanage, M.; Ok, Y. S.; Ahmad, M.; Ahmad, M.; Elfaki, J.; Abdulazeem, S. S.; Al-Wabel, M. I., 2015: Biochar production from date palm waste: charring temperature induced changes in composition and surface chemistry. Journal of Analytical and Applied Pyrolysis, 115: 392-400. https://doi.org/10.1016/j.jaap.2015.08.016
21. Woolf, D.; Amonette, J. E.; Street-Perrott, F. A.; Lehmann, J.; Joseph, S., 2010: Sustainable biochar to mitigate global climate change. Nature Communications, 1 (1): 1-9. https://doi.org/10.1038/ncomms1053

Corresponding address:

GHANBAR EBRAHIMI
Department of Wood and Paper Sciences, Faculty of Natural Resources, University of Tehran, Karaj, IRAN,
e-mail: ba_ebrahimi@yahoo.com

Justine Wepia Apungu[1], Kwaku Antwi[1], Emmanuel Appiah-Kubi[2], Francis Kofi Bih[1], Joseph Zakaria[1]

Investigating Physical and Mechanical Properties of Mahogany Root Wood (*Khaya ivorensis*) for its Utilization

Istraživanje fizičkih i mehaničkih svojstava drva korijena afričkog mahagonija (*Khaya ivorensis*) radi njegove uporabe

ORIGINAL SCIENTIFIC PAPER
Izvorni znanstveni rad
Received – prispjelo: 14. 8. 2024.
Accepted – prihvaćeno: 31. 1. 2025.
UDK: 630*81
https://doi.org/10.5552/drvind.2025.0228

ABSTRACT • *The growing need for wood in construction and furniture production has led to a gradual increase for interest in other tree components, such as the use of root wood. However, to evaluate the quality of wood, one must consider its mechanical, anatomical, and physical characteristics. African mahogany (Khaya ivorensis) is a hard and durable wood that has been over-exploited. However, its other tree components, such as root wood, are available and considered waste left to rot. This study investigated the physical and mechanical properties of mahogany root wood and known properties of other wood species as an alternative base for wood resources. Root samples were extracted from three trees with three roots each, with average diameters of 54.3 cm, 23.3 cm, and 20.6 cm for trees 1, 2, and 3, respectively, and prepared according to BS 373 standard. All tests were investigated at the Kumasi CSRI (FORIG) laboratory. The results indicated that the root wood of the species dried at 17 - 20 % MC proved to be as good a material as its stem wood and branch wood counterparts in terms of physical and mechanical properties. Basic density values averaged 508 kg/m³, 531 kg/m³, and 569 kg/m³ across the roots. The green moisture content was 80 %, 76 % and 70 % for tree 1, 2, and 3, respectively. Average shrinkage was 0.84 %, 4.58 %, and 6.28 %, respectively, in longitudinal, tangential, and radial direction. MOE recorded 6724.4 MPa, 9276.0 MPa and 10010.0 MPa, MOR was 54.3 MPa, 76.1 MPa, and 78.5 MPa, compressive strength parallel to the grain was 41.8 MPa, 54.4 MPa, and 59.2 MPa, shear strength values ranged from 14.3 MPa, 15.4 MPa, to 17.2 and Janka hardness from 3.81 kN to 4.01 kN for tree 1, 2, and 3. Most of the recorded root wood results were similar to those of the stem and branch wood, indicating that it was equally fit for structural purposes.*

KEYWORDS: *African mahogany (Khaya ivorensis); root wood; physical and mechanical properties*

SAŽETAK • *Sve veća potreba za drvom u graditeljstvu i proizvodnji namještaja dovela je do postupnog porasta zanimanja za ostale dijelove stabla, a time i do potrebe iskorištavanja korijena. Međutim, kako bi se procijenila*

* Corresponding author
[1] Authors are researchers at Akenten Appiah-Menka University of Skills Training and Entrepreneurial Development, Faculty of Technical Education, Department of Wood Science and Technology Education, Kumasi, Ghana. https://orcid.org/0009-0006-9863-4571, https://orcid.org/0000-0002-7715-3932, https://orcid.org/0000-0002-5197-5516, https://orcid.org/0009-0002-1711-3012
[2] Author is researcher at Akenten Appiah-Menka University of Skills Training and Entrepreneurial Development, Faculty of Engineering Technology, Department of Civil Engineering, Kumasi, Ghana. https://orcid.org/0000-0002-2783-0202

kvaliteta drva korijena, moraju se uzeti u obzir njegova mehanička, anatomska i fizička svojstva. Afrički mahagonij (Khaya ivorensis) tvrdo je i izdržljivo drvo koje se prekomjerno iskorištava. Međutim, drugi dostupni dijelovi njegova stabla, poput korijena, smatraju se otpadom ostavljenim da trune. Ovom studijom istražena su fizička i mehanička svojstva drva korijena afričkog mahagonija kao alternativne baze drvne sirovine u usporedbi s poznatim svojstvima drugih vrsta drva. Uzorci korijena uzeti su od tri stabla prosječnog promjera 54,3 cm (stablo 1.), 23,3 cm (stablo 2.) i 20,6 cm (stablo 3.) te su od njih pripremljeni uzorci za ispitivanje svojstava drva prema standardu BS 373. Sva ispitivanja provedena su u laboratoriju Kumasi CSRI (FORIG). Rezultati su pokazali da se drvo korijena osušeno na 17 – 20 % sadržaja vode u smislu fizičkih i mehaničkih svojstava pokazalo jednako dobrim materijalom kao i drvo debla i grana. Nominalna gustoća drva za pojedine je uzorke korijena prosječno iznosila 508 kg/m³, 531 kg/m³ i 569 kg/m³. Sadržaj vode u korijenu stabala 1., 2. i 3. u sirovom je stanju bio 80 %, 76 % i 70 %. Prosječno utezanje u uzdužnom, tangentnom i radijalnom smjeru iznosilo je 0,84 %, 4,58 % i 6,28 %. MOE je bio 6724,4 MPa, 9276,0 MPa i 10010,0 MPa; MOR je iznosio 54,3 MPa, 76,1 MPa i 78,5 MPa; čvrstoća na tlak paralelno s vlakancima bila je 41,8 MPa, 54,4 MPa i 59,2 MPa; vrijednosti smične čvrstoće kretale su se od 14,3 MPa, 15,4 MPa do 17,2 MPa, a tvrdoća po Janki za drvo korijena stabala 1., 2. i 3. iznosila je od 3,81 kN do 4,01 kN. Većina zabilježenih rezultata za svojstva drva korijena bila je slična onima za drvo debla i grana, što potvrđuje prikladnost tog drva za konstrukcijske namjene.

KLJUČNE RIJEČI: *African mahogany (Khaya ivorensis); drvo korijena; fizička i mehanička svojstva*

1 INTRODUCTION
1. UVOD

Mahogany wood was one of the first to be identified as a durable wood, and it can be found in northern Ghana. Its structural and aesthetic value is enormous. It is one of the exotic species with multi-functional uses, and its products may be found in every home in Ghana (Asare *et al.,* 2022). *Khaya ivorensis* is ranked as one of the best-known and most valuable tropical timbers on the international market, as indicated in the ITTO (2004) report.

Mahogany is distributed across Africa, Benin, Ghana, the Ivory Coast, Sudan, Togo, D.R. Congo, and Uganda. It grows in savannah and semi-deciduous forests, particularly the drier ones, however in the latter, it is typically found near water courses in regions with 1200–1800 mm of annual rainfall and a three–five-month dry season (Opoku *et al*., 2012).

The mahogany tree grows well in Ghana; it is observed that it is mainly found by river banks and lowland areas in the northern parts of the country, with large crown sizes producing a lot of canopies for relaxation, especially when grown in the community and along the major roads to serve as carbon sequestration to reduce environmental pollution (Nusir *et al.,* 2002). It is always well protected when planted in the community to prevent ruminants' destruction, as the leaves appear to be their delicacy.

Mahogany falls into the category of medium hardwood, in terms of density, stiffness, shear, compressive and good bending strength and it is simple to season and resistant to termite, bacterial, and fungal decay. The uses of mahogany in this part of the country are not different from what is established in other areas of the country and beyond. It is believed to be superior to teak wood in many ways, such as its ability to take a beautiful polish and other finishes and its widespread use in furniture, construction, turnery, panelling, tool handles, cooking utensils, and musical instruments. Other uses include car body building, floor joists, roof members, window and door frames, and veneer, among other industrial uses (Stephen *et al.,* 2016).

According to records, the West and Central African subregion is home to four main species of mahogany from the family Meliaceae: *Khaya anthotheca, Khaya ivorensis, Khaya grandifoliola*, and *Khaya senegalensis* (Bonsu *et al*., 2020).

All these species perform various functions in the wood industry. They are well known for their natural beauty when used for decoration works as well as their durability standards for structural works, and this has significantly increased the demand for these species, rendering them endangered amongst others, not losing sight of usage in the traditional areas for the treatment of ailments.

The demand for wood is driven by its use in construction, furniture, paper production, and energy (as fuelwood). With global population growth, urbanisation, and increasing consumerism, wood consumption continues to rise. Unsustainable harvesting contributes to deforestation, biodiversity loss, and climate change, making it critical to address both the demand and supply sides of the issue. Adopting sustainable forestry practices, including certified logging (e.g., FSC certification) and afforestation, ensures wood is sourced responsibly. Alternative materials like bamboo, engineered wood, recycled plastics, or metal can replace wood in construction, furniture, and packaging. Promoting recycling of paper and wood products reduces the need for virgin wood. Repurposing construction materials can extend their lifecycle. Advances like lab-grown wood or bioplastics offer promising ways to reduce dependence on natural wood. By integrating these solutions, the demand for wood can be met more sustainably, reducing environmental impact and ensuring resources for future generations (Antwi *et al.,* 2024).

The properties of mahogany root wood have not been thoroughly researched, even though some work has been done on species other than mahogany root wood. This study aims to study its properties for utilising the roots of harvested mahogany trees in the wood industry to promote a continued and sustainable wood resource base in the wake of the high demand for limited resources for local use.

In the savanna zones in Ghana, sometimes mahogany trees are uprooted either by storm or by erosion, yet the phenomenon of abandoning the roots is common after harvesting their trunks for lumber and the branches for charcoal and fuel wood; this may be attributed to a lack of knowledge on its alternative uses. It was also realised that 99.5 percent of the trees harvested, using the chainsaw machine could not produce shoots for regeneration; these suggest that the stumps and roots are left to waste; the course of the stumps inability to produce new shoots is yet to be established by research. Therefore, more studies must be conducted to find alternative uses for the unused parts of the species for economic benefits, which is the idea behind this research. The objective of this study is to investigate the physical and mechanical properties of mahogany (*Khaya ivorensis*) root wood for its utilisation.

2 MATERIALS AND METHODS
2. MATERIJALI I METODE

2.1 Study area and description
2.1. Područje i opis istraživanja

The Savannah region in Ghana was chosen for the study due to its large forest cover. It is one of the regions with vast forest land and Mole forest reserves located in the western part of the country toward the border with the Cote d'Ivoire.

The Savannah region is located nearby the Sahel and Sahara and it is significantly drier than the southern parts of Ghana. The predominant type of vegetation is grassland, particularly savanna, with pockets of drought-tolerant trees such as shea, dawadawa, ebony, nim, and baobabs. The dry season is considered to be from December to April. The average annual rainfall during the wet season, roughly from May to November, is between 750 and 1050 mm (30 and 40 inches). The end of the dry season brings the highest temperatures, while December and January bring the lowest. However, between December and the beginning of February, the hot Harmattan wind from the Sahara blows regularly. The temperature range is 14 °C (59 °F) at night to 40 °C (104 °F) during the day.

Data for this investigation were collected from Wangasi-Tudu, 55 km from Kpalbe in the north-east Gonja district in the savannah region with coordinates with latitude 9^0 9` N and longitude $1^0$ 36` W with elevation of 202 meters above sea level, with the digital address S J 15243-0154 where research materials were harvested.

2.2 Sampling
2.2. Uzorkovanje

Three (3) mature African mahogany trees yielded nine straight root boles for the study, with an average diameter of 16 cm to 20 cm and 24 cm. The trees were obtained from cassava and yam farmland in the same locality within the open forest area. The sample preparation process from logging to conversion is demonstrated in Figures a) - i). A purposive sampling technique was employed, targeting roots with a diameter greater than 16 cm, measured 75 cm from the stem and the overall straightness, and defect-free of the root bole. This approach ensured the selection of samples that met specific size criteria relevant to the study.

The samples were prepared in the Wood Technology Workshop of the Department of Wood Science and Technology Education of Akenten Appiah-Menka University of Skills Training and Entrepreneurial Development and the Anatomy laboratory at the Forestry Research Institute of Ghana, the Council for Scientific and Industrial Research of Ghana.

The samples were prepared in the dimensions shown in Table 1 for physical and mechanical tests according to the standards stated in Table 1. In total, sixty samples were tested for each property.

Table 1 Description of test samples
Tablica 1. Opis ispitnih uzoraka

Tests conducted *Provedena ispitivanja*	**Properties evaluated** *Ispitana svojstva*	**Standards used** *Primijenjene norme*	**Samples geometry** *Dimenzije uzoraka* mm	**Quantity of samples** *Broj uzoraka*
Physical properties *Fizička svojstva*	Moisture content / *sadržaj vode*	ASTM D4442-07	20 × 20 × 20	60
	Density / *gustoća*	ASTM D2395-07	20 × 20 × 20	60
	Shrinkage / *utezanje*	ASTM D1037-07	25 × 25 × 30	60
Mechanical properties *Mehanička svojstva*	Modulus of elasticity / *modul elastičnosti*	BS 373: 1957	20 × 20 × 300	60
	Modulus of rupture / *modul loma*	BS 373: 1957	20 × 20 × 300	60
	Compressive strength / *čvrstoća na tlak*	BS 373: 1957	20 × 20 × 60	60
	Shear strength / *smična čvrstoća*	BS 373: 1957	50 × 50 × 50	60
	Hardness (radial\tangential) / *tvrdoća (radijalna/tangentna)*	BS 373: 1957	50 × 50 × 150	60

Figure 1 Root wood samples preparation for physical and mechanical tests
Slika 1. Priprema uzoraka drva korijena za ispitivanje fizičkih i mehaničkih svojstava

The samples were air-dried at room temperature for three months and all particles on their edges were trimmed to keep the edges clean. Afterwards, they were transferred to a conditioning room, where the moisture was reduced to a uniform moisture content of 12 %. Each sample was labelled and grouped according to each test, e.g. R1, R2, R3…

2.3 Determination of basic density and moisture content
2.3. Određivanje nominalne gustoće i sadržaja vode

The basic density and moisture content were determined according to ASTM D 2395-07 and ASTM D4442-07, respectively. The same samples were used for both tests. Each strip was sawn into 20 mm × 20 mm sections and cross-cut into 20 mm cubes. The mass of the samples was taken immediately after preparation using a digital electronic balance (VWR Science Education RS232) with a precision of 0.001 g to obtain the initial mass (W_1). The samples were soaked in water for 24 hours to obtain the swollen volume (V_1) determined by the immersion method. Afterwards, the wood samples were oven-dried at (103 ± 2) °C with intermittent weighing until a constant mass (oven-dry mass) (W_0) was attained according to ASTM D 2395-07. The test was carried out under ambient temperature conditions of 20 °C. The duration of the basic density test was 24 hours. The basic density (BD) of the samples was calculated from oven-dry mass and swollen volume, as shown in Figures 2e-h.

2.4 Determination of shrinkage
2.4. Određivanje utezanja

Shrinkage was evaluated using 25×25×30 mm specimens. The four-sided specimen sizes were measured at 0.0001m accuracy of volume, then computed through weighing of specimens to obtain the initial weight, and then submerged horizontally under 25mm depth of clean water at room temperature for 72 hours. The specimens were then removed and put in a kiln until they attained the mandatory twelve per cent (12 %) moisture content. Volumetric shrinkage was calculated by Eq (1)

$$Volumetric\ shrinkage = \frac{Vf - Vo}{Vo} \times 100\ \% \qquad (1)$$

Where: Vo – initial volume of the specimen
Vf – final volume of the specimen

2.5 Testing instrument for mechanical properties
2.5. Uređaj za ispitivanje mehaničkih svojstava

Mechanical properties were tested using an automatic universal testing machine (UTM-Hegewald &

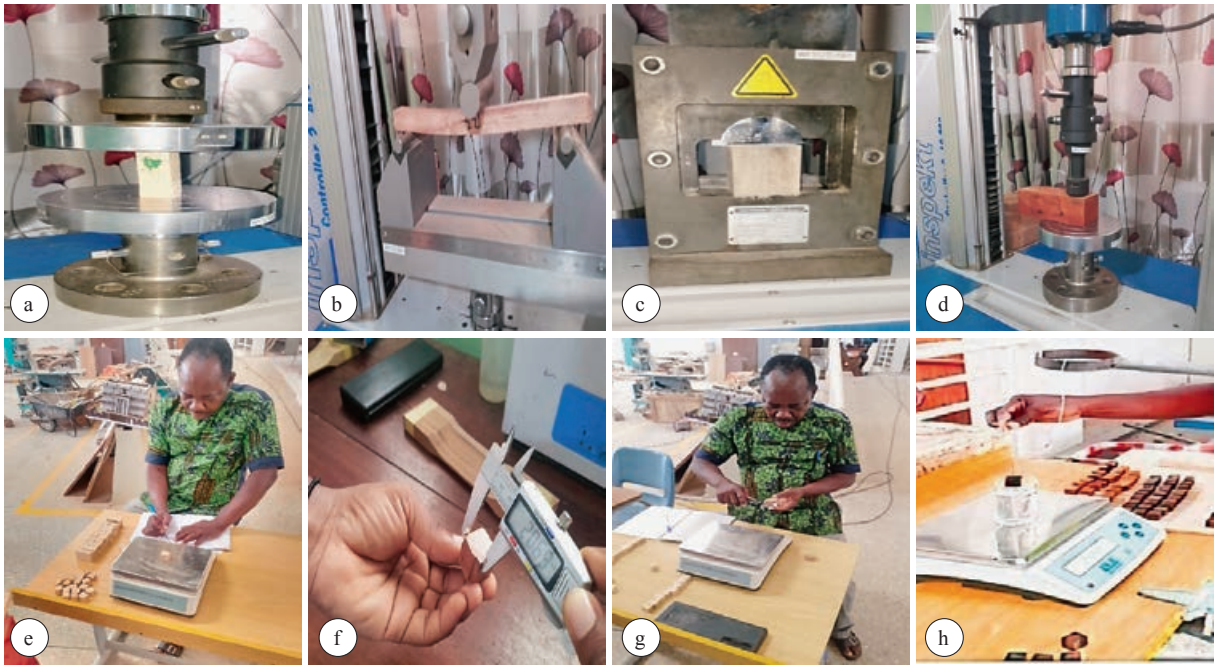

Figure 2 Testing of physical and mechanical properties of root wood
Slika 2. Ispitivanje fizičkih i mehaničkih svojstava drva korijena

Peschke mpt GmbH series no 10-030-000b2v1. 50 KN) according to standard BS 373 (1957). The testing machine consists of a jig where the samples are loaded for testing, and a head that moves up or down to exert stress on the sample. The computer used for this setup has the program "Winsoft", which senses deflection and stress and displays the load-by-deflection curve on the monitor concurrently with the test. The instrument was adjusted for the loading rate, and the sample dimensions by ISI 1708 (ISI, 1986).

Compressive strength was measured using the parallel to longitudinal grain method. Each sample was examined to ensure that the rectangular test pieces were smooth, parallel and expected to the axis. Plates containing the test component were parallel to each other throughout the test. Several checks were made to make sure that the correct conclusions were drawn, as shown in Figure 2a.

For static bending tests (modulus of elasticity and modulus of rupture), a three-point bending (central loading) system (Figure 2b) was used. The machine automatically applied the loading at a speed of 6.5 mm/min. Loading speed was maintained until the test sample failed. The computer component of the UTM recorded the maximum load at failure and the maximum load at the limit of proportionality between the outer points of loading. The tests were completed in (90 ± 30) seconds.

For the shear test samples, the load was applied at a speed of 0.635 mm/min. Shear strength was carried out in a longitudinal direction, parallel to the grain (Figure 2c). The samples were subjected to load until failure. The tests were completed in (90 ± 30) seconds.

For Janka hardness tests, a steel ball with a diameter of (11.3 ± 2.5) mm was located at one end of a steel bar, which was the fixture. The application of a load causes the hemispherical end (steel ball) to penetrate the test segment. The max force necessary to press the hemispherical end of the steel ball into the test piece to a depth of 5.64 mm is automatically recorded by the machine. The Janka hardness was calculated as the maximum force to imprint the steel ball into the wood. Both radial and tangential surfaces were tested, as shown in Figure 2 d.

2.6 Statistical procedures
2.6. Statistički postupci

Data were imported into the statistical software Origin (Version: Origin (Pro) 2021) for statistical analysis. Descriptive and inferential statistics were used to summarise the data numerically and graphically. Single factor one-way analysis of variance (ANOVA) was used to determine the significant difference within each root wood. The Turkey multiple comparison test and HSD post hoc were used to test the statistical significance of each pair of means and the variation in the physical and mechanical properties of the mahogany root wood. A 95 % confidence level was used to test the differences between all mean values.

3 RESULTS AND DISCUSSION
3. REZULTATI I RASPRAVA

3.1 Physical properties
3.1. Fizička svojstva

The results of the basic density for Root 1, Root 2, and Root 3 show that Root 3 recorded the highest

basic density of 569 kg/m³, while Root 1 recorded the lowest density of 508 kg/m³, as indicated in Figure 3 and Table 2. The ANOVA test shows that the roots significantly affect the basic density at a level of significance of 5 %. However, Turkey's multiple comparison tests show substantial density differences. This result is consistent with a similar result reported by Amoah *et al.* (2012b), who found that the Iroko root wood had the highest average density (760 kg/m³), ranging between 694 and 813 kg/m³. Again, the findings that Root 3 recorded the highest basic density (568.51 kg/m³) and Root 1 recorded the lowest (508.03 kg/m³) align with similar studies that highlight the influence of genetic and environmental factors on the basic density of wood. Variations in density among roots are commonly attributed to differences in wood anatomy, moisture distribution, and growth conditions, as supported by studies examining inter- and intra-tree wood property variations. This supports the study of Wiemann and Williamson (1988), who found significant variability in wood density across different parts of trees, emphasizing that root wood often exhibits lower densities due to increased porosity and moisture content. Similarly, Panshin and de Zeeuw (1980) identified that roots generally have a different structural composition compared to stems, leading to variation in density and mechanical properties.

Results of the green moisture content for Root 1, Root 2, and Root 3, respectively, show Root 1 with the highest moisture content of 80 % and Root 3 with the

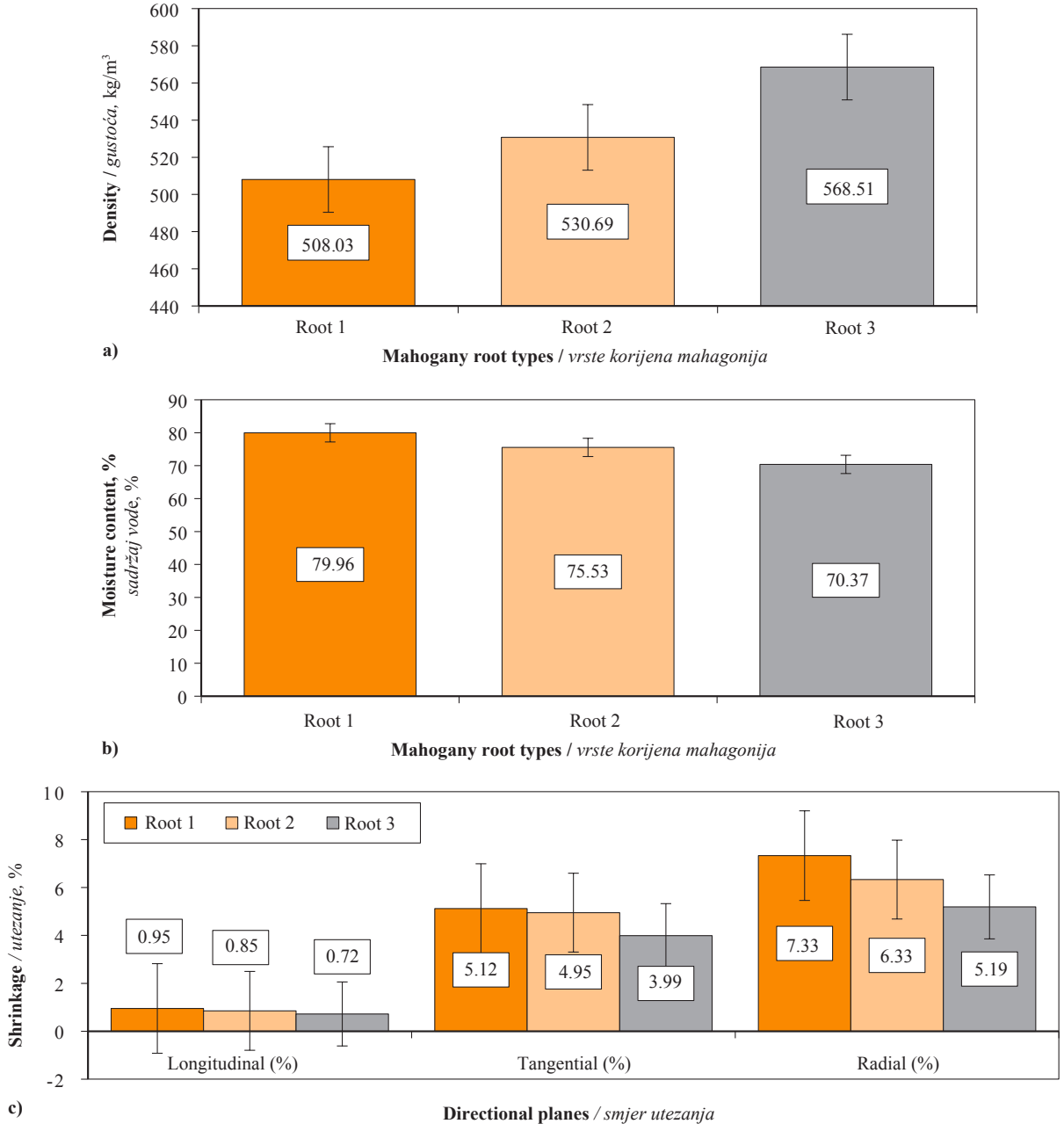

Figure 3 Average density, green moisture content, and shrinkage of mahogany root wood (Error bars = standard deviation)
Slika 3. Prosječna gustoća, sadržaj vode drva u sirovom stanju i utezanje korijena mahagonija (traka pogreške prikazuje standardnu devijaciju podataka)

lowest moisture content of 70 %. Furthermore, Turkey's multiple comparison tests show significant differences in moisture content between the three roots. These results can be compared with the findings of Hales and Miniat (2017), and Zhang *et al*. (2014), who reported that the moisture content of Chinese fir **(***Cunninghamia lanceolata***)** has a significant relationship with the strength of the wood. Their findings highlighted that variations in moisture content substantially affect the mechanical properties, including strength and stiffness, making moisture control crucial in the utilisation of this species.

The results demonstrate that Root 1 exhibits the highest shrinkage across longitudinal, tangential, and radial dimensions, likely due to differences in wood density, moisture content, or anatomical structure at the cellular level. High shrinkage values suggest that Root 1 may have a higher proportion of moisture-retentive tissues or a more variable grain structure, leading to greater dimensional changes during drying.

In contrast, Root 3 shows the lowest shrinkage**,** which could be attributed to a denser or more uniform cell structure, lower initial moisture content, or enhanced resistance to deformation under drying conditions. The reduced shrinkage values in Root 3 indicate better dimensional stability, making it potentially more suitable for applications requiring minimal warping or distortion. This variation highlights the importance of material selection based on shrinkage characteristics for specific woodworking or construction applications.

The shrinkage of Root 1, Root 2, and Root 3 shows a level of variability from 5.1 % to 54 %. This could be explained by root type and plane direction. However, the results of the ANOVA indicated a significant difference of shrinkage between the roots, while the Turkey multiple comparison tests prove that there was no significance. In their study, Glass *et al.* (2021) concluded that wood shrinks relatively little longitudinally or in a direction perpendicular to the grain. However, for most wood species, the average volumetric shrinkage from green to oven-dry is between 0.1 % and 0.2 %. However, depending on the species, it shrinks (swells) tangentially slightly more than radially. The study results are in line with Yang *et al.* (2016), who researched the moisture content and tensile strength of four tree roots *Betula platyphylla, Quercus mongolica, Pinus tabulae form, and Larix gmelinii*, with moisture content ranging from 26.00 to 33.00 %, 24.70 to 31.30 %, 37.00 to 45.00 % and 20.40 to 35.70 %, respectively.

Table 2 ANOVA test for physical properties of mahogany root wood
Tablica 2. ANOVA test rezultata fizičkih svojstava drva korijena mahagonija

Properties / *Svojstva*	***df***	***F*-value**	***P*-value**	**Var., %**
Density / *gustoća*	2	39.649	0.001**	
Moisture content *sadržaj vode*	2	75.095	0.001**	
Shrinkage / *utezanje*				
- Root type (RT) - *vrsta korijena (RT)*	2	4.550	0.012**	5.1
- Plane direction (PD) - *smjer utezanja (PD)*	2	101.876	0.001**	54.4
- RT × PD	4	1.053	0.382ns	2.4

** = significant at $p<0.05$, ns = not significant / ** = *značajno pri* $p < 0,05$, *ns = nije značajno*

3.2 Mechanical properties of mahogany root wood
3.2. Mehanička svojstva korijena mahagonija

3.2.1 Modulus of elasticity
3.2.1. Modul elastičnosti

The Modulus of Elasticity (*MOE*) results for Root 1, Root 2, and Root 3 are shown in Figure 4, accordingly. The results show that Root 3 recorded the highest *MOE* of 10010 MPa, while Root 1 recorded the lowest *MOE* value of 6724.4 MPa. The ANOVA results for the modulus of elasticity for roots 1, 2, and 3, respectively, are significant; Root 3 recorded the highest *MOE*, while root 1 recorded the lowest *MOE*. The reason could be the difference in root diameter resulting from the formation and maturity. The current results can be compared with the findings of Appiah-Kubi *et al.* (2016) on plantation-grown African mahogany (*Khaya ivorensis*) with *MOE* of 8603 MPa at the bottom, 10051 MPa at the middle, and 8718 MPa at the top of the stem wood with mean densities of 554, 518 and 491 kg/m^3, respectively. França *et al.* (2024) reported that the mean values of African mahogany *MOE* and *MOR* were 6367 MPa and 55.93 MPa, respectively.

3.2.2 Modulus of rupture
3.2.2. Modul loma

For Root 1, Root 2, and Root 3, the corresponding modulus of rupture (*MOR*) was obtained. The results show that Root 3 recorded the highest *MOR* of 78.48 MPa, while Root 1 recorded the lowest *MOR* value of 54.25 MPa. At the five percent significance level, the modulus of rupture for roots 1, 2, and 3 shows that they are significant, with Root 3 recording the highest value of 78.48 MPa, while Root 1 recorded the lowest *MOR* of 76.11 MPa. The current results are consistent with the findings of Ashaduzzaman *et al.* (2011), who investigated big-leaf mahogany (*Swietenia macrophylla king*) with *MOR* of 79.12 and 73.59 MPa, respectively. The results are also in accordance with the results of Amoah *et al.* (2012), who recorded that the *MOR* values of the branch, stem, and root wood ranged from 55 to 91, 60 to 88, and 56 to 90 MPa, respectively, and the *MOR* of the root wood was 74 MPa, varying between 53 and 85 MPa.

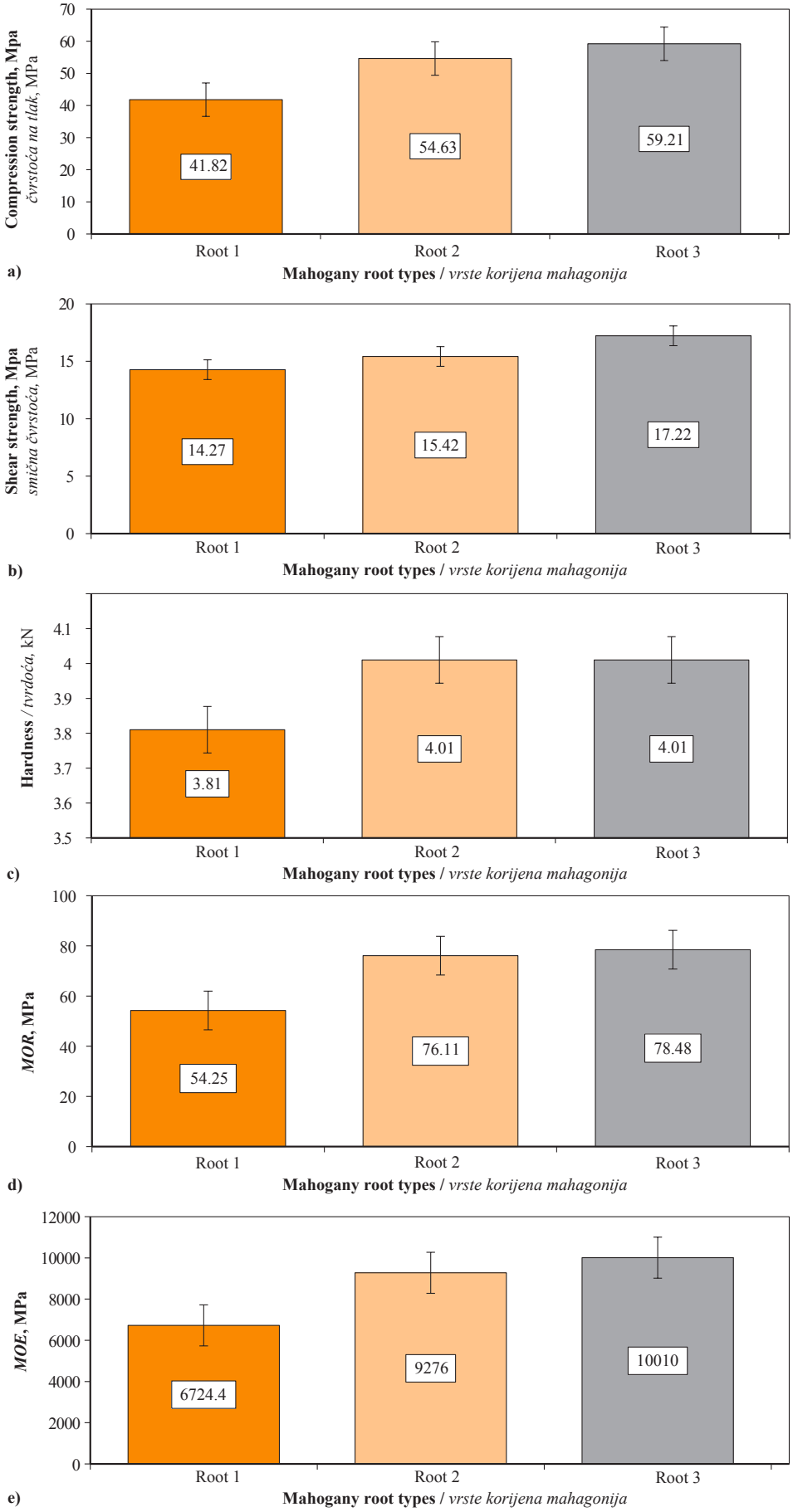

Figure 4 Average mechanical properties of mahogany root wood (Error bars = standard deviation)
Slika 4. Prosječna čmehanička svojstva korijena mahagonija (traka pogreške prikazuje standardnu devijaciju)

3.2.3 Compressive strength parallel to the grain
3.2.3. Čvrstoća na tlak paralelno s vlakancima

Figure 4 shows the results of the compressive strength parallel to the grain (*COM*) for R1, R2, and R3, respectively. R3 recorded the highest *COM* of 59.21 MPa, while R1 recorded the lowest *COM* of 41.82 MPa. The ANOVA test shows that the *COM* differences are significant between the roots. These variations could be attributed to the difference in properties within and between trees, the growth pattern, and environmental factors. The results are similar to those of Anoop *et al.* (2014), who reported that the compressive strength parallel to the grain varied significantly among different tropical wood species, reflecting how material properties are influenced by density and anatomical structure. Their findings showed that denser wood species tend to have higher compressive strength values, aligning with trends in our results where Root 3, likely denser, recorded the highest compressive strength (59.21 MPa), while Root 1, less dense, had the lowest (41.82 MPa). This correlation supports the significance of wood density in mechanical performance.

Table 2 indicates the ANOVA results, showing that, at a 5 % significance level, the root type significantly affects *MOE*. The results of Turkey's multiple comparison tests, as presented in Table 3, confirm that the *MOE* differences between the root types are significant.

The table also presents the ANOVA results for *MOR*, showing that, at a 5 % significance level, root type significantly affects *MOR*. Similarly, Turkey's multiple comparison tests reveal that the differences in *MOR* between the root types are significant. Results of the ANOVA (Table 3) indicate that root type significantly affects compressive strength at a 5 % significance level. Furthermore, Turkey's multiple comparison tests suggest that the differences in compressive strength between the root types are significant. The shear strength results for Root 1, Root 2, and Root 3 are presented in Figure 4. Root 3 recorded the highest shear strength of 17.22 MPa, while Root 1 recorded the lowest shear strength of 14.27 MPa as presented in Figure 4.

The ANOVA results (Table 3) indicate that root type significantly affects compressive strength at a 5 % significance level. Furthermore, Turkey's multiple comparison tests confirm that the differences in compressive strength between root types are significant. The ANOVA results show that root type significantly affects shear strength at a 5 % significance level. Additionally, Turkey's multiple comparison tests confirm that the differences in shear strength between the root types are significant. The ANOVA results indicate that root type has no significant effect on hardness at a 5 % significance level. Consistently, Turkey's multiple comparison tests show that the differences in hardness between the root types are insignificant.

Table 3 ANOVA test for mechanical properties of mahogany root wood
Tablica 3. ANOVA test rezultata mehaničkih svojstava korijena mahagonija

Properties / *Svojstva*	***df***	***F*-value**	***P*-value**
MOE	2	133.498	0.001**
MOR	2	492.841	0.001**
COM	2	289.059	0.001**
Shear strength *smična čvrstoća*	2	37.376	0.001**
Hardness / *tvrdoća*	2	1.017	0.368ns

** = significant at $p < 0.05$, ns = not significant; *MOE* – modulus of elasticity; *MOR* – modulus of rupture; *COM* – compressive strength parallel to the grain.
** = *značajno pri p < 0,05, ns = nije značajno; MOE – modul elastičnosti; MOR – modul loma; COM – čvrstoća na tlak paralelno s vlakancima*

3.2.4 Shear strength parallel to the grain
3.2.4. Smična čvrstoća paralelno s vlakancima

The results of the ANOVA for the shear strength of Root 1, Root 2, and Root 3, respectively, are significantly different between roots. Root 3 recorded the highest shear strength (17.22 MPa), while Root 1 recorded the least (14.27 MPa). This could be caused by genetic and growth factors as the root bole increases density and all mechanical test conducted increased. Mascarenhas *et al*. (2022) measured similar parameters of shear strength (10.4 MPa) when he researched the wood quality of *Khaya senegalensis*, while the average shear strength of the current study was 9.95 MPa.

3.2.5 Hardness
3.2.5. Tvrdoća

The ANOVA table shows that hardness values for Root 1, Root 2, and Root 3 show that Root 2 and Root 3 had the highest values, followed by Root 1; nonetheless, there was no discernible variation in hardness amongst the roots. This means that mahogany roots have similar hardness properties regardless of the environment and other genetic factors. It could also be the morphological structure of the roots and other anatomical structures within the tree, such as the fibre length and other chemical deposits. The current results fall in line with the parameters measured by França *et al.* (2024) on African mahogany, with results in Janka hardness, tangential, and radial, 4.58 kN, and 3.55 kN, respectively. However, the mahogany wood was lower in compressive strength parallel and perpendicular to the grain (46.19 MPa) (8.07 MPa) than the other mahogany wood. Mascarenhas *et al.* (2022) measured Janka hardness of 342 kN in their studies.

4 CONCLUSIONS
4. ZAKLJUČAK

The study on mahogany root wood was conducted to utilise roots that are usually abundant after felling and cutting their stems for wood and as an alternative to mahogany stem wood to increase the demand for mahogany wood to serve small-scale industries.

The study revealed a close relationship between the mahogany root wood and the stem wood of the same species for all the parameters measured, except hardness, which had a slightly lower value.

The root wood of *K. ivorensis* trees, based on density and strength properties, would be classified for use in class 3 and 4 according to EN 252 (CEN 2014) and considered appropriate for analogous applications of hardwood species (*Pterocarpus soyauxii*, *Diospyros spp*., *Tectona grandis, Dalbergia iatifolia*) often utilised as structural supports (beams and columns), bridges, flooring, railway sleepers, utility poles, mine props, boat building, as well as highly-priced furniture and cabinets.

Root wood exhibited high values in both physical and mechanical properties, which are the basis for wood utilisation and, therefore, can be used for structural and non-structural applications.

Acknowledgements – Zahvala

We are grateful to Sampson Antwi for his assistance, the director and the entire CSIR (FORIG) staff for allowing me to use laboratory equipment for this study; their kindness and support are greatly appreciated.

5 REFERENCES
5. LITERATURA

1. Asare, F., 2022: Sustainable biochar and charcoal production technologies. MsC Thesis, Purdue University, p. 47.
2. Amoah, M.; Appiah-Yeboah, J.; Okai, R., 2012a: Characterisation of physical and mechanical properties of branch, stem and mechanical properties of big-leaf mahogany (*Swietenia macrophylla Roxb*) and Root. Journal of Applied Sciences, Engineering and Technology, 4 (12): 1754-1760.
3. Amoah, M.; Appiah-Yeboah, J.; Okai, R., 2012b: Characterization of physical and mechanical properties of the branch stem and root wood of Iroko and Emire tropical trees. Research Journal of Applied Sciences, Engineering and Technology, 4 (12): 1755-1761.
4. Antwi, K.; Bih, F. K.; Adu, S.; Appiah, Y. J.; 2024: Variability of the chemical composition of the wood and bark of two tropical hardwoods from Ghana. Les/Wood, 73 (1): 35-44. https://doi.org/10.26614/les-wood.2024.v73n01a03
5. Anoop, E. V.; Jijeesh, C. M.; Sindhumathi, C. R.; Jayasree, C. E., 2014: Wood physical, anatomical and mechanical properties of big-leaf mahogany (*Swietenia macrophylla Roxb*) a potential exotic for South India. Research Journal of Agriculture and Forestry Sciences, 2 (8): 7-13.
6. Appiah-Kubi, E.; Kankam, C. K.; Frimpong-Mensah, K.; Opuni-Frimpong, E., 2016: The bending strength and modulus of elasticity properties of plantation-grown *Khaya ivorensis* (African Mahogany) from Ghana. Journal of the Indian Academy of Wood Science, 13: 48-54.
7. França, T. S. F. A.; Frederico, J. N.; França, R. A.; Arango, A. C.; Mercy, O., 2024: Properties of African Mahogany Wood Commercially Available in the United States. Forest Products Journal, 73 (4): 339-349.
8. Glass, S.; Zelinka, S., 2021: Moisture relations and physical properties of wood. Wood handbook: wood as an engineering material: Chapter 4. General technical report FPL; GTR-190. Madison, WI: U.S. Dept. of Agriculture, Forest Service, Forest Products Laboratory, 2010: p. 4.1-4.19.
9. Hales, T. C.; Miniat, C. F., 2017: Soil moisture causes dynamic adjustments to root reinforcement that reduce slope stability. Earth Surface Processes and Landforms, 42 (5): 803-813. https://doi.org/10.1002/esp.4039.
10. Mascarenhas, A. R. P.; Sccoti, M. S. V.; de Melo, R. R; de Oliveira Corrêa, F. L..; de Souza, E. F. M.; Pimenta, A. S., 2022: Wood quality of *Khaya senegalensis* trees from a multi-stratified agroforestry system established in an open ombrophilous forest zone. Wood Material Science and Engineering, 17 (6): 858-867. https://doi.org/10.1080/17480272.2021.1968490
11. Nuzir, F. A.; Kurniawan, A.; Chandra, S. D.; Munawaroh, A. S., 2022: Study on the potential of historical Mahogany trees in improving urban air quality. International Journal of Building, Urban, Interior and Landscape Technology, 19: 63-72.
12. Opoku, S. M., 2012: Growth and productivity of *Khaya grandifoliola* in the dry semi-deciduous forest of Ghana: a comparison in pure stands and in mixed stands. PhD Thesis, Kwame Nkrumah University of Science and Technology, Dspace KNUST.
13. Panshin, A. J.; de Zeeuw, C., 1980: Textbook of Wood Technology. McGraw-Hill.
14. Stephen, T. L.; Appiah-Kubi, E.; Essien, C.; Emmanuel, O. F.; James, K.; Pentsil, S.; Owusu, F. W., 2016: Wood and lumber quality of plantation-grown *Khaya ivorensis*. International Tropical Timber Organization, 4 (1).
15. Wiemann, M. C.; Williamson, G. B., 1988: Wood specific gravity gradients in tropical dry and montane rain forest trees. American Journal of Botany, 75 (6): 916-920.
16. Yang, Y.; Chen, L.; Li, N.; Zhang, Q., 2016: Effect of root moisture content and diameter on root tensile properties. PLOS ONE, 11 (3), e0151791. https://doi.org/10.1371/journal.pone.0151791
17. Zhang, C. B.; Chen, L. H.; Jiang, J., 2014: Why fine tree roots are stronger than thicker roots: The role of cellulose and lignin in slope stability. Geomorphology, 206: 196-202. https://doi.org/10.1016/j.geomorph.2013.09.024
18. ***ASTM D2395-07, 2007: Standard Test Methods for Specific Gravity of Wood and Wood-Based Materials, ASTM International, West Conshohocken, PA. https://doi.org/10.1520/D2395-07
19. ***ASTM D1037, 2007: Standard Test Methods for Small Clear Specimens of Timber. ASTM International, West Conshohocken, PA. https://doi.org/10.1520/D2395-0710.1520/D2395-07
20. ***ASTM D4442-07-19, 2007: Standard Test Methods for Mechanical Properties of Lumber and Wood-Based

Structural Materials. ASTM International, West Conshohocken, PA. https://doi.org/10.1520/D2395-0710.1520/D2395-07
21. ***BS 373, 1957: Methods of Testing Small Clear Specimens of Timber. London: British Standards Institution.
22. ***EN 252, 2014: Field Test Method for Determining the Relative Protective Effectiveness of a Wood Preservative in Ground Contact. Brussels: European Committee for Standardization.
23. *** ISI 1708, 1986: Methods of Testing Small Clear Specimens of Timber. New Delhi: Indian Standards Institution.
24. ***ITTO, 2004: Making the Mahogany Trade Work. Report of the workshop in capacity-building for the implementation of the CITES Appendix-II listing of mahogany. ITTO Technical Series 22, International Tropical Timber Organization, Yokohama, Japan, p. 54.

Corresponding address:

KWAKU ANTWI
Akenten Appiah-Menka University of Skills Training and Entrepreneurial Development, Kumasi, GHANA,
e-mail: kantwi@aamusted.edu.gh / antwikwaku10@gmail.com

Hadi Baseri*[1], Seyyed Khalil HosseiniHashemi*[2], Sayed Khosrow HossinAshrafi[2], Jakia Jerin Mehjabin[3]

Potential Antioxidants in Bio-oil Obtained by Pyrolysis of Yew (*Taxus baccata* L.) Tree Bark

Potencijalni antioksidansi u bioulju dobivenom pirolizom kore drva tise (*Taxus baccata* L.)

ORIGINAL SCIENTIFIC PAPER
Izvorni znanstveni rad
Received – prispjelo: 8. 10. 2024.
Accepted – prihvaćeno: 3. 3. 2025.
UDK: 630*86
https://doi.org/10.5552/drvind.2025.0233

ABSTRACT • *Bio-oil (BO), ethanol extract (EtE), and superheated ethanol extract (SHEtE) from the bark of Taxus baccata L. tree trunk fallen due to strong wind or landslide were obtained from pyrolysis of the crushed sample in the furnace at a temperature of 500 °C for 30 min, ordinary solvent extraction of air-dried powder sample for 24 hours using a 250 mL laboratory-scale Soxhlet extractor, and a small laboratory-scale reactor with a 50 ml cylindrical stainless steel vessel and maximum working temperatures of (300 ± 3) °C for superheated solvent extraction, respectively. The BO and extracts were analyzed for their antioxidant activities using the DPPH method. The presence of organic compounds in the BO and extracts was predicted by analyzing the functional groups using Fourier transform infrared (FTIR) spectroscopy. Among the BO and extracts from yew bark, the most active fraction was analyzed for its chemical composition using gas chromatography-mass spectrometry (GC/MS). BO was proven to have a higher antioxidant capacity (58.76 %) compared to the standard ascorbic acid (45.14 %) at a concentration of 1000 ppm. The FTIR analysis suggested the presence of active compounds in BO samples. The quantification of the BO and extracts showed that yew bark BO was richer in phenolic compounds than the extracts. The major components identified in the BO by GC/MS analysis were guaiacol (11.65 %), followed by phenol (8.48 %), β-D-Glucopyranose, 1,6-anhydro- (6.54 %), furfuryl alcohol (5.64 %), 3,4-dihydro-2H-pyran (5.52 %), p-cresol (4.50 %), 4-methylguaiacol (4.24 %), 3-methylcyclopent-2-enone (3.45 %), 2-hydroxy-3-methylcyclopent-2-en-1-one (3.29 %), and catechol (3.23 %).*

KEYWORDS: *Taxus baccata L.; bark bio-oil; chemical composition; antioxidant activity; GC/MS and FTIR*

SAŽETAK • *U radu su opisana istraživanja antioksidativne aktivnosti bioulja (BO), etanolnog ekstrakta (EtE) i pregrijanoga etanolnog ekstrakta (SHEtE) dobivenih iz kore debla Taxus baccata L., sruženoga zbog jakog vjetra ili klizišta. Bioulje je dobiveno pirolizom usitnjenog uzorka u peći, na temperaturi od 500 °C tijekom 30 minuta. Etanolni ekstrakt dobiven je iz uzorka praha kore osušene na zraku i ekstrahiranoga otapalom tijekom 24 sata uz pomoć laboratorijskog Soxhlet ekstraktora od 250 mL. Pregrijani etanolni ekstrakt dobiven je primjenom maloga laboratorijskog reaktora s cilindričnom posudom od nehrđajućeg čelika volumena 50 mL i maksimalnim radnim temperaturama od (300 ± 3) °C za ekstrakciju pregrijanim otapalom. Antioksidativna aktivnost bioulja i ekstraka-*

* Corresponding authors
[1] Author is associate professor at School of Chemistry, Damghan University, Damghan, Iran.
[2] Authors are associate professor and assistant professor at Department of Wood Science and Paper Technology, Karaj Branch, Islamic Azad University, Karaj, Iran.
[3] Author is PhD student at Hokkaido University, Graduate School of Environmental Science, Sapporo, Japan.

ta analizirana je DPPH metodom. Prisutnost organskih spojeva u bioulju i ekstraktima utvrđena je analizom funkcionalnih skupina primjenom Fourierove infracrvene spektroskopije (FTIR). Kemijski sastav najaktivnije frakcije dobivene od bioulja i ekstrakata iz kore drva tise analiziran je uz pomoć plinske kromatografije s masenom spektrometrijom (GC/MS). Dokazano je da bioulje pri koncentraciji od 1000 ppm ima veći antioksidativni kapacitet (58,76 %) od standardne askorbinske kiseline (45,14 %). FTIR analizom potvrđeno je postojanje aktivnih spojeva u uzorcima bioulja. Kvantifikacija bioulja i ekstrakata iz kore drva tise pokazala je da je bioulje bilo bogatije fenolnim spojevima od ekstrakata. Glavne komponente identificirane GC/MS analizom u bioulju bile su gvajakol (11,65 %), fenol (8,48 %), β-D-glukopiranoza, 1,6-anhidro-(6,54 %), furfurilni alkohol (5,64 %), 3,4-dihidro-2H-piran (5,52 %), p-krezol (4,50 %), 4-metilgvajakol (4,24 %), 3-metilciklopent-2-enon (3,45 %), 2-hidroksi-3-metilciklopent-2-en-1-on (3,29 %) i katehol (3,23 %).

KLJUČNE RIJEČI: *Taxus baccata L.; bioulje iz kore; kemijski sastav; antioksidativna aktivnost; GC/MS; FTIR*

1 INTRODUCTION
1. UVOD

A living system and organisms can produce a broad spectrum of reactive oxygen/nitrogen/chlorine species (RO/N/CS) and free radicals that play an essential role in regulating numerous physiological and metabolic functions of the body, where their reactivity and diffusibility are varied (Halliwell, 2003; Rajamanikandan *et al*., 2011). Hence, the excessive generation of RO/N/CS in living organisms can defeat these antioxidant defense mechanisms, give rise to oxidative stress (Mandal *et al*., 2011), cause damage to different biomolecules such as lipids, proteins, carbohydrates, and nucleic acids, and induce several types of degenerative diseases, for example, cancer, aging, atherosclerosis, cardiovascular disorders, neurodegenerative disorders, and inflammation (Finkel and Holbrook, 2000; Valko *et al*., 2007; Thitilertdecha *et al*., 2008). Antioxidant defense mechanisms of organisms directly scavenge or prevent the generation of RO/N/CS to protect living systems against their adverse effects (Rajamanikandan *et al*., 2011).

Forming complex organic compounds to restrain the accessibility of easily utilizable substrates, i.e., sugar and starches, is a defense strategy for trees to prevent their susceptibility to degradation (Scott Reading *et al*., 2003). The bark of trees works as a protective barrier against extreme weather conditions, insect pests, termites, and fungi, and it also has a significant role in wood fires (Hosseinashrafi *et al*., 2023). The softwood bark is composed of cellulose (18-38 %), hemicellulose (15-33 %), and lignin (30-60 %) (Díez *et al*., 2020).

Bio-oils from the bark have been used as protective substances obtained by pyrolytic methods (Singh and Singh, 2012). Phenols were major products in the bio-oil distillate from softwood lignin obtained by pyrolysis (Larson *et al*., 2017). Pyrolysis is an efficient technology in which lignin is converted into valuable chemicals, enhancing its valorization. Pyrolysis can yield phenolic compounds and/or aromatic hydrocarbons (AHs), demonstrating potential applications as biochemical intermediates and bio-fuel additives (Lu and Gu, 2022). When using bark as a source of biopesticide production, it must be taken in consideration that the bio-reactivity of bark extracts from different sources can differ (Singh and Singh, 2012).

Also, plants and their products have been shown to employ antioxidant activity against RO/N/CS, allowing their practical use as food preservatives, dietary supplements, and food flavoring agents (Huang *et al*., 2005; Lee *et al*., 2011).

Taxus baccata L. (European yew) is a member of the family Taxaceae, a native evergreen non-resinous gymnosperm that can grow up to 20-28 m and widely distributed in Europe and Asia (Thomas and Polwart, 2003). *Taxus baccata* L. is one of the four conifers indigenous to the Hyrcanian forests of Iran. This rare, native, old, and endangered tree species has recently been scrutinized due to its addition to the red list of threatened species (Alavi *et al*., 2019; Rezaei Karmozdi *et al*., 2022).

Sadeghi Aliabadi *et al*. (2009) examined different solvent-based extraction systems from the needles of yew. Their results indicated that the extract obtained with 100 % acetone contains the highest amount of taxol and other taxanes as well as alcohols, phenolic acids, simple sugars, disaccharides (sugar), free fatty acids, and resins found in the yew tree bark as the main compounds.

To the best of the authors' knowledge, the chemical composition of the bark of the yew (*Taxus baccata* L.) BO has yet to be reported. However, the chemical composition of the extract of this part has already been reported. Moreover, this novel approach investigated the antioxidant activity of its BO, EtE, and SHEtE and compared them with standard ascorbic acid (AA). This study investigated the antioxidant activity of the bark bio-oil of yew, which has not been reported before.

2 MATERIALS AND METHODS
2. MATERIJALI I METODE

2.1 Plant material
2.1. Biljni materijal

In the present study, three wooden discs with a thickness of 0.5 meters were prepared from the breast

height of three yew (*Taxus baccata* L.) tree trunks fallen due to strong wind or landslide. The fallen trunks were collected from Afratakhteh forests in Golestan province, Iran, in October 2017 (autumn). The bark of prepared discs was separated and poured into a glass jam jar with lids and then kept in a refrigerator at 4 ºC until pyrolysis and extraction. The plant material with voucher specimen 4657 was identified by Sayed Khosrow HossinAshrafi (Assistant Professor) and deposited to the Herbarium in the College of Agricultural and Natural Resources, Karaj Branch, Islamic Azad University, Karaj, Iran.

In this work, for the extraction of valuable compounds from the bark of the yew tree, three methods have been employed: pyrolysis, solvent extraction using a Soxhlet extractor, and superheated solvent extraction.

Prior to pyrolysis and extraction operations, yew bark samples were oven-dried at (103±2) ºC for 1 hour. The samples had a mass loss of 20 % due to the oven-dry procedure.

2.2 Experimental setup for pyrolysis
2.2. Eksperimentalna oprema za pirolizu

A small laboratory-scale electrical furnace was used to pyrolyze *Taxus baccata* dry bark. A schematic diagram of the furnace used in this study is shown in Figure 1.

This apparatus used a tubular ceramic core (5 cm ID and 30 cm length) equipped with an electrical heater (500 W) with a controlling temperature range of 100 to 600 ± 5 °C. The batch experiment was conducted in a closed system at the constant N_2 flow rate of 50 cm³/min. For conducting pyrolysis experiments, about 20 grams of the crushed sample were placed in the furnace, with

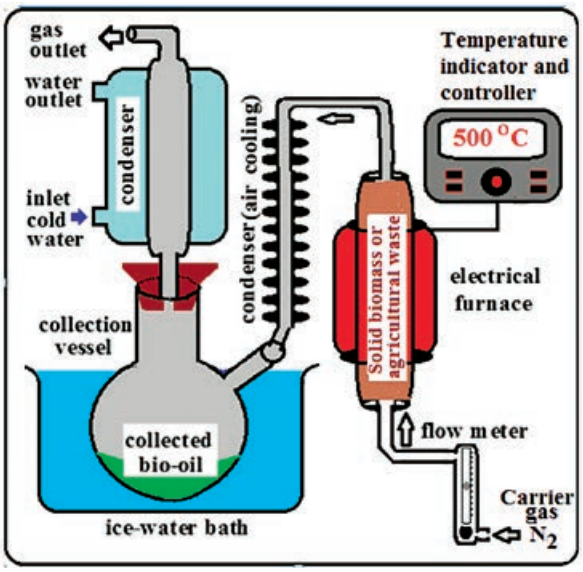

Figure 1 A schematic diagram of a small laboratory-scale electrical furnace (Bagi and Baseri, 2021)
Slika 1. Shematski dijagram male laboratorijske električne peći (Bagi i Baseri, 2021.)

both ends sealed by mineral wool. The samples were then pyrolyzed in the furnace at a temperature of 500 °C for 30 min. During the process, nitrogen gas was used as the carrier gas at a flow rate of 50 cm³/min.

During the pyrolysis process, the used carrier gas carried out the lighter products, and in the condensers, they were condensed into the liquid BO. However, the uncondensed gases were discharged into the atmosphere. The condensed BO was collected in the collection vessel at about 0 °C.

At the end of the experiment, the system was discharged, and the collected BO was weighed and stored in the closed vessel in the refrigerator until their compositions were characterized. Moreover, the solid residue was weighed, and the yields of the products (weight percentages) were calculated using Eq 1 (Bagi and Baseri, 2021; Raeisian *et al*., 2025).

$$Yield\ of\ product\,(\%) = \frac{M_2}{M_1} \times 100 \qquad (1)$$

Where M_2 and M_1 denote the weight of BO and the weight of biomass (dry feed), respectively.

2.3 Solvent extraction and superheated solvent extraction
2.3. Ekstrakcija otapalom i ekstrakcija pregrijanim otapalom

High-purity ethanol (99 %) was selected as the extraction solvent in the ordinary and superheated solvent extraction experiments. For the ordinary solvent extraction, 10 g of air-dried powder sample was placed into a thimble and was extracted for 24 hours using a 250 mL laboratory-scale Soxhlet extractor. After the extraction process, the solvent was removed under reduced pressure in a rotary evaporator, and the remaining extracts were weighed and stored in the closed flask in the refrigerator (Jayawardena and Smith, 2010; Vibala *et al*., 2020; Smith, 2022; Yu *et al*., 2023).

A small laboratory-scale reactor was used for superheated solvent extraction to extract *Taxus baccata* air-dried bark powder. A schematic diagram of the used reactor is shown in Figure 2.

In this system, a 50 mL cylindrical stainless steel vessel (18 mm ID and 200 mm length) is used as the extraction vessel, and the electrical heaters (500 W) with maximum working temperatures of (300 ± 3) °C to heat the vessel. The pressure of the vessel is increased by adding N_2 gas from the gas cylinder up to 4 MPa, and it is monitored by pressure indicators.

For a typical experiment, 5 g of air-dried powder sample is charged in the vessel, and 15 mL of solvent is added to the system. Then, the reactor is closed, and the air is discharged by purging of N_2 gas in the reactor. The pressure of the reactor increases to 7 bar by adding N_2 gas, which is controlled by a pressure control valve. Temperature of the system is adjusted to 110 (± 1 %) °C. To pre-

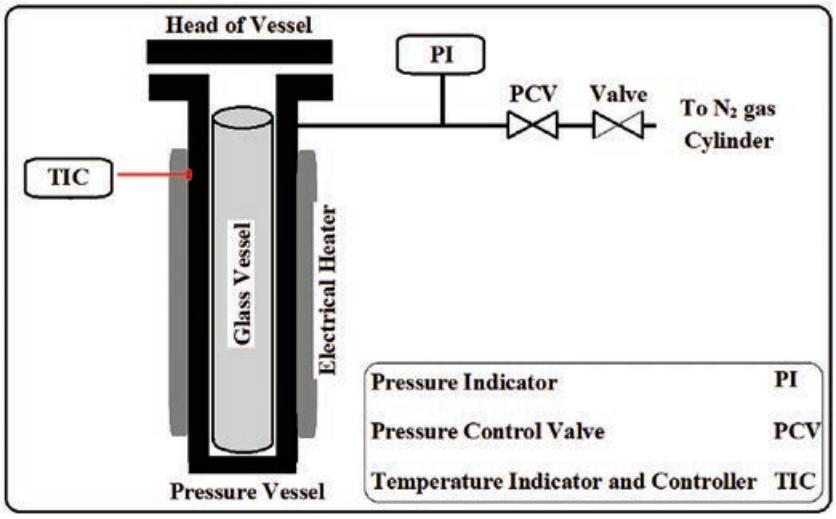

Figure 2 A schematic diagram of reactor used for superheated solvent extraction process (Mohseni and Baseri, 2022)
Slika 2. Shematski dijagram reaktora upotrijebljenog za proces ekstrakcije pregrijanim otapalom (Mohseni i Baseri, 2022.)

vent solvent evaporation, the system pressure is adjusted to values higher than the equilibrium vapor pressure of the extraction solvent in the system temperature.

At the end of the experiment, the reactor is cooled to room temperature, and the pressure is decreased by the constant rate of 15 bar/hour. Then, the reactor is opened, and the solid and liquid phases are separated by centrifuging (*RPM*=4000 and *t*=5 min). To calculate the total yield of extract, the remaining solid phase is dried at 100 °C for 1 hour and weighed.

Finally, the solvent is separated by a rotary evaporator under the reduced pressure, and the remaining extract is weighed and stored in the closed flask.

2.4 FTIR analysis bark bio-oil and extracts
2.4. FTIR analiza bioulja i ekstrakata iz kore drva tise

The functional groups of the yew bark BO and extracts were studied by Fourier transform infrared spectroscopic analysis with a Unicam 4600 FTIR spectrometer (Mattson, USA) over a scanning wave range of 400 to 4000 cm^{-1} (Wu *et al*., 2009; Packialakshmi and Naziya, 2014).

2.5 Antioxidant activity of yew bark bio-oil and extracts
2.5. Antioksidativna aktivnost bioulja i ekstrakata iz kore drva tise

The antioxidant potential of the yew bark BO and extracts was evaluated using a 1,1-Dipheny-2-picrylhydrazyl (DPPH) assay, according to the method described in the literature (Halliwell, 1997; Kim *et al*., 2002; Emami *et al*., 2010).

In short, 2.5 mL of a 0.1 mM DPPH solution in 70 % methanol (stock solution) was added to different concentrations (100 µL) of the BO, extracts, and ascorbic acid (AA) as the positive control. Serial dilutions were made from the stock solution and the working solution of the tested bark BO and solvent extracts to obtain concentrations of 1000, 500, 250, 125, 62.5, 31.25, 15.62, and 7.8 ppm. The preparation process of the working solution was conducted according to a previously reported method (Hosseinihashemi and Aghajani, 2017; Barzegari *et al*., 2023).

The control samples (DPPH solution) were prepared using an equal volume of solution without any test compounds or referenced standards, serving as the negative control (Pillai *et al*., 2019; Alam *et al*., 2021). Pure methanol (Sigma-Aldrich, Darmstadt, Germany) was used to prepare the control sample. Before analysis, the UV scanning spectrophotometer device (JENWAY 6320D, Standford, UK) was calibrated and adjusted using 70 % methanol. The reaction mixture was mixed for 10 s and left to stand at room temperature in a dark place for 30 min. The absorbance was measured at 517 nm, using a UV scanning spectrophotometer (Hosseinihashemi *et al*., 2017).

2.6 GC/MS analysis of yew bark bio-oil
2.6. GC/MS analiza bioulja iz kore drva tise

The yew bark BO was analyzed by GC/MS using a GC Agilent 7890A and MS Agilent 5975C mass spectrometer detector (Agilent Technologies, Palo Alto, CA, USA) equipped with an HP-5MS cross-linked capillary column (30 m long and 0.25 mm internal diameter, 0.25 µm film thickness).

100 µL of yew bark BO sample was dissolved separately with 900 µL of hexane. Samples (1 µL) were injected in the split mode (50:1) with a flow rate of 1 mL/min. The column temperature program was conducted as follows: injector temperature of 260 °C; transfer line of 270 °C; oven temperature program of 60 °C for 4 min, 3 °C/min to 100 °C for 2 min, then 4 °C/min to 250 °C for 5 min; carrier gas was He with a flow rate of 1 mL/min. The intrinsic energy that hits the

sample in the MS system was 70 eV. The total chromatographic run time was about 52 min.

The identification of yew bark BO components was carried out by comparing their mass spectra with those available on a NIST database mass spectral library, with spectra from literature (Joulain and Konig, 1988; Adams, 2001), as well as retention index and literature retention indices values calculated for each detected BO composition.

2.7 Statistical analysis
2.7. Statistička analiza

The results are given in mean values with their standard deviations. Statistical analysis was performed using the SPSS program, version 24.0 (International Business Machines (IBM) Corp., Armonk, NY, USA). Univariate analysis of variance (ANOVA) was conducted to determine the significance of differences between analytical results at $p<0.05$ significance level.

3 RESULTS AND DISCUSSION
3. REZULTATI I RASPRAVA

3.1 FTIR of yew bark bio-oil and extracts
3.1. FTIR bioulja i ekstrakata iz kore drva tise

Figure 3 depicts the FTIR spectrums of the components extracted with the ethanol, superheated ethanol, and the BO produced by the pyrolysis process. As can be seen, the spectrums of samples extracted by ethanol and superheated ethanol are relatively the same, with a slight increase in the intensity of some peaks. However, significant changes are observed in the BO produced by the pyrolysis process.

The main chemical groups in the ethanol extracts and the produced BO are as follows: the broad peak at about 3400 cm^{-1} represented the O-H stretch and H-bonded groups that may suggest the presence of phenols, alcohols, carboxylic acids, or water molecules. As can be seen, this peak strongly appeared in three samples studied.

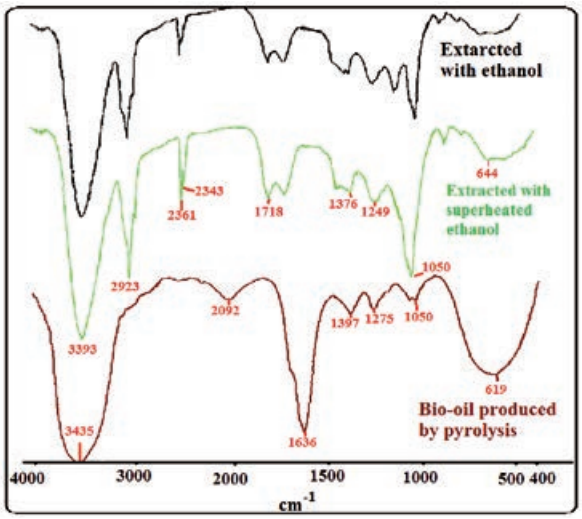

Figure 3 FTIR spectrums of components extracted with EtE, SHEtE, and BO produced by pyrolysis process
Slika 3. FTIR spektri ekstrakata EyE, SHEtE i bioulja proizvedenoga procesom pirolize

The absorption peak at about 2923 cm^{-1} was related to the C-H ($-CH_3$) stretching vibration of cycloalkanes and aliphatic hydrocarbons (Zhou *et al*., 2022). However, the binding vibration of $–CH_3$ groups was observed in about 1375 cm^{-1}.

The peaks that appeared in 1718 and 1450 cm^{-1} were caused by carbonyl groups (C=O) in carboxylic acids, ketones, or aldehydes (Zhou *et al*., 2022). In addition, the –C-O stretching and vibration of the –CH skeleton were depicted between 1267 and 1023 cm^{-1}. For the infrared spectra of BO, the broad peak bound at 1634 cm^{-1} may confirm the presence of aromatic functional groups or show the presence of amide I components in the produced BO (Kalisz *et al*., 2021). The broad peak in about 500 to 800 cm^{-1} can be assigned to benzene rings or vibration absorption of alkenes (Li *et al*., 2013).

3.2 Antioxidant activity of yew bark bio-oil and extracts
3.2. Antioksidativna aktivnost bioulja i ekstrakata iz kore drva tise

The yield of EtE and SHEtE from the bark of *T. baccata* was 10.3 % and 12.4 %, respectively. Pyrolysis of *T. baccata* gave dark BO with a yield of 17.41 mL/100 g, based on the dry weight of the bark.

The antioxidant activity of BO and extracts from the bark of *T. baccata* at eight different concentrations of 1000, 500, 250, 125, 62.5, 31.25, 15.62, and 7.8 ppm was measured in the present study by using the DPPH method and compared with AA as the reference standard (Table 1 and Figure 4). Statistically, substantial differences were observed among the treatments, including BO, EtE, SHEtE, AA, and their respective concentrations.

The data in Table 1 and Figure 4 show a higher antioxidant activity when tested at higher concentrations. The BO from yew bark exhibited excellent antioxidant activity overall compared to other extracts. The lowest antioxidant activity (-0.1 %) was observed in the EtE at the concentration of 7.8 ppm, which was lower than the value of AA (4.7 %) at the same concentration. The highest antioxidant activity was found in bark BO (58.7 %) at 1000 ppm, which was higher than the value of AA (45.1 %) at a similar concentration. The same trends were observed between the reference (AA) and BO after 250 ppm. Still, the antioxidant activity of the EtE and SHEt extracts has increased very slightly or remained constant with increasing concentration. There was a significant decrease in the concentration of DPPH radical as the concentration of BO increased due to its ability to scavenge free radicals

Table 1 Percentage of antioxidant activity (Mean ± SD) as affected by concentration of bark BO and extracts of *T. baccata* compared with AA
Tablica 1. Postotak antioksidativne aktivnosti (srednja vrijednost ± SD) u odnosu prema koncentraciji bioulja i ekstrakata iz kore drva *T. baccata* u usporedbi s AA

Treatment AOA, % *Tretman AOA, %*	**Concentration** / *Koncentracija*							
	1000	500	250	125	62.5	31.25	15.78	7.8
BO	58.76 ± 3.05 m	43.53 ± 1.69 l	12.98 ± 0.51 i	5.44 ± 0.19 bcd	0.90 ± 1.07 a	0.59 ± 0.92 a	0.07 ± 0.79 a	0.21 ± 1.32 a
EtE	13.14 ± 0.44 i	12.78 ± 0.91 i	8.96 ± 2.55 efg	2.65 ± 0.74 abc	2.43 ± 2.20 abc	1.32 ± 0.46 a	1.13 ± 0.97 a	-0.10 ± 1.62 a
SHEtE	18.86 ± 0.95 j	13.20 ± 4.76 i	12.19 ± 2.42 hi	7.72 ± 1.49 defg	1.19 ± 3.51 a	0.52 ± 0.83 a	0.66 ± 1.25 a	1.92 ± 1.21 ab
AA	45.14 ± 4.95 l	33.95 ± 0.49 k	9.86 ± 1.74 gh	9.23 ± 1.01 fg	6.68 ± 2.31 def	5.04 ± 0.37 cd	6.13 ± 1.40 de	4.69 ± 1.73 bcd

*Different letters in columns and rows indicate a statistical difference ($p<0.05$) among the treatment groups
**Različita slova u stupcima i redcima označavaju statističku razliku ($p<0,05$) među ispitivanim skupinama.*

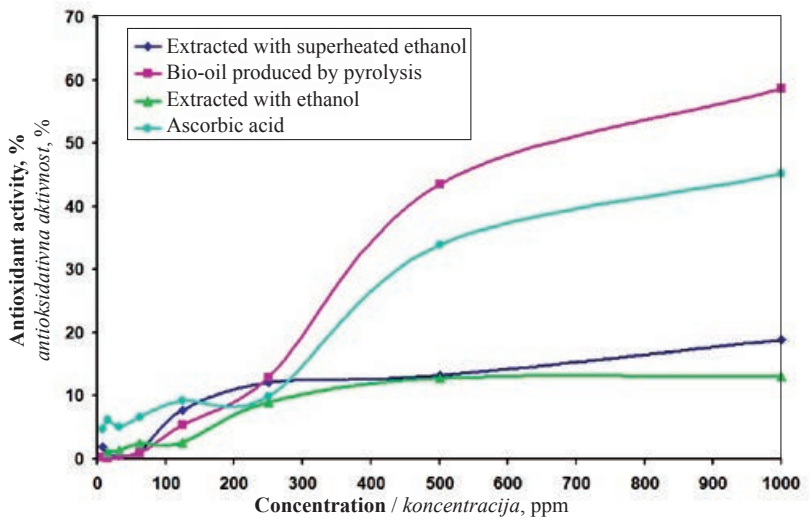

Figure 4 Antioxidant activity of components extracted with the EtE, SHEtE, and BO produced by pyrolysis process
Slika 4. Antioksidativna aktivnost ekstrakata EyE, SHEtE i bioulja proizvedenoga procesom pirolize

(Patra *et al*., 2015). The scavenging activity of BO is attributed to its ability to donate hydrogen ions or electrons to DPPH to neutralize free radicals (Rajamanikandan *et al*., 2011).

3.3 Chemical composition of yew bark bio-oil
3.3. Kemijski sastav bioulja iz kore drva tise

GC-MS analysis showed the chemical composition of volatile compounds in yew bark BO. The chemical profiles of yew bark BO have not been previously reported. Figure 5 shows the chromatogram of the BO of *T. baccata* bark obtained in October 2017 (autumn) at Afratakhteh forest station and it is analyzed in the HP-5MS column.

The identified constituents are presented in Table 2, where all compounds are listed in order of their elution from the HP-5 column. In total, 44 compounds comprising 98.75 % of the volatile compounds in the BO were selected and identified (Table 2) in this study.

The components of BO are mainly comprised of aldehydes, alcohols, acids, ether, phenols, and phenol derivatives. Among them, the top-seven most abundant compounds are guaiacol (11.65 %), phenol (8.48 %), *β*-D-Glucopyranose, 1,6-anhydro- (6.54 %), furfuryl alcohol (5.64 %), 3,4-dihydroxyphenol-*2H*-pyran (5.52 %), *p*-cresol (4.50 %) and 4-methylguaiacol (4.24 %).

In GC/MS analysis of the first harvest of biomass samples from *T. canadensis* shrubs, some compounds were identified such as phenol, 4-vinylphenol, 4-hydroxybenzaldehyde, 3,5-dimethoxyphenol, guaiacol, isoeugenol, and an anhydrosugar as some of the primary components of the pyrolysis oil based on published spectra (Cass *et al*., 2001). Jean *et al*. (1993) had previously identified 3,5-dimethoxyphenol as a major aglycone in *T. canadensis*; thus, its presence was ex-

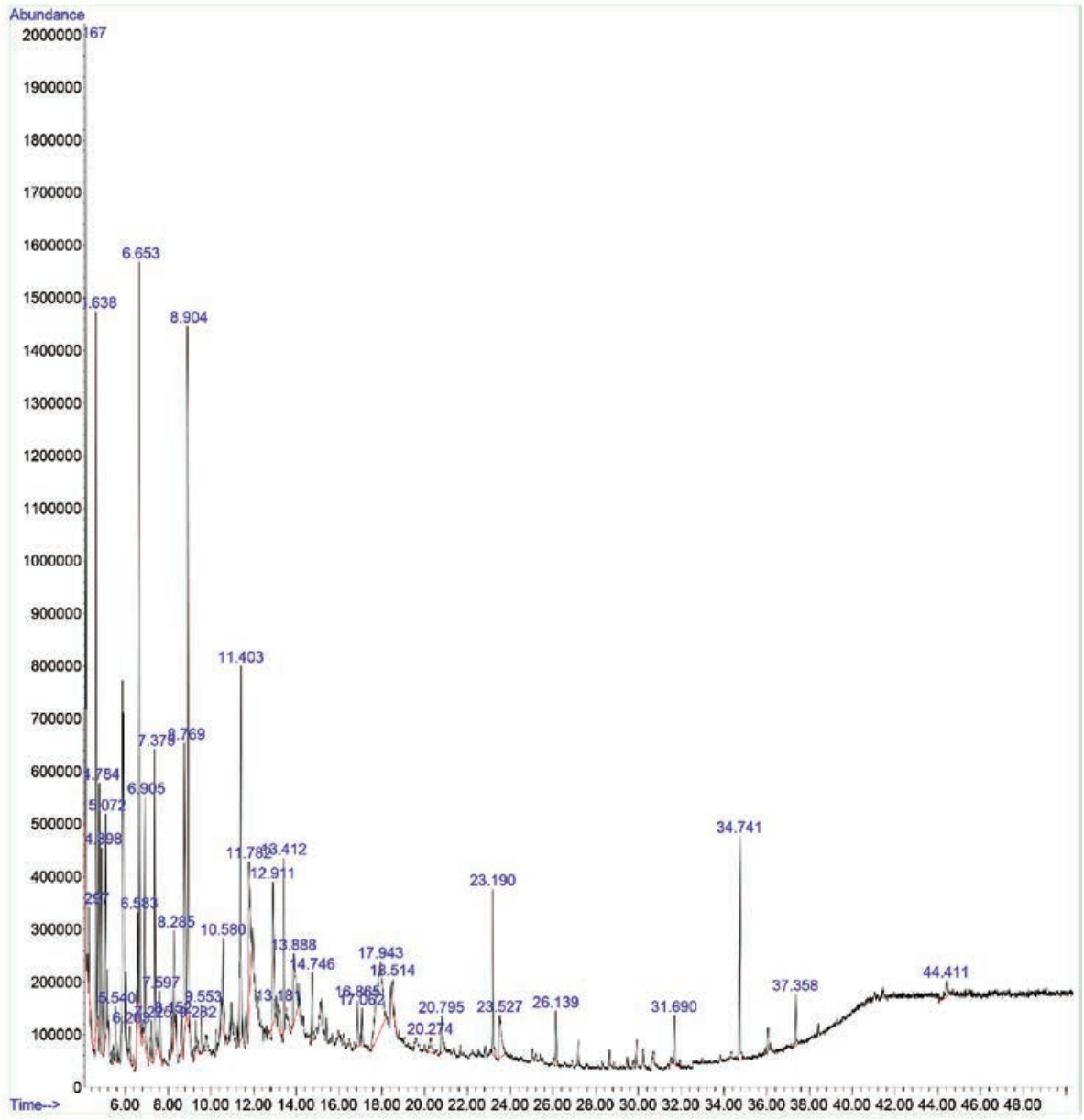

Figure 5 Chromatogram of BO from *T. baccata* bark harvested in October 2017 (autumn). Components: furfuryl alcohol (4.165 min), 3,4-dihydro-*2H*-pyran (4.637 min), phenol (6.650 min), *p*-cresol (8.767 min), guaiacol (8.902 min), and 4-methylguaiacol (11.403 min), *β*-D-Glucopyranose, 1,6-anhydro- (17.941 min)
Slika 5. Kromatogram bioulja iz kore *T. baccata*, srušene u listopadu 2017. (jesen). Sastojci: furfurilni alkohol (4,165 min), 3,4-dihidro-2H-piran (4,637 min), fenol (6,650 min), p-krezol (8,767 min), gvajakol (8,902 min) i 4-metilgvajakol (11,403 min), *β*-D-glukopiranoza, 1,6-anhidro- (17,941 min)

pected. Eugenol has also been identified in the essential oil and in the aglycone component of *T. canadensis* (Jean *et al*., 1993).

Among the identified compounds, some components such as phenol, *o*-cresol, and *p*-cresol in 2.19 %, 2.79 %, and (6.02 %) amounts were found in the bio-oil of Japanese red pine sawdust, respectively (Patra *et al*., 2015). Guaiacol, syringol, and 4-methylguaiacol in 3.60 %, 14.86 %, and 3.08 % amounts as well as in 1.26 %, 4.21 %, and 1.32 % amounts were also identified in the bio-oil from pyrolysis of undecayed and decayed *Fagus orientalis* wood, respectively (Hosseinihashemi *et al*., 2017).

According to the researchers' and our findings, the types of compounds in the essential oil and bio-oil of the yew plant are different from each other, but the class of some compounds may be the same (Radulović *et al*., 2011; Jian-chun *et al*., 2012; Yasar, 2013; Stefanović *et al*., 2016; Zhao *et al*., 2016; Wei and Yin, 2019; Huong *et al*., 2020; Benlembarek *et al*., 2021).

T. baccata of Algeria essential oil showed a moderate antioxidant activity (Benlembarek *et al*., 2021). In Algeria, Bekhouche *et al*. (2021) showed that the methanolic extract of *T. baccata* needles exhibits a greater antioxidant activity than the synthetic antioxidant BHT. The essential oil from the stems of *T. cuspi-*

Table 2 Bio-oil composition of *T. baccata* bark harvested in October 2017 (autumn)
Tablica 2. Sastav bioulja iz kore *T. baccata*, stabla srušena u listopadu 2017. (jesen)

No.	**Compound** / *Spoj*	***RT*, min**	**Area, %**	**KIL_{exp}**	**KI_{lab}**
1	Acetoxypropanone	4.134	1.46	856	839
2	Furfuryl alcohol	4.165	5.64	861	866
3	3-Methylpyridine	4.3	0.88	882	-
4	3,4-Dihydro-*2H*-pyran	4.637	5.52	912	705
5	2-Methylcyclopent-2-enone	4.782	1.96	920	893
6	2-Acetylfuran	4.896	2.15	927	902
7	Diisoamylether	5.073	1.97	936	-
8	2,4-Dimethylpyridine	5.54	0.69	959	933
9	5-methylfurfural	5.872	2.86	974	934
10	3-Methylcyclopent-2-enone	5.908	3.45	976	935
11	4-oxo-5-methoxy-2-penten-5-olide	6.028	0.50	981	-
12	1-Methyl-2-furoate	6.204	0.58	988	956
13	2-(1-Methylheptyl)-cyclopentanone	6.583	0.80	1005	1128
14	Phenol	6.65	8.48	1008	1002
15	Mepivacaine metabolite	6.904	2.94	1020	-
16	2-Hexene, 2-methyl-	7.226	0.73	1035	-
17	2-Hydroxy-3-methylcyclopent-2-en-1-one	7.382	3.29	1042	1015
18	2,3-Dimethylcyclopent-2-enone	7.6	1.08	1051	1018
19	*o*-Cresol	8.285	1.86	1079	1058
20	*p*-Cresol	8.767	4.50	1097	1090
21	Guaiacol	8.902	11.65	1103	1092
22	Maltol	9.281	0.53	1120	1093
23	3-Ethyl-2-hydroxycyclopent-2-en-1-one	9.556	0.58	1133	1100
24	Piperidine	10.578	0.80	1176	-
25	1,4:3,6-Dianhydro-*α*-d-glucopyranose	11.336	0.95	1206	-
26	4-Methylguaiacol	11.403	4.24	1209	-
27	Catechol	11.782	3.23	1227	-
28	3-Methoxycatechol	12.913	2.11	1276	1239
29	3-Methylcatechol	13.183	0.76	1287	1263
30	2-Methoxyphenethyl alcohol	13.411	1.73	1296	1309
31	4-Methylcatechol	13.888	2.22	1319	1246
32	Syringol	14.744	0.91	1358	1347
33	Dehydroacetic acid	16.867	0.67	1459	-
34	Isoeugenol	17.064	0.48	1469	1436
35	*β*-D-Glucopyranose, 1,6-anhydro-	17.941	6.54	1511	1491
36	2,3,5-Trimethoxytoluene	18.511	0.59	1540	1538
37	Propanamide, N-acetyl-	20.276	0.49	1630	-
38	Homovanillic acid	20.794	0.88	1658	1657
39	3,5-Diethoxycarbonyl-2,6-dimethylpyridine	23.192	1.88	1790	-
40	4-(1-Hydroxyethyl)benzaldehyde	23.529	1.42	1807	-
41	3,5-Diethoxycarbo	26.139	0.72	1945	-
42	2-ethylhexyl-3-(4-methoxyphenyl)acrylate	31.691	0.79	2341	-
43	Di(ethylhexyl) phthalate	34.741	2.72	2573	2509
44	Hexamethyl-cyclotrisiloxane	44.413	0.52	3356	-

RT – Mean retention time; KI_{exp} and KI_{lit} – experimental and literature Kovats indices, respectively, on HP-5MS column in reference to *n*-alkanes
RT– srednje vrijeme zadržavanja; KI_{exp} *i* KI_{lit} *– eksperimentalni i literaturni Kovatovi indeksi, redom na HP-5MS koloni u odnosu prema n-alkanima*

data has shown a strong antioxidant capacity against the DPPH radical (Bajpai and Baek, 2016). In India, the study of the antioxidant activity of *T. wallichiana* raw extracts from the leaves showed a very remarkable antioxidant activity (Ahmad *et al*., 2015).

Derivatives of methoxyphenol have shown a wide range of therapeutic benefits, primarily based on their antioxidant properties (Koleva *et al*., 2018). Volatile compounds of medicinal importance, such as furan, furan derivatives, catechol, and cresol, were found in the BO. Furan, as the basic skeleton of some compounds, has cardiovascular properties; it is also widely used for its antiviral, anti-inflammatory, antibacterial, antifungal, antitumor, and antihyperglycemic characteristics, as well as in the treatment of ventricular and atrial fibrillation (Hoyle and Roberts; 1973; Meotti *et al*., 2003; Verma *et al*., 2011). Cresols are used in the preparation of antioxidants and as abortives, diaphoret-

ics, and emmenagogue drugs (Hoyle and Roberts, 1973; Meotti *et al*., 2003; Kim *et al*., 2011; Syazana *et al*., 2011).

p-Cresol (4-methylphenol) was found in high concentration (4.5 %) in yew bark BO. It can be transformed using a Bronsted acid functionalized ionic liquid in the tert-butylation process to produce other valuable antioxidants and diphenol antioxidants with comparatively low toxicity (Fiege *et al*., 2000). According to Elavarasan *et al*. (2010), those conversion products may find application in the food, pharmaceutical, and cosmetic sectors.

4 CONCLUSIONS
4. ZAKLJUČAK

In this research, the antioxidant capacity of extracts and the chemical composition and antioxidant capacity of bio-oil from the bark of *T. baccata* were studied. The antioxidant activity of bio-oil from the bark of *T. baccata* indicated the high potential of this tree for nutrition and pharmaceutical purposes. Considering the findings of this research, the bio-oil extracted from *T. baccata* bark possessed an impressive capacity for scavenging DPPH free radicals compared to ascorbic acid. Regarding bio-oil chemical composition, the principal constituents shown in the bio-oil from bark included guaiacol, phenol, furfuryl alcohol, 3,4-dihydro-*2H*-pyran, *p*-cresol, and 4-methylguaiacol.

Acknowledgements – Zahvala

The authors are grateful for the support of the School of Chemistry, Damghan University and the Department of Wood Science and Paper Technology, Karaj Branch, Islamic Azad University.

5 REFERENCES
5. LITERATURA

1. Adams, R. P., 2001: Identification of essential oil components by gas chromatography/quadrupole mass spectroscopy, 3rd ed., Allured Publishing Corp., Carol Stream, IL, USA.
2. Ahmad, M.; Yaseen, M.; Bhat, A.; Ganai, B. A.; Zargar, M. A.; Ganie, S. A.; Qureshi, R., 2015: *Taxus wallichiana* as a potential in vitro antioxidant with good lethal effect on pathogenic bacterial strains. American Journal of Phytomedicine and Clinical Therapeutic, 3 (3): 209-221.
3. Alam, F.; Ali Khan, S. H.; Bin Asad, M. H. H., 2021: Phytochemical, antimicrobial, antioxidant and enzyme inhibitory potential of medicinal plant *Dryopteris ramosa* (Hope) C. Chr. BMC Complementary Medicine and Therapies, 21 (1): 197. https://doi.org/10.1186/s12906-021-03370-7
4. Alavi, S. A.; Ahmadi, K.; Hosseini, S. M.; Tabari, M., 2019: The response of English yew (*Taxus baccata* L.) to climate change in the Caspian Hyrcanian mixed forest ecoregion. Regional Environmental Change, 19 (5): 1495-1506. https://doi.org/10.1007/s10113-019-01483-x
5. Bagi, E.; Baseri, H., 2021: Pyrolysis of *Ligustrum vulgare* waste and the effects of various operating parameters on bio-oil upgrading. Biomass Conversion and Biorefinery, 13: 3153-3163. https://doi.org/10.1007/s13399-021-01374-4
6. Bajpai, V. K.; Baek, K. H., 2016: Characterization of microwave extracted essential oil from *Taxus cuspidata* stem and determination of its phenolic content, antioxidant and free radical scavenging activities. Journal of Essential Oil Bearing Plants, 19 (5): 1051-1065. https://10.1080/0972060X.2016.1194234
7. Barzegari, F.; Hosseinihashemi, S. K.; Baseri, H., 2023: Chemical composition and antioxidant activity of extracts from the fruit, leaf and branchlet of *Cupressus arizonica* Greene. BioResources, 18 (1): 19-38. https://doi.org/10.15376/biores.18.1.19-38
8. Bekhouche, M.; Morsli, A.; Slaoui, M. K.; Benyammi, R.; Krimat, S.; Khelifi, L., 2021: Free radical scavenging activity and detailed flavonoid profiling of Algerian yew. International Journal of Pharmaceutcal Sciences and Research, 12 (5): 2613-2619. https://10.13040/IJPSR.0975-8232.12(5).2613-19
9. Benlembarek, K.; Lograda, T.; Ramdani, M.; Figueredo, G.; Chalard, P., 2021: Chemical composition, antibacterial, antifungal and antioxidant activities of *Taxus baccata* essential oil from Algeria. Biodiversitas Journal of Biological Diversity, 22 (12): 5475-5483. https://10.13057/biodiv/d221231
10. Cass, B. J.; Piskorz, J.; Scott, D. S.; Legge, R. L., 2001: Challenges in the isolation of taxanes from *Taxus canadensis* by fast pyrolysis. Journal of Analytical and Applied Pyrolysis, 57 (2): 275-285. https://doi.org/10.1016/S0165-2370(00)00148-0
11. Díez, D.; Urueña, A.; Piñero, R.; Barrio, A.; Tamminen, T., 2020: Determination of hemicellulose, cellulose and lignin content in different types of biomasses by thermogravimetric analysis and pseudocomponent kinetic model (TGA-PKM method). Processes, 8 (9): 1048. https://doi.org/10.3390/pr8091048
12. Elavarasan, P.; Kondamudi, K.; Upadhyayula, S., 2010: Synthesis of antioxidants: Green chemistry route. International Journal of Chemical Science, 8: S578-S584.
13. Emami, S. A.; Fakhrjafary, M.; Tafaghodi, M.; Hasanzadeh, M. K., 2010: Chemical composition and antioxidant activities of the essential oils of different parts of *Cupressus arizonica* Greene. Journal of Essential Oil Research, 22 (3): 193-199. https://doi.org/10.1080/10412905.2010.9700301
14. Fiege, H., 2000: Cresols and Xylenols. In Ullmann's Encyclopedia of Industrial Chemistry; Wiley-VCH Verlas GmbH & Co., Weinhenim, Germany.
15. Finkel, T.; Holbrook, N. J., 2000: Oxidants, oxidative stress and the biology of ageing. Nature, 408 (6809): 239-247. https://doi.org/10.1038/35041687
16. Halliwell, B., 2003: Free radical chemistry as related to degradative mechanism. In: Wood Deterioration and Preservation, ACS Symposium Series No. 845, American Chemical Society, Washington, DC, 10-15.
17. Halliwell, B., 1997: Antioxidants and human diseases: A general introduction. Nutrition Review, 55 (1): 44-49. https://doi.org/10.1111/j.1753-4887.1997.tb06100.x
18. Hosseinashrafi, S. K.; Hosseinihashemi, S. K.; Gorji, P.; Akhtari, M., 2023: Environment-friendly waterborne fire retardants for protection of wood and bark against fire flames. BioResources, 18 (4): 7681-7699. https://doi.org/10.15376/biores.18.4.7681-7699

19. Hosseinihashemi, S. K.; Aghajani, H., 2017: Chemical composition and antioxidant capacity of extracts from the wood of *Berberis vulgaris* stem. Lignocellulose, 6 (1): 36-47.
20. Hosseinihashemi, S. K.; Hassani, S.; Jahan Latibari, A.; Ozbay, G., 2017: Chemical characterization of bio-oil from pyrolysis of undecayed and decayed *Fagus orientalis* wood. Drvna industrija, 68 (2): 113-119. https://doi.org/10.5552/drind.2017.1626
21. Hosseinihashemi, S. K.; Dadpour, A.; Lashgari, A., 2017: Antioxidant activity and chemical composition of *Juniperus excelsa* ssp. *Polycarpos* wood extracts. Natural Product Research, 31 (6): 681-685. https://doi.org/10.1080/14786419.2016.1209666
22. Hoyle, W.; Roberts, G. P., 1973: Potential antimicrobial furans. Journal of Medicinal Chemistry, 16 (6): 709-710. https://doi.org/10.1021/jm00264a031
23. Huang, D.; Ou, B.; Prior, R. L., 2005; The chemistry behind antioxidant capacity assays. Journal of Agricultural and Food Chemistry, 53 (6): 1841-1856. https://doi.org/10.1021/jf030723c
24. Huong, L. T.; Nguyen, T. H.; Chac, L. D.; Dai, D. N.; Ogunwande, A., 2020: Antimicrobial activity and chemical constituents of essential oils from the leaf and wood of *Taxus chinensis* (Rehder & E. H. Wilson) Rehder (Taxaceae) from Vietnam. Journal of Biologicaly Active Products from Nature, 10 (1): 8-17. https://10.1080/22311866.2020.1749128
25. Jayawardena, B.; Smith, R. M., 2010: Superheated water extraction of essential oils from *Cinnamomum zeylanicum* (L.). Phytochemical Analysis, 21 (5): 470-472. https://doi.org/10.1002/pca.1221
26. Jean, F.-I.; Garneau, F.-X.; Collin, G. J.; Bouhajib, M.; Zamir, L. O., 1993: The essential oil and glycosidically bound volatile compounds of *Taxus canadensis* Marsh. Journal of Essential Oil Research 5 (1): 7-11. https://doi.org/10.1080/10412905.1993.9698163
27. Jian-Chun, X.; Li-Huang, L.; Hui-Ying, Z.; Hui-Lan, H.; Bao-Guo, S., 2012: Volatile constituents of *Taxus wallichiana* var. Mairei leaves. Journal of Essential Oil Bearing Plants, 15 (5): 724-730. https://10.1080/0972060X.2012.10644112
28. Joulain, D.; Konig, W. A., 1988: The Atlas of Spectral Data of Sesquiterpene Hydrocarbons, EB. Verlag, Hamburg, Germany.
29. Kalisz, G.; Gieroba, B.; Chrobak, O.; Suchora, M.; Starosta, A. L.; Sroka-Bartnicka, A., 2021: Vibrational spectroscopic analyses and imaging of the early middle ages hemp bast fibres recovered from lake sediments. Molecules, 26 (5): 1314. https://doi.org/10.3390/molecules26051314
30. Kim, K. H.; Eom, I. Y.; Lee, S. M.; Choi, D.; Yeo, H.; Choi, I. G.; Choi, J. W., 2011: Investigation of physicochemical properties of bio-oils produced from yellow poplar wood (*Liriodendron tulipifera*) at various temperatures and residence times. Journal of Analytical and Applied Pyrolysis, 92 (1): 2-9. https://doi.org/10.1016/j.jaap.2011.04.002
31. Kim, J. K.; Noh, J. H.; Lee. S.; Choi, J. S.; Suh, H.; Chung, H. Y.; Song, Y. O.; Lee, C., 2002: The first total synthesis of 2,3,6-tribromo-4,5-dihydroxybenzyl methyl ether (TDB) and its antioxidant activity. Bulletin of Korean Chemical Society, 23 (5): 661-662. http://dx.doi.org/10.5012/bkcs.2002.23.5.661
32. Koleva, L.; Angelova, S.; Dettori, M.; Fabbri, D.; Delogu, G.; Kancheva, V., 2018: Antioxidant activity of selected O-methoxyphenols and biphenols: theoretical and experimental studies. Bulgarian Chemical Communications, 50 (Special Issue C): 238-246.
33. Larson, R. A.; Sharma, B. K.; Marley, K. A.; Scott, J. W., 2017: Potential antioxidants for biodiesel from a softwood lignin pyrolyzate. Industrial Crops and Products, 109: 476-482. https://doi.org/10.1016/j.indcrop.2017.08.053
34. Lee, H. M.; Khan, Z.; Kim, S. G.; Baek, N. I.; Kim, Y. H., 2011: Evaluation of the biocontrol potential of some medicinal plant materials alone and in combination with *Trichoderma harzianum* against *Rhizoctonia solani* AG 2-1. The Plant Pathology Journal, 27 (1): 68-77. http://dx.doi.org/10.5423/PPJ.2011.27.1.068
35. Li, Y.; Kong, D.; Wu, H., 2013: Analysis and evaluation of essential oil components of cinnamon barks using GC-MS and FTIR spectroscopy. Industrial Crops and Products, 41: 269-278. https://doi.org/10.1016/j.indcrop.2012.04.056
36. Lu, X.; Gu, X., 2022: A review on lignin pyrolysis: pyrolytic behavior, mechanism and relevant upgrading for improving process efficiency. Biotechnology for Biofuels and Bioproducts, 15 (1): 1-43. http://dx.doi.org/10.1186/s13068-022-02203-0
37. Mandal, S.; Hazra, B.; Sarkar, R.; Biswas, S.; Mandal, N., 2011: Assessment of the antioxidant and reactive oxygen species scavenging activity of methanolic extract of *Caesalphinia crista* leaf. Evidence-Based Complementary and Alternative Medicine, 2011: 173768. https://doi.org/10.1093/ecam/nep072
38. Meotti, F. C.; Silva, D. O.; Dos-Santos, A. R. S.; Zeni, G.; Rocha, J. B. T.; Nogueira, C. W., 2003: Thiophenes and furans derivatives: A new class of potential pharmacological agents. Environmental Toxicology and Pharmacology, 15 (1): 37-44. https://doi.org/10.1016/j.etap.2003.08.008
39. Mohseni, A. H.; Baseri, H., 2022: Optimization of process parameters on hydrothermal liquefaction of *Sambucus ebulus* for bio-oil production. Journal of Applied Chemical Research, 16 (4): 94-107.
40. Packialakshmi, N.; Naziya, S., 2014: Fourier transform infrared spectroscopy analysis of various solvent extracts of *Caralluma fimbriyata*. Asian Journal of Biomedical and Pharmaceutical Sciences, 4 (36): 20-25. https://doi.org/10.15272/ajbps.v4i36.569
41. Patra, J. K.; Kim, S. H.; Hwang, H.; Choi, J. W.; Baek, K.-H., 2015: Volatile compounds and antioxidant capacity of the bio-oil obtained by pyrolysis of Japanese red Pine (*Pinus Densiflora* Siebold and Zucc.). *Molecules*, *20* (3): 3986-4006. https://doi.org/10.3390/molecules20033986
42. Pillai, M. K.; Santi, L. I.; Magama, S., 2019: DPPH radical scavenging activity of extracts from *Rhamnus prinoides*. Journal of Medicinal Plants Research, 13 (15): 329-334. http://dx.doi.org/10.5897/JMPR2019.6793
43. Raeisian, M.; Izadi, M. E.; Ajloo, D., 2025: Experimental and theoretical study of cis-1,4-polyisoprene pyrolysis. Physical Chemistry Research, 13 (1): 115-127. https://doi.org/10.22036/pcr.2024.448894.2503
44. Radulović, N.; Blagojević, P.; Palić, R.; Zlatković, B., 2011: Chemical composition of the essential oil hydrodistilled from Serbian *Taxus baccata* L. Journal of Essential Oil Research, 22 (5): 458-461. https://10.1080/10412905.2010.9700371
45. Rajamanikandan, S.; Sindhu, T.; Durgapriya, D.; Sophia, D.; Ragavendran, P.; Gopalkrishnan, V. K., 2011: Radical

scavenging and antioxidant activity of ethanolic extract of *Mollugo nudicaulis* by in vitro assays. Indian Journal of Pharmaceutical Education and Research, 45 (4): 310-316.
46. Rezaei Karmozdi, M.; Tabari Kouch-Aksaraei, M.; Sadati, S. E., 2022: Effect of biochar on physiological characteristics of European yew (*Taxus baccata*) seedling in different light intensities. Ecopersia, 10 (1): 61-69.
47. Sadeghi Aliabadi, H.; Asghari, G.; Mostafavi, S. A.; Esmaeili, A., 2009: Solvent optimization on Taxol extraction from *Taxus baccata* L., using HPLC and LC-MS. DARU. Journal of Pharmaceutical Sciences, 17 (3): 192-208.
48. Scott Reading, N.; Welch, K. D.; Aust, S. D., 2003: Free radical reactions of wood-degrading fungi. In: Wood Deterioration and Preservation, ACS Symposium Series No. 845. American Chemical Society, Washington, DC, pp. 16-31.
49. Smith, R. M., 2002: Extractions with superheated water. Journal of Chromatography A., 975 (1): 31-46. https://doi.org/10.1016/S0021-9673(02)01225-6
50. Singh, T.; Singh, A. P., 2012: A review on natural products as wood protectant. Wood Science and Technology, 46 (5): 851-870. http://dx.doi.org/10.1007/s00226-011-0448-5
51. Stefanović, M.; Ristić, M.; Popović, Z.; Matić, R.; Nikolić, B.; Vidaković, V.; Obratov-Petković, D.; Bojović, S., 2016: Chemical composition and interpopulation variability of essential oils of *Taxus baccata* L. from Serbia. Chemistry and Biodiversity, 13 (7): 943-953. https://10.1002/cbdv.201500326
52. Syazana, M. S. N.; Halim, A. S.; Gan, S. H.; Shamsuddin, S., 2011: Antiproliferative effect of methanolic extraction of tualang honey on human keloid fibroblasts. BMC Complementary and Alternative Medicine, 11 (1): 82. http://dx.doi.org/10.1186/1472-6882-11-82
53. Thitilertdecha, N.; Teerawutgulrag, A.; Rakariyatham, N., 2008: Antioxidant and antibacterial activities of *Nephelium lappaceum* L. extracts. LWT Food Science and Technolog, 41 (10): 2029-2035. https://doi.org/10.1016/j.lwt.2008.01.017
54. Thomas, P. A.; Polwart, A., 2003: Biological flora of the British Isles, no. 229. *Taxus baccata* L. Journal of Ecology, 91 (3): 489-524. https://doi.org/10.1046/j.1365-2745.2003.00783.x
55. Valko, M.; Leibfritz, D.; Moncol, J.; Cronin, M. T. D.; Mazur, M.; Telser, J., 2007: Free radicals and antioxidants in normal physiological functions and human disease. The International Journal of Biochemistry & Cell Biology, 39 (1): 44-84. https://doi.org/10.1016/j.biocel.2006.07.001
56. Verma, A.; Pandeya, S. N.; Sinha, S., 2011: Synthesis and biological activities of furan derivatives. International Journal of Research in Ayurveda and Pharmacy, 2 (4): 1110-1116.
57. Vibala, B. V.; Praseetha, P. K.; Vijayakumar, S., 2020: Evaluating new strategies for anticancer molecules from ethnic medicinal plants through in silico and biological approach-A review. Gene Reports, 18: 100553. https://doi.org/10.1016/j.genrep.2019.100553
58. Wei, Q.; Yin, C. W., 2019: Chemical composition of essential oils from the stems of *Taxus chinensis* var. Mairei. Journal of Essential Oil Bearing Plants, 22 (4): 1144-1149. https://10.1080/0972060X.2019.1668864
59. Wu, H.; Liu, R.; Deng, C., 2009: Properties and Fourier transform infrared spectrum analysis on bio-oil from fast pyrolysis of poplar sawdust. Transactions of the Chinese Society of Agricultural Engineering, 25 (6): 219-223. https://doi.org/10.3969/j.issn.1002-6819.2009.06.041
60. Yasar, S., 2013: Volatile constituents of *Taxus baccata* L. leaves from western and southern Turkey. Asian Journal of Chemistry, 25 (16): 9123-9125. https://10.14233/ajchem.2013.15038
61. Yu, X.; Tu, X.; Tao, L.; Daddam, J.; Li, S.; Hu, F., 2023: Royal jelly fatty acids: Chemical composition, extraction, biological activity and prospect. Journal of Functional Foods, 111: 105868. https://doi.org/10.1016/j.jff.2023.105868
62. Zhao, C. J.; Xin, H.; Li, C. Y.; Lei, Y.; Yujie, F.; Kaiting, W.; Yukun, Z.; Yujiao, N., 2016: A microwave-assisted simultaneous distillation and extraction method for the separation of polysaccharides and essential oil from the leaves of *Taxus chinensis* var. Mairei. Applied Sciences, 6 (2): 1-19. https://10.3390/app6020019
63. Zhou, R.; Cao, R.; Liu, Y.; Ma, D.; Yao, Q.; Wang, J.; Sun, M.; Ma, X., 2022: Study on the characteristics and mechanism of fast co-pyrolysis of coal tar asphaltene and biomass. Journal of Analytical and Applied Pyrolysis, 161: 105409. https://doi.org/10.1016/j.jaap.2021.105409

Corresponding addresses:

Assoc. Prof. HADI BASERI
School of Chemistry, Damghan University, Damghan, IRAN, e-mail: baseri@du.ac.ir

Assoc. Prof. SEYYED KHALIL HOSSEINIHASHEMI
Department of Wood Science and Paper Technology, Karaj Branch, Islamic Azad University, Karaj, IRAN, e-mail: sk.hashemi@iau.ac.ir

Marin Dujmović[1], Branimir Šafran[1*], Matija Jug[1], Kristijan Radmanović[1]

Thermal Pre-treatments of Woody Biomass: A High-Level Overview

Toplinski predtretmani drvne biomase: opći pregled

REVIEW PAPER
Pregledni rad
Received – prispjelo: 19. 4. 2024.
Accepted – prihvaćeno: 24. 4. 2025.
UDK: 674.8
https://doi.org/10.5552/drvind.2025.0212

ABSTRACT • *The global demand to reduce CO_2 emissions has led large industrial pollutants, particularly power generation and metallurgical sectors, to search for alternatives to traditional fossil fuels like coal. Wood pellets have emerged as a recognized cleaner alternative. Yet, pellets fall short of coal key properties, notably in calorific value and storage stability. By subjecting the feedstock for wood pellet production, namely woody biomass, to thermal pre-treatments like torrefaction or steam explosion, these limitations can be mitigated. These treatments reduce moisture content, increase energy density, and enhance storage stability, making the wood pellets produced from thermally treated feedstock more similar to coal and compatible with existing coal infrastructure. While these pre-treatments offer potential energy savings and other benefits along the process of pellet production and supply chain, they might also necessitate significant capital investments. This review provides a concise overview of thermal pre-treatment technologies, necessary parameters, their impact on treated woody biomass, as well as final characteristics of treated woody biomass.*

KEYWORDS: *torrefaction; steam explosion; biofuel; industrial application; renewable energy*

SAŽETAK • *Globalna težnja za smanjenjem emisije CO_2 potaknula je velike industrijske onečišćivače, posebice iz sektora proizvodnje energije i metalurgije, da potraže alternative tradicionalnim fosilnim gorivima poput ugljena. Drvni pelet nameće se kao prepoznata čišća alternativa. Ipak, svojstva peleta zaostaju za ključnim svojstvima ugljena, posebice po kalorijskoj vrijednosti i stabilnosti pri skladištenju. Podvrgavanjem sirovine za proizvodnju drvnog peleta, prije svega drvne biomase, toplinskim predtretmanima poput torefakcije ili parne eksplozije, ti se nedostatci mogu smanjiti. Toplinskim predtretmanima smanjuje se sadržaj vode, povećava energetska gustoća te poboljšava stabilnost tijekom skladištenja, što drvni pelet proizveden od toplinski predtretirane sirovine čini sličnijim ugljenu i kompatibilnijim s postojećom infrastrukturom za upotrebu ugljena. Iako spomenuti predtretmani nude potencijalne energetske uštede i neke prednosti u procesu proizvodnje peleta i lanca opskrbe, oni ujedno zahtijevaju i znatna kapitalna ulaganja. Ovaj pregledni rad donosi sažeti pregled tehnologija toplinskih predtretmana, potrebnih parametara, njihova utjecaja na obrađivanu drvnu biomasu, kao i konačnih svojstava obrađene drvne biomase.*

KLJUČNE RIJEČI: *torefakcija; parna eksplozija; biogorivo; industrijska primjena; obnovljiva energija*

* Corresponding author
[1] Authors are researchers at University of Zagreb, Faculty of Forestry and Wood Technology, Department of Wood Technology, Institute of Processes Engineering, Zagreb, Croatia. https://orcid.org/0009-0004-9349-443X, https://orcid.org/0009-0009-5180-4272, https://orcid.org/0009-0009-2131-7094, https://orcid.org/0009-0001-4145-3968

1 INTRODUCTION
1. UVOD

Global demand to reduce CO_2 footprint and harmful emissions into the atmosphere has most recently become an imperative. This situation has led us to search for alternative fuel solutions for heat and energy generation, which will provide similar utilization properties (storage, transportation, handling, and energy outputs) as fossil fuels, while releasing less harmful gasses into the atmosphere and being economically feasible. Solid biomass has imposed itself as one of the main alternative options for these applications. Solid biomass is considered as residuals from the forestry and wood industry operations, as well as agricultural and municipal wastes (Malico *et al*., 2019). Currently, the most commonly used type of solid biomass is woody biomass, in the form of residuals from the wood processing industry, namely, sawdust, shavings, and wood chips (García *et al*., 2019; Nielsen *et al*., 2009). Other types of woody biomass, such as harvest residues and pulpwood can also be used. However, woody biomass in its original form has certain limitations as fuel when compared to fossil fuels. Specifically, biomass high moisture content and low bulk density make it less efficient when being handled and combusted (García *et al*., 2019). For these reasons, woody biomass is compressed/pelletized into wood pellets, in order to improve its energy density and handling characteristics, which consequently improve biomass performance along the supply chain (Dujmović *et al*., 2022; Abelha and Cieplik, 2021).

As a result of various policies and incentives to reduce harmful emissions, as well as to tackle increased prices of mainstream energy sources such as gas and power, wood pellets have been widely used by both residential and industry sectors (Eurostat, 2017) in Europe for the last couple of decades.

Most recently, even more intense global push to reduce emissions of harmful gasses has been implemented in the countries worldwide in the form of various laws and policies that primarily target larger industrial pollutants, such as power plants, iron and steel producers, and other heavy industries that still mainly rely on coal as their fuel. Consequently, the need for cleaner fuel solutions has further increased, mainly driven by these heavy industries complying with the newest demands for the reduction of emissions. Heavy industries were required to partially supplement or even completely replace their current fossil fuel needs with some form of cleaner alternative, such as wood pellets (McKechnie *et al*., 2016).

However, despite these benefits, wood pellets still fall short of coal properties. Heavy industry users specifically seek even higher energy density and superior mechanical properties to achieve greater similarity in transportation, storage, and combustion characteristics between wood pellets and coal.

Therefore, woody biomass requires additional treatment, in order to turn it into more desirable feedstock for the production of wood pellets, which could then replace fossil fuels in industrial applications such as steel and iron industries. These additional pre-treatments are typically of a thermal nature, where biomass is treated under various controlled conditions and raised temperature, all in order to upgrade biomass characteristics to make it more susceptible for further processing and utilization by the industry (Abelha and Cieplik, 2021; Cahyanti *et al.*, 2020).

This high-level overview intends to summarize and condense process technologies and necessary parameters of thermal pre-treatments of woody biomass. It also provides their chemical and physical impact on treated woody biomass, as well as final characteristics of the treated biomass, which is typically intended to be further pelletized and used as a biofuel by industrial users.

2 TYPES OF THERMAL TREATMENTS
2. VRSTE TOPLINSKIH POSTUPAKA

Thermal pre-treatments change chemical and physical characteristic of treated raw woody biomass. Changed physical properties and chemical composition of the processed feedstock has a positive impact on the whole biofuel supply chain, from production to final energy utilization (Christoforou and Fokaides, 2018; Christoforou and Fokaides, 2016). In particular, thermal treatments of feedstock prior or after pelletization, can decrease its moisture content while increasing its calorific value, improve chipping/milling and bonding/pelletization properties, as well as increase its final bulk density, hydrophobicity (Abelha and Cieplik, 2021), and even grindability, which becomes an important parameter if treated biofuels, as substitutes for coal, are to be pulverized prior to co-firing (Chen *et al*., 2015). Currently, torrefaction and steam explosion are among the most known thermal pre-treatments of woody biomass.

Torrefaction involves heating the feedstock at moderate temperatures, typically between 200 °C and 300 °C, to enhance its energy density and other fuel properties. In contrast, steam explosion employs high-temperature, high-pressure steam followed by rapid depressurization to disrupt the cell structure of the treated feedstock, thereby improving its suitability for subsequent processing and use as a fuel.

In addition to torrefaction and steam explosion, pyrolysis is another significant thermal treatment that should be acknowledged. Pyrolysis occurs at higher

temperatures (>300 °C) than the two above-mentioned treatments, in the absence of oxygen. This treatment leads to the decomposition of the feedstock, producing biochar, bio-oil, and syngas, all of which can be further utilized as biofuels for energy generation (Mohan *et al*., 2006).

Even though pyrolysis is an effective thermal treatment for enhancing the properties of woody biomass, this review will specifically concentrate on torrefaction and steam explosion, for which high-level overviews are provided in the following sections.

3 TORREFACTION
3. TOREFAKCIJA

3.1 Torrefaction technologies and parameters
3.1. Torefakcijske tehnologije i parametri

Torrefaction is a thermo-chemical biomass treatment, also considered as mild pyrolysis (Christoforou and Fokaides, 2018), as it is done inside an inert atmosphere under similar conditions to those of pyrolysis. It is carried out in the controlled non-oxygen environment, which is typically attained through flowing nitrogen gas inside the stainless steel-reactor (Kizuka *et al*., 2019).

Christoforou and Fokaides (2018) have summarized the existing torrefaction technologies, based on Cremers *et al*. (2015) study. They have listed the following types of reactors: rotary drum, screw conveyor, multiple heat furnace (MHF) or Herreshoff oven, fluidized bed reactor (torbed reactor), moving bed reactor, and microwave reactor. Each of the above reactors has their specific features, such as size and capacity, sensitivity to feedstock quality, maximum allowed temperature, energy consumption, and overall efficacy, all providing options for different torrefaction applications.

Torrefaction is considered mild pyrolysis as it takes place at temperatures between 190 °C and 320 °C (Tran *et al*., 2013; Cahyanti *et al*., 2020; Rousset *et al*., 2013; Föhr and Ranta, 2017; Kizuka *et al*., 2019), as opposed to regular pyrolysis, which takes place at higher temperatures, between 350 °C and 650 °C (Chen *et al*., 2015; Tran *et al*., 2013). Apart from the temperature, residence/duration time plays an important role in the torrefaction process. As reported by a number of studies (Shang *et al*., 2014; Föhr and Ranta, 2017; Kizuka *et al*., 2019), the typical duration of the torrefaction process is between a couple of minutes to up to two to three hours.

The level of torrefaction severity depends on two above-mentioned main parameters of the process: residence time and process temperature. Therefore, depending on the combination of these two said parameters, torrefaction can be classified into light, medium, and severe levels. However, within the typical range of torrefaction parameters (1-2 h, 200-300 °C), temperature has a prevailing influence on the properties of treated biomass (Chen *et al*., 2015), making it the crucial parameter that determines the level of severity. With that said, each temperature range of the process has a certain impact on the components of the treated woody biomass. Generally, lower process temperatures have lower impact on the material, while increased temperatures result in higher levels of degradation and weight loss.

3.2 Torrefaction process and its impact on treated woody biomass
3.2. Proces torefakcije i utjecaj na tretiranu drvnu biomasu

Woody biomass is mainly comprised of hemicellulose, cellulose, and lignin (Chen *et al*., 2018). The severity of the biomass torrefaction is then characterized by the level of degradation of these three components during the process. Specifically, the direct quantifier of the level of torrefaction is the weight loss of the treated biomass. The weight loss is mainly caused by decomposition of hemicellulose and cellulose during the process. Lignin, on the other hand, is the most difficult component to be thermally degraded, hence torrefaction impact on it is very low (Chen *et al*., 2015). Furthermore, the weight loss is also coming from the reduction of the moisture content of the treated biomass during the process, as well as due to the partial loss of the volatile matter (Kizuka *et al*., 2019; Acharya *et al*., 2015).

To summarize, Christoforou and Fokaides (2018) have provided five main stages of the torrefaction process, as described by Bergman (2015). The initial stage was described as the heating of the treated biomass, where the increase in feedstock temperature is observed. This stage is followed by the pre-drying stage, at around 100 °C, in which free water is evaporated from the biomass. Further increase of the temperature to up to 200 °C continues to increase feedstock temperature, starting to release some of the bound water. This is followed by the fourth stage, where the temperature rises above 200 °C, and the torrefaction itself begins. In this stage, treated feedstock is depolymerized, partially devolatilized, and carbonized (Christoforou and Fokaides, 2016). And finally, after the intense torrefaction stage, now torrefied feedstock is cooled down to desired temperature.

The impact of each temperature range classified into the level of torrefaction severity can be found in Table 1, derived from Chen *et al*. (2015), and Chen and Kuo (2011) studies.

Torrefied biomass, depending on the process severity, typically becomes darker in color, when compared to the initial biomass before treatment. As per Chen *at al*. (2015), light torrefaction results in brown

Table 1 Impact of toreffaction on main components of woody biomass
Tablica 1. Utjecaj torefakcije na glavne komponente drvne biomase

Severity level *Intenzitet*		**Light** *lagani*	**Medium** *srednji*	**Severe** *jaki*
Temperature, °C / *Temperatura,* °C		200-235	235-275	275-300
Impact on component *Utjecaj na komponentu*	Hemicellulose *hemiceluloza*	medium / *srednji*	medium to severe *srednji do jaki*	severe / *jaki*
	Cellulose / *celuloza*	slight / *blagi*	medium to severe *srednji do jaki*	medium to severe *srednji do jaki*
	Lignin / *lignin*	slight / *blagi*	slight / *blagi*	slight / *blagi*

Table 2 Impact of toreffaction on main chemical parameters of woody biomass
Tablica 2. Utjecaj torefakcije na glavne kemijske parametre drvne biomase

Torrefaction temperature, °C *Temperatura torefakcije,* °C	**Moisture content, %** *Sadržaj vode,* %	**Ash content, %** *Sadržaj pepela,* %	**Volatile matter, %** *Hlapljive tvari,* %	**Carbon content, %** *Sadržaj ugljika,* %	**Gross calorific value, MJ/kg** *Bruto kalorijska vrijednost,* MJ/kg
increase *povećava se*	decrease *smanjuje se*	increase *povećava se*	decrease *smanjuje se*	increase *povećava se*	increase *povećava se*

color, medium in darker brown, while severe torrefaction results in almost black color. Also, moisture content of the treated material is reduced approximately in half during the torrefaction process. For example, Shang *et al*. (2014) have torrefied wood chip samples and reduced their moisture content from initial 10 % down to final 5 %. Phanphanich and Mani (2011) have done a similar study, where they torrefied pine chip and logging residue samples, and tested them for numerous chemical properties. In summary, moisture content of the treated samples reduced from initial 6.69-7.94 %, down to between 3.30 and 1.57 %. Reduction in moisture content was directly correlated with the severity of the treatment, where higher temperatures resulted in lower moisture content. Ash content, on the other hand, increased with higher temperatures, from initial 0.27 % to up to 0.43 % for pine chips, and from 1.77 % to up to 6.52 % for logging residue samples. Furthermore, volatile matter was reduced approximately in half, while carbon content followed an upward trend with the severity of the treatment, from initial 47 % to up to > 60 %. Finally, reported gross calorific value has substantially increased with the torrefaction treatment, from around 18 MJ/kg to more than 25 MJ/kg. A very similar pattern in the results was reported by Park *et al*. (2012) as well, where torrefaction resulted in reduced moisture content and volatile matter, and increased ash content, carbon content, and gross calorific value. In both studies, the increase in the level of severity resulted in more distinct increases/decreases in the above-mentioned chemical parameters. Table 2 offers a simplified visual representation, derived from the research of Phanphanic and Mani (2011) and Park *et al*. (2012), showcasing the impact of torrefaction treatment on the fundamental chemical characteristics of woody biomass.

Even though torrefaction is considered a chemical treatment, it also changes some of the physical properties of the treated material. Impact on particle and bulk density of the treated woody biomass can also vary depending on the treatment temperature, with temperatures to up to 250 °C reducing the densities of the treated material, while further increase of the temperatures (300 °C) increases the densities of treated wood chips (Phanphanic and Mani, 2011). Torrefaction also has an effect on the grindability of treated materials. Grindability, quantified as a total energy (kWh/ton) required to grind the material, has been reported to improve after torrefaction treatment (Wang *et al*., 2017). This means that the total energy needed to grind torrefied woody biomass is lower than that of raw woody biomass, which directly translates into significant cost savings associated with size reduction of biomass intended to be utilized as a fuel. Again, higher torrefaction temperatures result in higher grindability, and consequently lower energy consumption needed for the size reduction of treated materials.

4 STEAM EXPLOSION
4. PARNA EKSPLOZIJA

4.1 Steam explosion technologies and parameters
4.1. Tehnologije i parametri parne eksplozije

Steam explosion, as a thermal pre-treatment that has both chemical and mechanical impact on treated woody biomass, was first described and patented by Mason in 1926. After a long period of stagnation of this technology, scientists and the wood industry have started to further explore capabilities and opportunities of steam explosion only 20 to 30 years ago. Since then, numerous studies have been done on this specific topic.

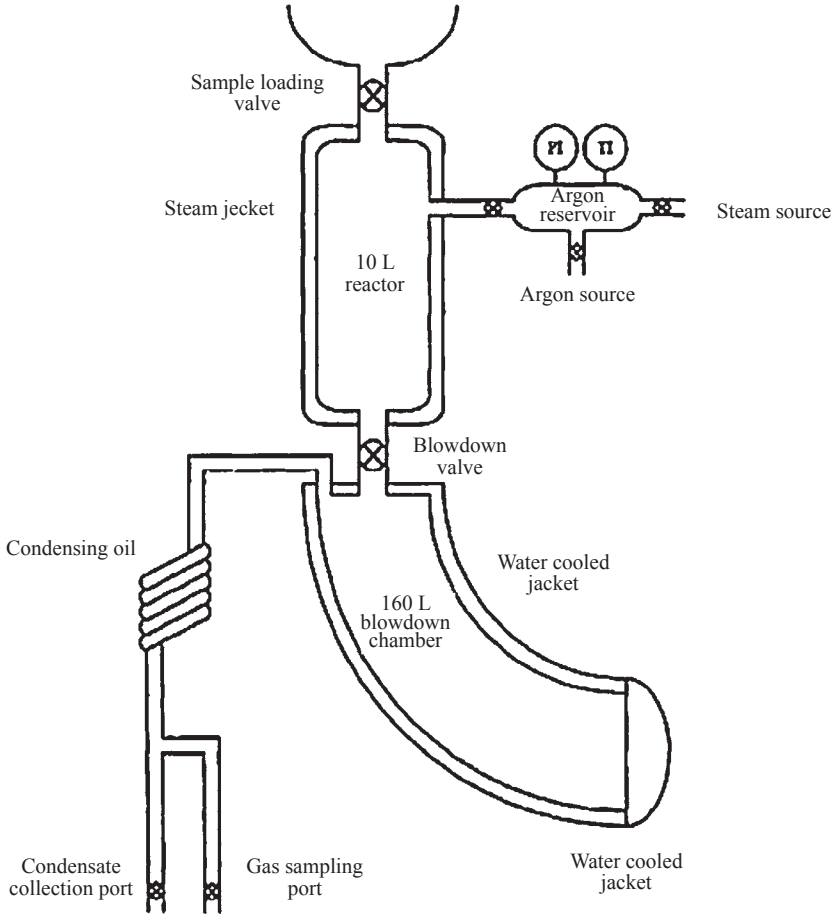

Figure 1 Steam explosion equipment line up (Turn *et al*., 1998)
Slika 1. Oprema za parnu eksploziju (Turn *et al*., 1998.)

As described by Mason (1926), Stelte (2013), and Turn *et al*. (1998), steam explosion of biomass has to be carried out in a steam explosion reactor that can provide controlled conditions for a successful treatment process. It usually consists of a steam generator, high pressure reactor/tank, discharge tank, and accompanying set of valves and piping (Figure 1).

Woody biomass, chipped into smaller pieces, is placed into a high-pressure chamber (reactor), which is sized on mass of treated material per the volume of the reactor basis (1 kg/10 L) (Stelte, 2013; Turn *et al*., 1998). Then, hot steam is forced into the reactor, until the target pressure and temperature are reached. After the certain retention time at a set pressure and temperature, biomass is released through a valve at the bottom of the reactor. According to the literature (Yu *et al*. 2012), the size and the opening speed of the release valve are crucial for a successful process, as the explosion happens at the moment when the valve is opened and when the biomass, forced by the pressure from inside the reactor, is pushed through the valve into the atmospheric conditions. Treated biomass is typically released into a discharge chamber, that according to the literature (Turn *et al*., 1998), needs to be 16 times larger in volume than the reactor itself, in order to capture both exploded material and released pressure.

Three crucial parameters for steam explosion process are temperature, pressure, and residence time. Numerous studies have provided different combinations of these three parameters that must be achieved inside a reactor in order to obtain steam explosion of treated biomass.

Steam explosion process can be done at a wide range of temperatures, ranging between 140 ºC and 280 ºC (Ziegler-Devin *et al*., 2021; Iroba *et al*., 2014; Jacquet *et al*., 2015). However, it seems that several studies that have done steam explosion on woody biomass opt for a narrower temperature range, from 180 ºC to 230 ºC (Tooyserkani *et al*., 2013; Jacquet *et al*., 2015). When compared to higher temperatures, the ~200 ºC process has proved to be more cost effective from the perspective of energy consumption, while yielding optimized quality of the treated material.

Furthermore, a relatively wide range of optimal pressures for achieving successful steam explosion was reported. Reported pressures range from 15 bar inside the reactor to up to 35 bar, while most studies have found the most optimal pressures to be in the range of 16 bar to 24 bar (Asada *et al*., 2012; Yu *et al*., 2012; Lam *et al*., 2013).

And finally, a duration/residence time that the treated material has to spend under the above-men-

tioned pressure and temperature has also been investigated by numerous studies, including the ones mentioned above as well as some additional ones, such as Jedvert *et al*. (2012), Stelte (2013), and Shimizu *et al*. (1998). As is the case with temperature and pressure, provided ranges of residence times are relatively wide, from 1 to up to 35 minutes. However, most steam explosion treatments last from 5 to 20 minutes.

Typically, the upper ends of the reported ranges of all of the parameters can be associated with experimenting with extreme levels of steam explosion, which often requires more energy consumption, thus being less economically viable for wider industrial applications.

4.2 Steam explosion process and its impact on treated woody biomass
4.2. Proces parne eksplozije i utjecaj na tretiranu drvnu biomasu

As per Ziegler-Devin *et al.* (2021), steam explosion treatment of woody biomass consists of two distinctive stages – chemical and mechanical. The initial stage involves conditions of elevated temperature and pressure caused by injecting hot steam into the reactor. This results in hydrolytic destabilization and breakdown of the lignocellulosic structure of the treated woody biomass and can be considered as a chemical stage. This stage, also known as cooking stage, generally leads to degradation of the cell wall, making treated biomass more susceptible to further treatment.

The chemical stage is then followed by a second stage with physical disruptions of the treated biomass particles and can be considered as a mechanical stage. The second stage occurs at the moment when the treated biomass is released from high temperature and high pressure conditions inside the reactor into the atmospheric conditions. At his moment of explosion, water vapor trapped inside the biomass structure is rapidly expanded, causing ruptures in the once rigid structure of the woody biomass particles.

To summarize, all main components of wood are impacted by the steam explosion. Hemicellulose and cellulose are deconstructed and thermally degraded (Stelte, 2013), while usually stable lignin is modified and relocated within the cells (Auxenfans *et al*., 2017) (Figure 2).

The severity of the steam explosion process, and its impact on the treated biomass, depends on the main parameters of the process: temperature, pressure, retention time, and decompression speed. Generally, the higher the temperature and pressure, coupled with longer retention times and faster decompression, the more severe the impact on the biomass and its structure.

The initial and most noticeable alteration in the characteristics of steam exploded woody biomass, compared to untreated biomass, occurs with the relocation of lignin, a naturally dark substance. This relocation results in a darker brown color of the treated biomass. Another physical change happens to particle size distribution, where studies have shown that the size reduction of the steam treated material is by around 25 % (Tooyserkani *et al*., 2013; Boussaid *et al*., 2000), which is due to rapid breakdown of the material into finer particles at the moment of explosion/decompression. Reduction in particle size is followed by the substantial increase in bulk density. It was reported that the bulk density increased from around 600 kg/m^3 for untreated material, to up to > 700 kg/m^3 for material after steam explosion, which consequently increased the energy density as well (Joronen *et al*., 2017). Ash content in steam exploded biomass is increased when compared to initial biomass before treatment (Joronen *et al*., 2017). Furthermore, increase in calorific value is directly related to a decrease in moisture content, as well as to thermal degradation of hemicellulose and an increase in carbon content (Stelte, 2013). Steam exploded biomass becomes more hydrophobic and generally more resistant to external influences. This is also due to the restructuring of the main woody biomass components, including lignin, which in this case acts as a repellent against water. Finally, as is the case with torrefaction, the grindability of steam exploded material improves (Stelte, 2013), and less energy is required to grind the steam exploded woody biomass, when compared to untreated raw biomass.

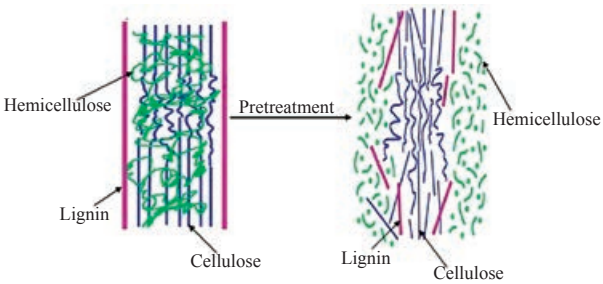

Figure 2 Impact of steam explosion on woody biomass structure (Wang *et al*., 2015; Harmsen *et al*., 2010)
Slika 2. Utjecaj parne eksplozije na strukturu drvne biomase (Wang *et al*., 2015.; Harmsen *et al*., 2010.)

5 COMPARISON OF QUALITY PROPERTIES OF WOOD PELLETS AND COAL
5. USPOREDBA KVALITATIVNIH SVOJSTAVA DRVNOG PELETA I UGLJENA

Here, an indicative and brief overview is provided of approximately typical final quality properties of different types of wood pellets, compared to those of coal (Table 3) based on papers of Kamperidou (2022), Gorzelany *et al.* (2020), Tumuluru *et al.* (2011), Joronen *et al.* (2017), Wolbers *et al.* (2018), Graham *et al.*

Table 3 Comparison of quality properties of different types of wood pellets and coal
Tablica 3. Usporedba kvalitativnih svojstava različitih vrsta drvnog peleta i ugljena

Quality property *Kvalitativno svojstvo*	**Wood pellet type** / *Vrsta drvnog peleta*				**Coal** *Ugljen*
	Conventional *Konvencionalni*	**Torrefied** *Torefakcionirani*	**Steam exploded** *Tretiran parnom eksplozijom*	**Pyrolyzed** *Pirolizirani*	
Moisture content, % *sadržaj vode, %*	5.0 – 10.0	1.0 – 5.0	8.0 – 10.0	4.8 – 5.5	10.0 – 15.0
Calorific value, MJ/kg *kalorijska vrijednost,* MJ/kg	17.0 – 19.0	20.0 – 24.0	19.0 – 21.0	21.0 – 30.0	23.0 – 28.0
Mechanical durability, % *mehanička izdržljivost, %*	96.0 – 99.4	50. 0 – 65.0	>92.0	45.0 – 57.0	Not applicable as testing methods for coal differ from methods for wood pellets. *Nije primjenjivo jer se metode ispitivanja ugljena razlikuju od metoda za drvene pelete.*
Ash content, % *sadržaj pepela, %*	0.3 – 1.9	Substantially increased compared to conventional. *Znatno povećan u usporedbi s konvencionalnim peletom.*	0.5 – 3.0	1.5 – 7.0	<8.0 – >16.0
Bulk density, kg/m^3 *nasipna gustoća,* kg/m^3	600 – 650	750 – 850	650 – 780	Increased compared to conventional. *Povećana u usporedbi s konvencionalnim peletom.*	800 – 850

(2017), Dyjakon *et al.* (2021), Phanphanich and Mani (2011), Park *et al.* (2012), Hashan *et al.* (2013), Saletnik *et al.* (2022) and Arous et al. (2021). Even though not covered in this high-level overview in detail, some data are also provided on pyrolyzed wood pellets for informative purposes.

6 CONCLUSIONS
6. ZAKLJUČAK

Thermal pre-treatments of woody biomass feedstock, through torrefaction or steam explosion, present substantial advantages for the production of industrial-grade wood pellets to be used as coal replacement in various industrial applications. Both pre-treatments result in feedstock with lower moisture content, higher calorific value and increased energy density, aligning more closely with coal properties. While torrefaction focuses more on enhancing calorific value of the treated feedstock, steam explosion provides feedstock resistant to environmental factors, making pellets produced from steam exploded feedstock more suitable for utilization at coal power plants and the like, due to its coal-like storage and handling properties. Apart from obvious improvements of quality properties of the treated feedstock, these thermal pre-treatments potentially offer energy savings and other benefits along the wood pellet supply chain. Higher energy density of pellets results in certain energy savings and reduced costs in the transportation of treated wood pellets (Wolber *et al.*, 2018). Furthermore, the grindability/pulverization properties of torrefied and steam exploded pellets, as opposed to untreated pellets, have shown to be substantially improved (Wang *et al.*, 2020; Wolber *et al.*, 2018). For example, the studies have shown that up to 50 % less energy is needed for grinding/pulverizing torrefied pellets, relative to untreated pellets (Wang *et al.*, 2020). Energy savings, as well as capital cost of installation of steam explosion and torrefaction equipment need to be further explored.

5 REFERENCES
5. LITERATURA

1. Abelha, P.; Cieplik, M. K., 2021: Evaluation of steam-exploded wood pellets storage and handling safety in a coal-designed power plant. Energy & Fuels, 35: 2357-2367. https://dx.doi.org/10.1021/acs.energyfuels.0c04246

2. Acharyia, B.; Dutta, A.; Minaret, J., 2015: Review on comparative study of dry and wet torrefaction. Sustainable Energy Technologies and Assessments, 12: 26-37. https://doi.org/10.1016/j.seta.2015.08.003
3. Arous, S.; Koubaa, A.; Bouafif, H.; Bouslimi, B.; Braghiroli, F. L.; Bradai, C., 2021: Effect of pyrolysis temperature and wood species on the properties of biochar pellets. Energies, 14: 6529. https://doi.org/10.3390/en14206529
4. Asada, C.; Sasaki, C.; Uto, Y.; Sakafuji, J.; Nakamura, Y., 2012: Effect of steam explosion pretreatment with ultra-high temperature and pressure on effective utilization of softwood biomass. Biochemical Engineering Journal, 60: 25-29. https://doi.org/ 10.1016/j.bej.2011.09.013
5. Auxenfans, T.; Crônier, D.; Chabbert, B.; Paës, G., 2017: Understanding the structural and chemical changes of plant biomass following steam explosion pretreatment. Biotechnol Biofuels, 10: 36. https://doi.org/10.1186/s13068-017-0718-z
6. Bergman, P. C. A., 2005: Combined torrefaction and pelletisation. The TOP process. Technical Report ECN-C-05-073, Netherlands, 2005. https://scholar.google.hr/scholar?q=bergmann+pca+combined+torrefaction+and+pelletisation&hl=en&as_sdt=0&as_vis=1&oi=scholart (Accessed Mar. 1, 2024).
7. Boussaid, A. L.; Esteghlalian, R.; Gregg, J.; Lee, K. H.; Saddler, J. N., 2000: Steam pretreatment of Douglas fir wood chips. Applied Biochemistry and Biotechnology, 84-86 (1-9): 693-705. https://doi.org/10.1385/abab:84-86:1-9:693
8. Cahyanti, M. N.; Doddapanenin, T. R. K. C.; Kikas, T., 2020: Biomass torrefaction: An overview on process parameters, economic and environmental aspects and recent advancements. Bioresource Technology, 301: 122737. https://doi.org/10.1016/j.biortech.2020.122737
9. Chaula, Z.; Said, M.; Jogn, G.; Manyele, S.; Mhilu, C., 2014: Modelling the suitability of pine sawdust for energy production via biomass steam explosion. Smart Grid and Reneable Energy, 5 (1): 7. https://doi.org/10.4236/sgre.2014.51001
10. Chen, D.; Gao, A.; Cen, K.; Zhang, J.; Cao, X.; Ma, Z., 2018: Investigation of biomass torrefaction based on three major components: hemicellulose, cellulose and lignin. Energy Conversion and Management, 169: 228-237. https://doi.org/10.1016/j.enconman.2018.05.063
11. Chen, W. H.; Kuo, P. C., 2011: Torrefaction and co-torrefaction characterization of hemicellulose, cellulose, lignin as well as torrefaction of some basic constituents in biomass. Energy, 36 (2): 803-811. https://doi.org/10.1016/j.energy.2010.12.036
12. Chen, W. H.; Peng, J.; Bi, X. T., 2015: A stet-of-the-art review of biomass torrefaction, densification and applications. Renewable and Sustainable Energy Reviews, 44: 847-866. http://dx.doi.org/10.1016/j.rser.2014.12.039
13. Christoforou, E. A.; Fokaides, P. A., 2016: Life cycle assessment (LCA) of olive husk torrefaction. Renew Energy, 90: 257-266. https://doi.org/10.1016/j.renene.2016.01.022
14. Christoforou, E. A.; Fokaides, P. A., 2018: Recent advancements in torrefaction of solid biomass. Current Sustainable/Renewable Energy Reports, 5: 163-171. https://doi.org/10.1007/s40518-018-0110-z
15. Cremers, M.; Koppejan, J.; Middelkamp, J.; Witkamp, J.; Sokhansanj, S.; Melin, S., 2015: Status overview of torrefaction technologies – a review of the commercialisation status of biomass torrefaction. IEA Bioenergy, https://www.ieabioenergy.com/wp content/uploads/2015/11/IEA_Bioenergy_T32_Torrefaction_update_2015b.pdf (Accessed Feb. 23, 2024).
16. Dujmović, M.; Šafran, B.; Jug, M.; Radmanović, K.; Antonović, A., 2022: Biomass pelletizing process: A review. Drvna industrija, 73 (1): 99-106. https://doi.org/10.5552/drvind.2022.2139
17. Dyjakon, A.; Noszcyk, T.; Mostek, A., 2021: Mechanical durability and grindability of pellets after torrefaction process. Energies, 14: 6772. https://doi.org/10.3390/en14206772
18. Föhr, J.; Ranta, T., 2017: Manufacturing of torrefied pellets without a binder from different rwa wood materials in the pilot plant. Wood Research, 62 (3): 481-494.
19. García, R.; Gil, M. V.; Rubiera, F.; Pevida, C., 2019: Pelletization of wood and alternative residual biomass blends for producing industrial quality pellets. Fuel, 251: 739-753. https://doi.org/10.1016/j.fuel.2019.03.141
20. Gorzelany, J.; Zardzewiały, M.; Murawski, P.; Matłok, N., 2020: Analysis of selected quality features of wood pellets. Agricultural Engineering, 24: 25-34. https://doi.org/10.1515/agriceng-2020-0003
21. Graham, S.; Eastwick, C.; Snape, C.; Quick, W., 2017: Mechanical degradation of biomass wood pellets during long term stockpile storage. Fuel Processing Technology, 160: 143-151. https://doi.org/10.1016/j.fuproc.2017.02.017
22. Harmsen, P.; Huijgen, W.; Bermudez, R.; Bakker, R., 2010: Literature review of physical and chemical pretreatment processes for lignocellulosic biomass. Energy Research Center of the Netherlands, 2010.
23. Hashan, M.; Howladar, M. F.; Nusrat, L.; Deb, P. K., 2013: Ash content and its relevance with the coal grade and environment in bangladesh. International Journal of Scientific & Engineering Research, 4 (4): 669-676.
24. Iroba, K. L.; Tabil, L. G.; Sokhansanj, S.; Meda, V., 2014: Producing durable pellets from barley straw subjected to radio-frequency-alkaline and steam explosion pretreatments. International Journal of Agricultural and Biological Engineering, 7 (3): 68-82. https://doi.org/10.3965/j.ijabe.20140703.009
25. Jacquet, N.; Maniet, G.; Vanderghem, C.; Delvigne, F.; Richel, A., 2015: Application of steam explosion as pretreatment on lignocellulosic material: A review. Industrial & Engineering Chemistry Research, 54: 2593-2598. https://doi.org/10.1021/ie503151g1
26. Jedvert, K.; Saltberg, A.; Lindström, M. E.; Theliander, H., 2012: Mild steam explosion and chemical pre-treatment of Norway spruce. BioResources, 7 (2): 2051-2074. https://doi.org/10.15376/biores.7.2.2051-2074
27. Joronen, T.; Björklund, P.; Bohlàr-Nordenkampf, M., 2017: High quality fuel by steam explosion. In: Proceeding of the European Biomass Conference, 14-18th May.
28. Kamperidou, V., 2022: Quality analysis of commercially available wood pellets and correlations between pellets characteristics. Energies, 15: 2865. https://doi.org/10.3390/en15082865
29. Kizuka, R.; Ishii, K.; Sato, M.; Fujiyama, A., 2019: Characteristics of wood pellets mixed with torrefied rice straw as biomass fuel. International Journal of Energy and Environmental Engineering, 10: 357-365. https://doi.org/10.1007/s40095-019-0305-0
30. Lam, P. S.; Lam, P. Y.; Sokhansanj, S.; Bi, X. T.; Lim, C. J., 2013: Mechanical and compositional characteristics of steam-treated Douglas fir (*Pseudotsuga menziesii L.*) during pelletization. Biomass and Bioenergy, 56: 116-126. https://doi.org/10.1016/j.biombioe.2013.05.001
31. Malico, I.; Pereira, R. N.; Gonçalves, A. C.; Sousa, A. M. O., 2019: Current status and future perspectives for energy production from solid biomass in the European in-

dustry. Renewable and Sustainable Energy Reviews, 112: 960-977. https://doi.org/10.1016/j.rser.2019.06.022
32. Mason, W. H., 1926: Process and Apparatus for Disintegration of Wood and the Like. Unites States Patent Office. 1, 578, 609. Serial No. 739, 748.
33. McKechnie, J.; Saville, B.; MacLean, H. L., 2016: Steam-treated wood pellets: Environmental and financial implications relative to fossil fuels and conventional pellets for electricity generation. Applied Energy, 180: 637-649. https://dx.doi.org/10.1016/j.apenergy.2016.08.024
34. Mohan, D.; Pittman, C. U.; Steele, P. H., 2006: Pyrolysis of wood/biomass for bio-oil: A critical review. Energy & Fuels, 20: 848-889. https://doi.org/10.1021/ef0502397
35. Nielsen, N. P. K.; Gardner, D. J.; Poulsen, T.; Felby, C., 2009: Importance of temperature, moisture content and species for the conversion process of wood residues into fuel pellets. Wood and Fiber Science, 41: 414-425.
36. Park, S. W.; Jang, C. H.; Baek, K. R.; Yang, J. K., 2012: Torrefaction and low-temperature carbonization of woody biomass: Evaluation of fuel characteristics of the products. Energy, 45: 676-685. https://doi.org/10.1016/j.energy.2012.07.024
37. Phanphanich, M.; Mani, S., 2011: Impact of torrefaction on the grindability and fuel characteristics of forest biomass. Bioresource Technology, 102: 1246-1253. https://doi.org/10.1016/j.biortech.2010.08.028
38. Rousset, P.; Fernandes, K.; Vale, A.; Macedo, L.; Benoist, A., 2013: Change in particle size distribution of torrefied biomass during fluidization. Energy, 51: 71-77. https://doi.org/10.1016/j.energy.2013.01.030
39. Saletnik, B.; Saletnik, A.; Zaguła, G.; Bajcar, M.; Puchalski, C., 2022: The use of wood pellets in the production of high quality biocarbon materials. Materials, 15: 4404. https://doi.org/10.3390/ma15134404
40. Shang, L.; Nielsen, N. P. K.; Stelte, W.; Dahl, J.; Ahrenfeldt, J.; Holm, J. K.; Arnavat, M. P.; Bach, L. S.; Henriksen, U. B., 2014: Lab and bench-scale pelletization of torrefied wood chips – Process optimization and pellet quality. Bioenergy Resources, 7: 87-94. https://doi.org/10.1007/s12155-013-9354-z
41. Shimizu, K.; Sudo, K.; Ono, H.; Ishihara, M.; Fujii, T.; Hishyama, S., 1998: Integrated process for total utilization of wood components by steam-explosion pretreatment. Biomass and Bioenergy, 14: 195-203. https://doi.org/10.1016/S0961-9534(97)10044-7
42. Stelte, W., 2013: Steam explosion for biomass pre-treatment. Danish Technological Institute. Resultat Kontrakt (RP) Report. pp 15.
43. Tooyserkani, Z.; Sokhansanj, S.; Bi, X.; Lim, J.; Lau, A.; Saddler, J.; Kumar, L.; Lam, P. S.; Melin, S., 2013: Steam treatment of four softwood species and bark to produce torrefied wood. Applied Energy, 103: 514-521. https://doi.org/10.1016/j.apenergy.2012.10.016
44. Tran, K. Q.; Luo, X.; Seisenbaeva, G.; Jirjis, R., 2013: Stump torrefaction for bioenergy application. Applied Energy, 112: 539-546. https://doi.org/10.1016/j.apenergy.2012.12.053
45. Tumuluru, J. S.; Sokhansanj, S.; Hess, J. R.; Wright, C. T.; Boardman, R. D., 2011: A review on biomass torrefaction process and product properties for energy applications. Industrial Biotechnology, 7 (5): 384-402. https://doi.org/10.1089/.2011.0014
46. Turn, S. Q.; Kinoshita, C. M.; Kaar, W. E.; Ishiimura, D. M., 1998: Measurements of gas phase carbon in steam explosion biomass. Bioresource Technology, 64 (1): 71-75. https://doi.org/10.1016/S0960-8524(97)00144-2
47. Wang, K.; Chen, J.; Sun, S. N.; Sun, R. C., 2015: Steam Explosion. In: Pretreatment of Biomass, pp. 75-104. https://doi.org/10.1016/B978-0-12-800080-9.00006-2
48. Wang, L.; Barta-Rajnai, E.; Skreiberg, Ø.; Khalil, R.; Czégény, Z.; Jakab, E.; Barta, Z.; Grønli, M., 2017: Impact of torrefaction on woody biomass properties. Energy Procedia, 105: 1149-1154. https://doi.org/10.1016/j.egypro.2017.03.486
49. Wang, L.; Riva, L.; Skreiberg, Ø.; Khalil, R.; Bartocci, P.; Yang, Q.; Yang, H.; Wang, X.; Chen, D.; Rudolfsson, M.; Nielsen, H. K., 2020: Effect of torrefaction on properties of pellets produced from woody biomass. Energy Fuels, 34: 15343-15354. https://dx.doi.org/10.1021/acs.energyfuels.0c02671
50. Wolber, P.; Cremers, M.; Robinson, T.; Madrali, S.; Touringy, G., 2018: Biomass pre-treatment for bioenergy – Case study 4: The steam explosion process technology. IEA Bioenergy.
51. Yu, Z.; Zhang, B.; Yu, F.; Xu, G.; Song, A., 2012: A real explosion: The requirement of steam explosion pretreatment. Bioresource Technology, 121: 335-341. https://doi.org/10.1016/j.biortech.2012.06.055
52. Ziegler-Davin, I.; Chrusciel, L.; Brosse, N., 2021: Steam explosion pretreatment of lignocellulosic biomass: A mini-review of theoretical and experimental approaches. Frontiers in chemistry. Frontiers Media, 9: 705358. https://doi.org/10.3389/fchem.2021.705358
53. ***Eurostat. http://ec.europa.eu/eurostat/data/database; 2017.

Corresponding address:

BRANIMIR ŠAFRAN
University of Zagreb Faculty of Forestry and Wood Technology, Department of Wood Technology, Institute of Processes Engineering, Svetošimunska cesta 23, 10000 Zagreb, CROATIA, e-mail: bsafran@sumfak.unizg.hr

Drvo poljskog jasena *Fraxinus angustifolia* Vahl

OPĆENITO O VRSTI

Fraxinus angustifolia Vahl vrsta je drva iz porodice *Oleaceae*. Trgovački su nazivi te vrste Desert ash (Australija), Narrow-leaved ash (Velika Britanija), fresno, fresno de hoja estrecha, fresno de la tierra (Španjolska), freixo-de-folhas-estreitas (Portugal). Poljski jasen je široko rasprostranjen od regije Kavkaza, preko središnje i južne Europe do sjeverozapadne Afrike. Uspijeva u riječnim dolinama, obalnim šumama te poplavnim ravnicama i močvarama, a najviše mu odgovaraju vlažna, plodna tla u blagim klimatskim uvjetima. Često stvara velike, kontinuirane populacije, ali može kolonizirati i oslabljena područja. Tipično pokazuje visoku genetsku raznolikost i nisku do umjerenu genetsku diferencijaciju, što je očekivano od vrste poput jasena, slično drugom drveću koje se oprašuje vjetrom (Temunović i dr., 2012.). Plantažni uzgoj jasena u Europi nije baš čest jer se uglavnom sadi u kombinaciji s drugim vrstama.

Zbog atraktivnog lišća i načina rasta poljski se jasen u urbanim krajolicima sadi kao ukrasno drveće. Budući da vrlo brzo raste, plantažno se sadi za potrebe industrije celuloze i papira. Također, kao sirovina se upotrebljava i u proizvodnji šperploča te lameliranog drva.

Drvo poljskog jasena ima slična svojstva kao obični jasen, iako mu je kvaliteta lošija u smislu čvrstoće i elastičnosti. Drvo veće kvalitete, usporedivo s običnim jasenom, može se dobiti uzgojem na sušnijim staništima, gdje stabla sporije rastu. Na području sjeverozapadne Turske, gdje se više iskorištava uskolisni jasen iz brzorastućih plantaža na močvarnim nizinama, kvaliteta njegova drva sličnija je topolovini i prikladna je za dobivanje celuloznog drva i proizvoda od lijepljenog drva poput šperploče i lamelirane građe od furnira te za proizvodnju lijepljenoga lameliranog drva.

Poljski jasen nije na popisu ugroženih vrsta međunarodne organizacija CITES, dok se prema IUCN-u vodi kao vrsta drva najmanje zabrinjavajućeg opstanka.

RELEVANTNE SPOZNAJE O DRVU POLJSKOG JASENA

Drvo poljskog jasena jednolično je žućkasto do crvenkastobijelo (Trajković i Hasan, 2022.). Srednje je do grube teksture, poput hrastova drva. Pore i go-

GENERAL INFORMATION ON SPECIES

Fraxinus angustifolia Vahl is a wood species in the *Oleaceae* family. Common names are: Desert ash (Australia), Narrow-leaved ash (Great Britain), fresno, fresno de hoja estrecha, fresno de la tierra (Spain), freixo-de-folhas-estreitas (Portugal). Narrow-leaved ash is widely distributed from the Caucasus region, through central and southern Europe to northwestern Africa. It thrives in river valleys, riparian forests, floodplains, and wetlands, preferring moist, fertile soils in mild climates. It often forms large, continuous populations, but it can also colonize disturbed areas. It typically shows high genetic diversity and low to moderate genetic differentiation, as expected in ashes and other wind-pollinated trees (Temunović et al., 2012). Timber plantations are not very common over Europe, as it is mainly planted in combination with other species.

The tree is used for ornamental purposes in urban landscapes for its attractive foliage and growth habit. Due to its very fast growth, it is planted on plantations for the needs of the pulp and paper industry. It is also used as a raw material in the production of plywood and laminated wood.

The wood of narrow-leaved ash has similar properties to the common ash, although the quality is inferior in terms of strength and elasticity. Higher wood quality, comparable to common ash, can be obtained on drier sites where tree growth is slower. In the northwest of Turkey, where narrow-leaved ash is more used in fast-growing plantations on swampy lowlands, the wood quality is more similar to the poplars and is suitable for pulpwood and bonded wood products, such as plywood, laminated veneer lumber and glued laminated timber.

This wood species is not listed in the international organization CITES Appendices and is reported by the IUCN as a species of least concern.

RELEVANT KNOWLEDGE ABOUT NARROW-LEAVED ASH WOOD

The wood of narrow-leaved ash is of uniform yellowish to reddish-white color (Trajković and Hasan 2022). It is considered to be medium to coarse-textured, similar to oak. Vessels and annual growth rings are clearly visible to the naked eye. It is ring-porous wood with large earlywood pores (2-4 in rows), and

dovi dobro su vidljivi običnim okom. Prstenasto je porozno drvo s krupnim porama ranog drva (2 – 4 u nizu) i sitnim pojedinačnim ili radijalnim nizovima od 2 – 3 pore kasnog drva. Poljski jasen nema prave srži. Fakultativno obojena srž u deblima poljskog jasena dopire do prvih grana te u pojedinim stablima na različitim mjestima može imati različite nijanse (Trajković i Hasan, 2022.).

Pregled novijih istraživanja drva poljskog jasena donosi spoznaje o (a) sličnostima svojstava tog drva s drvom *F. excelsior* (Fraxigen, 2005.); (b) o najboljim mehaničkim svojstvima drva iz regija s najvećim razmakom stabala (Guler i dr., 2015.); (c) o otpornosti drva poljskog jasena na djelovanje gljiva, što bi se moglo povećati toplinskom obradom drva (Yalcin i Sahin, 2015.); (d) o smanjenju širine godova u smjeru od baze debla prema krošnji u vrijeme napredovanja odumiranja stabala jasena (Tulik i dr., 2017.); (e) o naglom smanjenju prirasta u godini nakon rezidbe stabala, dok se širina zone ranog drva nije promijenila, a kasnog drva gotovo i nema (Candel-Pérez i dr., 2022.).

Napomena: podatci o tehničkim i tehnološkim svojstva drva poljskog jasena dostupni su na web stranicama navedenima u literaturi.

VAŽNOST ISTRAŽIVANJA POLJSKOG JASENA U HRVATSKOJ

Poljski je jasen na području Hrvatske uglavnom vezan za područja uz rijeke crnomorskoga i jadranskog slijeva i uz njihove pritoke. U Hrvatskoj je poljski jasen prvi istraživao Fukarek (1954., 1955., 1957.), a u svojim radovima opisuje osam podvrsta, varijeteta i formi poljskoga jasena: *var. angustifolia*, *var. australis* Gay, *var. oxycarpa* Willdenow, *var. pannonica*, *var. nova*, *var. obliqua* Tausch, *subsp. pallisae* Wilmott, *var. oligophylla* Boissier te *f. rotundifolia* Miller. Isti autor detaljno opisuje rasprostranjenost poljskog jasena u Istri, Hrvatskom primorju (uključujući otoke Krk, Rab i Pag), kao i u Dalmaciji (područja rijeke Zrmanje, Ravnih kotara, rijeke Krke, Čikole, Cetine i Neretve). Detaljna istraživanja autohtonih populacija poljskog jasena na području cijele Hrvatske pokazala su znatne razlike u genskoj strukturi između populacija kontinentalnoga i jadranskog područja (Temunović i dr., 2012.).

Najnovije istraživanje šteta koje jelen obični (*Cervus elaphus* L.) uzrokuje na kori i strukturi drva mladih stabala poljskog jasena provedeno je na Fakultetu šumarstva i drvne tehnologije Sveučilišta u Zagrebu, u Zavodu za zaštitu šuma i lovno gospodarenje te u Zavodu za znanost o drvu (Kranjec Orlović i dr., 2024.). Prema najvažnijim zaključcima, prouzročena su oštećenja u potpunosti zatvorena, a promjene boje i propadanje ograničeni su na središnji dio debla, dok su

small latewood pores solitary and radial multiples of 2-3. Narrow-leaved ash has no proper heartwood. The facultatively colored heartwood in narrow-leaved ash trunks reaches the first branches and may have different shades in color in trees growing in different places (Trajković and Hasan 2022).

A review of later research on narrow-leaved ash wood provides knowledge on: (a) *F. angustifolia* wood characteristics similarities to *F. excelsior* (Fraxigen 2005); (b) the best mechanical properties obtained from the region with the widest tree spacing (Guler et al. 2015); (c) the durability of narrow-leaved ash wood against fungi could be increased through heat treatment (Yalcin and Sahin 2015); (d) the decrease in the width of annual tree rings in the direction from the base of the trunk toward the crown during the progress of ash dieback (Tulik et al. 2017); (e) a sudden growth reduction observed a year after pruning, earlywood width not altered that year, but latewood almost absent (Candel-Pérez et al. 2022).

Note: data on technical and technological properties of narrow-leaved ash wood are available on web pages listed in the literature section.

THE IMPORTNACE OF NARROW-LEAVED ASH RESEARCH IN CROATIA

In Croatia, narrow-leaved ash is generally associated with areas along the rivers of the Black Sea and Adriatic Basins and their tributaries. In Croatia, it was first investigated by Fukarek (1954, 1955, 1957), who describes eight subspecies, varieties and forms of the field ash: *var. angustifolia*, *var. australis* Gay, *var. oxycarpa* Willdenow, *var. pannonica, var. nova*, *var. obliqua* Tausch, *subsp. pallisae* Wilmott, *var. oligophylla* Boissier and *f. rotundifolia* Miller. The same author describes in detail the distribution of the field ash in Istria, the Croatian Littoral (including the islands of Krk, Rab and Pag), as well as in Dalmatia (the areas of the Zrmanja River, Ravni Kotari, the Krka River, Čikola, Cetina and Neretva rivers). Detailed research of autochthonous populations of the narrow-leaved ash throughout Croatia has shown significant differences in the genetic structure between populations in the continental and Adriatic areas (Temunović et al. 2012).

The latest research into the damage caused by red deer (*Cervus elaphus* L.) to the bark and wood structure of young narrow-leaved ash trees was conducted at the Faculty of Forestry and Wood Technology of the University of Zagreb, at the Institute for Forest Protection and Wildlife Management and the Institute for Wood Science (Kranjec Orlović et al., 2024). According to the most important conclusions, the wounds were completely closed, and discoloration and decay were limited to the central part of the stem, while ear-

stanice u ranom drvu ozlijeđenog tkiva manjih promjera lumena u usporedbi s onima u zdravom tkivu, a s obzirom na različita stabla i visinu debla. Pri tome je identificirana i invazivna patogena gljiva prisutna u tkivu koje je bilo izloženo oštećenju.

lywood cells in wounding zone made by red deer had narrower lumens compared to those in adjacent healthy zone regarding different trees and stem heights. At the same time, an invasive pathogenic fungus was also identified in the tissue exposed by wounding.

LITERATURE

1. Candel-Pérez, D.; Hernández-Alonso, H.; Mutke, S.; García-Hidalgo, M.; Castro, F.; Sangüesa-Barreda, G.; Rozas, V.; Olano, J. M., 2022: 250-Year reconstruction of pollarding events reveals sharp management changes in Iberian ash woodlands. Trees, 36: 1909-1921. https://doi.org/10.1007/s00468-022-02343-8
2. Caudullo, G.; Houston Durrant, T., 2016: Fraxinus angustifolia in Europe: distribution, habitat, usage and threats. U: San-MiguelAyanz, J.; de Rigo, D.; Caudullo, G.; Houston Durrant, T.; Mauri, A. (eds.), European Atlas of Forest Tree Species. Publ. Off. EU, Luxembourg, pp. e0101d2+
3. Çiçek, E.; Yilmaz, M., 2002: Proceeding of International IUFRO Meeting: Management of Fast Growing Plantations, 11-13 September 2002. Izmit, Turkey, pp. 192-202.
4. Coello, J.; Beckuey, J.; Gonin, P.; Ortisset, J.-P.; Desombre, V.; Baiges, T.; Pique, M., 2013: Ecology and silviculture of the main valuable broadleaved species in the Pyrenean area and neighbouring regions – Centre de la Propietat Forestal, Generalitat de Catalunya, Santa Perpètua de Mogoda (Spain).
5. Fraxigen, 2005: Ash Species in Europe: Biological Characteristics and Practical Guidelines for Sustainable Use. A summary of Findings from the Fraxigen Project EU Project EVKCT00108. Oxford Forestry Institute, University of Oxford, UK.
6. Fukarek, P., 1954: Poljski jasen (*Fraxinus angustifolia* Vahl). Šumarski list, 78 (9-10): 433-453.
7. Fukarek, P., 1955: Dodatak članku Poljski jasen (*Fraxinus angustifolia* Vahl). Šumarski list, 79 (-2): 16-21.
8. Fukarek, P., 1957: Novi podaci o poljskom jasenu (*Fraxinus angustifolia* Vahl). Šumarski list, 81 (1-2): 30-35.
9. Guler, C.; Sahin, H. I.; Aliogullari, S., 2015: Effect of spacing on some mechanical properties of narrow leaved ash (*Fraxinus angustifolia*) wood. Maderas. Ciencia y Tecnología 17(4): 773-788. https://10.4067/S0718-221X2015005000067
10. Kranjec Orlović, J.; Diminić, D.; Ištok, I.; Volenec, I.; Hodak, L.; Grubešić, M.; Tomljanović, K., 2024: Fungal Presence and Changes of Wood Structure in Bark Stripping Wounds Made by Red Deer (*Cervus elaphus* L.) on Stems of *Fraxinus angustifolia* (Vahl). Forests, 15: 314. https://doi.org/10.3390/f15020314
11. Temunović, M.; Franjić, J.; Šatović, Z.; Grgurev, M.; Frascaria-Lacoste, N.; Fernández-Manjarrés, J. F., 2012: Environmental Heterogeneity Explains the Genetic Structure of Continental and Mediterranean Populations of *Fraxinus angustifolia* Vahl. PLoS ONE, 7, e42764.
12. Trajković, J.; Hasan, M., 2022: Anatomska svojstva drva poljskog jasena i njegova prirodna trajnost. U: Anić, I. (ur.): Poljski jasen u Hrvatskoj. Akademija šumarskih znanosti Zagreb, 539-548.
13. Tulik, M.; Zakrzewski, J.; Adamczyk, J.; Tereba, A.; Yaman, B.; Nowakowska, J. A., 2017: Anatomical and genetic aspects of ash dieback: a look at the wood structure. iForest 10: 522-528. https://doi.org/10.3832/ifor2080-010
14. Yalcin, M.; Sahin, H. I., 2015. Changes in the chemical structure and decay resistance of heat-treated narrow-leaved ash wood. Maderas. Ciencia y Tecnología, 17 (2): 435-446. https://doi.org//10.4067/S0718-221X2015005000040
15. https://bdc.univie.ac.at/fileadmin/user_upload/i_bdc/dashboard/Fraxinusangustifolia.html (pristupljeno 20. svibnja 2025.)
16. https://www.euforgen.org/species/fraxinus-angustifolia (pristupljeno 20. svibnja 2025.)
17. https://www.iucnredlist.org/species/203366/96445347 (pristupljeno 23. svibnja 2025.)
18. https://www.wood-database.com/european-ash/ (pristupljeno 23. svibnja 2025.)

doc. dr. sc. Iva Ištok Pandur

Upute autorima

Opće odredbe

Časopis *Drvna industrija* objavljuje znanstvene radove (izvorne znanstvene radove, pregledne radove, prethodna priopćenja), stručne radove, izlaganja sa savjetovanja, stručne obavijesti, bibliografske radove, preglede te ostale priloge s područja biologije, kemije, fizike i tehnologije drva, pulpe i papira te drvnih proizvoda, uključujući i proizvodnu, upravljačku i tržišnu problematiku u drvnoj industriji.

Predaja rukopisa podrazumijeva uvjet da rad nije već predan negdje drugdje radi objavljivanja ili da nije već objavljen (osim sažetka, dijelova objavljenih predavanja ili magistarskih radova odnosno disertacija, što mora biti navedeno u napomeni) te da su objavljivanje odobrili svi suautori (ako rad ima više autora) i ovlaštene osobe ustanove u kojoj je istraživanje provedeno. Cjelokupni sadržaj Drvne industrije dostupan je za skidanje s interneta, tiskanje, daljnju distribuciju, čitanje i ponovno korištenje bez ograničenja sve dok se naznače autor(i) i originalni izvor prema Creative Commons Attribution 4.0 International License (CC BY). Autor(i) zadržavaju izdavačka prava bez ograničenja.

Znanstveni i stručni radovi objavljuju se na engleskom jeziku, uz sažetak na hrvatskome. Također, naslov, podnaslovi i svi važni rezultati trebaju biti napisani dvojezično. Uredništvo osigurava inozemnim autorima prijevod na hrvatski. Ostali se članci uglavnom objavljuju na hrvatskome. Znanstveni i stručni radovi podliježu temeljitoj recenziji najmanje dvaju recenzenata. Izbor recenzenata i odluku o klasifikaciji i prihvaćanju članka (prema preporukama recenzenata) donosi Urednički odbor.

Svi prilozi podvrgavaju se jezičnoj obradi. Urednici će od autora zahtijevati da tekst prilagode preporukama recenzenata i lektora, te zadržavaju i pravo da predlože skraćivanje ili poboljšanje teksta. Autori su potpuno odgovorni za svoje priloge. Podrazumijeva se da je autor pribavio dozvolu za objavljivanje dijelova teksta što su već negdje objavljeni te da objavljivanje članka ne ugrožava prava pojedinca ili pravne osobe. Radovi moraju izvještavati o istinitim znanstvenim ili tehničkim postignućima. Autori su odgovorni za terminološku i metrološku usklađenost svojih priloga. Radovi se šalju elektronički putem poveznice http://journal.sdewes.org/drvind

Upute

Predani radovi smiju sadržavati najviše 15 jednostrano pisanih A4 listova s dvostrukim proredom (30 redaka na stranici), uključujući i tablice, slike te popis literature, dodatke i ostale priloge. Dulje je članke preporučljivo podijeliti na dva ili više nastavaka. Tekst treba biti u *doc formatu*, u potpunosti napisan fontom *Times New Roman* (tekst, grafikoni i slike), normalnim stilom, bez dodatnog uređenja teksta.

Prva stranica poslanog rada treba sadržavati puni naslov, ime(na) i prezime(na) autora, podatke o zaposlenju autora (ustanova, grad i država) te sažetak s ključnim riječima (duljina sažetka približno 1/2 stranice A4).

Posljednja stranica treba sadržavati titule, zanimanje, zvanje i adresu (svakog) autora, s naznakom osobe s kojom će Uredništvo biti u vezi.

Znanstveni i stručni radovi moraju biti sažeti i precizni. Osnovna poglavlja trebaju biti označena odgovarajućim podnaslovima. Napomene se ispisuju na dnu pripadajuće stranice, a obrojčavaju se susljedno. One koje se odnose na naslov označuju se zvjezdicom, a ostale uzdignutim arapskim brojkama. Napomene koje se odnose na tablice pišu se ispod tablica, a označavaju se uzdignutim malim pisanim slovima, abecednim redom.

Latinska imena trebaju biti pisana kosim slovima (italicom), a ako je cijeli tekst pisan kosim slovima, latinska imena trebaju biti podcrtana.

U uvodu treba definirati problem i, koliko je moguće, predočiti granice postojećih spoznaja, tako da se čitateljima koji se ne bave područjem o kojemu je riječ omogući razumijevanje ciljeva rada.

Materijal i metode trebaju biti što preciznije opisane da omoguće drugim znanstvenicima ponavljanje pokusa. Glavni eksperimentalni podaci trebaju biti dvojezično navedeni.

Rezultati trebaju obuhvatiti samo materijal koji se izravno odnosi na predmet. Obvezatna je primjena metričkog sustava. Preporučuje se upotreba SI jedinica. Rjeđe rabljene fizikalne vrijednosti, simboli i jedinice trebaju biti objašnjeni pri njihovu prvom spominjanju u tekstu. Za pisanje formula valja se koristiti Equation Editorom (programom za pisanje formula u MS Wordu). Jedinice se pišu normalnim (uspravnim) slovima, a fizikalni simboli i faktori kosima (italicom).

Formule se susljedno obrojčavaju arapskim brojkama u zagradama, npr. (1) na kraju retka.

Broj slika mora biti ograničen samo na one koje su prijeko potrebne za objašnjenje teksta. Isti podaci ne smiju biti navedeni i u tablici i na slici. Slike i tablice trebaju biti zasebno obrojčane, arapskim brojkama, a u tekstu se na njih upućuje jasnim naznakama ("tablica 1" ili "slika 1"). Naslovi, zaglavlja, legende i sav ostali tekst u slikama i tablicama treba biti napisan hrvatskim i engleskim jezikom.

Slike je potrebno rasporediti na odgovarajuća mjesta u tekstu, trebaju biti izrađene u rezoluciji 600 dpi, crno-bijele (objavljivanje slika u koloru moguće je na zahtjev autora), formata jpg ili tiff, potpune i jasno razumljive bez pozivanja na tekst priloga.

Svi grafikoni i tablice izrađuju se kao crno-bijeli prilozi (osim na zahtjev). Tablice i grafikoni trebaju biti na svojim mjestima u tekstu te originalnog formata u kojemu su izrađeni radi naknadnog ubacivanja hrvatskog prijevoda. Ako ne postoji mogućnost za to, potrebno je poslati originalne dokumente u formatu u kojemu su napravljeni (*excel* ili *statistica* format).

Naslovi slika i crteža ne pišu se velikim tiskanim slovima. Crteži i grafikoni trebaju odgovarati stilu časopisa (fontovima i izgledu). Slova i brojke moraju biti dovoljno veliki da budu lako čitljivi nakon smanjenja širine slike ili tablice. Fotomikrografije moraju imati naznaku uvećanja, poželjno u mikrometrima. Uvećanje može biti dodatno naznačeno na kraju naslova slike, npr. "uvećanje 7500 : l".

Diskusija i zaključak mogu, ako autori žele, biti spojeni u jedan odjeljak. U tom tekstu treba objasniti rezultate s obzirom na problem postavljen u uvodu i u odnosu prema odgovarajućim zapažanjima autora ili drugih istraživača. Valja izbjegavati ponavljanje podataka već iznesenih u odjeljku *Rezultati*. Mogu se razmotriti naznake za daljnja istraživanja ili primjenu. Ako su rezultati i diskusija spojeni u isti odjeljak, zaključke je nužno napisati izdvojeno. Zahvale se navode na kraju rukopisa. Odgovarajuću literaturu treba citirati u tekstu, i to prema harvardskom sustavu (*ime – godina*), npr. (Bađun, 1965).

Nadalje, bibliografija mora biti navedena na kraju teksta, i to abecednim redom prezimena autora, s naslovima i potpunim navodima bibliografskih referenci. Popis literature mora biti selektivan, a svaka referenca na kraju mora imati naveden DOI broj, ako ga posjeduje (http://www.doi.org) (provjeriti na http://www.crossref.org).

Primjeri navođenja literature

Članci u časopisima: Prezime autora, inicijal(i) osobnog imena, godina: Naslov. Naziv časopisa, godište (ev. broj): stranice (od – do). Doi broj.

Primjer

Kärki, T., 2001: Variation of wood density and shrinkage in European aspen (*Populus tremula*). Holz als Roh- und Werkstoff, 59: 79-84. http://dx.doi.org/10.1007/s001070050479.

Knjige: Prezime autora, inicijal(i) osobnog imena, godina: Naslov. (ev. izdavač/editor): izdanje (ev. svezak). Mjesto izdanja, izdavač (ev. stranice od – do).

Primjeri

Krpan, J., 1970: Tehnologija furnira i ploča. Drugo izdanje. Zagreb, Tehnička knjiga.

Wilson, J. W.; Wellwood, R. W., 1965: Intra-increment chemical properties of certain western Canadian coniferous species. U: W. A. Cote, Jr. (Ed.): Cellular Ultrastructure of Woody Plants. Syracuse, N.Y., Syracuse Univ. Press, pp. 551- 559.

Ostale publikacije (brošure, studije itd.)

Müller, D., 1977: Beitrag zür Klassifizierung asiatischer Baumarten. Mitteilung der Bundesforschungsanstalt für Forstund Holzvvirt schaft Hamburg, Nr. 98. Hamburg: M. Wiederbusch.

Web stranice

***1997: "Guide to Punctuation" (online), University of Sussex, www.informatics.sussex.ac.uk/department/docs/punctuation/node 00.html. First published 1997 (pristupljeno 27. siječnja 2010).

Autoru se prije konačnog tiska šalje pdf rada. Rad je potrebno pažljivo pročitati, ispraviti te vratiti Uredništvu s listom ispravaka. Autori znanstvenih i stručnih radova besplatno dobivaju po jedan primjerak časopisa. Autoru svakog priloga također se dostavlja besplatan primjerak časopisa.

Dodatne informacije o načinu pisanja znanstvenih radova mogu se naći na web adresi:
www.ease.org.uk/publications/author-guidelines

Instructions for authors

General terms

The "Drvna industrija" ("Wood Industry") journal publishes scientific papers (original scientific papers, review papers, previous notes), professional papers, conference papers, professional information, bibliographical and survey articles and other contributions related to biology, chemistry, physics and technology of wood, pulp and paper and wood products, including production, management and marketing issues in the wood industry.

Submission of a paper implies that the work has not been submitted for publication elsewhere or published before (except in the form of an abstract or as part of a published lecture, review or thesis, in which case it must be stated in a footnote); that the publication is approved by all co-authors (if any) and by the authorities of the institution where the research has been carried out. The complete content of the journal *Drvna industrija* (Wood Industry) is available on the Internet permitting any users to download, print, further distribute, read and reuse it with no limits provided that the author(s) and the original source are identified in accordance with the Creative Commons Attribution 4.0 International License (CC BY). The authors retain their copyrights.

The scientific and professional papers shall be published in English with summary in Croatian. The titles, headings and all the relevant results shall be also presented bilingually. The Editor's Office shall provide the translation into Croatian for foreign authors. Other articles are generally published in Croatian. The scientific and professional papers will be subject to a thorough review by at least two selected referees. The Editorial Board shall make the choice of reviewers, as well as the decision about the classification of the paper and its acceptance (based on reviewers' recommendations).

All contributions are subject to proofreading. The editors will require authors to modify the text in the light of the recommendations made by reviewers and language advisers, and they reserve the right to suggest abbreviations and text improvements. Authors are fully responsible for the contents of their contributions. It shall be assumed that the author has obtained the permission for the reproduction of portions of text published elsewhere, and that the publication of the paper in question does not infringe upon any individual or corporate rights. Papers shall report on true scientific or technical achievement. Authors are responsible for the terminological and metrological consistency of their contributions. The contributions are to be submitted by the link http://journal.sdewes.org/drvind

Details

Papers submitted shall consist of no more than 15 single-sided DIN A-4 sheets of 30 double-spaced lines, including tables, figures and references, appendices and other supplements. Longer papers should be divided into two or more continuing series. The text should be written in doc format, fully written using Times New Roman font (text, graphs and figures), in normal style without additional text editing.

The first page of the paper submitted should contain full title, name(s) of author(s) with professional affiliation (institution, city and state), abstract with keywords (approx. 1/2 sheet DIN A4).

The last page should provide the full titles, posts and address(es) of each author with indication of the contact person for the Editor's Office.

Scientific and professional papers shall be precise and concise. The main chapters should be characterized by appropriate headings. Footnotes shall be placed at the bottom of the same page and consecutively numbered. Those relating to the title should be marked by an asterix, others by superscript Arabic numerals. Footnotes relating to the tables shall be printed under the table and marked by small letters in alphabetical order.

Latin names shall be printed in italics and underlined.

Introduction should define the problem and if possible the framework of existing knowledge, to ensure that readers not working in that particular field are able to understand author's intentions.

Materials and methods should be as precise as possible to enable other scientists to repeat the experiment. The main experimental data should be presented bilingually.

The results should involve only material pertinent to the subject. The metric system shall be used. SI units are recommended. Rarely used physical values, symbols and units should be explained at their first appearance in the text. Formulas should be written by using Equation Editor (program for writing formulas in MS Word). Units shall be written in normal (upright) letters, physical symbols and factors in italics. Formulas shall be consecutively numbered with Arabic numerals in parenthesis (e.g. (1)) at the end of the line.

The number of figures shall be limited to those absolutely necessary for clarification of the text. The same information must not be presented in both a table and a figure. Figures and tables should be numbered separately with Arabic numerals, and should be referred to in the text with clear remarks ("Table 1" or "Figure 1"). Titles, headings, legends and all the other text in figures and tables should be written in both Croatian and English.

Figures should be inserted into the text. They should be of 600 dpi resolution, black and white (color photographs only on request), in jpg or tiff format, completely clear and understandable without reference to the text of the contribution.

All graphs and tables shall be black and white (unless requested otherwise). Tables and graphs should be inserted into the text in their original format in order to insert them subsequently into the Croatian version. If this is not possible, original document should be sent in the format in which it was made (excel or statistica format).

The captions to figures and drawings shall not be written in block letters. Line drawings and graphs should conform to the style of the journal (font size and appearance). Letters and numbers shall be sufficiently large to be readily legible after reduction of the width of a figure or table. Photomicrographs should have a mark indicating magnification, preferably in micrometers. Magnification can be additionally indicated at the end of the figure title, e.g. "Mag. 7500:1".

Discussion and conclusion may, if desired by authors, be combined into one chapter. This text should interpret the results relating to the problem outlined in the introduction and to related observations by the author(s) or other researchers. Repeating the data already presented in the "Results" chapter should be avoided. Implications for further studies or application may be discussed. A conclusion shall be expressed separately if results and discussion are combined in the same chapter. Acknowledgements are presented at the end of the paper. Relevant literature shall be cited in the text according to the Harvard system ("name – year"), e.g. (Bađun, 1965). In addition, the bibliography shall be listed at the end of the text in alphabetical order of the author's names, together with the title and full quotation of the bibliographical reference. The list of references shall be selective, and each reference shall have its DOI number (http://www.doi.org) (check at http://www.crossref.org).:

Example of references

Journal articles: Author's second name, initial(s) of the first name, year: Title. Journal name, volume (ev. issue): pages (from - to). DOI number.

Example:
Kärki, T., 2001: Variation of wood density and shrinkage in European aspen (*Populus tremula*). Holz als Roh- und Werkstoff, 59: 79-84. http://dx.doi.org/10.1007/s001070050479.

Books:
Author's second name, initial(s) of the first name, year: Title. (ev. Publisher/editor): edition, (ev. volume). Place of publishing, publisher (ev. pages from - to).

Examples:
Krpan, J. 1970: Tehnologija furnira i ploča. Drugo izdanje. Zagreb: Tehnička knjiga.
Wilson, J.W.; Wellwood, R.W. 1965: Intra-increment chemical properties of certain western Canadian coniferous species. U: W. A. Cote, Jr. (Ed.): Cellular Ultrastructure of Woody Plants. Syracuse, N.Y., Syracuse Univ. Press, pp. 551-559.

Other publications (brochures, studies, etc.):
Müller, D. 1977: Beitrag zur Klassifizierung asiatischer Baumarten. Mitteilung der Bundesforschungsanslalt für Forst- und Holzwirtschaft Hamburg, Nr. 98. Hamburg: M. Wiederbusch.

Websites:
***1997: "Guide to Punctuation" (online), University of Sussex, www.informatics.sussex.ac.uk/department/docs/punctuation/node00.html. First published 1997 (Accessed Jan. 27, 2010).

The paper will be sent to the author in pdf format before printing. The paper should be carefully corrected and sent back to the Editor's Office with the list of corrections made. Each contributor will receive 1 copy of the journal.

Further information on the way of writing scientific papers can be found on the following website:

www.ease.org.uk/publications/author-guidelines

HRVATSKA KOMORA
INŽENJERA ŠUMARSTVA
I DRVNE TEHNOLOGIJE

HRVATSKA KOMORA INŽENJERA ŠUMARSTVA I DRVNE TEHNOLOGIJE

Osnovana je na temelju Zakona o Hrvatskoj komori inženjera šumarstva i drvne tehnologije.

Komora je samostalna i neovisna strukovna organizacija koja obavlja povjerene joj javne ovlasti, čuva ugled, čast i prava svojih članova, skrbi da ovlašteni inženjeri obavljaju svoje poslove savjesno i u skladu sa zakonom, promiče, zastupa i usklađuje njihove interese pred državnim i drugim tijelima u zemlji i inozemstvu.

Članovi komore:

inženjeri šumarstva i drvne tehnologije koji obavljaju stručne poslove iz područja šumarstva, lovstva i drvne tehnologije.

Stručni poslovi:

projektiranje, izrada, procjena, izvođenje i nadzor radova iz područja uzgajanja, uređivanja, iskorištavanja i otvaranja šuma, lovstva, zaštite šuma, hortikulture, rasadničarske proizvodnje, savjetovanja, ispitivanja kvalitete proizvoda, sudskoga vještačenja, izrade i revizije stručnih studija i planova, kontrola projekata i stručne dokumentacije, izgradnja uređaja, izbor opreme, objekata, procesa i sustava, stručno osposobljavanje i licenciranje radova u šumarstvu, lovstvu i preradi drva.

Zadaci Komore:

- promicanje razvoja struke i skrb o stručnom usavršavanju članova,
- poticanje donošenja propisa kojima se utvrđuju javne ovlasti Komore,
- reagiranje struke na pripremu propisa iz područja šumarstva, lovstva i drvne tehnologije,
- suradnja s nadležnim institucijama i zastupanje struke u odnosu prema njima,
- organizacija stručnoga usavršavanja,
- zastupanje interesa svojih članova,
- izdavanje pečata i iskaznice ovlaštenim inženjerima,
- briga i nadzor poštivanja kodeksa strukovne etike,
- osiguravanje članova Komore za štetu koja bi mogla nastati investitorima i trećim osobama i sl.

Članovima Komore izdaje se rješenje, pečat i iskaznica ovlaštenoga inženjera.
Za uspješno obavljanje zadataka te za postizanje ciljeva ravnopravnoga i jednakovrijednoga zastupanja struka udruženih u Komoru, članovi Komore organizirani su u razrede:

- Razred inženjera šumarstva
- Razred inženjera drvne tehnologije

HRVATSKA KOMORA INŽENJERA ŠUMARSTVA I DRVNE TEHNOLOGIJE
Prilaz Gjure Deželića 63
10000 ZAGREB

telefon:
++ 385 1 376-5501
e-mail:
info@hkisdt.hr

www.hkisdt.hr

Drvodjelac d.o.o.
Petra Preradovića 14, Ivanec, Hrvatska
+385 (0)42 781 922 | www.drvodjelac.hr